Deltares

Enabling Delta Life

Development of a Water Quality Modelling Framework for the Hauraki Plains Catchment

Deltares

Development of a Water Quality Modelling Framework for the Hauraki Plains Catchment

Marc Weeber (DairyNZ & Deltares)
Joost van den Roovaart
Erwin Meijers
Neeltje Goorden
Daniel Tollenaar
David Burger (DairyNZ)

1210754-000

Deltares

Development of a Water Quality Modelling Framework for the Hauraki Plains Catchment

Marc Weeber (DairyNZ & Deltares)
Joost van den Roovaart
Erwin Meijers
Neeltje Goorden
Daniel Tollenaar
David Burger (DairyNZ)

1210754-000

Deltares

Title
Development of a Water Quality Modelling Framework for the Hauraki Plains Catchment

Client	Project	Reference	Pages
DairyNZ Limited	1210754-000	1210754-000-ZWS-0006	

Keywords
Hauraki Plains catchment, Catchment water quality model, nitrogen and phosphorus loading, Water Framework Directive Explorer, WFLOW, FEWS, New Zealand

Summary
In 2014 Deltares and DairyNZ developed and applied an integrated catchment hydrological-water quality modelling approach for the Waituna catchment in Southland, New Zealand. A distributed hydrological model (WFLOW) was combined with a spatially refined water quality model (WFD Explorer) to quantify farm and catchment scale total nitrogen (TN) and total phosphorus (TP) loading to the Waituna Lagoon.

This current study builds further on the Waituna Modelling Framework to test and apply the modelling approach to a much larger and more complex catchment, the Hauraki Plains catchment in Waikato, New Zealand (area 346,000 ha). The catchment represents a significant dairying region (53% of land area) and consists of the Waihou, Piako and Waitakaruru River sub-catchments, which discharge to the Firth of Thames. A marine spatial plan is currently being developed for the Firth and wider Hauraki Gulf Marine Reserve. This precedes a future catchment water quality limit setting process which will commence in the Hauraki Catchment from 2017. As part of this process a greater understanding of catchment load sources is required.

The WFLOW hydrological model was set up on a daily time step and spatial resolution of 25 by 25 m. The water balance of the catchment is strongly influenced by spring flows and the limited knowledge available to spatially and temporally parameterise these sources influenced the overall performance of the hydrological model, especially for the Waihou and Waitoa catchments.

Catchment water quality was simulated using the WFD-Explorer model. Nutrient load input to the model reflected sources related to specific agricultural land-uses, background loads and point sources. Different types of land-uses, and for farms even block types, were defined in the WFD Explorer as separate emission types. Nutrient losses for Dairy farms were based on 12 model farms with other land-use values acquired from the literature whilst point source estimates were derived from empirical data from literature sources. The results suggest that model performance is good for the simulation of periodic (approximately monthly) TN load and reasonable for annual TN load. When TN prediction is compared annually between rivers, model performance for the Piako is good but other rivers poor. For TP model performance was determined to be reasonable for periodic loads and good for annual loads. Between rivers model performance for TP was good downstream and poor upstream for the Piako River, reasonable for the Ohinemuri River, and poor for all other rivers. Poor model performance in some rivers can mostly be attributed to uncertainties in simulated flows. The model was assessed against RLoadest estimates estimated from continuous flow data and monthly measurements. Access to more temporally refined water quality data, especially over high flow periods, would help improve model performance.

The calibrated model framework is considered fit for purpose to be used as a management screening tool to test the likely impact of various nutrient load scenarios in the Hauraki Plains catchment. The model also provides a first overall estimate of TN and TP loading from the entire Hauraki Plains catchment, including the large areas of land situated below the current monitoring locations, to the Firth of Thames.

Deltares

Title
Development of a Water Quality Modelling Framework for the Hauraki Plains Catchment

Client	Project	Reference	Pages
DairyNZ Limited	1210754-000	1210754-000-ZWS-0006	

This study represents a collaboration between DairyNZ and Deltares and has been funded by DairyNZ (model application) and the Netherlands Ministry of Economic Affairs Knowledge and Innovation Program on Delta technology (model code development).

Version	Date	Author	Initials	Review	Initials	Approval	Initials
1	December 2016	Marc Weeber and Joost vd Roovaart		Simon Groot		Sacha de Rijk	
2	January 2017						

State
final

Contents

1 Introduction

1.1 Background

In 2014 Deltares and DairyNZ developed and applied an integrated catchment hydrological-water quality modelling approach for the Waituna catchment in Southland, New Zealand (van den Roovaart et al. 2014). A distributed hydrological model (WFLOW) was combined with a spatially refined water quality model (WFD Explorer) to quantify farm and catchment scale total nitrogen (TN) and total phosphorus (TP) loading to the Waituna Lagoon. The Waituna study was considered a test case to provide learnings towards the development of a spatially refined catchment water quality modelling framework which could be applied by DairyNZ to assist the catchment limit setting process in other New Zealand agricultural catchments.

An integrated catchment modelling approach offers one of the best means to quantify and assess the relative importance of individual load sources across a catchment. Such a model can also be applied as a complete catchment management tool to explore and evaluate the impacts of different management solutions to reach water quality targets together with land owners and water managers. A spatially-refined modelling approach permits individual load sources to be implemented individually, to capture possible differences in loading rates and best solutions for each source.

The Waituna model application was undertaken on a relatively small catchment (20,000 ha, 100 farms) with short groundwater lag times. It is currently uncertain whether the same modelling approach can be applied to a much larger catchment where groundwater processes are more dominant. It is also desirable that the model is refined temporally, to provide information around monthly as opposed to seasonal loading.

This study builds further on the Waituna Modelling Framework to test and apply the modelling approach to a much larger and more complex catchment, the Hauraki Plains catchment in Waikato, New Zealand (area 346,000 ha). As well as testing model applicability, the study aims to quantify monthly nitrogen and phosphorus loads from all sources, including diffuse land-use loads and point sources, to the Firth of Thames and Hauraki Gulf Marine Reserve.

The Hauraki Plains catchment is a significant dairying region with over 1510 dairy herds present (LIC/DNZ, 2015). The catchment is made up of the Waihou River (Waihou and Ohinemuri River sub-catchments, area 197,658 ha), the Piako River (Piako and Waitoa sub-catchments, area 148,147 ha) and the Waitakaruru River (no sub-catchments, area 15,416 ha) systems (DairyNZ, unpublished work). The Hauraki Plains Catchment is one of the key water catchments being assessed through a larger catchment management plan to improve the water quality of the Hauraki Gulf Marine Reserve (including the Firth of Thames). This plan precedes any nutrient limitations that might be added by the future legislatorial limit-setting process to be undertaken by Waikato Regional Council from 2017.

1.2 Study approach

This study represents a collaboration between DairyNZ and Deltares and has been funded by DairyNZ (Model application) and the Netherlands Ministry of Economic Affairs Knowledge and Innovation Program on Delta technology (model code development). Water quantity and quality data as well as land-use information required for set up of the model was provided by Waikato Regional Council. Study approach.
The Hauraki Plains catchment model development approach involved seven key activities:

1. Set up, calibrate and validate a 1D distributed hydrological model framework to compute daily discharges from the Piako-Waihou catchments (Hauraki Plains catchment) to the Hauraki Gulf based on WFLOW. Key characteristics of the flow modelling approach are:
   - A daily model time step with a minimum simulation period of seven years (2008-2014) and calibration period of two years.
   - Model calibration against continuous flow data covering at least seven Waikato Regional Council (WRC) monitoring locations.
   - The implementation of groundwater inputs to the head of the catchment.
2. Coupling of the hydrological model to a data, workflow and visualisation framework with Delft-FEWS.
3. Set up of a catchment water quality model framework to estimate total nitrogen and total phosphorus loads to the Firth of Thames using the WFD-Explorer model on a seasonal and on a monthly time step, including the implementation of spatially refined catchment nutrient sources into the water quality model schematisation. Key features include:
   - A simulation period of six years, calibration period of four years and a validation period of two years.
   - Mean annual total nitrogen and total phosphorus losses associated with individual farm titles, including approximately 1510 dairy farms represented as unique sources in the model framework.
   - The inclusion of point sources discharging to the two river systems, including municipal sewerage treatment plant discharges.
   - Model visualisation area extending to the Firth of Thames (Inner Hauraki Gulf).
4. Coupling of hydrological model output to the water quality modelling environment.
5. Calibration and final quantification of TN and TP loads to the Hauraki Gulf after attenuation, based on water quality measurements collected monthly at at least five monitoring locations.
6. Application and testing of the complete modelling framework as a management tool for assessing the impacts of a number of preliminary mitigation scenarios.
7. Reporting and model handover, including a user guide on how to run the model, update input information and apply management scenarios.

Because the river network in the lower Hauraki catchment is tidally influenced with the tidal range extending just upstream of each monitoring location, the simulated flows downstream of these monitoring points represent only uncalibrated freshwater discharges. Flood control structures in the lower catchment below the monitoring sites were not explicitly modelled as part of the project.

1.3 TKI Matching

This project was co-funded in part by the Netherlands Ministry of Economic Affairs Knowledge and Innovation Program on Delta technology (TKI). The following specific activities were undertaken through the TKI program and reflect mostly model software developments:

1. Set up of the software to enable the WFLOW hydrological model to be dynamically coupled with a ModFlow groundwater model.
2. Temporal disaggregation of the WFD-Explorer model calculations to enable model time step calculations on a more detailed level than the existing seasonal level (month, decade, week).
3. Set up of a Delta Data Viewer application for the Hauraki Plains-Waituna Catchment Modelling Framework. This interactive tool can be used in stakeholder workshops.

4. Improvement and extension of the functionalities regarding the report and output information of the WFD-Explorer.
5. Associated consultation and communication.

These activities mostly reflect model software developments which were required for full application of the Hauraki Plains and Waituna catchment model frameworks. Under the TKI agreement any new model software developed through the study will also be available for use by other users of the Modelling Framework components, both in the Netherlands and abroad.

1.4 Report outline

Chapter 1 provides an introduction to the study and its key aims, objectives and research activities. Chapter 2 provides an overview of the modelling approach applied and describes the various sub-models which make up the final model instrumentation. Chapter 3 describes the analysis of measured flows and loads. The setup of the hydrological model is described in Chapter 4. In Chapter 5 the WFD-Explorer water quality model is further explained. Chapter 6 tests the application of the model framework for nutrient load management scenarios while Chapter 7 describes the extension of the model framework using the Delta Data Viewer. A summary of the study, recommendations for further model refinement and expansion and overall conclusions are provided in Chapter 8. Supplementary background information about the model framework is documented as appendices.

2 Modelling Framework

2.1 Requirements

The main purpose for applying a catchment water quality modelling framework to the Hauraki Plains catchment is to (a) quantify total catchment nitrogen and phosphorus loading from the Piako and Waihou catchments to the Firth of Thames after attenuation and (b) provide an integrated management tool which can be applied to explore possible management solutions to reduce loading together with land owners and water managers.

For the modelling tool to be effective, the following functionalities were desired:

- A spatially refined approach which allows farms and other load sources to be implemented individually in the model framework. This is to capture the heterogeneity in nutrient losses between individual farms, for example due to differences in stocking rates, system type, soil type and other variables.
- An integrated catchment load management tool which can be applied to test a wide range of possible scenarios targeting different load sources, locations, soil types, land-use types and activities.
- The ability to generate and visualise spatial and temporal model estimates of stream nutrient concentrations and loading.
- Rapid model run times to allow scenarios to be simulated and analysed quickly together with land owners and stakeholders.
- An adaptable and flexible approach which allows more complex model functionalities, for example groundwater and in-stream processes, or other substances to be added in future without the need to reconfigure the existing set up and approach.
- Open-source software or freeware, to ensure that the model could be applied by anyone to any catchment without constraints. This improves model applicability and transparency and helps understand the capabilities and limitations of the model.

As the overall objective of the model is to assist catchment management planning, the main requirement of model output is mean, steady-state seasonal load estimates.

This Chapter introduces the overall modelling framework applied in the current study. More detailed information on the set up and application of each model component is documented in Chapters 4 (hydrology) and 5 (water quality model).

2.2 Selected modelling approach

To meet the specified requirements for the model, a framework based on the following individual sub-models was applied:

1. A 1D distributed catchment hydrological model for the simulation of rainfall runoff and sub-surface flows on a daily time step and spatial resolution of 25 x 25 m (Deltares WFLOW).
2. A data, workflow and visualisation platform to serve as a user interface for the hydrological model and to assist data management and result mapping (Delft-FEWS).
3. A lumped, steady state catchment water quality model to quantify catchment nutrient loading after attenuation and to conduct nutrient management scenarios (Deltares WFD-Explorer).
4. A model setup tool in Python which automates the WFD-Explorer model generation.

5. A Delta Data Viewer (DDV) application of the model which is used as a user friendly stakeholder engagement tool.

The modelling framework applied is based on the suite of models applied earlier to the Waituna Catchment (van den Roovaart et al. 2015). A schematic overview of the complete modelling framework and individual sub-models is shown in Figure 2.1. Each individual model is described in more detail in the following sections.

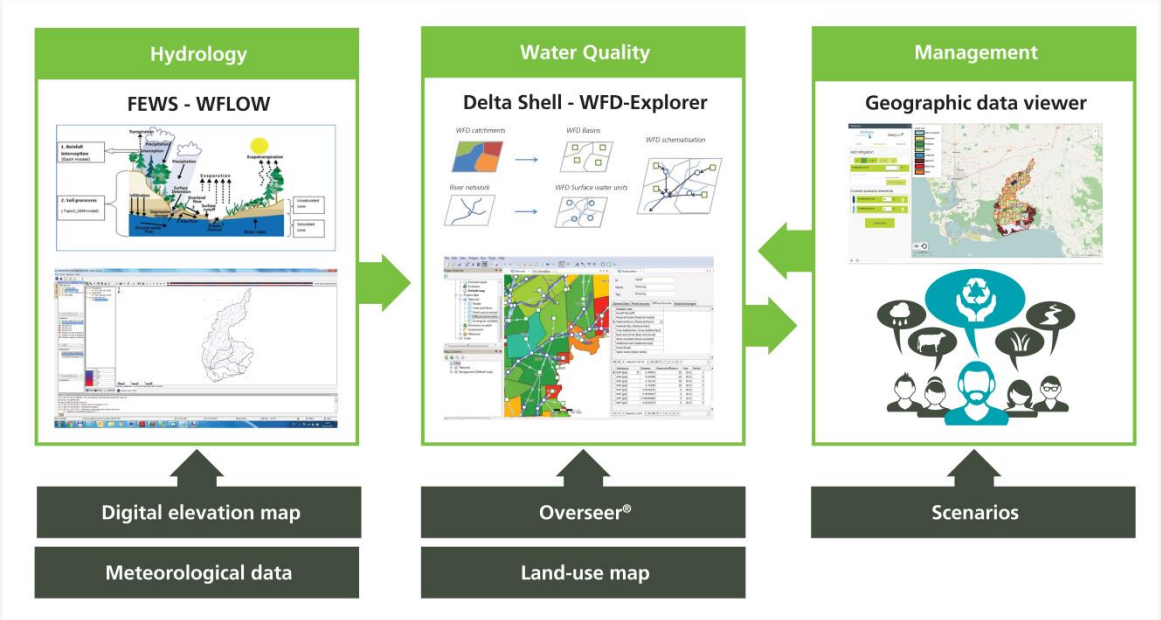

Figure 2.1 Schematic overview of the complete modelling framework including coupling between the WFLOW model, WFD Explorer model and Delta Data Viewer.

2.3 WFLOW hydrological model

WFLOW is a process-based distributed hydrological model developed by Deltares (Appendix A). Distributed hydrological models are grid-cell based and take into account the spatial variability of model input (e.g. meteorology, terrain, soils). Conceptually WFLOW is based on the TOPOG_SBM model concept (Vertressy and Elsenbeer, 1999). Hydrological processes are simulated at the spatial scale of model elements, which in the case of WFLOW are cells on a square grid. The model is programmed in a dynamic GIS environment based on PCRaster (Burrough et al., 2005), a dynamic programming language especially developed for spatial grid computations. Key inputs to the model include measured precipitation and potential evapotranspiration data.

WFLOW incorporates the most important processes of the hydrological cycle as schematized in Figure 2.2.

Different components of the cycle are modelled through a combination of sub-models nested in the model code, including:

1. Rainfall interception schematized by the Gash model (Gash, 1980; 1995).
2. Channel and overland flow modelled with the kinematic wave model.

3. Soil processes schematized by the HBV-96 model (Bergström, 1995). Alternatively, soil processes can be modelled with the TOPOG_SBM model concept (Vertressy and Elsenbeer, 1999).
4. Unsaturated zone.
5. Saturated zone.

WFLOW solves the governing equations for surface and subsurface flow routines using a finite difference scheme. The equations are solved in time for each grid cell, providing continuous simulated values for the hydrological state variables (e.g. runoff volumes, saturation) for each cell. Channel flow processes are simulated using the kinematic wave model. Model output can be visualized as a sequence of spatial maps (gridded raster data) of hydrological variables. For selected locations across the catchment, time series of hydrological variables such as discharge or soil saturation can be generated.

WFLOW has been developed to simulate surface and shallow sub-surface flow paths. Deeper, regional groundwater flows are not modelled explicitly but can instead be represented in the overall model framework as specific or point source discharges.

A detailed description of the WFLOW model is provided in Appendix A.

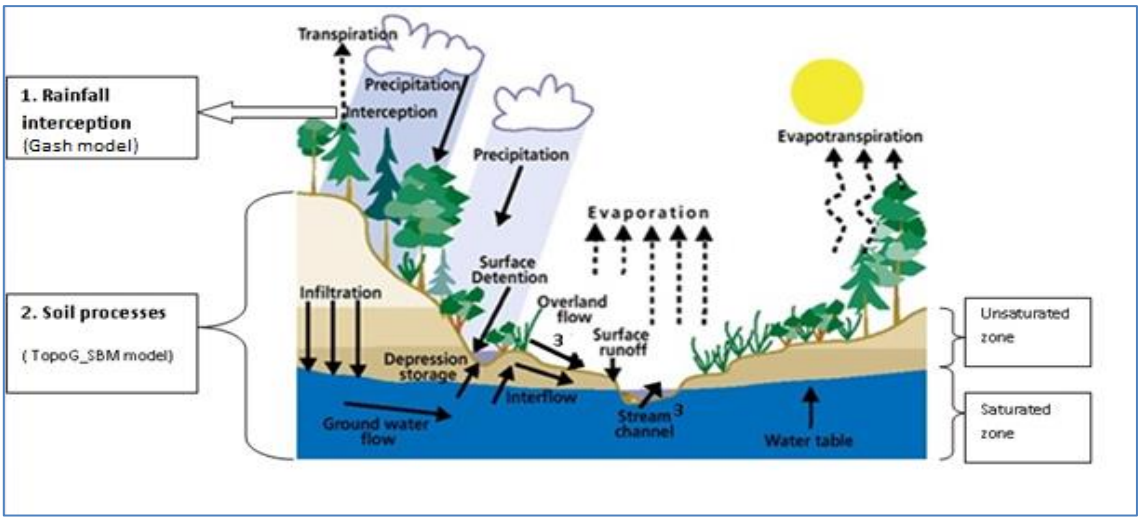

Figure 2.2 The basic components of the hydrological cycle represented in the WFLOW model.

2.4 FEWS platform environment

WFLOW was applied in combination with Delft-FEWS as the model does not have a user-interface, making it difficult to run and analyse model results or demonstrate output to end users in an interactive way. In this approach Delft-FEWS acts as the WFLOW user-interface as well as a data management system for importing and retrieving model inputs and outputs.

Delft-FEWS is an open software environment utilized for the application of various modelling tools built around a central database (Werner et al, 2013). Delft-FEWS offers the benefit of tools related to data handling, including modules for importing and exporting data, validating and interpolating data (both temporally and spatially) and transforming data (aggregation, disaggregation and transformation).

Delft-FEWS is an open system that allows a wide range of models to be used in tandem. This concept is supported by the provision of a General Adapter module, which allows

communication to external modules using an open, XML based, published interface. The XML published interface in combination with the General Adapter effectively enables “plugging-in” of any module to Delft-FEWS. A module adapter is typically required to convert the published interface files to the native module data formats.

Delft-FEWS is shown schematically in Figure 2.3. The WFLOW model is linked to FEWS following the same approach as all other models linked to FEWS:

1. Forcing data is imported into FEWS, in this case measured precipitation and potential evapotranspiration as required for the hydrological model;
2. Data is exported to the WFLOW model in a defined format (Published Interface - PI). For the WFLOW model the defined format is PCRaster “map”-files;
3. Model runs are complete using the native format of the model code;
4. Data is imported from the model in the same defined format (PI).

More background information about Delft-FEWS can be found on the Deltares wiki site (http://publicwiki.deltares.nl/display/FEWSDOC/Home). Running WFLOW in Delft-FEWS is described in Appendix B.

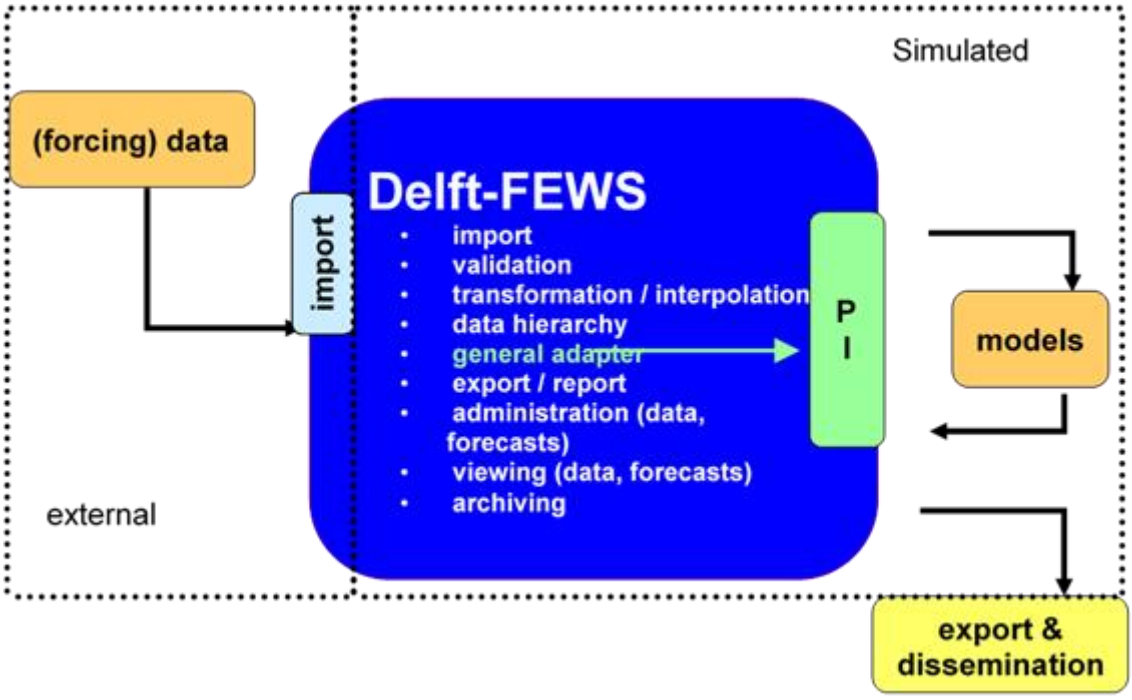

Figure 2.3 Conceptual architecture of Delft-FEWS.

2.5 WFD Explorer model

WFD Explorer is a lumped, steady state model developed to support catchment water quality management (Deltares, 2006). The model was initially developed in response to modelling requirements for the Water Framework Directive (WFD) in the European Union. The WFD requires water managers to improve the chemical and ecological status of degraded water bodies. The chemical and ecological status of a water body is defined by so-called ecological quality ratios (EQRs). The EQR includes metrics based on concentrations of total nitrogen, total phosphorus, chlorophyll-a, and species composition and/or abundance of phytoplankton, macro fauna, macrophytes and fish.

To improve the chemical and ecological status of water bodies, water managers define sets of mitigation strategies. However, it is often not clear to what extent the strategies identified will improve the EQR of a water body. As mitigation measures are expensive, having prior insights on the likely effectiveness and cost efficiency of different mitigation scenarios is extremely helpful as part of the catchment management planning process. The WFD Explorer has been developed to support water managers in making decisions on what measures should be implemented to improve the chemical and ecological functioning of a water body. The WFD-Explorer is also a useful communication tool to assist stakeholders with identifying different management options and outcomes in an interactive way.

The WFD Explorer consists of a water mass balance, a substance mass balance, an ecological module and a mitigation module (including a cost module) (Figure 2.4). In short, the WFD Explorer works as follows: the water balance constructs a water flow through a network of water bodies, for example ditches, streams and lakes. The water mass balance is used as input for the substance mass balance and transports the substances throughout the hydrological network. From this, nutrient concentrations are generated. These are used together with the characteristics of the water body (e.g., sheet piling, weirs) as input for the ecological module.

To preform scenario analyses in the WFD Explorer model mitigations can be added. These mitigations can express their influence on any substance or ecological level. The WFD Explorer generates output in the form of tables and maps. These outputs contain information on substance concentrations and chemical and ecological EQRs.

In this study only the water mass balance and substance mass balance of the WFD Explorer are used.

2.5.1 WFD Explorer model set up tool

The Waituna catchment model has been set up manually. However, because the Hauraki Plains catchment is significantly larger than the Waituna catchment, an automated model set up tool has been developed (Figure 2.5). A tutorial to this Tool is provided in Appendix 0. Both the Waituna and the Hauraki Plains catchment model have been setup by the process described in Figure 2.6. All land uses and point sources are derived to a single spatial location (WFD Basin). The hydraulic schematisation (WFD Surface water units and WFD Links) of the model is derived from the river network. Point sources will be attached to one single nearest spatial location on the hydraulic schematisation, instead of land uses which will as a diffuse source be connected to multiple nearest spatial locations on the hydraulic schematisation. All together this composes the WFD Schematisation.

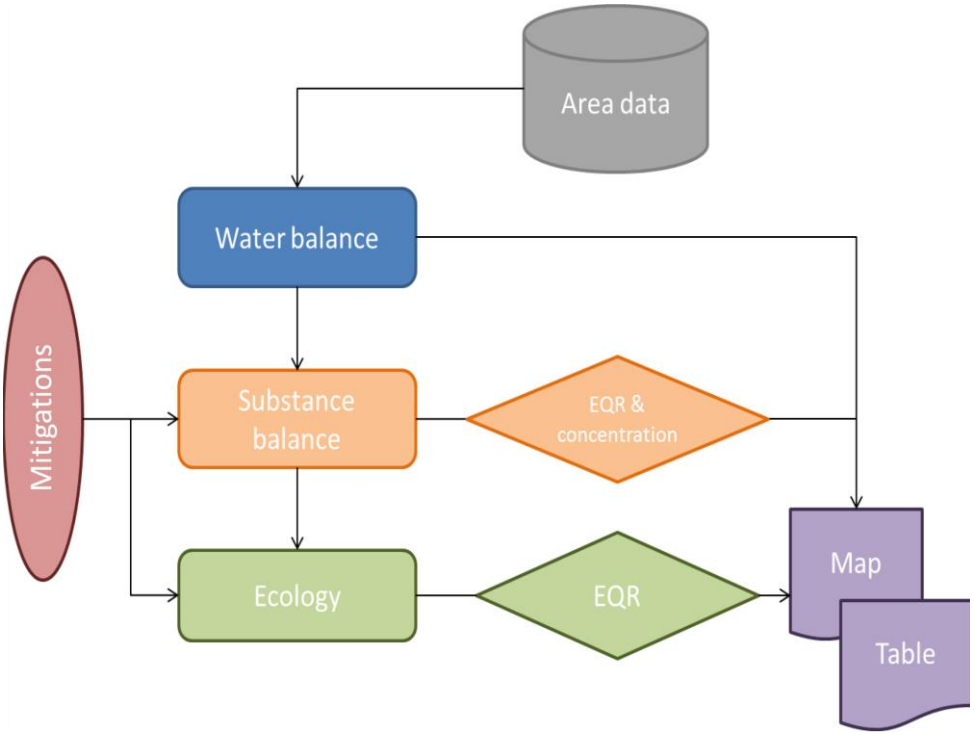

Figure 2.4 Flow chart of operations in the WFD Explorer.

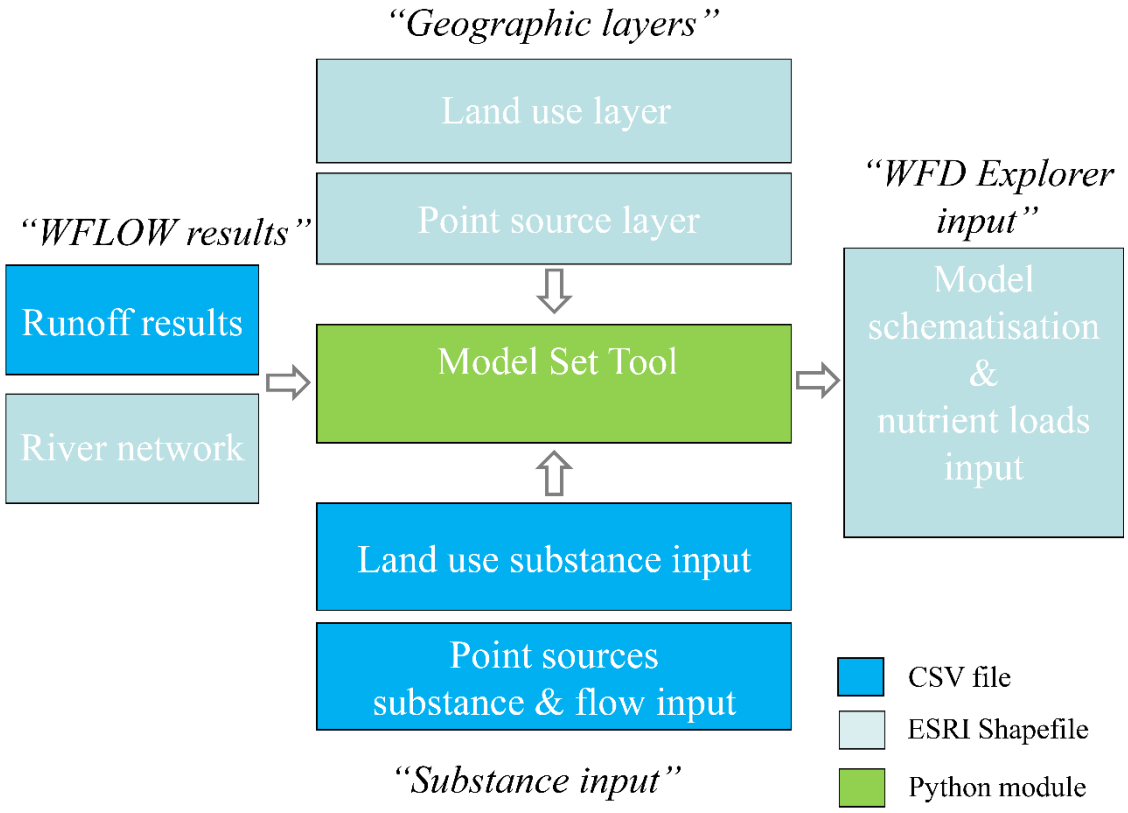

Figure 2.5 Schematic overview of the Model Setup Tool used to setup the input files for the WFD Explorer model.

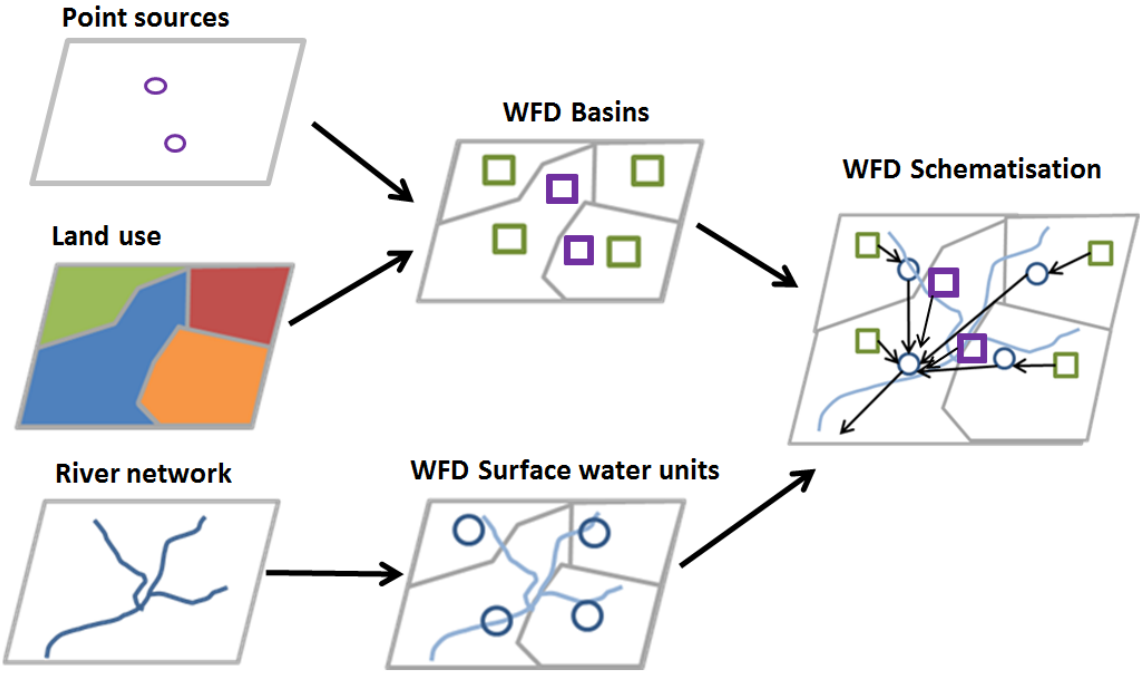

Figure 2.6 WFD Explorer model schematisation as applied to the Waituna Lagoon and Hauraki Plains model.

2.6 Delta Data Viewer

The Delta Data Viewer (DDV), developed by Deltares, is a smart geographic data viewer which can be tailored for any data application. The DDV can work with multiple geographic file formats (e.g., KML/KMZ, WPS/WMS, GeoJSON, SHP, TMS) and provides multiple interactive functions (e.g., drawing of polygons, lines and points; server file browser; accessing attribute files of data layers; view capturing). DDV applications can be hosted on a webserver, making them accessible by internet via different browsers (e.g. Internet Explorer, Chrome, Firefox) and on different platforms (e.g., PC, tablets, smart phones). The applications work through touch screen and with mouse-driven actions.

With the help of TKI matching generated by the Waituna and Hauraki projects, Deltares has developed a DDV application specific for WFD Explorer model applications. This DDV application permits users to view spatial catchment information to make policy decisions (e.g. land-use, soil type and farm locations); generate and inspect output for mitigation scenarios. Due to the smart aspect of the DDV and the WFD Explorer, the application requires a short calculation time (±5 seconds depending on the model application) which makes it suitable for interactive stakeholder discussions).

2.7 Final model workflows

The final model workflows for the complete framework as applied to the Hauraki case study can be summarised as follows:

Delft-FEWS:

1. Catchment hydrology is computed with WFLOW for the unsaturated zone and the river network.
2. The WFLOW model is fed by static data (e.g. a Digital Elevation Model, land-use parameters and soil parameters) and dynamic (hydro-meteorological forcing) data.
3. The WFLOW output is generated and manually transferred to WFD Explorer.

WFD-Explorer:

1. The WFD Explorer model setup tool converts the WFLOW output data to the WFD Explorer format, including spatial and time aggregation and conversion of the load sources to WFD Explorer format, enables prescribing of load attenuation and the seasonal distribution.
2. The WFD Explorer interface imports data from the model setup tool, combines the individual farm loads with loads from other land-use types and point sources, and calculates nutrient concentrations for the schematized parts of the river network.
3. Within the WFD Explorer different emission scenarios are defined and calculated, either by varying the load input files or manipulation of the loads related to specific farms, land-use, soil type or geographical location of the farms.
4. The model validation tool and post processing scripts combine measured and computed values for nutrient concentrations and loads, generate maps with loads per farm or per hectare, and present overviews with the contribution of the flows from the different sub-catchments to the Hauraki Gulf.

DDV:

1. The Delta Data Viewer application (DDV) is a graphical representation of the WFD Explorer model and enables users to perform catchment based calculations. The DDV enables the user to explore important spatial characteristics of the catchment (e.g., land use, soil types, surface water) and to select property boundaries (individually or grouped) to specify mitigations.
2. When mitigations have been specified and the DDV application was commanded to perform a calculation, the DDV application sends the mitigation information to the calculation server. This server starts a WFD Explorer calculation to determine the effect of the mitigations and return post processed results back to the DDV application.
3. The DDV application receives the results from the calculation server and projects these results spatially to the user.

3 Analysis of flows and loads based on existing monitoring data

3.1 Introduction

Prior to set up of the detailed modelling approach (Chapters 4 and 5), total catchment flow discharge, N and P loads were first estimated based on existing literature and a detailed analyses of available hydrological and water quality monitoring data. The Hauraki Plains Catchment area has been subject of several water quality studies by the Waikato Regional Council (Vant, 2011, 2012), NIWA (Toenepi stream catchment, Wilcock et al., 2014) and Lincoln Agritech (groundwater attenuation rates, Stenger et al., 2014).

As a first step total N and P loads were generated for the catchment based on a similar approach as applied by Vant (2011) and Vant (2014), which estimated total load based on flow and water quality measurements at the catchment scale. Discharge values for point sources used in this study were derived directly from Vant (2011) and Vant (2014), whereas representative flow stations for ungauged water quality stations were derived from Jenkins & Vant (2007).

The approach used in Vant (2011 & 2014) represents a spreadsheet calculation to determine mean annual load based on monthly measurements collected by Waikato Regional Council (WRC). The current modelling study extends this approach by capturing the relationship between flows, land-use and nutrient load in more detail using a statistical modelling approach to provide a more temporally and spatially refined estimate of loading.

Stephens (2015) evaluated different methods for quantifying river loads using the Hauraki Plains Catchment as a test case. This work is used as a comparison between the modelled loads and calculated loads in Section 0.

3.2 Data availability and approach

There are 18 WRC water quality measurement stations in the Hauraki Plains catchment, including stations located at Coxhead Rd and Mangawhero Stm in the Waitakaruru (Figure 3.1). For each station the following water quality parameters are measured:

- Concentrations of:
    - Dissolved Oxygen (DO)
    - Dissolved reactive phosphorus (DRP)
    - Ammonium (NH4)
    - Total Kjeldahl Nitrogen (TKN)
    - Total Phosphorus (TP)
    - Nitrate/Nitrite (NNN)
    - E. Coli bacteria (E.coli)
    - F. Coli bacteria (F.coli)
- Dissolved oxygen percentage (%DO),
- pH

- Water temperature (Temp)
- Turbidity (Turb_Misc)

All water quality stations are monitored on a monthly time interval. The flow gauges measure on a 5-minute interval.

In this study the Kauaeranga River catchment (containing the water quality station Smiths Cableway) was not analysed or represented in the model framework as this catchment consists mostly of indigenous forest and presumably has a negligible influence on the nitrogen and phosphorus loading compared to the rest of the study area (e.g., Stephens [2015] demonstrated <1% of combined Hauraki Rivers TN or TP load is attributed to the Kauaeranga River catchment).

Across the 17 remaining stations, only 8 possess a regularly monitored flow gauge (e.g., Kiwitahi, Paeroa-Tahuna Rd Br, Landsdowne Rd Br, Mellon Rd, Okauia, Te Aroha, Queens Head and Karangahake). The stations at Te Aroha and Karangahake are managed by NIWA, whereas the rest of the stations are managed by WRC. All water quality monitoring stations without a flow gauge have been linked to a flow gauge in a corresponding catchment with a similar rainfall regime (Jenkins & Vant, 2008). The 8 water quality stations with flow gauge were used for the data analyses. The data available for these stations overlap for the years 2005 to 2013. These stations have also been used for calibrating and validating the WFD Explorer model (Chapter 5). For calibration of the WFLOW model the Pinedale flow station was added (Chapter 4).

To quantify nutrient loads associated with different land-uses a spatial land-use layer was developed. Vant (2011) also used a catchment scale land-use layer, derived from Jenkins & Vant (2008). This layer is based on the Land Cover Database (LCDB) Version 2 in combination with Agribase Version 2011. In this study more detailed classes have been used (Section 5.2).

Vant (2011) determined average flows and mass flows for the 8 water quality stations for the period 2000 – 2009.

*Table 3.1 Average flows and loads of total nitrogen and total phosphorus for the years 2000 – 2009 as derived in Vant (2011). * Note that the concentration – and thus the mass flow – of TP at this site fell markedly during the decade (2006-09 was 70% lower than 2000 – 05).*

Catchment	Station	Flow (m^3/s)	Total nitrogen (t/yr)	Total phosphorus (t/yr)
Waihou	Okauia	26.6	1246	89
	Te Aroha	37.2	1581	125
Ohinemuri	Queens Head	5.0	265	8
	Karangahake	11.1	299	9
Waitoa	Landsdowne Rd Br	1.4	123	6
	Mellon Rd Rec	4.8	535	58*
Piako	Kiwitahi	1.7	212	7
	Paeroa-Tahuna Rd Br	6.9	775	55

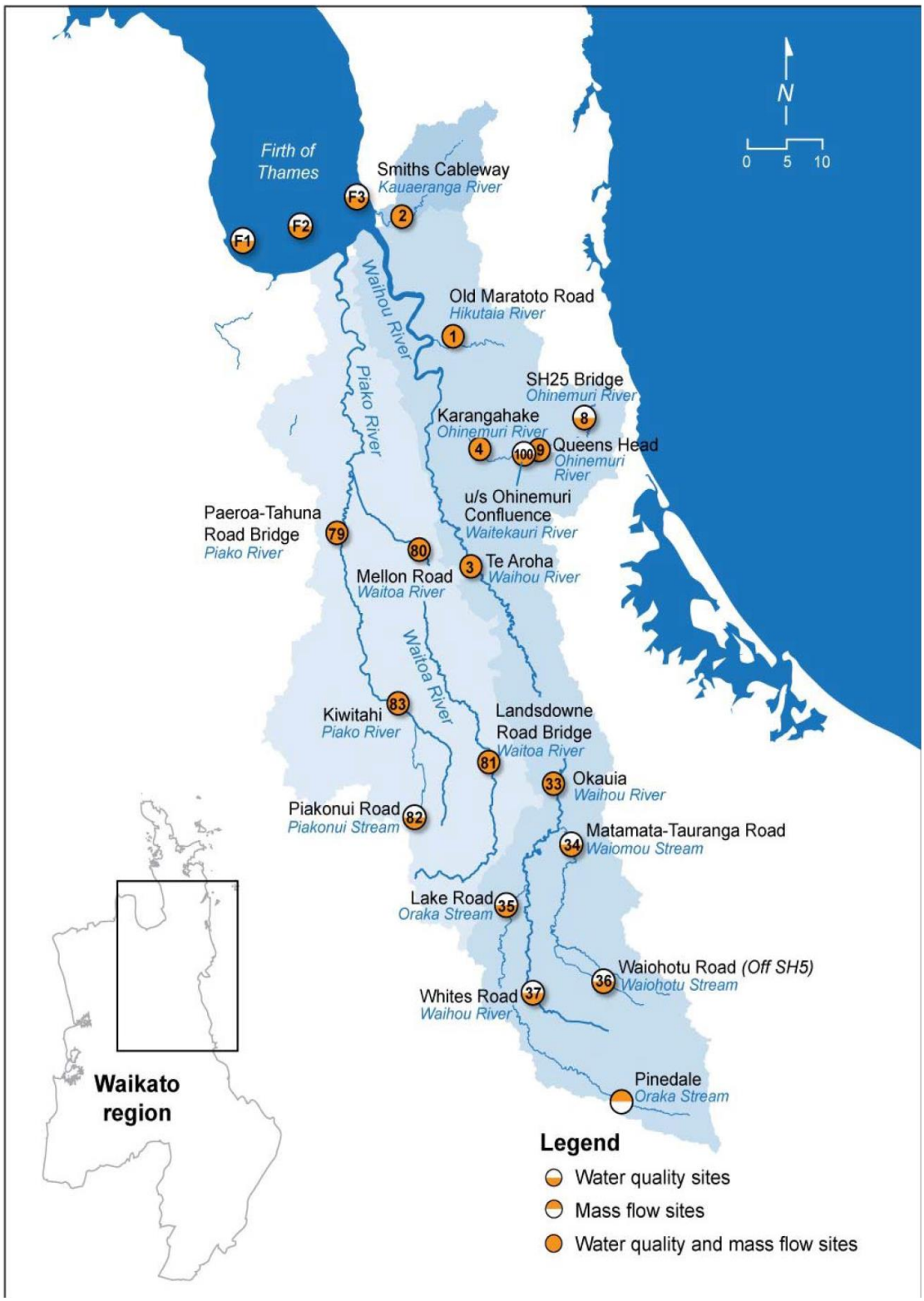

Figure 3.1 Location of the measurement stations in the Hauraki Plains Catchment (Vant, 2011).

3.3 Flow analysis

Flow data were normalised using the Normal Quantile Transformation. A One-way ANOVA statistical analysis was performed to determine if there were any significant differences between years for flow. The results indicate clear inter-annual variability in flow over the time series analysed (for 2005-2013; $p<0.05$ at all 8 stations). Posthoc Tukey tests were used to determine which years differed. Unusually there was little similarity in inter-annual variation to flow between stations in the same sub-catchments (see Appendix D.1 and Table 3.2).

Despite dissimilar inter-annual patterns of change to flow, the effect of climate (rainfall and evapotranspiration) does influence at the catchment-scale. For instance, the year 2008 stands out with a large range in flow measurements in all sub-catchments except for the Ohinemuri River. Also 2013 stands out with a large range in flow in the Piako and Waitoa sub-catchments. This indicates that even though the flow pattern among flow gauges is statistically dissimilar, some spatially broad patterns are apparent and likely driven by climatic influences.

Table 3.2 Comparison of the flow between years per station in the Piako and Waihou catchment. The flow data has been normalised using the Normal Quantile Transformation. A One-way ANOVA was performed to determine if there are significant differences between years within the station. Posthoc Tukey test were used to determine which years differed. The stations have been labelled A for the upstream station and B for the downstream station within the sub-catchment (e.g., Waihou : A = Okauia, B = Te Ahora; Ohinemuri : A = Queens Head, B = Karangahake; Piako : A = Kiwitahi, B = Paeroa-Tahuna Rd Br; Waitoa : A = Landsdowne Rd (Wahoroa Ctrl), B = Mellon Rd Rec).

Catchment	***Sub-catchment***	***Station***	***One - Way ANOVA***	***Posthoc Tukey test***								
			P- value	*2005*	*2006*	*2007*	*2008*	*2009*	*2010*	*2011*	*2012*	*2013*
Waihou	Waihou	A	<0.05	a	a	bc	b	b	c	a	a	b
		B	<0.05	be	ab	ac	c	ac	ac	d	e	c
	Ohinemuri	A	<0.05	ab	abcd	abc	abc	acd	b	e	de	bc
		B	<0.05	ac	ab	ab	ab	ac	b	d	cd	ac
Piako	Piako	A	<0.05	ad	ab	c	cd	acd	ab	b	ad	e
		B	<0.05	ab	a	b	b	a	ac	c	ac	d
	Waitoa	A	<0.05	ab	ab	c	cd	ad	ad	b	ab	c
		B	<0.05	a	ab	c	c	a	a	b	a	c

3.4 Concentration analysis

Total nitrogen and total phosphorus data, as described in Section 3.3, was normalised using the Normal Quantile Transformation method and subsequently analysed using the “One-way ANOVA” and “Posthoc Tukey test”.

Table 3.3 Comparison of the total nitrogen (TN) between years per station in the Piako and Waihou catchment. The TN data has been normalised using the Normal Quantile Transformation. A One-way ANOVA was preformed to determine if there are significant differences between years within the station. Posthoc Tukey test were used to determine which years differed. The stations have been labelled A for the upstream station and B for the downstream station within the sub-catchment (e.g., Waihou : A = Okauia, B = Te Ahora; Ohinemuri : A = Queens Head, B = Karangahake; Piako : A = Kiwitahi, B = Paeroa-Tahuna Rd Br; Waitoa : A = Landsdowne Rd (Wahoroa Ctrl), B = Mellon Rd Rec).

Catchment	***Sub-catchment***	***Station***	***One - Way ANOVA***	***Posthoc Tukey test***								
			P- value	*2005*	*2006*	*2007*	*2008*	*2009*	*2010*	*2011*	*2012*	*2013*
Waihou	Waihou	A	0.39	-	-	-	-	-	-	-	-	-
		B	0.18	-	-	-	-	-	-	-	-	-
	Ohinemuri	A	< 0.05	a	a	a	a	a	a	a	a	a
		B	0.25	-	-	-	-	-	-	-	-	-
Piako	Piako	A	0.64	-	-	-	-	-	-	-	-	-
		B	0.40	-	-	-	-	-	-	-	-	-
	Waitoa	A	0.43	-	-	-	-	-	-	-	-	-
		B	0.87	-	-	-	-	-	-	-	-	-

Table 3.4 Comparison of the total phosphorus (TP) between years per station in the Piako and Waihou catchment. The TP data has been normalised using the Normal Quantile Transformation. A One-way ANOVA was preformed to determine if there are significant differences between years within the station. Posthoc Tukey test were used to determine which years differed. The stations have been labelled A for the upstream station and B for the downstream station within the sub-catchment (e.g., Waihou: A = Okauia, B = Te Ahora; Ohinemuri: A = Queens Head, B = Karangahake; Piako: A = Kiwitahi, B = Paeroa-Tahuna Rd Br; Waitoa: A = Landsdowne Rd (Wahoroa Ctrl), B = Mellon Rd Rec).

Catchment	***Sub-catchment***	***Station***	***One - Way ANOVA***	***Posthoc Tukey test***								
			P- value	*2005*	*2006*	*2007*	*2008*	*2009*	*2010*	*2011*	*2012*	*2013*
Waihou	Waihou	A	< 0.05	a	a	a	a	a	ab	a	a	b
		B	< 0.05	ab	a	ab	ab	ab	b	ab	ab	ab
	Ohinemuri	A	< 0.05	a	abc	ab	ac	bc	bc	ab	abc	c
		B	0.43	-	-	-	-	-	-	-	-	-
Piako	Piako	A	< 0.05	a	a	ab	ab	ab	ab	a	ab	b
		B	0.32	-	-	-	-	-	-	-	-	-
	Waitoa	A	< 0.05	ab	a	ab	ab	ab	b	ab	ab	ab
		B	< 0.05	c	a	a	ab	b	ab	ab	ab	ab

Concentrations of TP exhibited significant inter-annual variation at most stations (all but Karangahake and Paeroa-Tahuna Rd Br) whereas TN concentration only varied significantly between years at Queens Head (see Appendix D.2, Table 3.3 and Table 3.4). More detailed trend analysis in Stephens (2015) has demonstrated marked, significant trends for decreasing TP concentrations across all Hauraki Rivers with the exception of the Kauaeranga, over a similar period (2004-2013; -13.1%/yr to -1.0%/yr, $p < 0.05$). Likewise, Stephens (2015) also demonstrated more mixed changes in TN – only 5 of the 17 stations experience a significant decrease and 2 headwater stations (Okauia and Queens Head) in the Waihou experience a significant increase ($p<0.05$).

When TP and TN concentrations are correlated against corresponding flow measurements varying relationships are observed (see Appendix D.3). Overall TN concentration tends to increase with flow. In the Waihou River TP concentration tends to linearly increase with flow upstream (measurement station Okauia), but stays relatively uniform with flow at Te Aroha. In the Ohinemuri River there seems to be a threshold at high flows where TP concentration increases exponentially. In both the Piako and Waitoa Rivers the relation seems linear, but with clear exceptions.

Taken together, these findings give an overview of the detail and complexity required for the Hauraki Plains catchment water quality model. The model must handle marked upstream-downstream, inter-river and inter-annual variations in flow and concentration of nutrients, including long-term trends that will alter the nature of any flow and load-driven relationships to instream concentration.

3.5 Load analysis

This section is separated in two parts. First, the measured loads were quantified and analysed (Appendix D.4). The yearly loads were then modelled from flow-load regressive relationships, using the module RLoadest in R (R Core Team, 2016). RLoadest can compute daily, monthly or annual loads from flow, season and/or year predictors (Lorenz, 2014).

The loads, that have been generated at a daily resolution, are scaled up to periodic loads. For the Hauraki Plains catchment water quality model, a year is build-up of 12 periods (30 days per period, with the last period containing 35-36 days). By aggregating the daily RLoadest loads in the same way these can be used to validate the Hauraki Plains water quality model (Chapter 5).

3.5.1 RLoadest

To determine the daily load per station the R package RLoadest (Lorenz, 2014) was used. RLoadest has been developed by USGS on an earlier version (USGS, 2004) and has been widely used for estimating constituent loads in streams and rivers (water.usgs.gov/software/loudest/apps, visited: 23-08-2016). It assists the user in developing optimal rating curves for flow and loading from up to nine regression model structures. Those structures vary in both the linear form of explanatory variables (e.g., x, x^2) as well as the choice of explanatory variables (e.g., flow, decimal time like date, season and year). RLoadest uses adjusted maximum likelihood estimation, maximum likelihood estimate or least absolute deviation to provide uncertainty measures about predicted mean load (e.g., standard errors and 95 percent confidence intervals). The user specifies the regressive approach – here the adjusted maximum likelihood estimation was used based on its recommendation by Runkel et al (2004).

For the stations Kiwitahi, Paeroa-Tahuna Rd Br, Landsdowne Rd Br, Mellon Rd Rec, Te Aroha, Queens Head and Karangahake, an RLoadest model was setup for both TN and TP load. The TN and TP load models tend to differ from each other, but overall have a good prediction capacity. The prediction capacity has been determined statistically using the corrected Akaike information criterion (AICc), r-squared (R^2), model bias (Bias) and Nash-Sutcliff statistic (NS).

It is important to note that the RLoadest output is only based on the observed daily flow and water quality measurements provided by monthly sampling and is validated against those same measurements. It is therefore possible that the model accurately predicts these individual measurements, but under or overestimates load peaks as the measurements are skewed towards certain conditions (i.e., only lower flows due to only sampling in dry weather).

Table 3.6 and Table 3.7 demonstrate generally good performance (e.g., $R^2 > 0.8$, bias < 25%, NS > 0.5), permitting widespread application in the Hauraki Plains catchment. However, prediction of TP at Mellon Rd Rec and Queens Head is moderate-to-poor given, high model bias and lowered NS, suggesting greater caution is needed about calibration of later modelled loading at those stations. Both are subject to point-source contributions (Vant, 2011), which have likely altered the nature of flow-load relationships on a stochastic basis and outside the range of continuous variables available to RLoadest (e.g., decimal time and flow).

Table 3.5 RLoadest predictions for the yearly load at the downstream measurement stations.

Year	**Total Nitrogen Load** Modelled by WFD-Explorer per station (ton / yr)				**Total Phosphorus Load** Modelled by WFD-Explorer per station (ton / yr)			
	Te Aroha	Karangahake	Paeroa-Tahuna Rd br	Mellon Rd Rec	Te Aroha	Karangahake	Paeroa-Tahuna Rd Br	Mellon Rd Rec
2008	2313	393	1552	1269	181	26	93	84
2009	2154	211	1102	950	172	26	78	68
2010	2208	338	1237	1114	170	26	77	71
2011	2141	245	1092	982	170	26	78	73
2012	2424	330	1092	997	191	26	74	68
2013	2014	190	829	853	158	26	54	61

Table 3.6 Model selection and performance for RLoadest total nitrogen (TN) load calculation from flow. The prediction capacity of the chosen model has been determined using the corrected Akaike information criterion (AICc), r-squared (R^2), model bias (Bias) and Nash-Sutcliff statistic (NS).

River	Stations	Model	AICc	R^2 (%)	Bias (%)	NS
Paiko	Kiwitahi	8	58.12	97.64	5.37	0.94
	Paeroa-Tahuna Rd Br	9	54.81	96.82	6.25	0.88
Waitoa	Landsdowne Rd Br	8	-73.35	98.39	2.20	0.94
	Mellon Rd Rec	6	-15.36	96.81	0.24	0.97
Waihou	Okauia	6	-236.10	95.34	-0.06	0.96
	Te Aroha	4	-164.30	94.12	-0.13	0.89
Karangahake	Queens Head	9	173.20	88.66	7.50	0.89
	Karangahake	4	110.50	92.60	3.62	0.87

Table 3.7 Model selection and performance for RLoadest total phosphorus (TP) load calculation from flow. The prediction capacity of the chosen model has been determined using the corrected Akaike information criterion (AICc), r-squared (R^2), model bias (Bias) and Nash-Sutcliff statistic (NS).

River	Stations	Model	AICc	R^2 (%)	Bias (%)	NS
Paiko	Kiwitahi	8	114.70	92.03	-8.24	0.71
	Paeroa-Tahuna Rd Br	8	69.42	92.42	-1.10	0.94
Waitoa	Landsdowne Rd Br	8	153.30	92.55	-6.74	0.69
	Mellon Rd Rec	9	190.40	85.96	14.83	0.36
Waihou	Okauia	9	-62.68	85.29	0.04	0.95
	Te Aroha	7	-29.59	83.20	-0.87	0.70
Karangahake	Queens Head	9	237.00	83.44	-29.13	0.46
	Karangahake	9	119.60	91.84	-12.11	0.87

3.5.2 Periodic loading distribution

The RLoadest results include daily load distribution from daily flow estimates, for the period 2005-2013, at 8 stations. As RLoadest uses flow as the main input parameter, it is not surprising that the load calculations closely follow patterns in flow even after transformation by the Normal Quantile Transformation (DairyNZ, unpublished work). The generally good loading regression performance has ensured that earlier significant differences in flow between years are also reproduced in the RLoadest results.

As the Hauraki Plains catchment water quality model will operate with artificial months the daily RLoadest results are aggregated to 12 periods per year (30 days per period, with the last period containing 35-36 days).

Total Nitrogen

When the daily loads calculated by RLoadest are summed for each period and spread out over the years, the results differ strongly between stations (see Appendix D.5).

The highest annual N load is observed at measurement station Te Aroha (46% of total, see Appendix D.5). The largest loads at this site were generally well-distributed over the year, although a large load is distributed in summer (Periods 12, 1 and 2, approximately December to February). However, at Paeroa-Tahuna Rd Br, the largest loads per period are reported for Period 8 (August). This might be because high flow events haven't been captured by the monitoring and are thereby over predicted by the RLoadest model (see Appendix D.4).

Total Phosphorus

Phosphorus loads also vary strongly between stations (see Appendix D.5). At measurement station Te Aroha the load is evenly distributed over the year. Depending on the time of year, the highest loads were observed at either Karangahake or Te Aroha (see Appendix D.5). At Karangahake the highest load is primarily observed in Periods 7 and 8 (Jul and Aug), corresponding to the periods with highest flow. This corresponds well to the relationship between phosphorus load and flow as shown in the graphs in Appendix D. However, in this case the RLoadest model most likely over-predicts the load as not enough water quality measurements have been performed during extreme flow events in the Ohinemuri River.

4 Catchment hydrological model set up, calibration and results

4.1 Introduction

Spatially distributed estimates of rainfall-runoff from the Waitakaruru, Piako and Waihou River catchments to the Hauraki Gulf were simulated using the WFLOW hydrological model. Model output, including water balances generated for each individual farm title in the catchment, were subsequently used as input to the water quality model to simulate river water quality and total catchment contaminant loads (see Chapter 5).

This chapter describes the setup of the WFLOW hydrological model, including data inputs and model parameterisation, calibration and results.

4.2 Model inputs

The input data required to execute a simulation in WFLOW can be separated into *i)* static data concerning the description of the land surface, and *ii)* dynamic data, represented by the hydro-meteorological forcing of the model. Table 4.1 reports the key data requirements for the model and their respective sources as used for the current application.

Table 4.1 WFLOW data requirements and data sources within the Hauraki Plains catchment.

Static Data	
Digital Elevation Model (DEM) on 5x5 meter grid resolution	• A 25m resolution DEM from Landcare Research NZ Ltd, processed from 'spot heights' 20m contours, lake shorelines and the coastline. • WRC 5m resolution DEM derived from LIDAR
Soil physical parameters	FSL New Zealand soil classification by Landcare Research NZ Ltd, supplied as a shape-file
Land-use	WRC Catchment Land Use for Environmental Sustainability (CLUES) Land-use type layer 2012
Dynamic data	
Precipitation and potential evaporation	NIWA daily precipitation records (13 stations), WRC daily precipitation station records (7 stations), WRC hourly precipitation stations (4 stations), covering the period 2008-2015
Discharge data (for calibration and validation)	Continuous flow monitoring data from WRC. 5 min. interval data at Karangahake, Queens Head, Kiwitahi, Paeroa-Tahuna Road Bridge, Te Aroha, Mellon Road and Wahaoa stations. 10-minute data interval at Pinedale station.

4.2.1 Digital elevation data and river network

Digital elevation models were available from Landcare Research NZ Ltd (Landcare Research, 2007) (25m resolution) and Waikato Regional Council (WRC) (5m resolution). It is assumed that both source elevation models (see Table 4.1) are referenced to mean sea level (msl). Only the vertical date of the LIDAR is specified to be at Moturiki 1953 and Tarararu 1952 (Hannah, 2001). In Figure 4.1 a merge of both DEMs is shown for which (1) the 25m DEM was resampled to 5m and (2) the resampled DEM was used to fill in no-data areas of the 5m LIDAR.

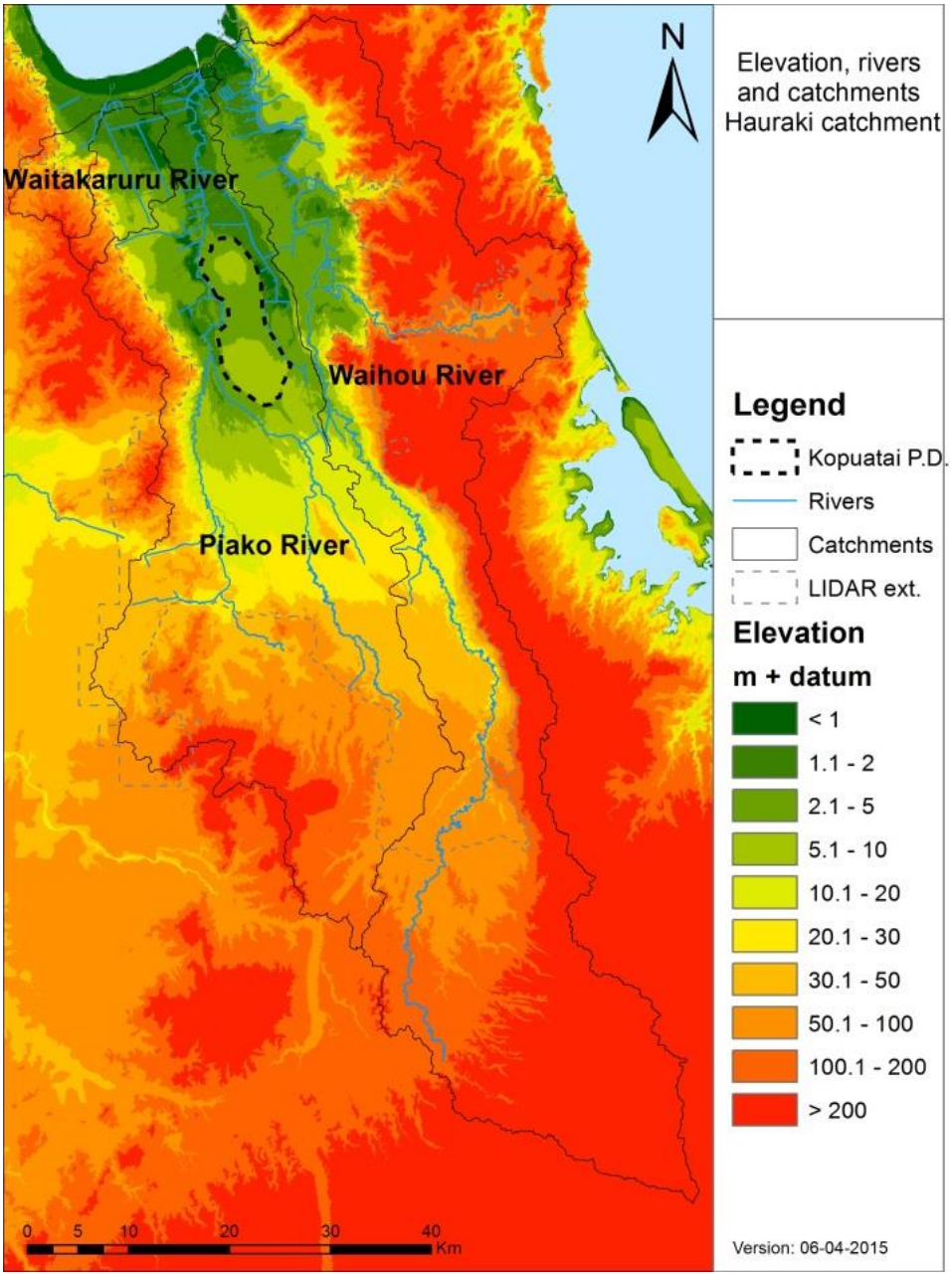

Figure 4.1 Catchment elevation and river network.

River and drainage vector layers were available via the Topo50 maps (see: http://www.linz.govt.nz/land/maps/linz-topographic-maps/topo50-maps, accessed on 09-04-2015). These layers vary in accuracy and completeness for the location of the river and drainage network and were therefore edited to meet the requirements for WFLOW (see Figure 4.1). In particular, areas below 10m + msl are generally very flat (<5º) and drained by extensive networks of small and larger artificial surface drains, crossing the Piako and Waihou River catchment boundaries. Although the primary flow direction follows the natural elevation under flood conditions, flow direction can be reversed due to the operation of flood control structures such as pumps and gates.

These structures are found at many locations along Piako and Waihou Rivers, of which some examples are shown in Figure 4.2. Information regarding the operational control of these flow structures were not available and this aspect was therefore excluded from the current model application.

Note: In WFLOW, river-flow is assumed to be governed by friction and gravity forces (using the kinematic wave), where only one route to the catchment outlet is available, following topography. For a more accurate description of hydraulic processes within a river, including backwater effects and structures, hydrodynamic packages solving full shallow water (Saint Venant) and structure equations should be used.

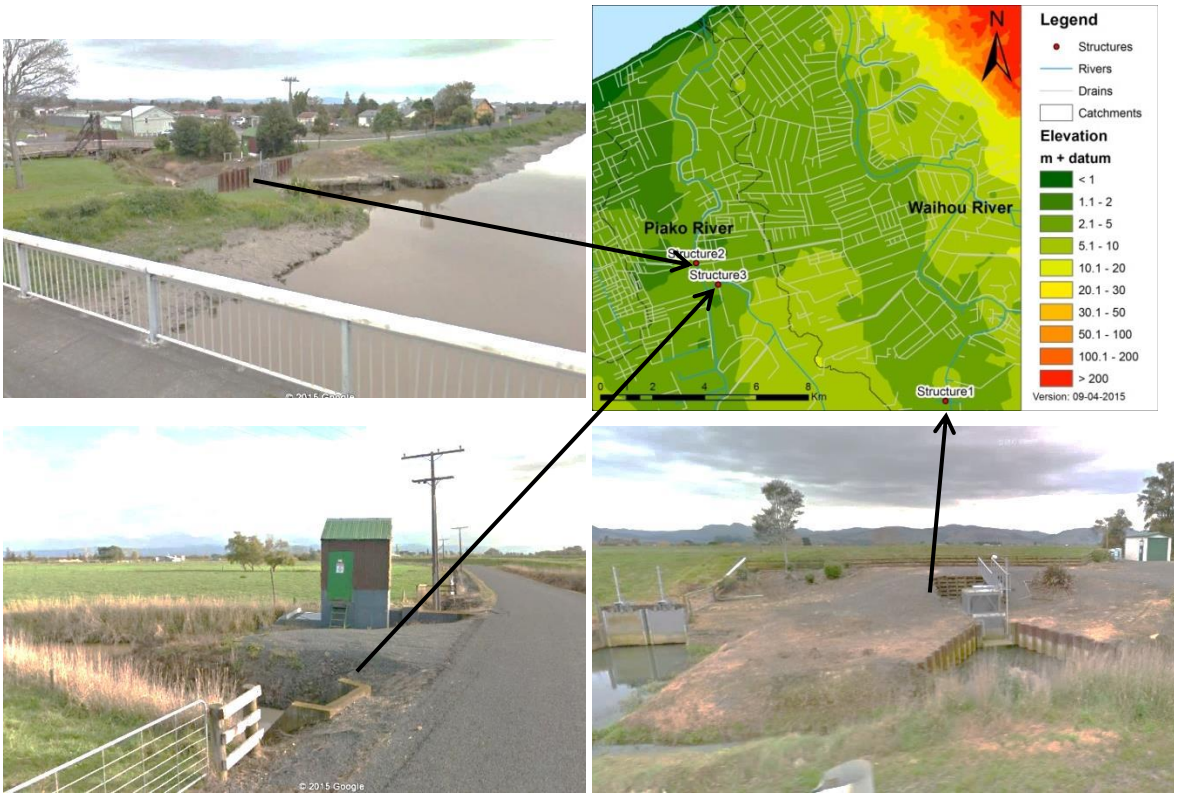

Figure 4.2 Structures and drains at Piako and Waihou rivers (Google Streetview, 2015).

4.2.2 Land-use type

Land-use type was classified based on information provided by WRC, which includes a modified Catchment Land Use for Environmental Sustainability (CLUES) catchment model land-use type layer (2012) of the full catchment. The Hauraki Plains catchment is predominantly made up of livestock farms (75%), forest (18%) and wetland (5%). In Table 4.2 the reclassification from CLUES land-use types to the standard WFLOW land-use classes is shown. Six classes are differentiated, including a unique class representing the Kopuatai peat dome.

This information was subsequently used to derive WFD Explorer land-use classes on a finer spatial scale than what is available in CLUES. The WFLOW model was setup without regard for individual farm property boundaries as this will have little effect on meteorology or model parameterisation. However, the scale of CLUES data set is appropriate for the WFLOW model as shown by the model performance.
An overview of the land-use classification of the Hauraki catchment is given in Figure 4.3.

Table 4.2 Reclassification of CLUES to WFLOW and their comparison to the WFD Explorer land-use classes.

CLUES class	WFLOW class		WFD Explorer class
APPLES	1	Horticulture	Horticulture
DAIRY	2	Livestock	Dairy & Dairy Support
DEER	2	Livestock	Other farming
GRAPES	1	Horticulture	Horticulture
KIWIFRUIT	1	Horticulture	Horticulture
MAIZE	1	Horticulture	Horticulture
NAT_FOR	3	Forest	Indigenous Forest
ONIONS	1	Horticulture	Horticulture
OTHER	4	Other (peat dome)	Wetland
OTHER_ANIM	2	Livestock	Other farming
PLANT_FOR	3	Forest	Exotic forest
POTATOES	1	Horticulture	Horticulture
SBHIGH	2	Livestock	Drystock
SBHILL	2	Livestock	Drystock
SBINTEN	2	Livestock	Drystock
SCRUB	5	Grassland	Shrubland
TUSSOCK	5	Grassland	Other landscape
UNGR_PAST	5	Grassland	Other landscape
URBAN	6	Urban	Res / Com

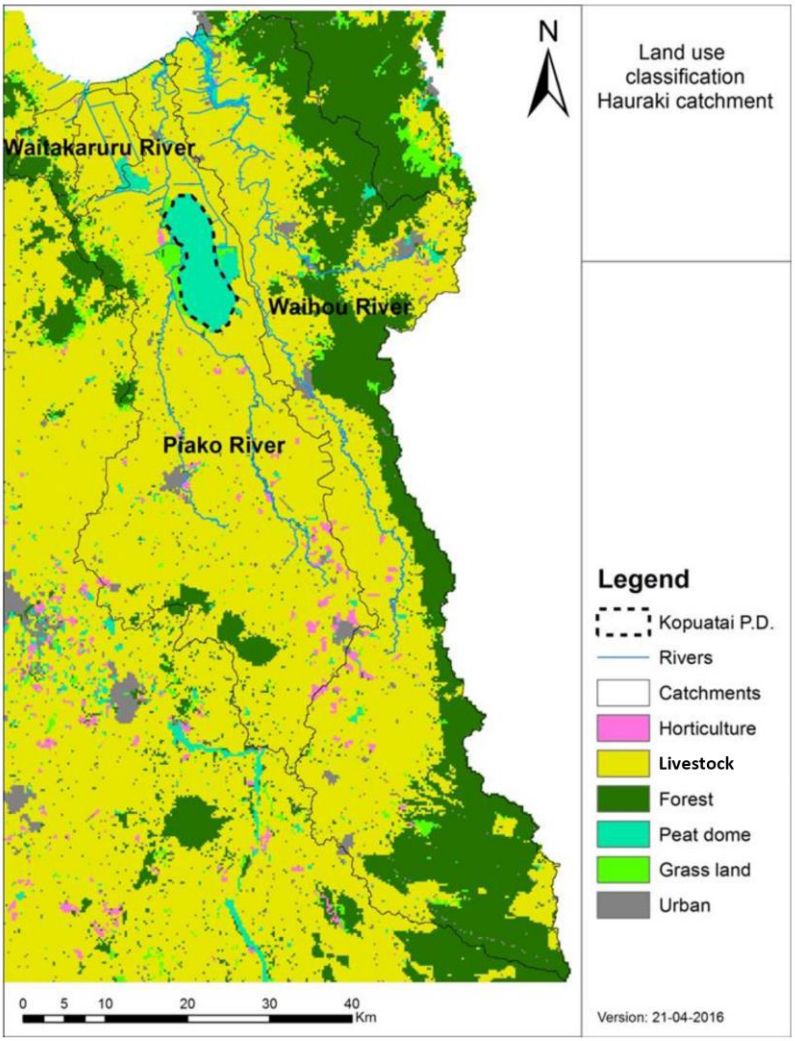

Figure 4.3 Land-use classification for WFLOW.

4.2.3 Soil type classification

Catchment soil type was derived from the FSL New Zealand soil classification scheme from Landcare Research (https://soils.landcareresearch.co.nz/describing-soils/nzsc/soil-order/, visited: 26 – 08 - 2016). Soil data was supplied as an ESRI shape-file, which was reclassified into the classes (1) Brown, (2) Gley, (3) Melanic, (4) Organic and (5) Ultic soils prior to rasterization (Fig. 3.4):

- Brown Soils: Brown soils have a moderate base saturation and are not waterlogged in winter. Brown soils occur in the Eastern part of the Waihou river catchment as well as at some places in the Piako River.
- Gley soils: Together with Organic soils, represent the original extent of New Zealand wetlands, which have been greatly restricted in historic area by drainage. Groundwater tables are high, the rooting depth for plants is shallow and the bulk density of the soil is high. Waterlogging occurs in winter and spring. In the Hauraki plains, Gley soils occur in low-lying and coastal areas.
- Melanic soils: Naturally fertile soils, which occur in association with lime-rich rocks or dark volcanic rocks. In the Hauraki plains catchment, Melanic soils occur upstream of low-lying areas, where Organic and Gley soils are found.

- Organic soils: Serving as giant sponges in the landscape, these soils can hold up to 20 times their weight in water. Organic Soils are formed from the partially decomposed remains of wetland plants (peat) or forest litter. Some mineral material may be present but the soil is dominated by organic matter. In Hauraki, the Kopuatai Peat Dome is a large area with undrained organic soil. More West, in parts of the Piako and Waitakaruru catchments, drained organic soils are also found.
- Ultic soils: Strongly weathered soils that have a well-structured, clay enriched subsoil horizon. This soil type occurs in clay or sandy clay material derived by strong alteration of quartz-rich rocks over long periods of time. Clayey subsoils with slow permeability are characteristic. Upstream in the Piako River Ultic soils occur.

Figure 4.4 shows the soil classification map, used as static input for WFLOW.

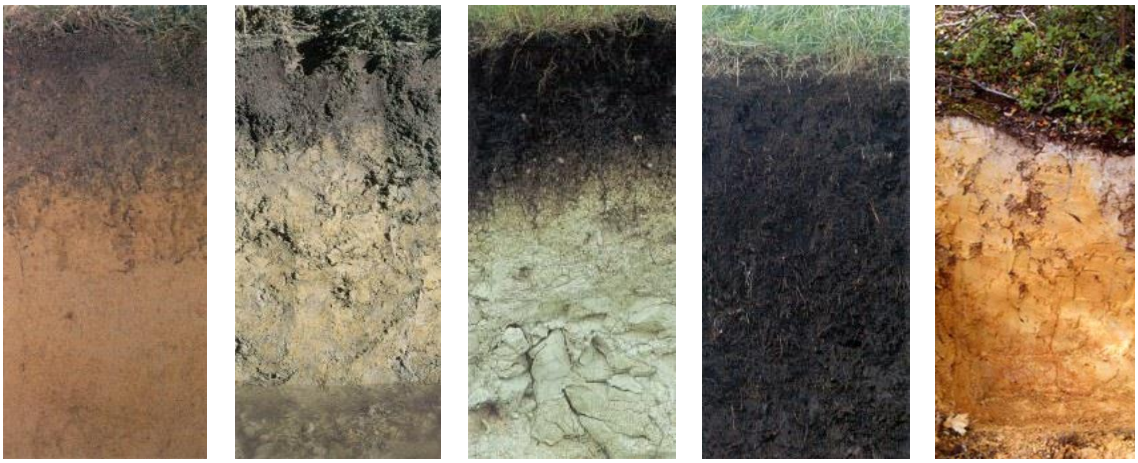

Figure 4.4 From left to right (1) Brown soils, (2) Gley soils, (3) Melanic soils, (4) organic soils and (5) Ultic soils (source and images: http://soils.landcareresearch.co.nz/).

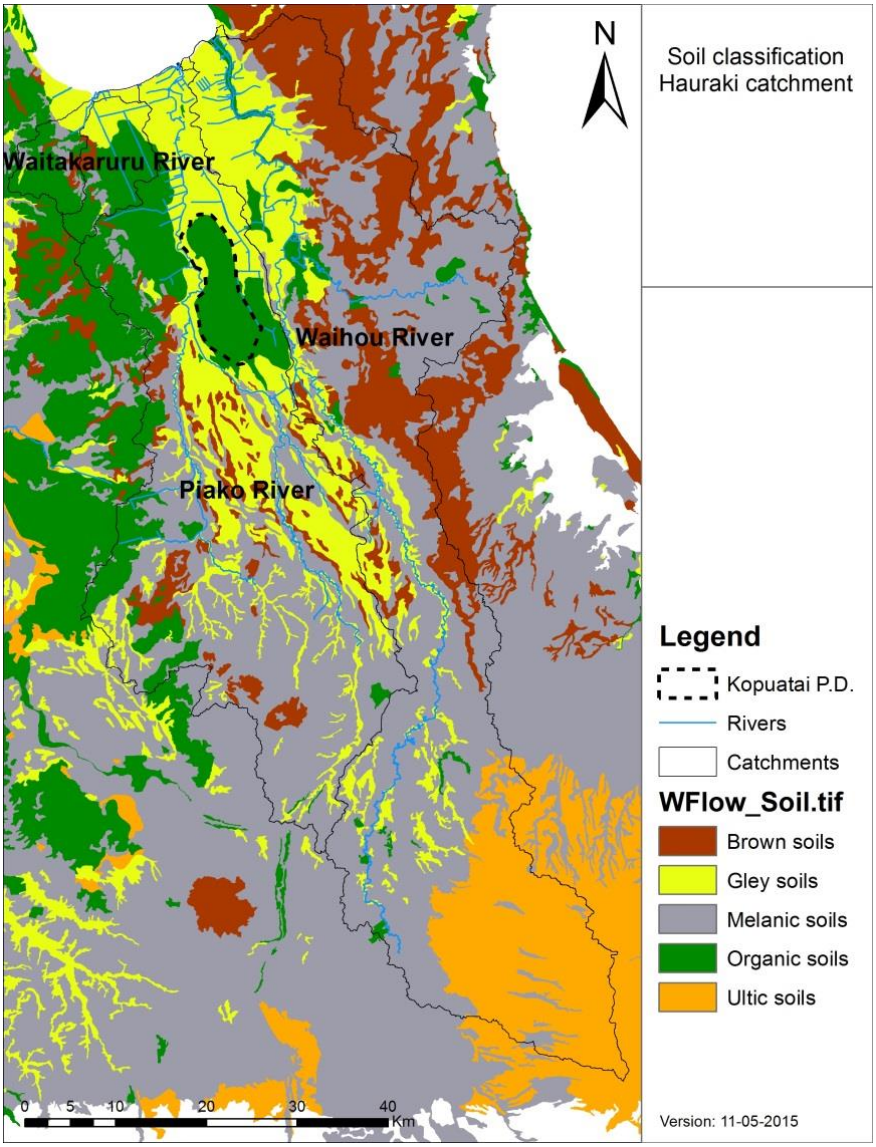

Figure 4.5 Soil classification for WFLOW.

4.2.4 Precipitation and potential evapotranspiration

4.2.4.1. Available data

Precipitation data were obtained from NIWA (13 stations) and WRC (11 stations) for a range of locations across the catchment (Figure 4.6). Evapotranspiration data were obtained for 11 of these stations.

Table 4.3 Precipitation (P) and Evapotranspiration (ET) data, observed on daily (d) or hourly (h) time intervals as derived from NIWA and Waikato Regional Council (WRC).

Source	CODE	Site Name	Latitude	Longitude	P(h)	P(d)	ET(d)
NIWA	17030	Matamata Hinuera	-37.877	175.735		X	
NIWA	23908	Toenepi	-37.7196	175.5853		X	X
NIWA	1547	Paeroa	-37.373	175.684		X	X
NIWA	38619	Firth of Thames	-37.2152	175.4503		X	X
NIWA	38671	Mamaku	-38.066	176.062		X	
NIWA	37656	Lake Karapiro	-37.925	175.54		X	X
NIWA	26645	Holland Road	-37.748	175.367		X	X
NIWA	26117	Hamilton	-37.7757	175.3051		X	X
NIWA	2112	Hamilton Aws	-37.865	175.336		X	
NIWA	12325	Wiri	-36.993	174.87		X	X
NIWA	2006	Pukekohe	-37.2064	174.8638		X	X
NIWA	25162	Whatawhata	-37.7883	175.0691		X	X
NIWA	1962	Auckland Aero	-37.0081	174.7887		X	X
NIWA	1529	Thames 2	-37.1586	175.5514			X
WRC		Old Netherton Rd Rainfall	-37.3405	175.6199		X	
WRC		Hauraki Rd Rainfall	-37.295	175.5979		X	
WRC		Putaruru Leslie Rd Rainfall	-37.2193	175.7971		X	
WRC		Springdale Rainfall	-37.5225	175.5462		X	
WRC		Morrinsville Tahuna Rd Rainfall	-37.5396	175.5049		X	
WRC		Kurere Rainfall	-37.3201	175.6801		X	
WRC		Kaimai Te Poi Rainfall	-37.8793	175.8879		X	
WRC		Maukoro Landing Rd	-37.4295	175.51	X		
WRC		Paeroa WRC	-37.373	175.684	X		
WRC		Matamata Aerodrome	-37.7324	175.7433	X		
WRC		Te Aroha	-37.5466	175.7067	X		

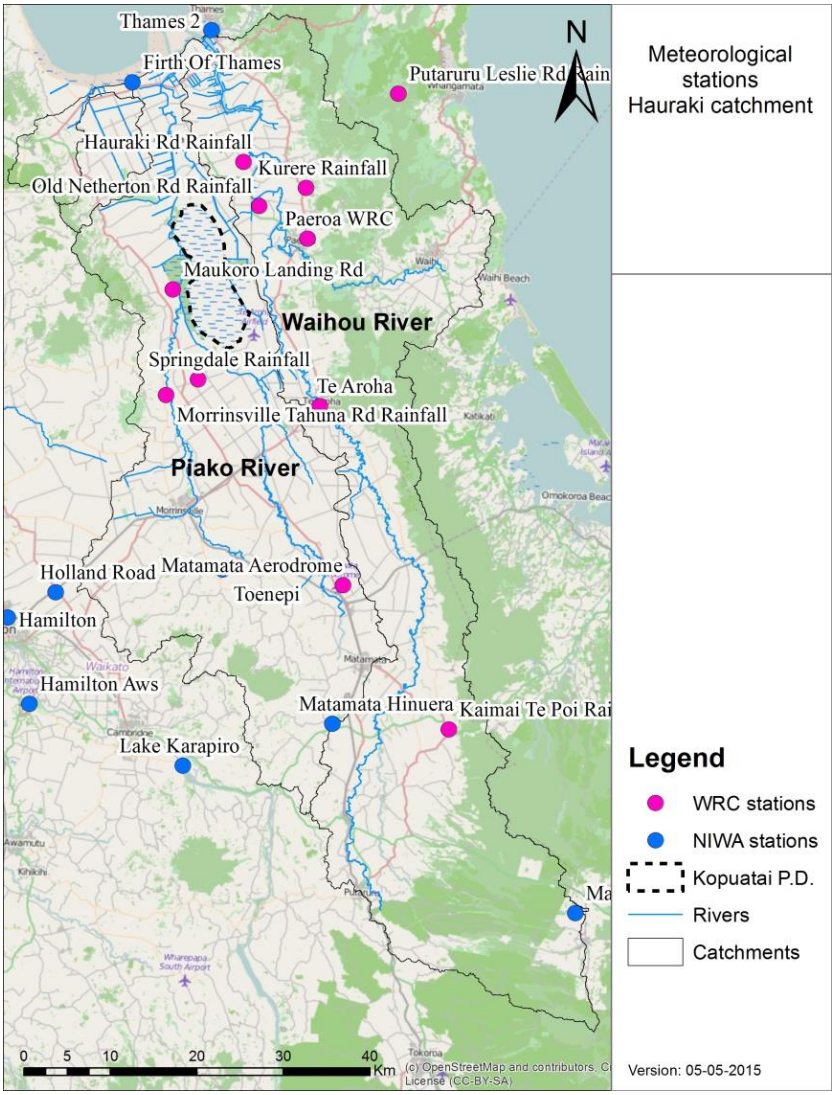

Figure 4.6 Meteorological stations in and around the Hauraki Plains catchment.

4.2.4.1. *Data processing*

FEWS was used to process and interpolate the raw meteorological data from WRC and NIWA to the required format for forcing for the WFLOW model. Station data was converted into gridded model forcing data using the inverse distance weighting (IDW) method. In this approach forcing values for grid cells where data were absent are derived from the distance to nearby stations ($dist_{c,s}$, see eq 4-1) and a relative weight (W_s, see eq 4-2) by which station values are multiplied and summed to the cell forcing value (F_c, see eq 4-3).

$$dist_{c,s} = \sqrt{(c_x - s_x)^2 + (c_y - s_y)^2} \quad \text{eq 4-1}$$

with:

$dist_{c,s}$	*distance between cell and station*
c	*cell*
s	*station*
x	*x-coordinate*
y	*y-coordinate*

$$W_s = \frac{1}{dist_{c,s}^{power}} \quad \text{eq 4-2}$$

with:

W_s	*Relative weight of station*
power	*power on distance between station and cell*

$$F_c = \sum_{s=n}^{n} \frac{F_s \cdot W_s}{\sum_{s=1}^{n} W_s} \quad \text{eq 4-3}$$

with:

F_c	*Forcing-value of cell*
F_s	*Forcing-value of station*
n	*Number of stations*

4.2.5 Natural springs

In the upper Waihou River a significant proportion of base flow is supplied by natural springs (Vant, 2011; Stephens, 2015). Here, groundwater from deeper aquifers enters the surface water system with little variability in flow over time. Exfiltration from deep aquifers is not included in this WFLOW model and therefore in the current model application, natural springs were simulated as a boundary condition using the kinematic wave routine.

The locations of significant natural springs known to be present in the catchment are shown in Figure 4.7 (WRC, unpublished data). There is no routine flow monitoring program in place for these headwater spring systems and data availability is limited to discrete measurements for ten locations (Table 4.4).

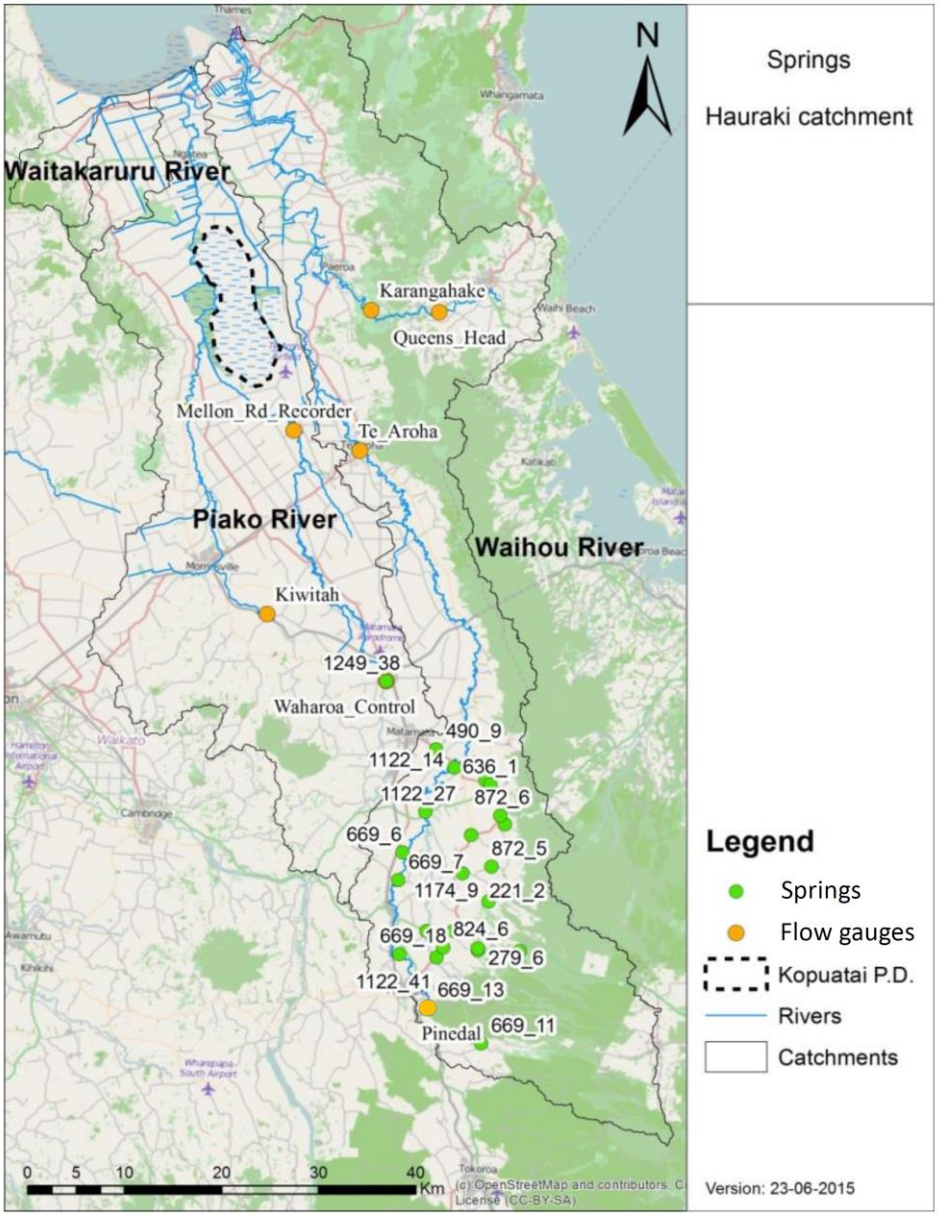

Figure 4.7 Spring sites and considered river gauges.

Flow gauging was carried out at several up and downstream river locations in the upper catchment by WRC in early 2014 to estimate specific discharge between sample locations under dry, base flow conditions (Table 4.5). This specific discharge was assumed to represent mostly groundwater inputs and accordingly was used as a direct input to the hydrological model framework to represent spring flows.

The results of uncalibrated WFLOW model simulations over predicted base flow relative to the measurements at the Te Aroha monitoring location, which is downstream of all known spring inputs to the model. Subsequent calibration suggested a multiplication factor of 0.3 for the spring flow data was needed to represent the monitored base flow at Te Aroha (see Figure 4.8).

Table 4.4 Summary of flow data held for Natural spring discharge for all known significant springs in the catchment (data provided by WRC).

Site name	Sample period	Number of samples	Mean flow (m^3/sec)
Pungapunga Stm @ Spring 2	1982-1989	2	0.0004
Purere Stm @ Spring 3 Jenkins Waterwheel	1980-1984	18	0.3556
Purere Stm @ Spring 4 Wiiliams Prop	1981-1984	18	0.0789
Purere Stm Trib @ Spring 3	1980-1983	4	0.0403
Tui Stm Trib @ Spring Discharge Pipe	1979	1	0.0054
Waihou River @ Spring 6 Dillon Farm	1981	1	0.6070
Blue Bull Stm Trib @ Blue Spring	1988	1	0.0133
Waipare Stm Spring @ Spring2 U/S Water Wheel	1980-1988	18	0.0908
Waihou River @ Blue Spring	2001	0	0.4985
Oraka Special Survey @ Site 5 Spring On Deihl Road	2006	1	0.0155

Table 4.5 Natural spring discharge for all known significant springs in the catchment (data provided by WRC).

Site No	Upstream area [km^2]	Discharge [m^3/s]	Specific runoff [$l/s/km^2$]	X (NZTM2000)	Y (NZTM2000)
1122_14	483.3	13.519	28	1848886	5808042
1122_27	465.7	13.358	28.7	1845891	5803435
1122_29	59.9	5.243	87.5	1846010	5791029
1122_41	43	4.452	103.5	1847029	5788310
1158_1	87.9	4.001	45.5	1848811	5791033
1174_10	72.4	1.71	23.6	1849703	5797037
1174_4	199.4	2.829	14.2	1852089	5806746
1174_6	133.5	2.407	18	1850597	5801041
1174_9	37.1	1.116	30.1	1852408	5794140
1204_5	52.5	1.795	34.2	1851315	5789035
1249_38	122.5	0.138	1.1	1841868	5817036
221_2	34.8	0.482	13.9	1852703	5797742
279_1	16.3	0.175	10.7	1855618	5788942
279_6	21.6	1.077	49.9	1851315	5789236
490_9	51.9	0.681	13.1	1846982	5809940
636_1	16.1	0.213	13.2	1852590	5806247
669_11	103.8	0.589	5.7	1851629	5779331
669_13	129.8	1.802	13.9	1846121	5783025
669_18	206.8	2.042	9.9	1843211	5788624
669_6	252.5	2.614	10.4	1843532	5799203
669_7	242.4	2.612	10.8	1843100	5796327
824_6	7.5	0.748	99.7	1847713	5789330
872_5	25.8	0.264	10.2	1854098	5802147
872_6	25.8	0.264	10.2	1853596	5803047

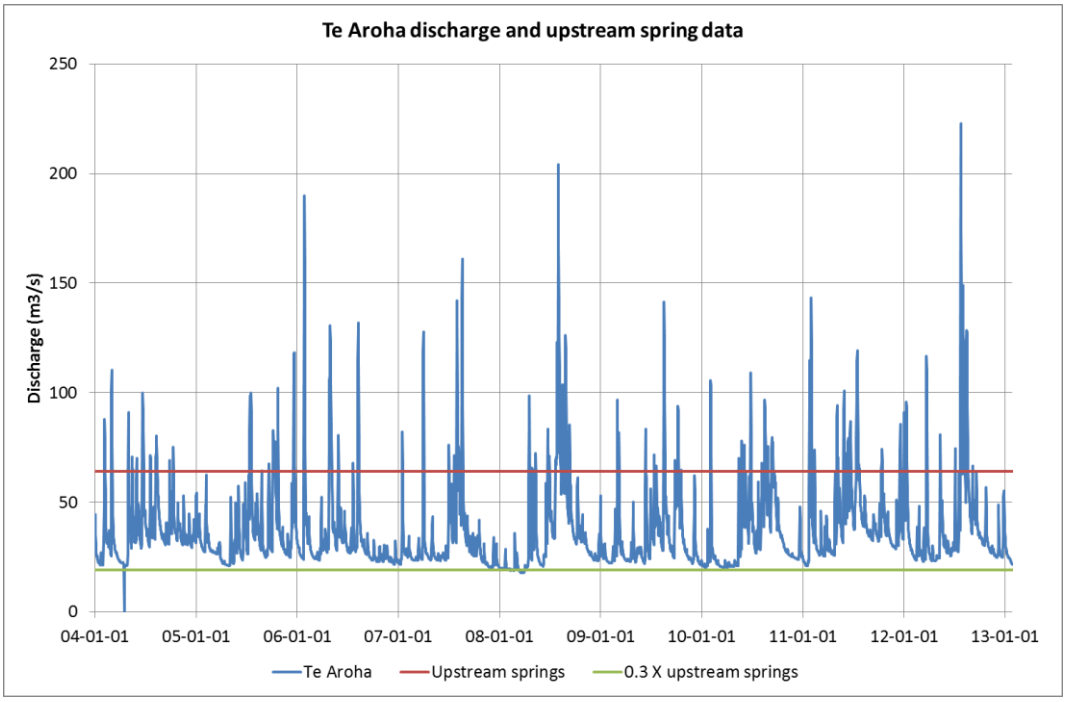

Figure 4.88 Observed discharge at Te Aroha, uncalibrated base flow (upstream springs) and calibrated base flow (0.3x upstream springs) from 04-01-01 till 13-01-01.

4.3 Model parameterisation

4.3.1 Model coefficients

Model coefficients used to prescribe water storage and runoff in the unsaturated and free surface water routines of WFLOW were specified for each land-use type based on default settings and expert judgment. Most parameters were retained as the default model settings across all soil and land-use classes (Table 4.6). The fraction of compacted soil, PathFrac [-] and RootingDepth [mm], where varied for different land-use classes (Table 4.7). Saturated conductivity and FristZoneKsatVer [mm/day] were varied over different soil classes (Table 4.8).

Table 4.6 Model default parameters applied to all soil and land-use classes.

	PathFrac	default value
Canopy Gap Fraction [-]	Fraction of precipitation that is not intercepted by canopy	0.80
EoverR [-]	Ratio of average wet canopy evaporation rate over rainfall rate	0.10
Max Canopy Storage [mm]	Canopy interception storage	1.00
FirstZoneCapacity [mm]	Thickness of the first aquifer	3000.00
FirstZoneMinCapacity [mm]	Minimum Thickness of the first aquifer upstream in the catchment	500.00
InfiltCapSoil [mm/day]	Infiltration capacity on soil	200.00
InfiltCapPath [mm/day]	Infiltration capacity in compacted areas	5.00
M [-]	Calibration parameter; decay of saturated conductivity over depth	100.00
N_river [s/m$^{1/3}$]	Manning friction applied in rivers	0.04
N [s/m$^{1/3}$]	Manning friction applied on overland	0.10
thetaR [-]	Residual water content	0.05
thetaS [-]	saturated water content	0.15

Table 4.7 Land-use-specific model input parameters.

	PathFrac	Rooting Depth [mm]
Horticulture	0.01	300
Livestock	0.01	300
Forest	0.01	4000
Other (peat dome)	0.00	300
Grass land	0.01	300
Urban	0.50	100

Table 4.8 Soil type-specific model input parameters.

	FirstZoneKsatVer [mm/day]
Brown	500
Gley	200
Melanic	100
Organic	1000
Ultic	500

4.3.2 Model spatial and temporal resolution

A daily model computational time step was selected to reflect the temporal resolution of the available meteorological forcing data. The model can be run on a much finer time step (e.g. minutes, but in the absence of more temporally refined input data this would not improve model accuracy.

Two model applications were constructed. A 250m model (linear distance of grid cells) was used for calibration purposes to ensure a fast computation time (+/- 5min per year simulated). As the 250m model is rather coarse, a 25m model was also generated to compute the water budget at farm-level. The computational time of the refined model is considerably larger (+/- 3.5h per year simulated).

4.3.3 Integration into Delft-FEWS

The full procedure (*'workflow'*) to convert imported WRC and NIWA rainfall into the required WFLOW forcing data comprised of the following five steps:

1. Aggregation of hourly WRC precipitation to daily precipitation
2. Merging of the daily aggregated WRC precipitation (1), daily WRC precipitation and NIWA precipitation into daily precipitation stations

3. Interpolation of daily precipitation stations (2) to a grid with a cell length of 1000m using inverse distance weighting (power=3, number of stations(n) = 6)
4. Interpolation of NIWA daily potential evapotranspiration stations to a grid with a cell length of 1000m, using inverse distance weighting (power=3, number of stations(n) = 6)
5. Generation of the model forcing from the gridded precipitation and evapotranspiration time series (3 and 4), to the spatial (25m or 250m, see Section 4.2.1) and temporal (daily timestep) resolution of the model.

4.4 Model calibration

4.4.1 Calibration approach

Continuous flow measurements collected and provided by WRC as part of their regional monitoring program were used for model calibration (see Section 3.3). In Table 4.9 and Figure 4.7, the locations of the available discharge monitoring stations are shown. Monitoring data was available in upstream tributaries of the Paiko and Waihou Rivers only. For all stations, discharge data was provided from 01-01-2005 until 31-12-2014 except for Te Aroha, where the data is available from 02-01-2004 until 31-12-2013.

Table 4.9 Discharge gauge locations.

Location	X	Y	Start	End	River
Te Aroha	1839127	5841042	02-01-2004	31-12-2013	Waihou
Karangahake	1840302	5855651	01-01-2005	31-12-2014	Ohinemuri
Queens Head	1847306	5855463	01-01-2005	31-12-2014	Ohinemuri
Pinedale	1846121	5783025	01-01-2005	31-12-2014	Waihou
Kiwitah	1829552	5824019	01-01-2005	31-12-2014	Piako (small trib.)
Paeroa-Tahuna Rd Br	1821514	5845214	01-01-2005	31-12-2014	Piako
Mellon Rd Recorder	1832321	5843131	01-01-2005	23-12-2014	Waitoa (Piako trib.)
Waharoa Control	1841868	5817036	01-01-2005	31-12-2014	Waitoa (Piako trib.)

Observed precipitation and discharge data overlap for the period 01-01-2008 to 01-01-2015. The model was calibrated over the period 01-01-2011 to 01-01-2015 and validated over the period 01-01-2008 to 01-01-2011. Model performance was optimized by undertaking the following steps:

1. Analysing the performance of the default model.
2. Manual calibration over the period 01-01-2011 to 01-01-2015 until acceptable model runs were obtained.
3. Model validation over the period 01-01-2008 to 01-01-2011 to assess model validation in scenario analysis.

For steps 2 and 3, model performance was assessed by a combination of the Nash-Sutcliffe coefficient (NS, eq 4-4) and relative volume error (RVE, eq 4-5). Both performance functions are combined to derive an objective function (25% NS and 75% RVE), as shown in eq 4-6. The Coefficient of Fit (COF) was optimized to 0.

$$NS = 1 - \frac{\sum(s-o)^2}{\sum(s-\bar{o})^2} \qquad \text{eq 4-4}$$

with:

s	*simulated value*
o	*observed value*
ō	*average of observed series*

$$RVE = \frac{\sum(s-o)}{\sum o} \qquad \text{eq 4-5}$$

$$COF = 1 - (0.75 \cdot (1 - abs(RVE)) + 0.25 \cdot NS) \qquad \text{eq 4-6}$$

Based on the work by Moriasi et al. (2007) for defining the performance of the NS, and Dawson et al.(2006) on the RVE, an arbitrary criteria was created to determine model performance based on the COF (Table 4.10). It should be noted that the RVE analysis is data dependent, with best performance at 0 and worst performance at ±∞.

Table 4.10 Arbitrary model performance criteria based on the COF derived from the NS and RVE. The criteria for NS were taken from Moriasi et al. (2007) and for RVE were arbitrary set based on Dawson et al. (2006).

Performance rating	NS	RVE	COF
Very good	0.75 < X < 1.00	- 0.25 < X < 0.25	0.2500 < X ≤ 0.0000
Good	0.65 < X < 0.75	- 0.5 < X < 0.5	0.4625 < X < 0.2500
Satisfactory	0.50 < X < 0.65	-1 < X < 1	0.8750 < X < 0.4625
Unsatisfactory	0.00 < X < 0.50	-2.5 < X < 2.5	2.1250 < X < 0.8750
Unsuitable	X < 0.00	-∞ < X < ∞	X > 2.1250

4.4.2 Default model performance

The results of model performance for the default, uncalibrated simulation for each discharge monitoring station, using the parameters given in Section 4.3.1 are shown in Table 4.11. At stations with a lower COF, model performance is better.

Model performance varied over the catchment. The model reflects patterns in observed discharge for the Ohinemuri, a lower Waihou tributary, at Karangahake and Queens head, as well as for the Piako River at Kiwitahi (see Figure 4.9) and Paeroa-Tahuna Road Bridge. At the other locations the model preforms worse than the mean of the observed flows (NS < 0). At all gauges an overestimate of peak discharge events is observed under semi-saturated conditions. These conditions occur in the periods April to June in 2013 and 2014.

Table 4.11 Model performance at each discharge monitoring station based on the default parameter settings (2011-2015) and assessed using the Nash-Sutcliff statistic (NS), Relative volume error (RVE) and the derived coefficient of fit (COF). The model performance rating is based on the COF. Note the poor performance of the WFLOW model at Pinedale.

Catchment	Station	NS	RVE	COF	Performance rating
Waihou	Pinedale	-82.99	0.72	21.54	Unsuitable
	Te Aroha	-3.71	0.27	1.38	Unsatisfactory
Ohinemuri	Queens-Head	0.48	-0.41	0.44	Good
	Karangahake	0.57	-0.39	0.40	Good
Waitoa	Waharoa Control	-0.68	0.57	0.85	Satisfactory
	Mellon Rd Recorder	-4.05	0.77	1.84	Unsatisfactory
Piako	Kiwitahi	0.56	0.28	0.32	Good
	Paeroa-Tahuna	0.03	0.30	0.47	Good

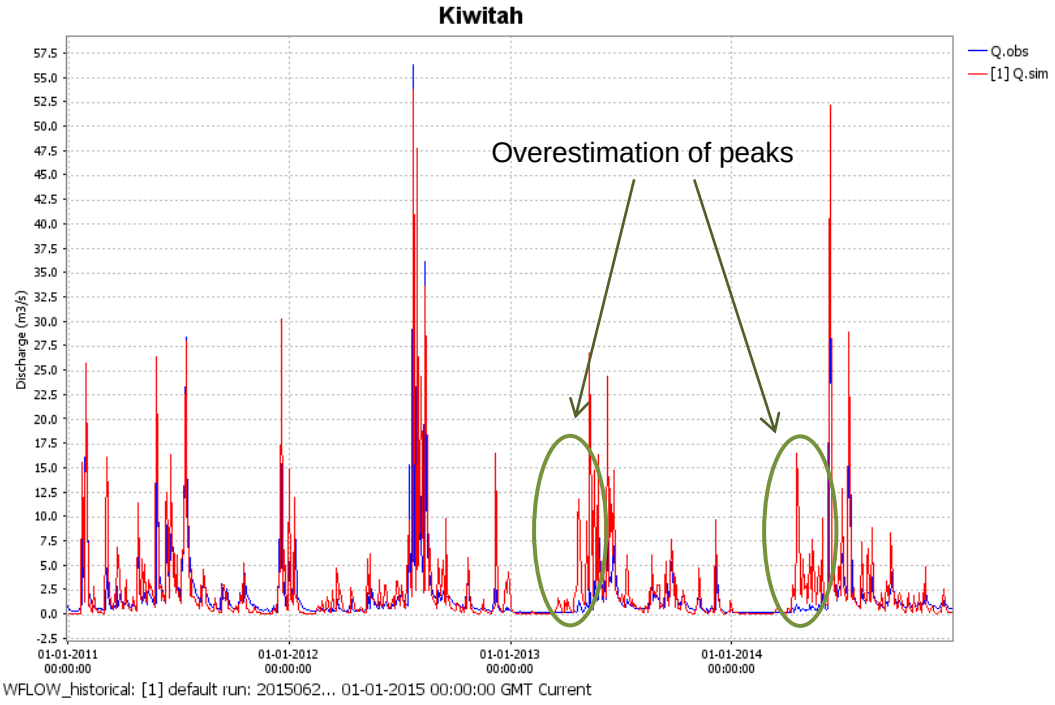

Figure 4.9 Result with default model parameters at Kiwitah (2011-2015).

Uncalibrated model performance for the Waitoa River, the Eastern tributary of the Piako, as well as the Waihou River at Te Aroha is considerably lower. At these locations the model appears to overestimate variability in peak flow. At Pinedale uncalibrated model performance is classified unsuitable, with runoff volumes, especially peak flows, significantly overestimated. Possible explanations for the overestimation of peak flows at all these stations, include:

1. The spatial cover of rainfall gauges is limited in these areas and as a result (peak) rainfall is systematically over-estimated.
2. Model input parameters are not correct, especially for the Waitoa River and the Eastern tributary of the Paiko, where model performance could be considerably improved by applying different model parameters, in particular increasing storage in the first soil layer. This could be updated by improved data on the soil characteristics.
3. Upstream of Pinedale complex interactions with deeper groundwater aquifers is highly likely. In this case, WFLOW may not capture all the important hydrological processes, in particular springs contributing to recharge of deep ground water next to their contribution to overland runoff.

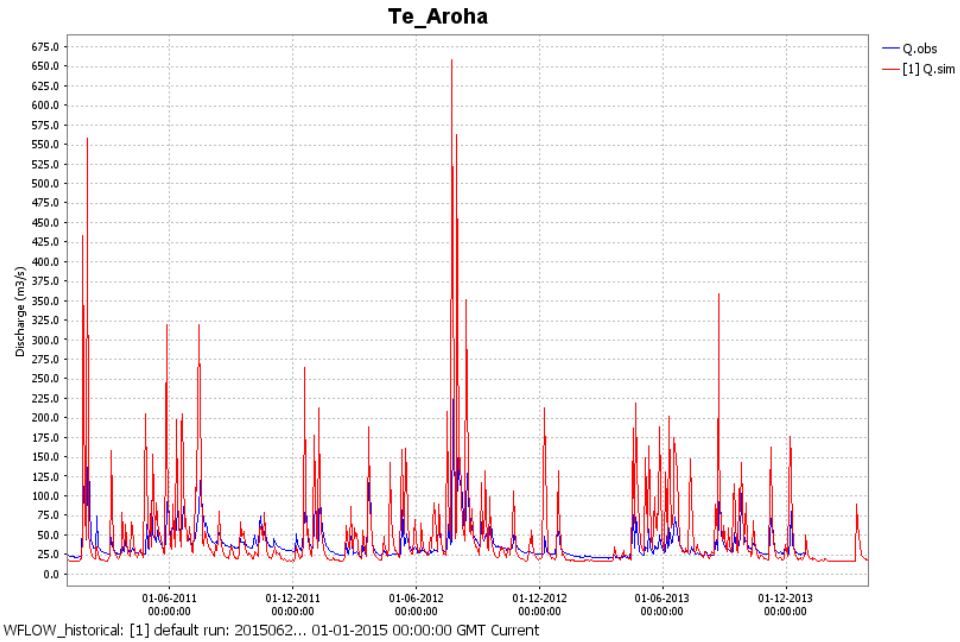

Figure 4.10 Uncalibrated model (Q sim) and observed (Q obs) flow results Te Aroha (2011-2015).

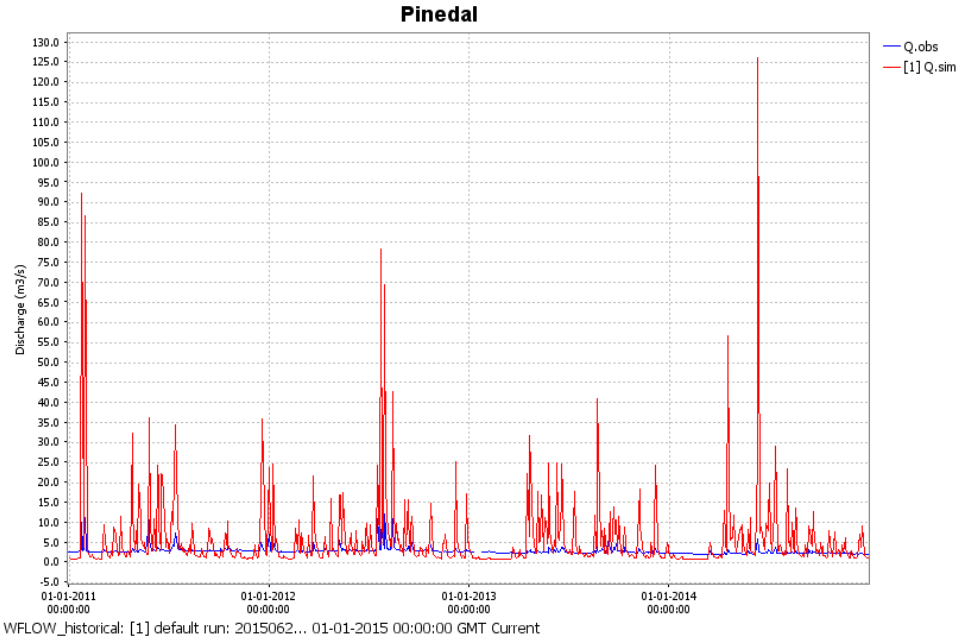

Figure 4.11 Uncalibrated model (Q sim) and observed (Q obs) flow results Pinedale (2011-2015).

4.4.3 Model calibration

Complex (multi-variate) sensitivity analysis and automated calibration techniques are now standard practice to understand model sensitivity and to 'tune' model performance in areas where dominant hydrological processes are well understood and covered by the model concept.

In the Hauraki Plains catchment, where we still lack an understanding of geo-hydrological behaviour in many places, such calibration techniques could lead to calibration towards an optimised model based on the selection of parameter sets for the wrong reason.

The causes for the varying performance of the model across the Hauraki Plains catchment was discussed between DairyNZ and GNS (pers. comm.). It seems that in some areas, for example in the Ohinemuri sub-catchment, there is less storage in the sub-soil than in other areas, for example Waitoa. In the Waihou River catchment upstream of Te Aroha the description of surface-groundwater interactions seems to be more complex than suitable for the WFLOW concept.

In light of this the following steps were undertaken to manually calibrate the hydrological model:

Four calibration zones (see Figure 4.12) of different hydrological characteristics were applied. Variations in these zones could not be explained by variations in soil class or land-use alone.

1. The *first zone capacity* (FZC) and *first zone minimum capacity* (FZMC) coefficients were independently increased for all calibration zones to increase storage in the hydrological model.
2. The rooting depth of grass and horticulture land-use types was increased to a maximum of 500mm (a justifiable maximum, particularly on peat soils), to allow for more depletion due to evapotranspiration.

3. Canopy storage upstream of Pinedale (calibration zone 4) was enlarged to a maximum of 4mm and the canopy gap fraction to a maximum of 0.4 for forested areas. This leads to more storage upstream of Pinedale.
4. The saturated soil moisture content upstream of Pinedale was increased to 0.2 for Ultic soils.

These steps were taken to improve model performance by increasing storage and varying storage values over the catchment (see Table 4.15). The sensitivity of runoff-response to rainfall under different hydraulic conductivity values was further assessed by varying the *FirstZoneKsatVer* between 50 and 2000 mm/day and *M*-value between 50 and 500.

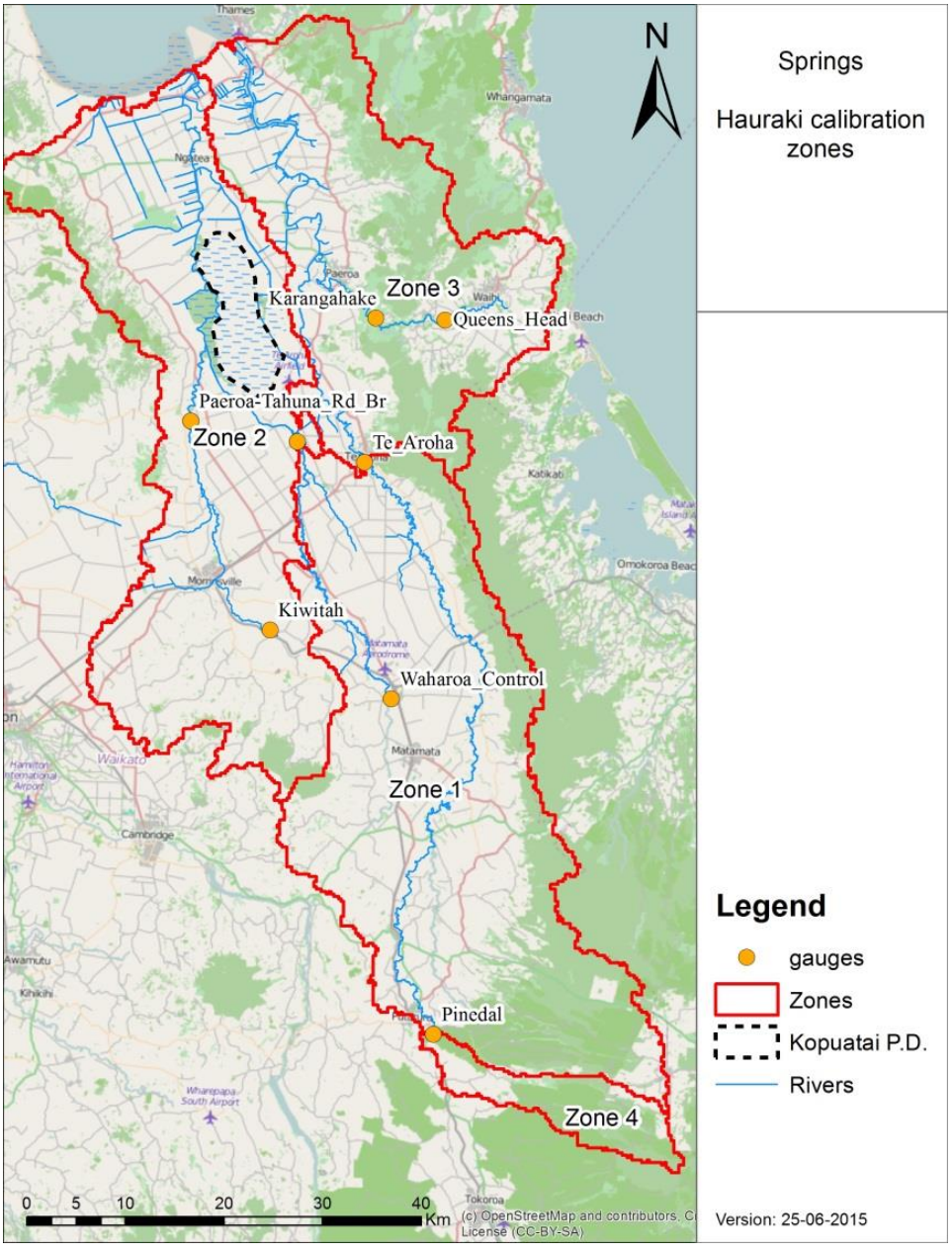

Figure 4.12 Zones by which model parameters can be varied.

Table 4.12 Parameter adjustments per zone.

	Default model		Calibrated model	
	FirstZone Capacity [mm]	**FirstZone MinCapacity [mm]**	**FirstZone Capacity [mm]**	**FirstZone MinCapacity [mm]**
Zone 1	3000	500	5000	5000
Zone 2			3000	3000
Zone 3			2000	500
Zone 4			8000	8000

Table 4.13 Parameter adjustments per land-use class.

	Can.GapFrac [-]		Max. Can.Storage [mm]	
	Default model	**Calibrated model**	**Default model**	**Calibrated model**
Horticulture	0.8	0.9	0.1	0.1
Livestock		0.9		0.1
Forest		0.4		0.4
Other (peat dome)		0.9		0.1
Grass land		0.9		0.1
Urban		0.9		0.1

Table 4.14 Parameter adjustments per soil type class.

	thetaS [-]	
	Default model	**Calibrated model**
Brown	0.15	0.15
Gley		0.15
Melanic		0.15
Organic		0.15
Ultic		0.20

4.5 Final Hydrological model results

In this section the model validation results are shown and the model performance is further discussed per sub-catchment. The figures shown in the sections below depict model results for 2008-2015 for different tributaries. The x-axis in the figures shows the model time step (days) since 01-01-2008.

4.5.1 Model validation

The calibration improved all model results (Table 4.15), however only for Te Aroha this is visible in the model performance results (Table 4.16).

Table 4.15 Model performance before and after manual calibration (over the period 2011-2015) and for the validation after manual calibration (2008 – 2011) expressed in the Nash-Sutcliff statistic (NS), Relative volume error (RVE) and the derived coefficient of fit (COF).

		Default model			Calibration			Validation		
Catchment	**Station**	**NS**	**RVE**	**COF**	**NS**	**RVE**	**COF**	**NS**	**RVE**	**COF**
Waihou	Pinedale	-82.99	0.72	21.54	-26.51	0.41	7.18	-59.9	0.38	15.51
	Te Aroha	-3.71	0.27	1.38	-1.00	0.12	0.59	-0.78	0.19	0.59
Ohinemuri	Queens-Head	0.48	-0.41	0.44	0.47	-0.43	0.45	0.62	-0.32	0.34
	Karangahake	0.57	-0.39	0.4	0.56	-0.40	0.41	0.68	-0.33	0.33
Waitoa	Waharoa Control	-0.68	0.57	0.85	0.22	0.36	0.46	-1.12	0.40	0.83
	Mellon Rd Recorder	-4.05	0.77	1.84	-2.68	0.58	1.36	-2.84	0.55	1.37
Piako	Kiwitahi	0.56	0.28	0.32	0.75	0.02	0.08	0.73	-0.05	0.10
	Paeroa-Tahuna	0.03	0.30	0.47	0.55	0.09	0.18	0.62	0.10	0.17

Table 4.16 Model performance rating before and after manual calibration (over the period 2011-2015) and for the validation after manual calibration (2008 – 2011) based on the coefficient of fit (COF).

		Performance rating		
Catchment	**Station**	**Default model**	**Calibration**	**Validation**
Waihou	Pinedale	Unsuitable	Unsuitable	Unsuitable
	Te Aroha	Unsatisfactory	Satisfactory	Satisfactory
Ohinemuri	Queens-Head	Good	Good	Good
	Karangahake	Good	Good	Good
Waitoa	Waharoa Control	Satisfactory	Good	Satisfactory
	Mellon Rd Recorder	Unsatisfactory	Unsatisfactory	Unsatisfactory
Piako	Kiwitahi	Good	Very good	Very good
	Paeroa-Tahuna	Good	Very good	Very good

4.5.2 Waihou River

Based on the statistical assessment protocols applied, the results of model prediction for the Waihou River ranges between satisfactory (Te Aroha) to unsuitable (Pinedale) (COF 0.59 and 15.51, respectively). This catchment is known to have dominant groundwater-surface water interaction which should be captured in the modelling framework by adding the groundwater model (iMOD). In Pinedale average discharge is highly overestimated (Figure 4.13). It is believed most rainfall captured in the catchment infiltrates to the groundwater where it probably contributes to discharges of adjacent rivers outside the topographic boundary. At Te Aroha, the model underestimates base and peak flow, which can only be explained to a limited extent by the overestimation in Pinedale (Figure 4.14).

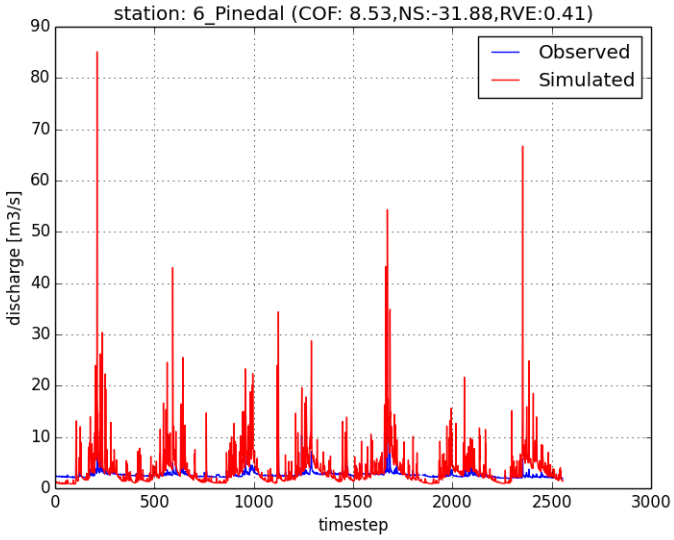

Figure 4.13 Observed and simulated discharge at Pinedale (2008-2015).

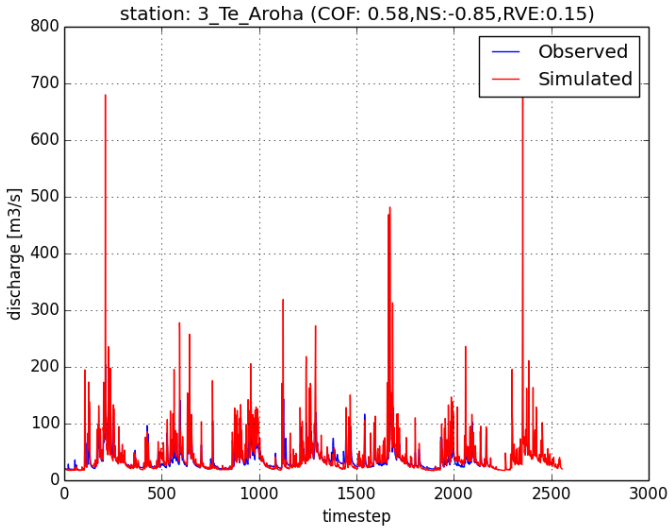

Figure 4.14 Observed and simulated discharge at Te Aroha (2008-2015).

4.5.3 Ohinemuri River

The Ohinemuri River has a good model performance (COF: 0.33 and 0.34). However, it is very difficult to accurately predict discharge peaks and base flow as there are only few rainfall stations in and around the upstream part of the Ohinemuri River. Due to both peak flow and base flow are underestimated, there is a considerable underestimation of flow at peaks by 30-40% at both Queens Head (Figure 4.15) as Karangahake (Figure 4.16).

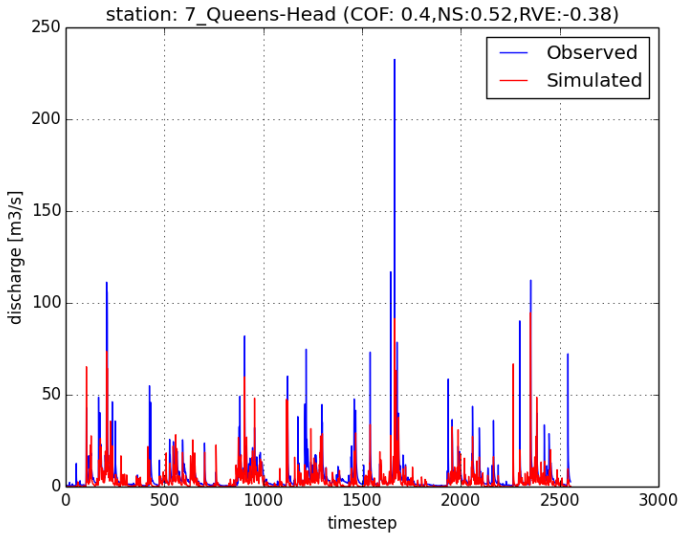

Figure 4.15 Observed and simulated discharge at Queens Head (2008-2015).

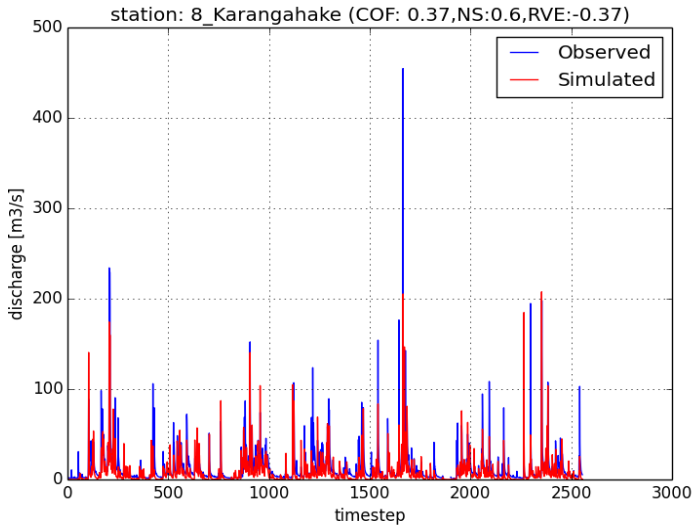

Figure 4.16 Observed and simulated discharge at Karangahake (2008-2015).

4.5.4 Waitoa River

The Waitoa River has a satisfactory to unsatisfactory model performance (COF: 0.83 and 1.37). The model is well capable of capturing the base flow, but especially at the start of the wet season, April till June, discharge peaks are overestimated. The capacity of the river catchment and system to retain peak rainfall under semi-saturated conditions seems to be

much higher than estimated by the hydrological model. These results were to some extent improved by increasing storage during manual calibration (Figure 4.17 and Figure 4.18).

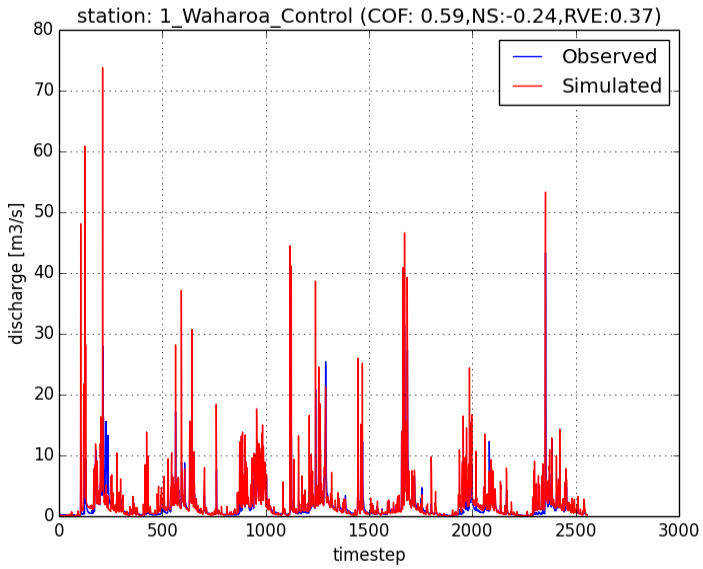

Figure 4.17 Observed and simulated discharge at Waharoa (2008-2015).

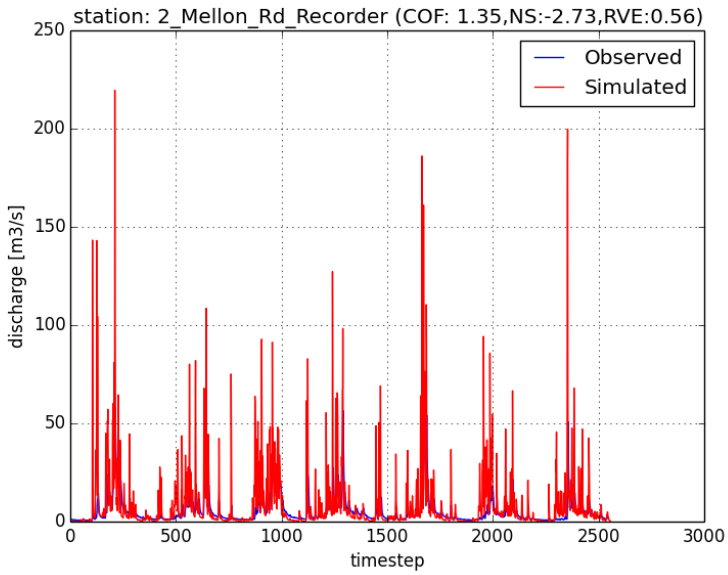

Figure 4.18 Observed and simulated discharge at Mellon Road (2008-2015).

4.5.5 Piako River

The Piako River results demonstrate very good model performance (COF: 0.10 and 0.17). The model provides a good representation of base flow in this system. A small error in peak flow is mainly caused by occasional overestimations of event flows at the start of each new wet season (April till June). This overestimation also results in a relatively small error in total discharge volume of between 5-10% (Figure 4.19 and Figure 4.20).

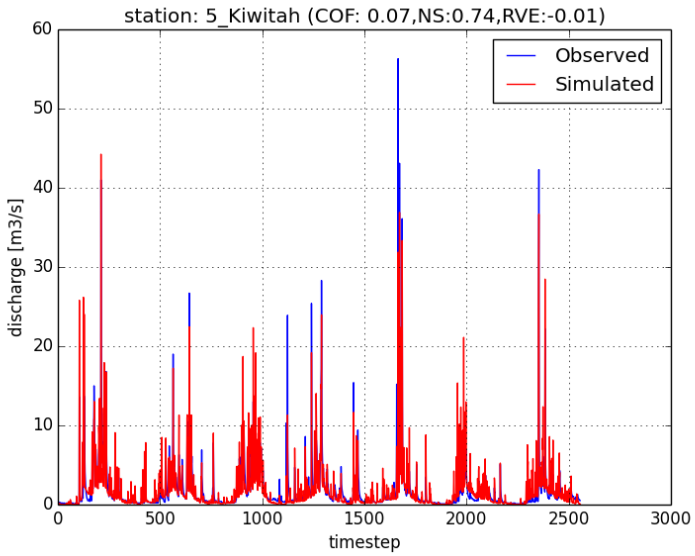

Figure 4.19 Observed and simulated discharge at Kiwitahi (2008-2015).

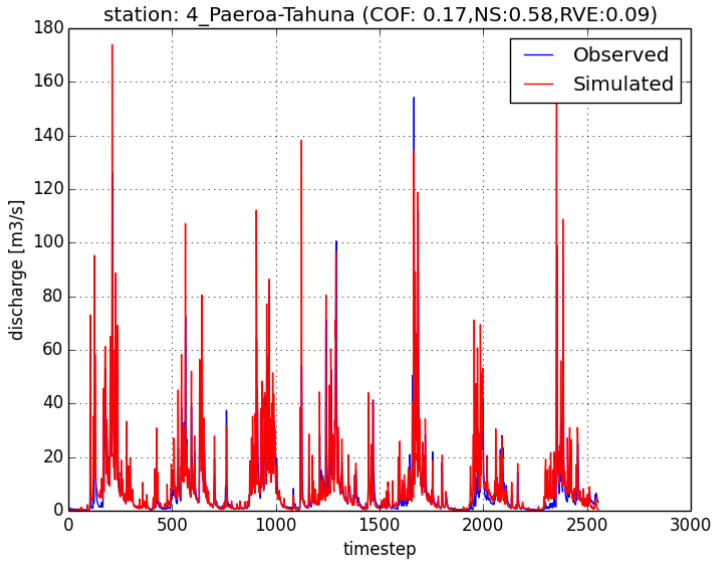

Figure 4.20 Observed and simulated discharge at Paeroa-Tahuna (2008-2015).

5 Catchment water quality model set up

5.1 Introduction

The WFD Explorer water quality model was applied to quantify total nitrogen and total phosphorus loads discharging from the Hauraki Plains to the Firth of Thames. The WFD Explorer is a lumped, steady state model developed to support catchment water quality management (Chapter 2). The WFD Explorer model was applied by coupling a water balance model to the water quality model on a time scale of 12 evenly disturbed periods.

The catchment water balance was driven by runoff estimated on a 25 x 25m spatial resolution using the WFLOW hydrological model (see Chapter 4). The water quality model adds emission values for all individual farm properties in the catchment as well as additional loading associated with other sources.

The final modelling framework used is based on the suite of models applied earlier to the Waituna Catchment (van den Roovaart et al., 2015, Chapter 2). The set-up of the Hauraki Plains catchment model differs from the Waituna catchment model in the following ways:

- Farm nutrient losses were not available for each specific farm and are instead based on upscaling of OVERSEER nutrient loss output derived from 12 representative case study farms.
- Point sources have been added to the model schematisation to represent municipal and industrial wastewater discharges.
- More effort was spent on determining the quantity and land-use source of phosphorus loads associated with other sources than explained by OVERSEER (e.g., erosion, overland runoff).
- The model has been set up to deliver results for 12 evenly distributed periods throughout the year, as opposed to only 4 periods.

The processes described in this chapter are depicted in Figure 2.5 and Figure 2.6.

The results of the model include flows of water through the river network, estimates of in-river nutrient concentrations and total nutrient loads as contributions to the coastal waters by each sub-catchment. The complete model framework can be applied as a management tool to evaluate the impacts of different mitigation scenarios on catchment nutrient loading.

5.2 Land-use categories

The WFD model is driven by spatially variable land-use sources of nitrogen and phosphorus. These diffuse sources consist of loads associated with different land types (anthropogenic and natural). To create this spatial layer information from LCDB4, AGRIBASE and CLUES GIS layers were used (for elaborate land-use classification tables see Appendix G). The AGRIBASE and CLUES layers were provided by WRC.

These layers differ in their spatial resolution and the information they contain. AGRIBASE contains the most spatially refined detail as this layer depicts property boundaries as well as different land-use classes for farming. For natural land-uses (e.g. wetland, native forest, exotic forest), the LCDB4 layer was used as these are not described in AGRIBASE. The CLUES layer is low in spatial resolution and strongly rasterized. Therefor this layer was only used for validation and to provide information for areas of the catchment where AGRIBASE and LCDB4 did not contain sufficient data. The layers where CLUES provided information were visually validated and manually added by making use of Open Street Map and satellite imagery.

The remaining non-farming area was intersected with the land-uses of the LCDB4 layer. Areas still remaining after the intersection with LCDB4 were manually separated into residential and commercial (Res/com), roads, rivers and slivers. Slivers mostly represent the small, remaining area between property boundaries. For the land-use Res/com only areas that intersect with a CLUES Urban class raster cluster larger than 17 acres (70.000 m^2) were taken into account.

All natural, forestry and farming land-uses were further classified using the categories in the AGRIBASE, LCDB4 and CLUES layers, resulting in a divide of the Hauraki Plains Catchment in 15 land-use classes, of which 12 land-use classes were assigned to property boundaries (excluding roads, rivers and slivers).

The final property based land-use classes derived and applied to the catchment model are summarised in Table 5.1. The result of the final land-use classification is shown in Figure 5.1.

Table 5.1 Property based land-use classes used in the Hauraki Plains Catchment model.

Category	Land-use
Farming	Dairy
	Dairy support
	Drystock
	Horticulture
	Lifestyle
	Other farming
Forestry	Exotic forest
Residential	Res/Com
Natural	Wetland
	Shrubland
	Indigenous forest
	Other landscape

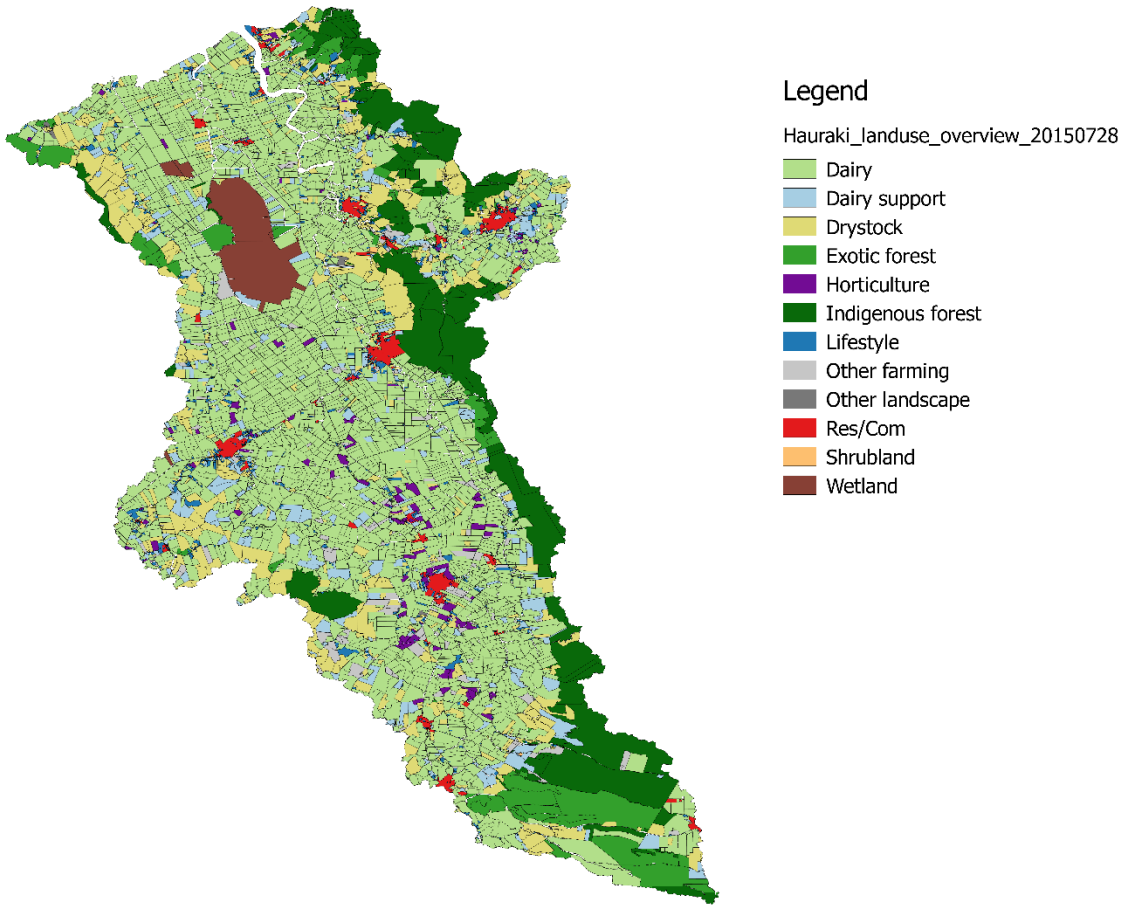

Figure 5.1 Final land-use classification used in the Hauraki Plains Catchment water quality model.

The final land-use map was used to create part of the basin nodes in the WFD-Explorer schematisation, as shown in Figure 2.5. These land-use classes have been coarsely validated with the help of local residents working at DairyNZ. Further detail on the land-use classification can be found in Appendix G.

Table 5.2 Land-uses distribution through the Hauraki Plains catchment derived from the created land-use layer. For the geographic location of the catchments see Figure 5.2.

Catchment	***Hauraki Plains***		*Waihou*			*Piako*			*Waitakaruru*		
Land-use	Area (Ha)	Catchment (%)	Area (Ha)	Sub-catchment (%)	Catchment (%)	Area (Ha)	Sub-catchment (%)	Catchment (%)	Area (Ha)	Sub-catchment (%)	Catchment (%)
Horticulture	4302.96	1.23	1841.05	0.97	0.53	2364.39	1.64	0.68	97.51	0.63	0.03
Res/Com	5210.55	1.49	3311.68	1.75	0.95	1898.87	1.32	0.54	0.00	0.00	0.00
Drystock	42378.50	12.15	21931.66	11.58	6.29	17059.97	11.84	4.89	3386.88	21.97	0.97
Lifestyle	6202.59	1.78	3239.30	1.71	0.93	2702.96	1.88	0.77	260.33	1.69	0.07
Wetland	9794.10	2.81	0.00	0.00	0.00	9769.58	6.78	2.80	24.52	0.16	0.01
Shrubland	63.89	0.02	63.82	0.03	0.02	0.07	0.00	0.00	0.00	0.00	0.00
Other farming	6947.19	1.99	3138.11	1.66	0.90	3804.80	2.64	1.09	4.28	0.03	0.00
Dairy	186449.09	53.45	86203.06	45.53	24.71	91138.22	63.25	26.13	9107.81	59.08	2.61
Other landscape	272.85	0.08	153.13	0.08	0.04	45.49	0.03	0.01	74.23	0.48	0.02
Indigenous forest	48016.09	13.76	44558.12	23.53	12.77	3094.62	2.15	0.89	363.35	2.36	0.10
Exotic forest	19373.12	5.55	15430.77	8.15	4.42	2344.73	1.63	0.67	1597.62	10.36	0.46
Dairy support	19823.01	5.68	9466.79	5.00	2.71	9857.09	6.84	2.83	499.12	3.24	0.14
Total	348833.94	100.00	189337.50	100.00	54.28	144080.79	100.00	41.30	15415.64	100.00	4.42

5.3 Coupling of WFLOW with WFD Explorer

5.3.1 River schematisation

As described in Chapter 3, WFLOW was used to create a rainfall runoff model for the Hauraki Plains Catchment. Based on the Digital Elevation Map (DEM) and visual corrections derived from the Open Earth layer the river network was created and all flows have been routed to this network (see Figure 5.2).

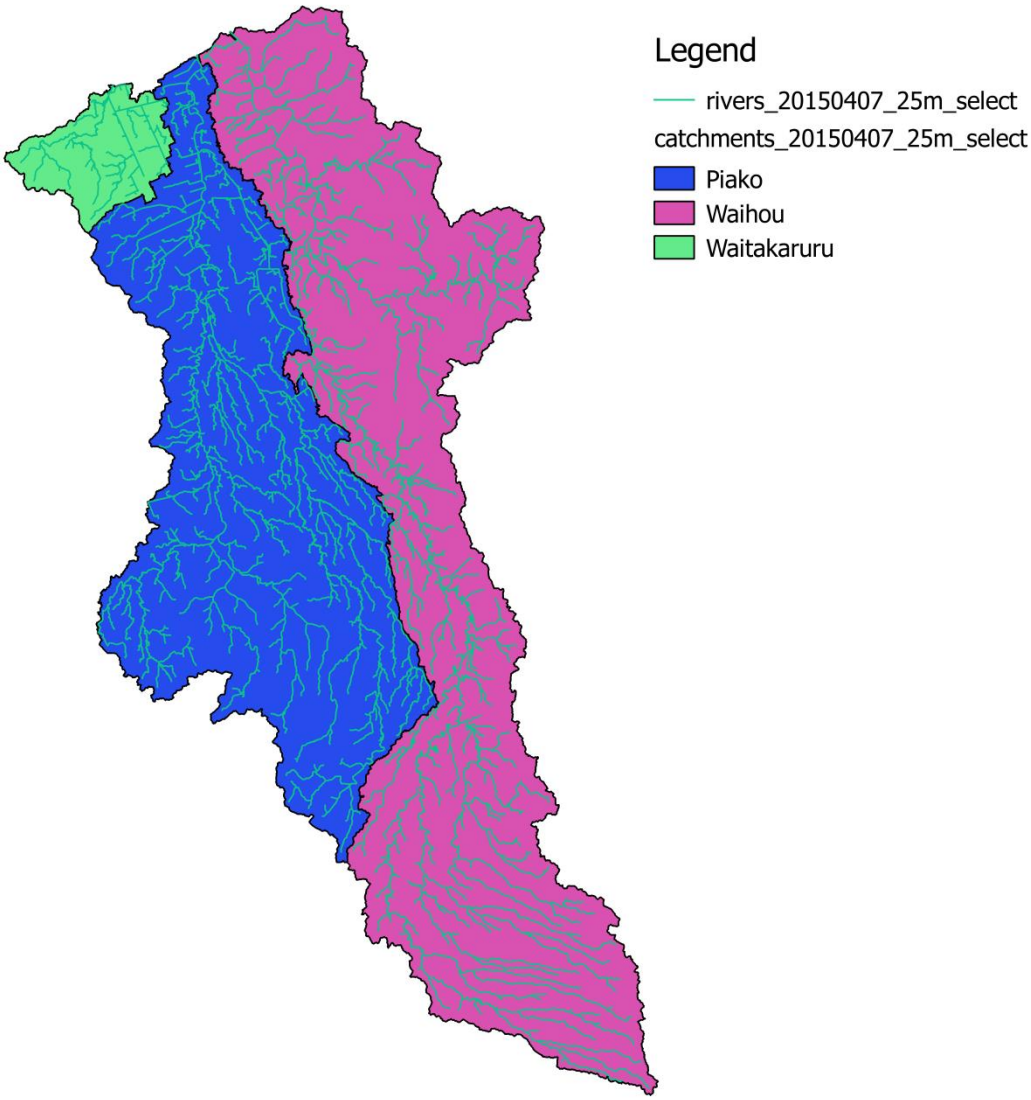

Figure 5.2 WFLOW river network placed over the three catchments.

5.3.2 Flow transformation

To produce concentrations and loads within the WFD Explorer model, flows derived from the hydrological model were added to the basin nodes. The runoff results which are fed from WFLOW to the WFD Explorer represent mean daily flow in mm per day per concatenated property polygon. These concatenated property polygons represent concatenates of a single land-use polygon with the nearby gridded river, road and sliver polygons. By multiplying the mean daily mm with the area of the concatenated property polygon the flow contribution in cubic meters per day for that basin node is obtained.

5.4 Nutrient sources from land-use

5.4.1 Loads Dairy land-use

Nutrient loading associated with dairy land-use was based on the results of OVERSEER modelling on 12 representative case study farms distributed throughout the Hauraki Plains catchment and reported by Longhurst et al. (2016). Due to farmer confidentiality the exact name and location of the modelled farms is not reported. OVERSEER assumes that modelled farms practise good farming standards (e.g., not applying fertilizer when it is about to rain, sealed effluent pond systems). Hence, the modelled output assumes good practice throughout all dairy farms in the water quality model.

The leaching results for each modelled farm were separated into the block types pastoral, cropping, stock excluded, wetland and other (as defined in OVERSEER). Pastoral block types were further separated by soil class, including Marine (Gley Soils), Volcanic (Allophanic, Brown, Granular/Volcanic, Ultic/Sedimentary and Recent soils) and Organic (Peat/Organic soils) (see Section 4.2.3). Pastoral has been defined in more detail than for other block types as the expectation is that the majority of the nutrient load attributed by dairying is from pastoral land. Leaching from pastoral land is also highly influenced by soil type (Longhurst et al., 2016). All results have been re-calculated to derive a load in kilograms TN and TP per hectare per year. From these values the median for farms on a similar soil type was assumed to be an indicatory leaching loss value per area for all dairy farms on that soil type in the Hauraki Plains Catchment. Due to the limited amount of data acquired from the 12 modelled farms, not all load categories could be assumed to be normally distributed (see Table 5.3).

Table 5.3 The mean, median, min, max, normality and number of measurements of data for the defined block types and their total nitrogen and total phosphorus load leaching (in Kg/Ha/Yr). The block type "Wetland" is missing as this block type has not been implemented on any of the model farms, and therefore has not been used in the Hauraki Plains Catchment model. SD is standard deviation, LB is lower boundary, UB is upper boundary of an 95% interval, and n is number of samples.

Nitrogen Load on Hauraki Model farms											
Source		N Kg/Ha/Yr							Shapiro - Wilk test		
Block type	Soil class	mean	median	min	max	SD	LB	UB	n	P value	Normality
Pastoral	Marine	19.45	18.37	16.65	26.55	2.93	13.59	25.31	8	0.02	FALSE
Pastoral	Vulcanic	20.75	20.83	8.80	36.35	7.94	4.86	36.64	15	0.62	TRUE
Pastoral	Organic	19.27	17.75	12.50	29.09	6.06	7.15	31.40	4	0.24	TRUE
Crop	-	23.94	22.86	6.27	47.50	14.41	-4.88 *	52.77	7	0.63	TRUE
Stock Excluded	-	3.59	2.96	0.38	10.67	2.74	-1.90 *	9.07	10	0.04	FALSE
Other	-	1.66	1.29	0.52	4.36	1.10	-0.54 *	3.87	10	0.01	FALSE

Phosphorus Load on Hauraki Model farms											
Source		P Kg/Ha/Yr							Shapiro - Wilk test		
Block type	Soil class	mean	median	min	max	SD	LB	UB	n	P value	Normality
Pastoral	Marine	0.70	0.63	0.45	1.05	0.21	0.29	1.11	8	0.39	FALSE
Pastoral	Vulcanic	0.99	0.62	0.10	5.32	1.32	-1.65	3.63	15	<0.01	FALSE
Pastoral	Organic	1.17	1.30	0.70	1.39	0.28	0.61	1.73	4	0.10	TRUE
Crop	-	1.59	1.34	1.00	2.21	0.43	0.74	2.45	7	0.33	TRUE
Stock Excluded	-	0.07	0.03	0.00	0.33	0.09	-0.12 *	0.25	10	<0.01	FALSE
Other	-	0.34	0.32	0.20	0.64	0.11	0.12	0.57	10	0.04	FALSE

* Negative values for TN and TN leaching are not feasible, however here the LB represents the spread of the values.

As shown in Table 5.3, the current data availability for nitrogen and phosphorus leaching from dairy farms is insufficient to reliably assign average or median leaching values for all soil and block types across the catchment, as they don't pass the statistical test for normality.

Accordingly, the final model setup supports the possibility for more detailed farm-specific loads to be implemented in future, should these values become available for each farm.

In the current model setup the leaching values derived for the three soil classes have been distributed over all nine soil types present in the catchment, to enable model scenarios to be carried out for mitigations targeted at specific soil types (see Table 5.4). Podzol, Pumice and Raw were not represented in the OVERSEER model farm results but are present in the catchment. These were filled with values derived for Volcanic soils.

Total farm area was distributed as a percentage of block type use derived as a mean from the 12 OVERSEER model farms. The loads have been assigned accordingly to surface area per block type (see Table 5.5). For the block type "Pastoral" the area per block type was further divided by the proportion of each soil type present within individual farm boundaries.

Table 5.4 Leaching values for total nitrogen and total phosphorus for the land-use Dairy assigned per block type, soil type and drainage combination. As leaching values, the means estimated in table X are used. The medians for the soil classes Marine, Volcanic and Organic have been distributed over the soil category and drainage combinations.

Block type	Soil type	Drainage	N (kg/ha)	P (kg/ha)
Pastoral	Gley	Poor	18.37	0.63
	Allophanic	Imperfect	20.83	0.62
	Allophanic	Well	17.75	0.62
	Peat / Organic	Poor	20.83	1.3
	Brown	Imperfect	20.83	0.62
	Granular / Volcanic	Moderatly Well	20.83	0.62
	Ultic / Sedimentary	Moderatly Well	20.83	0.62
	Recent	Imperfect	20.83	0.62
	Granular / Volcanic	Poor	20.83	0.62
	Podzols	Moderatly Well	20.83	0.62
	Pumice	Moderatly Well	20.83	0.62
	Raw	Moderatly Well	20.83	0.62
Crop	-	-	22.86	1.34
Stock excluded	-	-	2.96	0.03
Wetland	-	-	0	0
Other	-	-	1.29	0.32

Table 5.5 Mean distribution of farm area per block type for the land-use Dairy, as used to determine total nitrogen and total phosphorus leaching of the farm.

Block type	Area of farm (%)
Pastoral	92.3
Crop	3.5
Stock excluded	4.2
Wetland	0
Other	100.0*

** as the kg/ha is applicable to the complete farm*

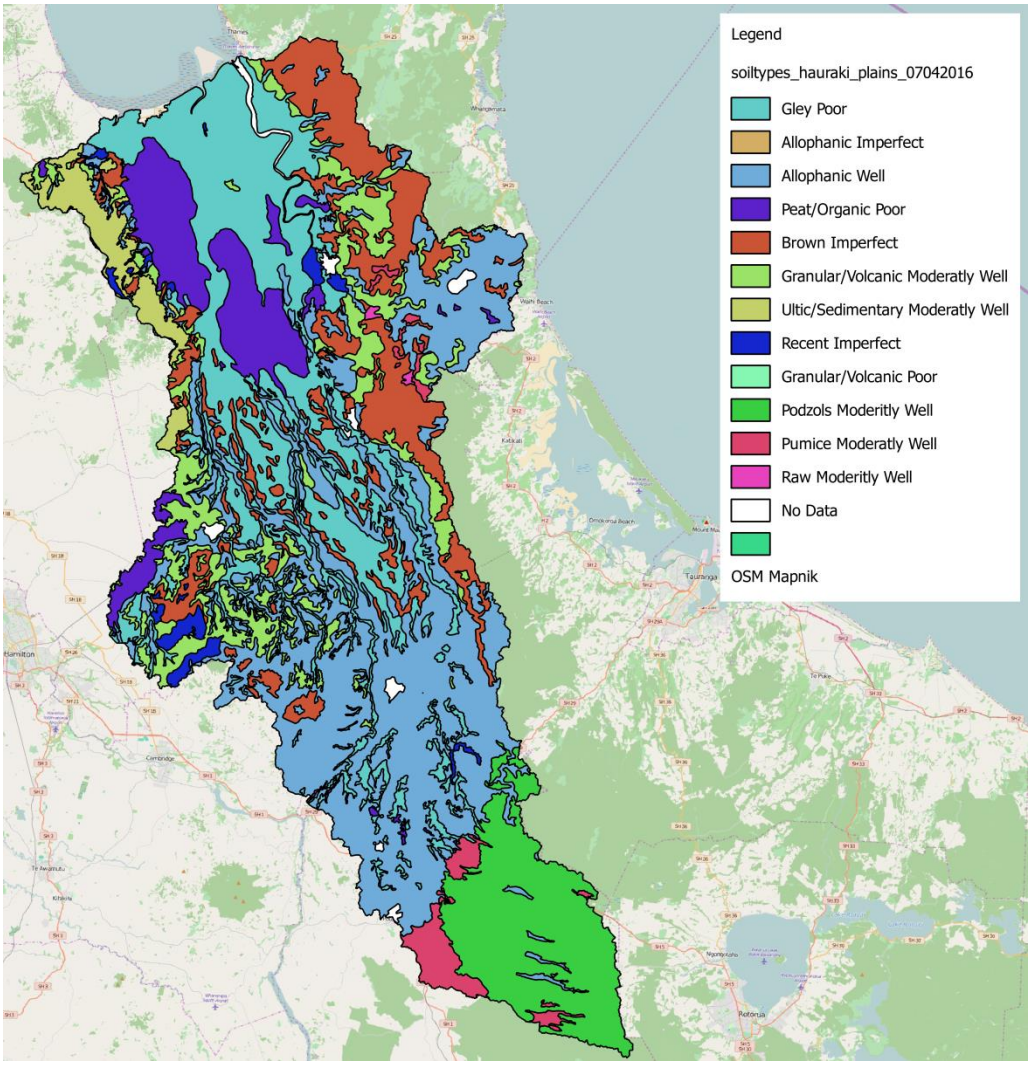

Figure 5.3 Soil types in combination with drainage class distribution in the Hauraki plains.

Table 5.6 Soil / drainage class distribution through the Hauraki Plains catchment derived from the created soil / drainage layer. For the geographic location of the catchments see Figure 5.2.

Catchment	***Hauraki Plains***		*Waihou*			*Piako*			*Waitakaruru*		
Soil / Drainage class	Area (Ha)	Catchment (%)	Area (Ha)	Sub-catchment (%)	Catchment (%)	Area (Ha)	Sub-catchment (%)	Catchment (%)	Area (Ha)	Sub-catchment (%)	Catchment (%)
Gley Poor	98899.32	26.22	34731.32	17.54	9.21	60603.48	37.12	16.07	3564.52	22.47	0.95
Allophanic Imperfect	0.01	0.00	0.01	0.00	0.00	0.00	0.00	0.00	0.00	0.00	0.00
Allophanic Well	111909.44	29.67	66462.10	33.56	17.62	44555.32	27.29	11.81	892.02	5.62	0.24
Peat/Organic Poor	27147.32	7.20	2353.13	1.19	0.62	20756.98	12.71	5.50	4037.21	25.45	1.07
Brown Imperfect	47589.06	12.62	34900.87	17.62	9.25	11707.87	7.17	3.10	980.32	6.18	0.26
Granular/Volcanic Moderatly Well	32391.40	8.59	14516.65	7.33	3.85	16951.64	10.38	4.49	923.10	5.82	0.24
Ultic/Sedimentary Moderatly Well	10414.73	2.76	0.00	0.00	0.00	5352.99	3.28	1.42	5061.74	31.91	1.34
Recent Imperfect	4954.59	1.31	1338.55	0.68	0.35	3211.41	1.97	0.85	404.63	2.55	0.11
Granular/Volcanic Poor	0.03	0.00	0.00	0.00	0.00	0.03	0.00	0.00	0.00	0.00	0.00
Podzols Moderitly Well	35768.61	9.48	35741.51	18.05	9.48	27.10	0.02	0.01	0.00	0.00	0.00
Pumice Moderatly Well	7645.14	2.03	7645.14	3.86	2.03	0.00	0.00	0.00	0.00	0.00	0.00
Raw Moderitly Well	470.42	0.12	351.93	0.18	0.09	118.49	0.07	0.03	0.00	0.00	0.00
NoData	3162.18	0.84	2481.76	1.25	0.66	680.42	0.42	0.18	0.00	0.00	0.00
Total	377190.06	100.00	198041.21	100.00	52.50	163285.30	100.00	43.29	15863.54	100.00	4.21

5.4.2 Loads non-dairy land-use

For loads associated with land-uses other than dairy, land-use specific TN and TP loss values were derived from current research and the previous modelling project of the Waituna catchment (van den Roovaart et al., 2014) (Table 5.7). For some land-use types information was not available and instead expert judgement was used (see Appendix H).

Table 5.7 Mean leaching values for total nitrogen and total phosphorus per non-dairy land-use as used in the Hauraki Plains Model.

Land-use	total nitrogen (kg/ha)	total phosphorus (kg/ha)	Source
Dairy support	21.00	0.44	DairyNZ, unpublished data
Drystock	13.09	0.95	Olubode-Awosola et al., unpublished/confidential
Lifestyle	7.00	0.10	DairyNZ, unpublished data
Other farming	15.00	1.00	Judge and Ledgard, 2009
Horticulture	55.00	1.30	The AgriBusiness Group, 2014; pers. comm. Stuart Ford (The agribusiness Group)
Res/Com	3.00	0.10	DairyNZ, unpublished data
Shrubland	3.00	0.30	Jenkins & Vant, 2007
Indigenous forest	3.00	0.30	Jenkins & Vant, 2007
Exotic forest	3.00	0.30	Jenkins & Vant, 2007
Wetland	3.00	0.30	DairyNZ, unpublished data
Other landscape	3.00	0.30	Jenkins & Vant, 2007
Road	2.50	0.10	DairyNZ, unpublished data
Sliver	2.50	0.10	DairyNZ, unpublished data
River and flood plains	2.50	0.10	DairyNZ, unpublished data

5.4.3 Phosphorus load from erosion

Similar to the Waituna Catchment water quality study, the phosphorus load is under predicted in the model when load sources only reflect land-use and point sources. In the Waituna Catchment model this missing load was attributed to phosphorus associated with bankside erosion.

In this study, an exploration of where additional phosphorus loads due to erosion might be derived from and to which land-uses this can be attributed, was undertaken. Based on a linear modelling approach an additional particulate phosphorus (PP) load was determined for land-uses Dairy and Exotic Forest (Table 5.8, full details in Appendix I). Likely causes for the extra P load in dairy-dominated parts of the catchment could be overland erosion, bank side treading by cattle, bank-side collapse and upstream supply and deposition into bankside deposits by flood pulses. For example, Swales et al. (2016) determined >90% of sediment in the upper Waihou at Te Aroha was attributed to bankside erosion, of which 80% was linked directly to forestry upstream. Likely causes for additional sediment and P losses from exotic forest are leaf litter deposition, overland erosion after harvesting and bank collapse. The additional loads (see Table 5.8) are only applied to Dairy and Exotic forest land-use tiles located on slopes greater than 3º. A study performed by NIWA on sources of eroded soils underpins that exotic forest (Waihou, pine forest contributes 80-90% of bankside eroded material) and dairy (Piako, dairy contributes 75% of bankside erosion) are the main contributors of eroded soils to the Firth of Thames (Swales et al., 2016).

Table 5.8Additional mean annual total phosphorus per land-use due to erosion (No slope is <3º, Slope is >3º).

Land-use	Specific	TP (Kg/Ha/Yr)
Dairy	No Slope	0.00
Dairy	Slope	0.47
Exotic forest	No Slope	0.00
Exotic forest	Slope	0.86

5.5 Point sources

Point sources were separated into anthropogenic point sources and groundwater springs.

5.5.1 Point sources

A total of 22 major point sources including factory and sewage treatment plant discharges present in the catchment are described in Vant (2011) (see Table 5.11). Collectively these represent an average TP load of 73.43 T per year and TN load of 254.36 T per year. Corresponding flow values make a small contribution to total flow (<1% of volume flowing out in the Firth of Thames). These sources and associated mean annual load were added directly to the model schematisation. Figure 5.4 taken from Vant (2011) shows the location of these sources. Further detail on the temporal distribution of discharges from individual load sources has not been measured.

5.5.2 Springs

The position of significant springs was determined from the difference in water balance between the WFLOW model and monitored flow at several locations in the catchment (see Section 4.2.5). These springs occur mostly in the Pinedale region, an area known to have complex hydrological interactions between surface and deeper groundwater. For all springs in the Hauraki Plains catchment, water quality measurements are only available for the Blue Springs in 2011 (WRC springs and boreholes water quality measurements). Therefore, measured concentrations at the Blue Springs were used to derive mean annual loads for all other springs (see **Error! Reference source not found.**). This was important only for total n itrogen as measured total phosphorus concentration at Blue Springs is negligible (see **Error! Reference source not found.**).

Groundwater spring flows were directly derived from estimates obtained through the calibrated hydrological model (see Figure 4.7). Spring flows were considered to be constant through time across all locations.

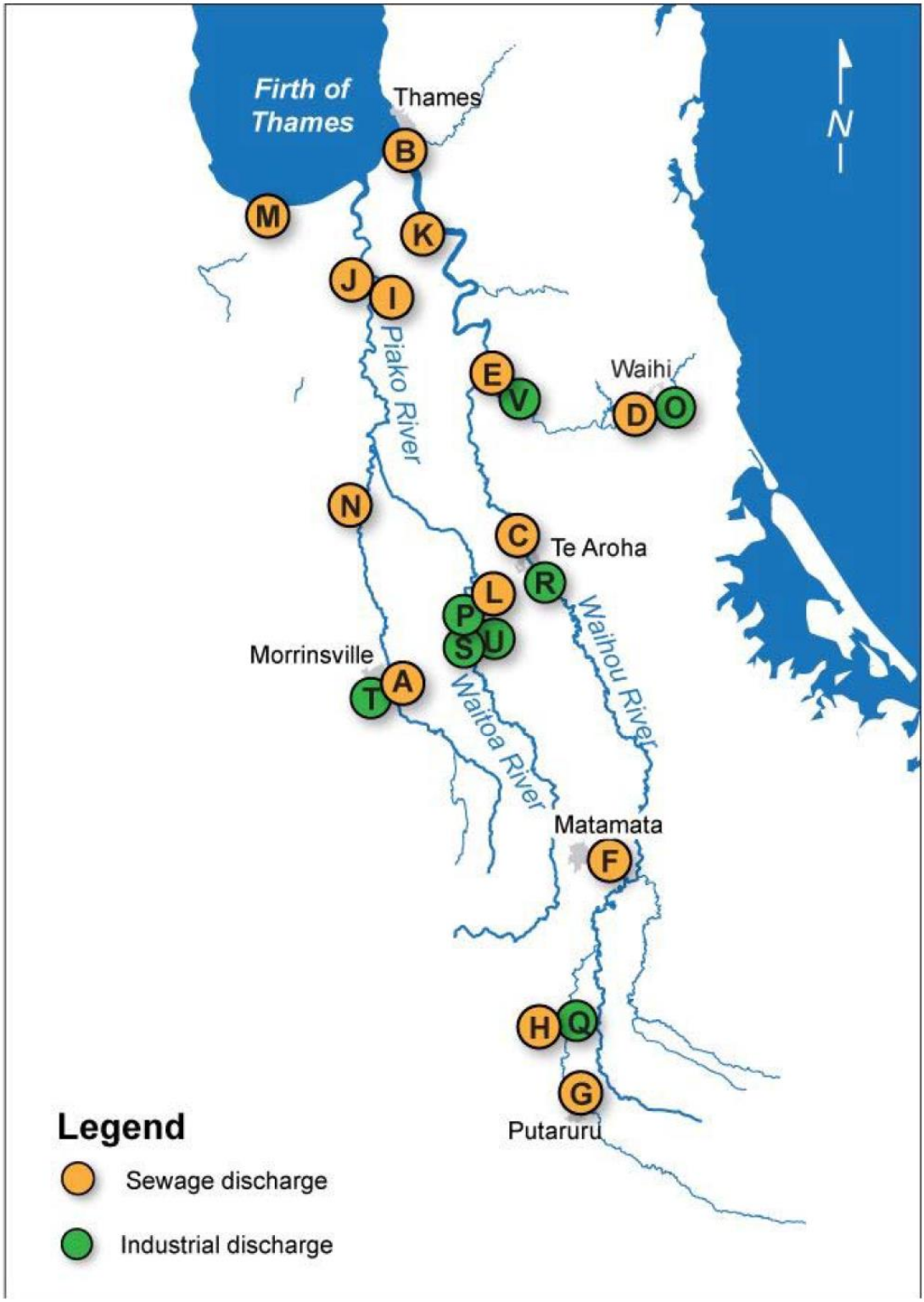

Figure 5.4 Location of the point sources in the Hauraki Plains Catchment (Vant, 2011). Sewage discharges represent municipal wastewater treatment plants.

Table 5.9 Total nitrogen and total phosphorus loads applied to anthropogenic point sources in the Hauraki Plains model (the code corresponds with the spatial Figure 5.4).

Source	Code	Flow (1*10^6 m3/yr)	N (T/Yr)	P (T/Yr)
UWWTP	A	1.51	16.66	10.00
UWWTP	B	1.42	39.65	4.96
UWWTP	C	0.76	16.02	1.60
UWWTP	D	0.68	8.19	2.87
UWWTP	E	0.65	8.49	2.09
UWWTP	F	0.60	14.97	5.27
UWWTP	G	0.44	11.39	3.20
UWWTP	H	0.11	3.81	0.59
UWWTP	I	0.06	0.81	0.41
UWWTP	J	0.03	0.79	0.21
UWWTP	K	0.03	0.46	0.25
UWWTP	L	0.01	0.44	0.13
UWWTP	M	0.01	0.34	0.08
UWWTP	N	0.01	0.08	0.05
INDUS	O	3.26	6.52	0.00
INDUS	P	1.99	27.85	21.28
INDUS	Q	0.87	31.40	8.55
INDUS	R	0.23	26.16	6.05
INDUS	S	0.16	34.33	5.27
INDUS	T	0.14	0.14	0.03
INDUS	U	0.09	2.37	0.23
INDUS	V	0.04	3.49	0.31

Table 5.10 Nitrogen and phosphorus loads applied to springs in the Hauraki Plains model (the code corresponds with the spatial Figure 5.4).

Source	Code	Flow (1*10^6 m3/yr)	N (T/Yr)	P (T/Yr)
SPRING	1122_14	142.11	86.69	0
SPRING	1122_27	140.42	85.66	0
SPRING	1122_29	55.11	33.62	0
SPRING	1122_41	46.80	28.55	0
SPRING	1158_1	42.06	25.66	0
SPRING	1174_10	17.98	10.97	0
SPRING	1174_4	29.74	18.14	0
SPRING	1174_6	25.30	15.43	0
SPRING	1174_9	11.73	7.16	0
SPRING	1204_5	18.87	11.51	0
SPRING	1249_38	1.45	0.88	0
SPRING	221_2	5.07	3.09	0
SPRING	279_1	1.84	1.12	0
SPRING	279_6	11.32	6.91	0
SPRING	490_9	7.16	4.37	0
SPRING	636_1	2.24	1.37	0
SPRING	669_11	6.19	3.78	0
SPRING	669_13	18.94	11.56	0
SPRING	669_18	21.47	13.09	0
SPRING	669_6	27.48	16.76	0
SPRING	669_7	27.46	16.75	0
SPRING	824_6	7.86	4.80	0
SPRING	872_5	2.78	1.69	0
SPRING	872_6	2.78	1.69	0

5.6 Model setup tool

5.6.1 The model setup tool

As the Hauraki Plains Catchment is substantually larger than the Waituna Catchment (about 16 times larger in area), the choice was made to automise generation of the model schematisation. For this automisation process a Python module was created to generate the WFD Explorer model schematisation and input based on the WFLOW results, as well as the land-use layer, position of the point sources and nutrient load inputs. In addition, another Python module was created to automise the translation of the model results for validation. A more detailed description of both modules can be found in Appendix 0.

A WFD-Explorer model schematisation consists of three elements. These are:

- Basins, representing the property boundaries or a point source
- Surface water units, representing stretches of river network
- Links between the Basin and Surface water units.

The year and period specific model input consist of two elements. These are:

- Flow distribution between the links of the model schematisation
- Sources of flow and nutrients that are added to the model schematisation.

Nutrient loads and flows have been assigned to individual farms, each represented by a Basin node in the model schematisation. The contribution of individual farm title flow and load for each year and period is stored in the sources file.

The layout of the files described can be found in Appendix C.2.

5.6.2 Basins

Each property boundary in the Hauraki Plains catchment was represented as an individual basin in the WFD-Explorer model schematisation. Property boundary information as well as land-use type and land area were derived from the created land-use layer. Several additional attributes were included in the Basins file to make it ready for importing in the WFD-Explorer.

5.6.3 River Network

The river network generated by WFLOW (see Chapter 3) was intersected to create unique river reaches within each individual property boundary. To each individual reach a SWU node was added and following the river network these SWU nodes were connected to each other by links. These links force flows and loads to accumulate towards the river mouth.

5.6.4 Sources

All Basins and Surface water units were linked to each other in the model schematisation. As there is free flow from upstream to downstream and all river branches accumulate to a single reach in the hydrological model, the river routing was relatively simple to implement in the WFD-Explorer.

Two steps were taken to generate the complete routing of the model. First, the river routing was setup. These links were labelled with a tag ”River”. All River links have a 100% routing of the outflowing water to the next downstream node.

Secondly, the Basins were connected to the river network. The diffuse sources were partitioned primarily based on the overlap with a river stretch. When no overlap was found the diffuse source was partitioned to the nearest river stretches. Point sources were always partitioned to the nearest river reach. When a source is connected to several (n) river reaches, the outflow of that source is distributed evenly across all river reaches (100% outflow / n river stretches).

5.7 Calibration of the nutrient model

5.7.1 Calibration approach mean annual load

The years 2008, 2010, 2011 and 2013 were used to calibrate the modelled load estimations. The years 2009 and 2012 were reserved for validation of the model, as these years are within the year range to avoid the effect of possible load trends on the model performance and as both year are average flow years (Section 3.3). The model was calibrated by adding a fixed catchment wide attenuation factor for total nitrogen and by periodically distributing and scaling the annual land-use loads according to the flow for both nutrients.

This periodical scaling is only applied to loads coming from anthropogenic land-uses. This scaling factor is the applied solution to achieve temporal and spatial variability in loads and concentrations in the absence of more detailed loading information for all individual farms or more temporally refined measurements of point sources and field measurements on nutrient leaching and management practices.

5.7.2 Attenuation

The loads used as input to the model reflect either losses to the root zone (load from land-use), direct discharges to the river (load from springs and anthropogenic point sources) or a combination of overland flow and in-stream erosion (runoff/erosion load from land-use). These loads are reduced as they travel through groundwater and surface waters due to attenuation. These processes will diminish the load further before the eventual discharge to the Hauraki Gulf. Most of the attenuation is likely to occur between the root zone and immediate area downstream of discharge to the river. Part of this attenuation is created by uptake and adsorption to sediment, bacterial processes and uptake by in river and spring vegetation.

Attenuation is considered to mainly have an effect on the total nitrogen load as nitrogen can be transformed to nitrogen gas and leave the system. Phosphorus can be stored in biomass and the sediment but will remain in the system and still be available for circulation until eventual discharge to the receiving environment. As the Hauraki Plains Catchment model is a steady state model, it is assumed that the system is in balance and thereby no net losses will occur through uptake by organisms (i.e. aquatic plants) or other biogeochemical processes such as binding with the sediment.

To estimate the global attenuation factor for TN, comparisons were made between uncalibrated modelled loads and the measured loads (see Figure 5.5). To compare these, the loads of each downstream measurement station were summed. These downstream stations consist of Paeroa-Tahuna Road Bridge, Mellon Road Recorder, Te Aroha and Karangahake.

In the absence of more detailed measurements, the chosen approach for deriving an attenuation factor for the model was to apply a single attenuation factor to the entire catchment. There is insufficient data to make the attenuation factor specific to sub-catchments, different land-uses and soil-types, or retention time in groundwater, although this can be implemented should new data become available.

The uncalibrated model slightly over-predicts total nitrogen load (approximately 4%). This over- prediction is likely due to attenuation, the inability to validate input loads for specific years, as well as the possibly that the model is underestimating source inputs, as attenuation rates for nitrogen are typically assumed to be much greater than the 4% estimated here. In the final model set up an attenuation factor of 4% was applied to all N sources (anthropogenic and natural, diffuse and point source) to scale the loads towards the averaged measured annual load.

For the total phosphorus load no attenuation was implemented. The model is assumed to predict the phosphorus load accurately, assuming that land-use TP sources and erosion processes have been adequately represented. As can be seen in the graph (Figure 5.6) the model has a slight under prediction (approximately -4%).

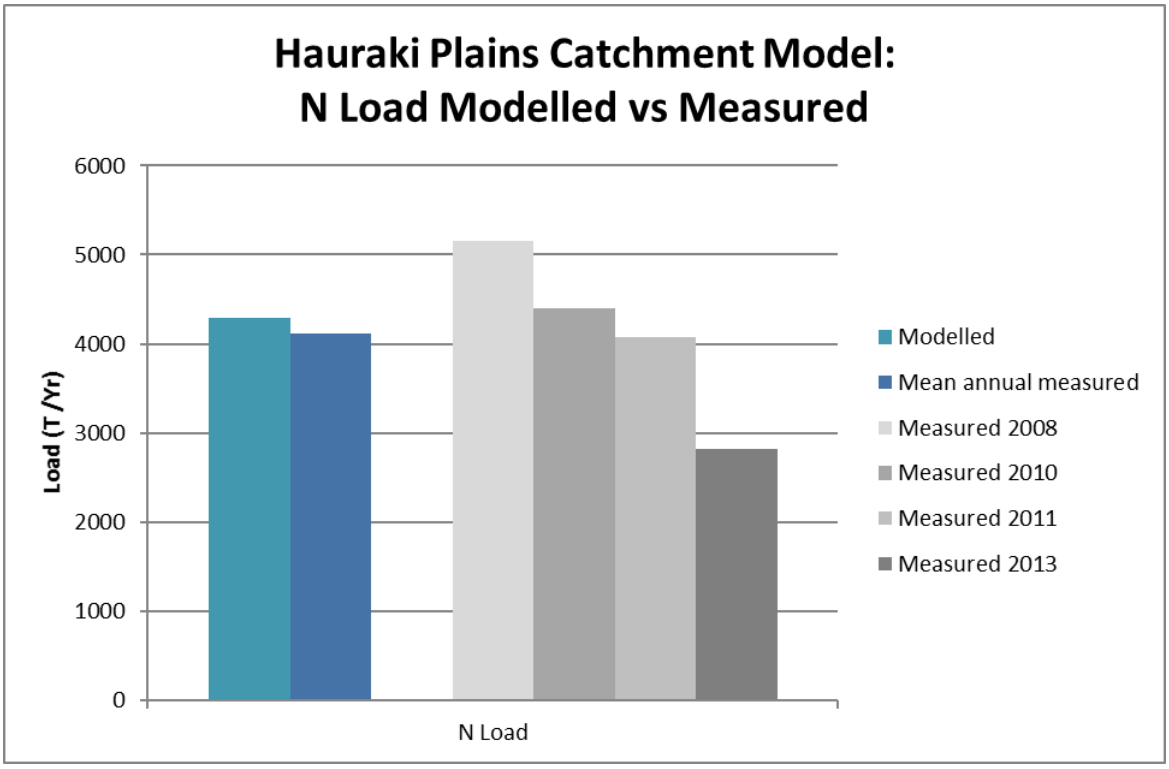

Figure 5.5 Comparison between mean annual measured and modelled total nitrogen load, based on the sum of all four downstream measurement stations (Te Aroha, Karangahake, Mellon Rd Rec and Paeroa-Tahuna Rd Br. The measured total annual load for individual years (2008, 2010, 2011 & 2013) is also shown.

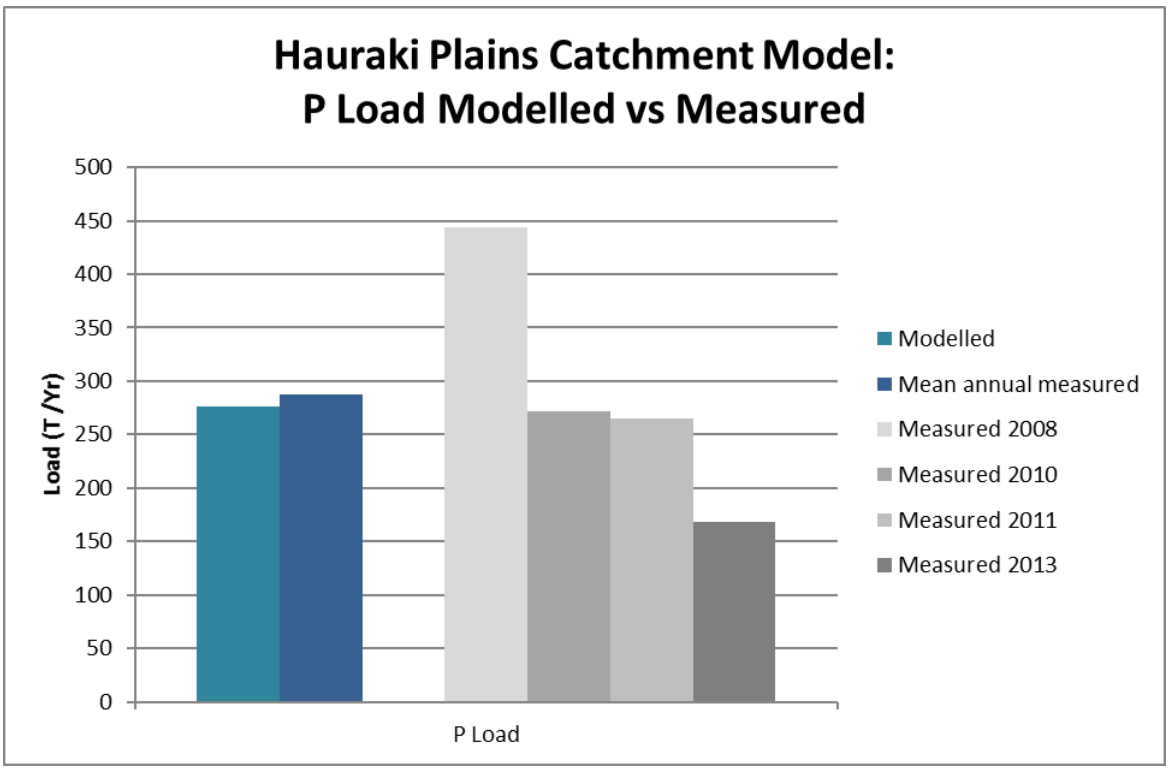

Figure 5.6 Comparison between mean annual measured and modelled total phosphorus load, based on the sum of all four downstream measurement stations (Te Aroha, Karangahake, Mellon Rd Rec and Paeroa-Tahuna Rd Br. The measured total annual load for individual years (2008, 2010, 2011 & 2013) is also shown.

After applying attenuation to the model input the default model setup per station shows a comparable result with the averaged year load derived from RLoadest results (Figure 5.7 and Figure 5.8). For TP in the Ohinemuri River, a clear under prediction is visible for both stations, which is likely caused by the extreme year 2008. At Mellon Rd Rec TP appears to be over predicted (Figure 5.8).

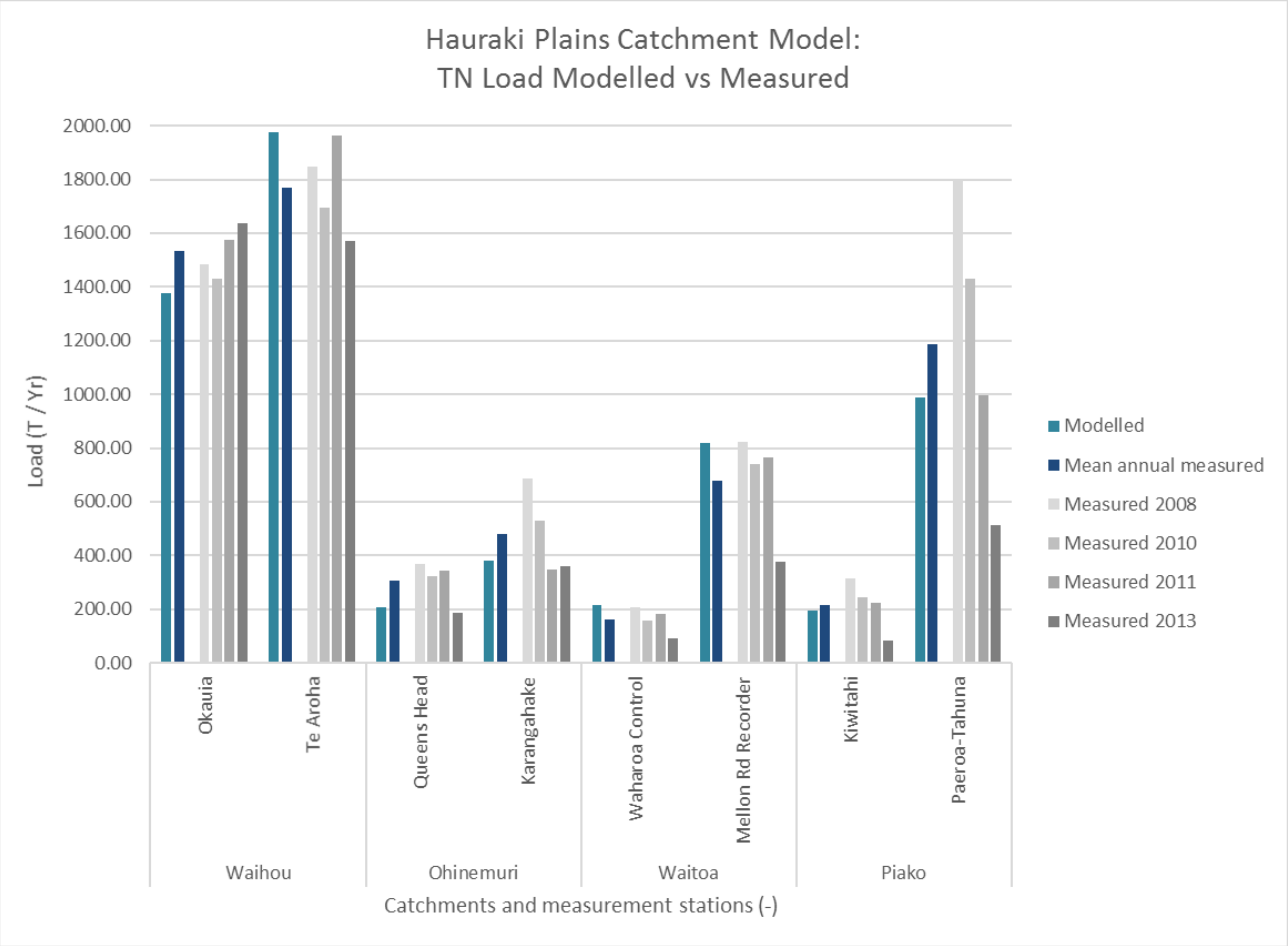

Figure 5.7 Nitrogen load of the default Hauraki Plains Model after attenuation spread out over the measurement stations and compared against average year load and RLoadest calculated loads for the calibration years 2008, 2010, 2011 and 2013.

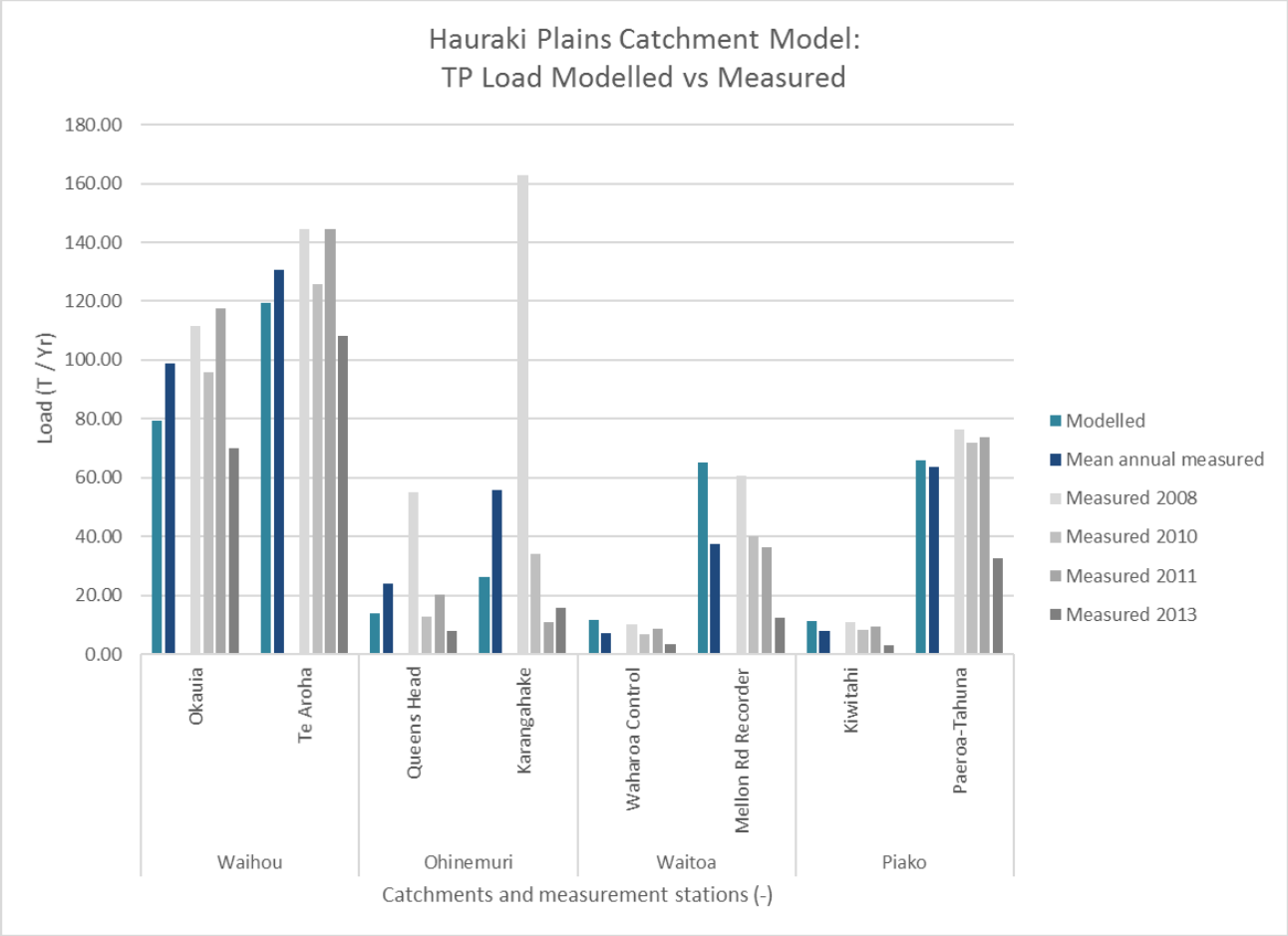

Figure 5.8 Phosphorus load of the default Hauraki Plains Model including phosphorus load from erosion spread out over the measurement stations and compared against average year load and RLoadest calculated loads for the calibration years 2008, 2010, 2011 and 2013.

5.8 Periodic and annual load distribution

The intention of the Hauraki Plains catchment study was to move towards a more temporally refined model output time step (i.e. monthly basis). However, as there is insufficient information on the specific land-use loads in space and time, it was not possible to use empirical spatial and time specific leaching losses by land-use within the model. Also there is insufficient information on the distribution of the flows and loads released by point sources to resolve these on a monthly basis.

To derive monthly time steps in model output the choice was made to divide 365-366 days into 12 equivalent length periods (periods of 30 days with the remaining 5-6 days assigned to the last period).

The Hauraki Plains catchment was split into 5 scaling zones based on the downstream measurement stations Te Aroha, Karangahake, Mellon Rd Rec and Paeroa-Tahuna Rd Br (Figure 5.9). The remaining area which was not upstream of any of these measurement stations was classified as Other (Figure 5.9).

In Section 3.5.2 the relation between measured flow and loads has been determined for downstream stations for the years 2005 - 2013. This relation was used to derive a formula to predict the load based on flow by approximating the relation with a line of best fit (see Figure 5.11, Figure 5.12 & Figure 5.13, Table 5.13, Table 5.14, Table 5.15). These formulas were specifically derived for each station and period to account for the effects of seasonality, for example due to rainfall distribution, management practices and uptake by plants. The flow-load rating curve for Other was derived by a flow weighted result of all four downstream measurement stations. The load-flow rating curves as derived from RLoadest results is shown in Appendix D.6 for load vs. flow per period.

The periodic load was determined per year by using the station-specific flow-load rating curves. As input for the flow the periodic WFLOW results for that specific year were used. These loads were than summed to a year load.

As there is insufficient data to distribute the point sources within and between years, the approach taken assumes point sources discharge an equivalent flow and load throughout the year. The approach also assumes that inter-annual variability is only due to variability in loads associated with anthropogenic land-uses. Therefore, Indigenous forest, Wetland, Shrub and springs were classified as background loads and their leaching loads are also kept constant within and between periods. The remaining load is assumed to be contributed by anthropogenic land-use and were assumed to vary in time.

By subtracting the load accounted for by sources other than anthropogenic land-use (background loads and point sources) per period, the load accountable to this land-use is determined. The calculated anthropogenic land-use load is compared to the default model anthropogenic land-use load (as shown in Table 5.11 and Table 5.12*)* to derive a scaling factor for each modelled year. The scaling percentage is used to scale the load contribution of anthropogenic land-uses to the model in comparison to the default setup (which are in Kg/Ha/Yr). Based on the distribution of the calculated periodic anthropogenic land-use load the input model is spread over the periods (Kg/Ha/Period). A schematic overview of this process is given in Figure 5.10.

As noted in Section 3.5.2, this step is underpinned by the statistically strong rating curve relationships at all 8 stations tested for both nitrogen and phosphorus, with exception of Ohinemuri River at Karangahake and at Queen’s Head for TP. This approach is underpinned on the assumption that the RLoadest rating curves offer sufficient coverage of the wide range in flows over the 9 years of monthly concentration sampling.

As the TP flow-load rating curve at Karangahake differs significantly from the patterns observed at other locations, this is further discussed in a separate Section 5.8.3.

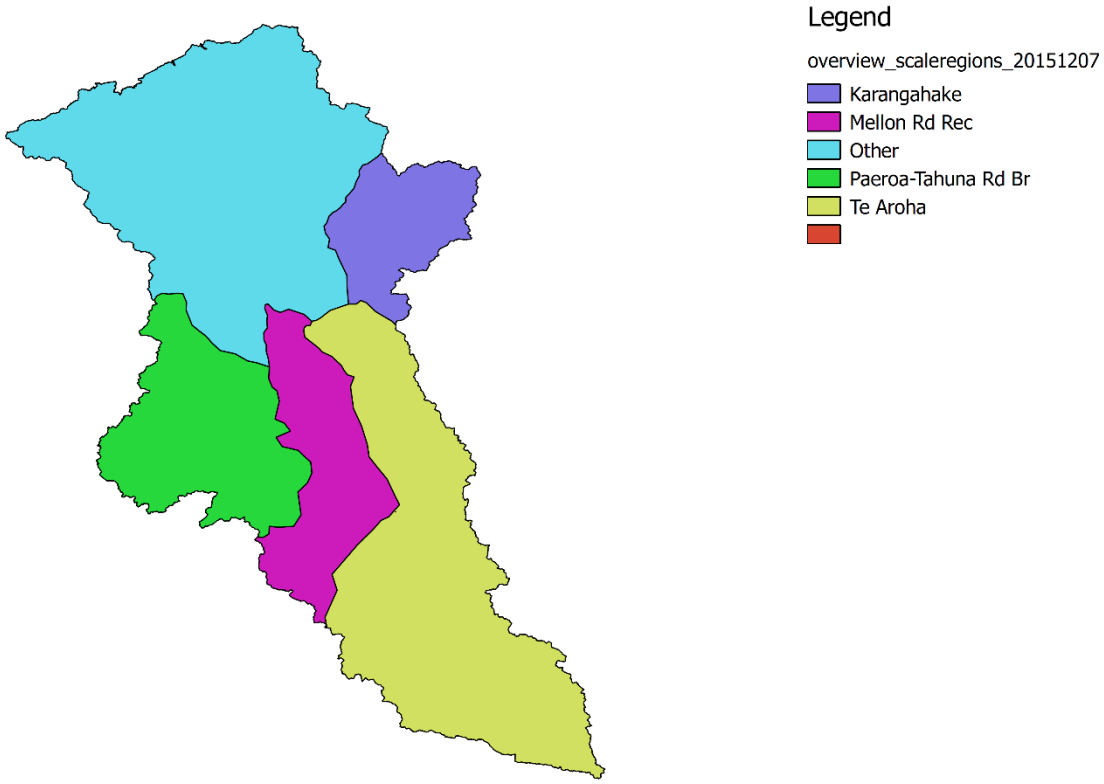

Figure 5.9 Overview of the scaling regions used to calibrate the water quality model. All land-uses within the region will be scaled to the flow-load relation derived per period from that catchment station. The region "Other" is scaled to the weighted average flow-load relation.

5.8.1 Anthropogenic land-use calculation

The load distributions as derived from the default Hauraki Plains catchment model setup and separated in the sources point source, background and anthropogenic land-use are quantified in Table 5.11 and Table 5.12.

Table 5.11 Loads originating from point sources, background and land-use per measurement location in Tons TN per year calculated from the default model setup.

Load (T TN / Year)	**Paeroa_Tahuna_RdBr**	**Mellon_RdRec**	**Te Aroha**	**Karangahake**
Point sources	16.80	64.99	87.73	14.71
Background	8.67	1.79	481.93	35.46
Land-use	983.06	805.23	1446.80	338.53
Sum	1008.52	872.01	2016.46	388.70

Table 5.12 Loads originating from point sources, background and land-use per measurement location in Tons TP per year calculated from the default model setup.

Load (T TP / Year)	Paeroa_Tahuna_RdBr	Mellon_RdRec	Te Aroha	Karangahake
Point sources	10.02	26.92	23.66	2.87
Background	0.81	0.04	6.93	3.45
Land-use	54.96	38.26	88.70	19.74
Sum	65.79	65.23	119.29	26.05

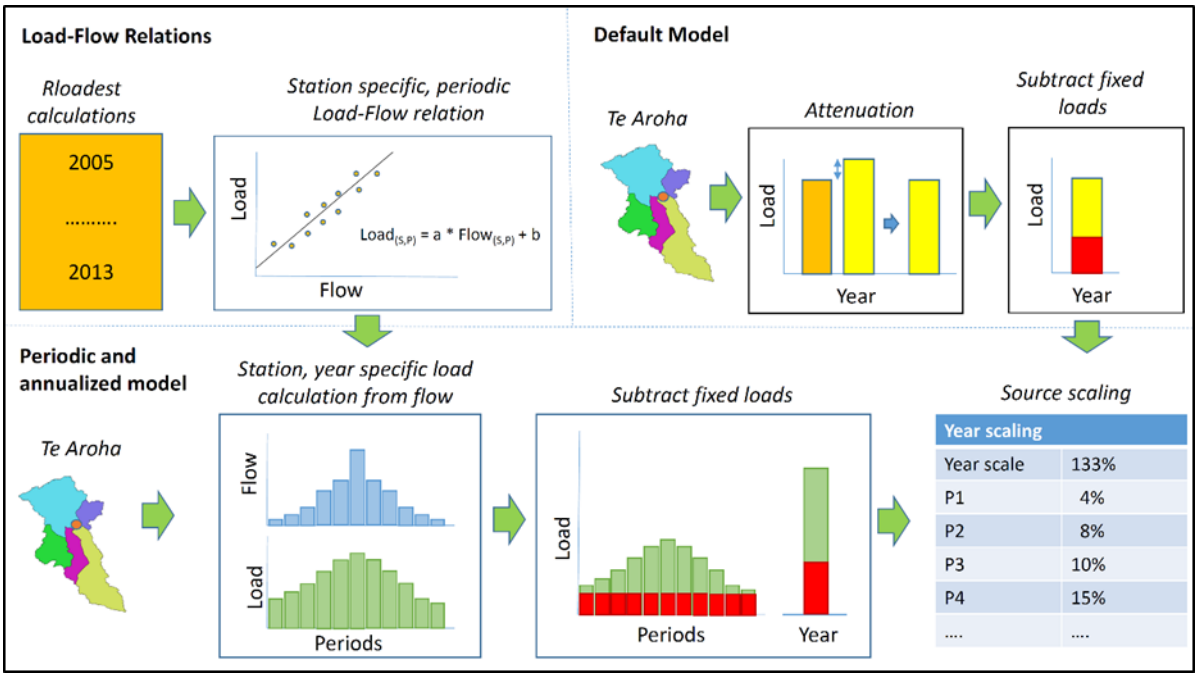

Figure 5.10 A schematic representation of the steps followed to create a periodic and yearly load distribution for each model year. In brief the steps taken were: (a) ***Load-Flow Relations*** *contains the load per flow per period relation derived for every station from year- period RLoadest results for the years 2005 till 2013. These formulas are used to calculate the period load per model year based on WFLOW flow results for that period. (b) The* ***Default Model*** *results in a modelled load, which scaled attenuation (only for TN) to the average RLoadest year load (data years 2008 till 2013). By subtracting the fixed loads (background and point sources) the default anthropogenic land-use load remains. (c) The* ***Periodic and annualized model*** *anthropogenic land-use loads are determined by scaling the default loads. With the Load-Flow relations the year specific periodic load distribution was calculated. After subtracting fixed loads (background and point sources) the anthropogenic land-use loads remain. The measured annual load is compared to the annual load of the default model, which results in a scaling percentage of the annual load. This scaling percentage is disturbed over the periods based on the proportion that they form within the annual load. After these period and yearly scaling percentages are derived they are applied to the anthropogenic land-use load input file which generates a year specific model setup.*

5.8.2 Flow-Load relationships

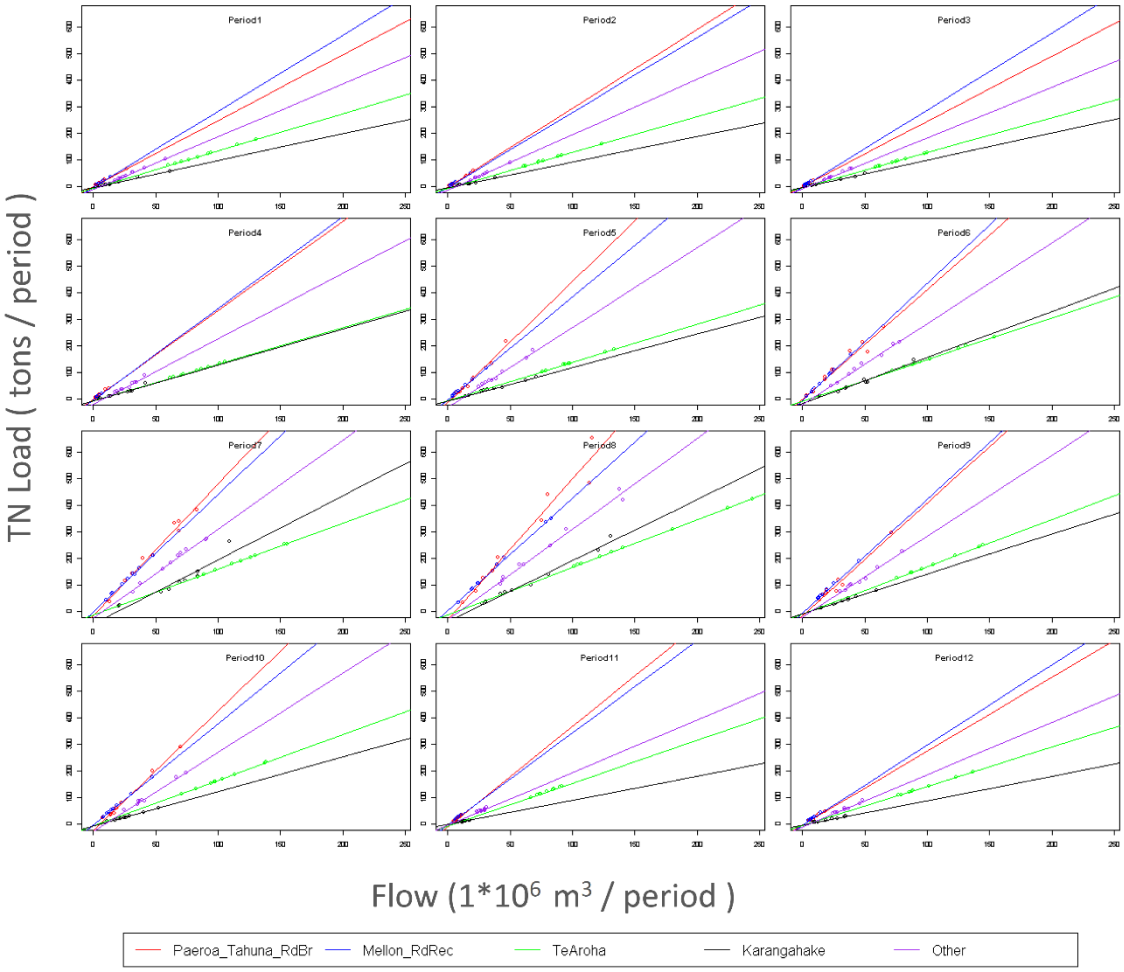

Figure 5.11 Linear total nitrogen load to flow relation for the measurement stations Paeroa-Tahuna Rd Br, Mellon Rd Rec, Te Aroha and Karangahake.

Table 5.13 Load total nitrogen in T derived from Flow (10^6 m^3/period). Do mind that the visualisation in the graphs is in Tons.These formulas are derived by approximating the flow-load relationships per period and per station with a linear line of best fit.

Period	Paeroa_Tahuna_RdBr	Mellon_RdRec	TeAroha	Karangahake	Other
1	2.49x - 1.28	2.87x - 3.24	1.4x - 7.33	1.01x - 5.07	1.99x - 12.35
2	2.98x - 2.67	2.83x - 2.83	1.35x - 7.57	0.97x - 5.67	2.09x - 15.33
3	2.45x - 0.63	2.91x - 2.5	1.32x - 5.84	1.02x - 4.54	1.91x - 8.98
4	3.36x - 2.32	3.46x - 3.47	1.37x - 7.17	1.36x - 8.43	2.46x - 19.58
5	4.57x - 13.74	3.88x - 3.65	1.44x - 6.67	1.27x - 8	3x - 30.57
6	4.12x - 0.2	4.41x - 4.94	1.57x - 8.19	1.74x - 19.18	3.05x - 20.47
7	4.97x - 15.57	4.44x - 1.97	1.73x - 13.84	2.41x - 46.77	3.34x - 24.24
8	5.31x - 30.46	4.25x + 2.65	1.79x - 12.23	2.31x - 38.93	3.41x - 30.05
9	4.25x - 16.14	4.28x - 4.75	1.78x - 9.85	1.51x - 10.91	3.05x - 21.52
10	4.5x - 24.23	3.82x - 4.06	1.73x - 9.13	1.3x - 8.97	2.99x - 28.57
11	3.8x - 10.31	3.49x - 4.77	1.62x - 7.09	0.91x - 3.7	1.98x - 3.93
12	2.78x - 4.23	3.02x - 4.13	1.48x - 7.01	0.91x - 4.64	1.97x - 11.12

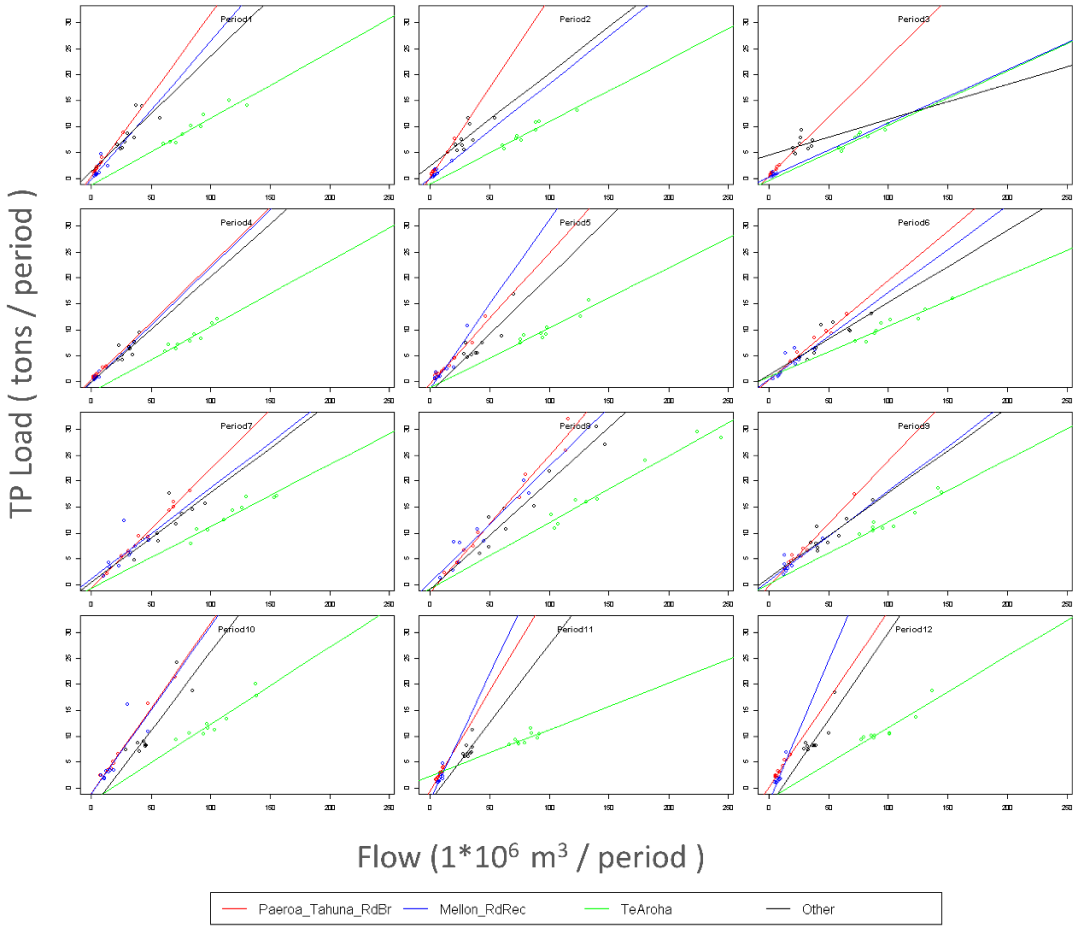

Figure 5.12 Linear total phosphorus load to flow relation for the measurement stations Paeroa-Tahuna Rd Br, Mellon Rd Rec and Te Aroha. Karangahake is excluded from this graph as this location has an exponential relation.

Table 5.14 Load total phosphorus in T derived from Flow (10^6 m^3/period). Karangahake is excluded from this graph due to the strong exponential relationship. Karangahake could not be captured by the direct relationship to flow. Based on these relations the WFLOW result will be used to scale the load for the different years and periods in the WFD-Explorer model. For predicting the TP load at Karangahake another approach is used.

Period	Paeroa_Tahuna_RdBr	Mellon_RdRec	TeAroha	Other
1	0.31x + 0.58	0.27x - 0.05	0.13x - 1.22	0.22x + 1.44
2	0.35x + 0.32	0.18x + 0.14	0.12x - 1.06	0.18x + 2.45
3	0.23x + 0.48	0.1x + 0.26	0.11x - 0.35	0.07x + 4.56
4	0.22x + 0.33	0.22x - 0.2	0.13x - 2.16	0.2x + 0.02
5	0.25x - 0.39	0.33x - 1.21	0.12x - 1.28	0.22x - 1.91
6	0.19x + 0.32	0.17x + 0.48	0.1x + 0.84	0.14x + 1.38
7	0.23x - 0.61	0.18x + 1.17	0.12x - 0.64	0.17x + 0.49
8	0.26x - 1.36	0.22x + 0.54	0.13x - 0.81	0.21x - 0.83
9	0.24x - 0.18	0.17x + 0.9	0.12x + 0.14	0.16x + 1.4
10	0.33x - 0.93	0.32x - 1	0.15x - 2.46	0.3x - 3.99
11	0.38x - 0.42	0.48x - 2.08	0.09x + 2.29	0.3x - 2.37
12	0.34x + 0.33	0.54x - 2.38	0.14x - 2.22	0.33x - 3.45

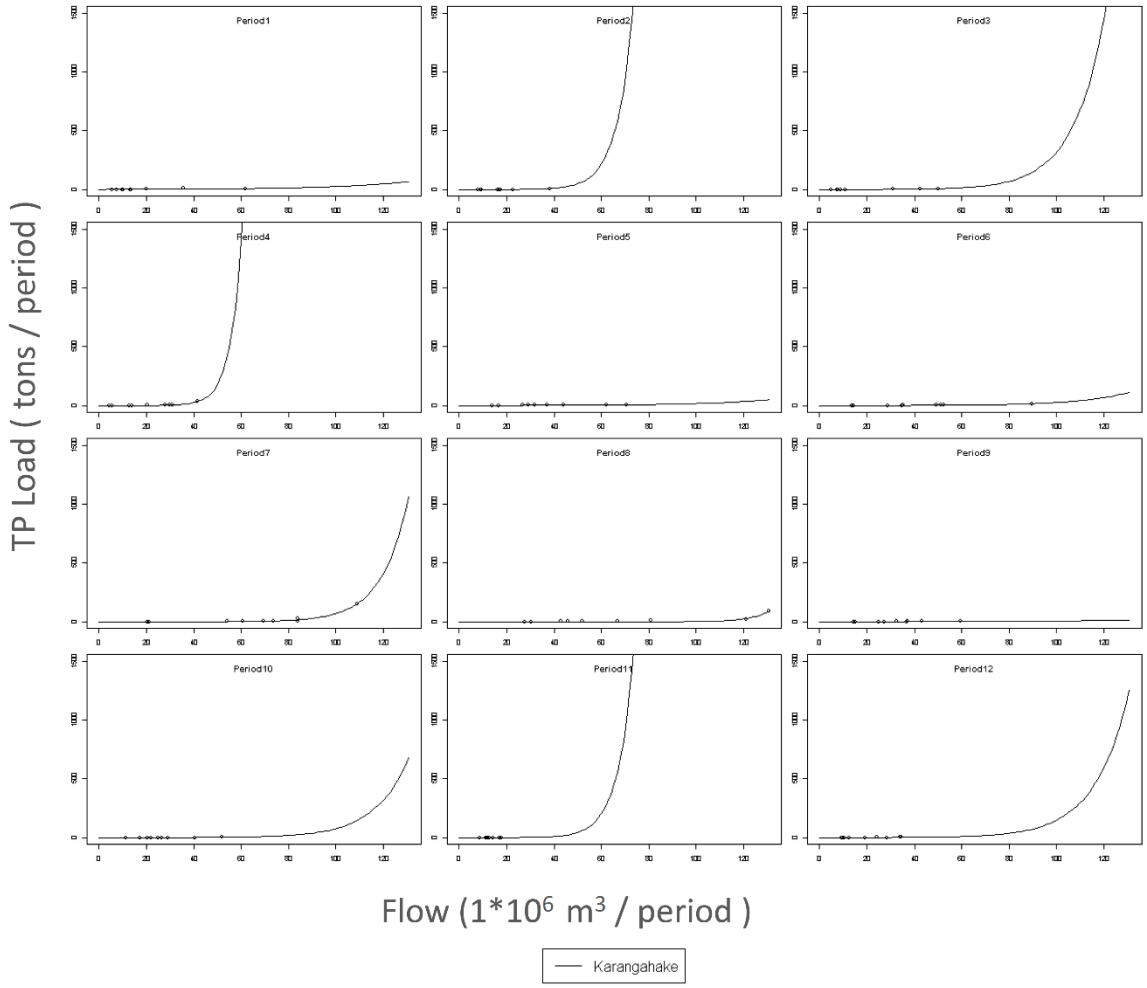

Figure 5.13 Exponential phosphorus load to flow relation for the measurement station Karangahake.

Table 5.15 Load Phosphorus in T derived from Flow (10^6 m^3/period).

Period	Karangahake
1	1.12 * exp(0.03x)
2	3.13E-02 * exp(0.15x)
3	1.67E-01 * exp(0.08x)
4	6.78E-03 * exp(0.2x)
5	4.70E-01 * exp(0.04x)
6	1.83E-01 * exp(0.05x)
7	9.22E-03 * exp(0.09x)
8	2.11E-05 * exp(0.12x)
9	4.64E-01 * exp(0.03x)
10	7.10E-02 * exp(0.07x)
11	2.39E-02 * exp(0.15x)
12	1.47E-01 * exp(0.07x)

5.8.3 Karangahake : Flow-load relationship TP

The total phosphorus load for Karangahake appears to be significantly influenced by high flows (Figure 5.13). The data depicts an exponential relationship. Therefore, the flow-load rating curve at Karangahake was derived using an exponential relation in contrary to the other locations (Table 5.15). The reason that this exponential relation is required is that the exact source of this increase of phosphorus was not investigated in this study.

5.8.4 Final anthropogenic land-use scaling factors

For each station the load was calculated using the flow-load rating curve in combination with the periodic yearly WFLOW flow results. These flow-load results have been derived for the total load at the station. To derive the anthropogenic fraction of the load the evenly distributed loads originating from point sources and background loads were subtracted. In most cases this subtraction left a remaining load that could be attributed to the anthropogenic land-use. However, for total phosphorus at Mellon Rd Rec and Karangahake this resulted in several periods with a negative load. To correct for these negative loads a zero anthropogenic load was implemented in these instances. For TP at Karangahake negative loads were so severe that this approach would lead to only a few periods per year with a positive anthropogenic load. Therefore, the default TP load input was used for Karangahake in all modelled years.

The periodic flow-load relationships are used to determine the assumed load for the different years. In this case a scaling percentage of 100% means that the anthropogenic land-use load source stays the same as the default model setup, where >100% means that the allocated load increases and <100% a decrease of the allocated load. These percentages are then distributed over the periods based on the portion of load calculated for that specific period. Please note that the percentages of the periods add up to the calculated scaling percentage for that specific year.

The percentages with which the default anthropogenic land-use loads needed to be calibrated for TN varied between measurement stations with at Te Aroha 105 – 135%, at Karangahake 41 – 103%, at Paeroa-Tahuna Rd Br 85% -162%, at Mellon Rd Rec 102 – 156% and at Other 71-109%. In Table 5.16 an example is shown for Te Aroha (see Appendix J for all anthropogenic land-use scaling).

Table 5.16 Scaling of nitrogen land-use loads in percentage for Te Aroha compared with the default Hauraki Plains catchment model anthropogenic load input.

Nitrogen scaling (%)	Period1	Period2	Period3	Period4	Period5	Period6	Period7	Period8	Period9	Period10	Period11	Period12	Total
2008	2.36	2.19	2.23	7.19	11.53	11.80	20.16	35.27	13.21	10.61	5.74	4.61	126.87
2009	3.70	4.98	4.14	4.12	7.62	10.30	17.70	19.03	12.51	18.95	5.86	6.72	115.64
2010	3.21	5.23	2.46	2.64	9.44	16.58	12.44	25.98	24.07	8.77	4.64	3.89	119.34
2011	9.74	3.68	5.21	5.63	11.86	17.85	21.53	10.21	8.72	7.59	4.68	7.91	114.61
2012	6.98	3.92	5.78	4.86	9.23	8.80	20.90	38.15	15.62	8.56	5.55	7.34	135.70
2013	2.89	2.25	2.29	6.43	12.17	16.52	10.65	13.57	15.02	9.31	7.12	7.36	105.58

The percentages with which the default anthropogenic land-use loads needed to be calibrated for TP varied between measurement stations with at Te Aroha 145 – 170%, at Paeroa-Tahuna Rd Br 78% -150%, at Mellon Rd Rec 88 – 149% and at Other 129-175%. In Table 5.17 an example is shown for Te Aroha (see Appendix J for all anthropogenic land-use scalings). The scaling percentage of Karangahake was kept at 100% for all modelled years. The periodic distribution of anthropogenic loads for Karangahake was scaled to the periodic WFLOW flow distribution at this station.

Table 5.17 Scaling of phosphorus land-use loads in percentage for Te Aroha compared with the default Hauraki Plains catchment model anthropogenic load input.

Phosphorus scaling (%)	Period1	Period2	Period3	Period4	Period5	Period6	Period7	Period8	Period9	Period10	Period11	Period12	Total
2008	5.03	4.59	4.75	11.64	16.42	14.32	24.00	42.86	16.16	14.86	8.32	7.94	170.89
2009	7.06	8.64	7.35	6.89	11.11	12.77	21.21	23.63	15.39	26.66	8.44	11.12	160.27
2010	6.32	9.00	5.06	4.59	13.58	19.29	15.26	31.86	28.10	12.26	7.33	6.76	159.41
2011	16.21	6.75	8.80	9.22	16.87	20.61	25.55	13.18	11.22	10.60	7.36	12.97	159.34
2012	12.04	7.11	9.57	8.03	13.29	11.21	24.83	46.28	18.80	11.97	8.15	12.16	183.45
2013	5.84	4.68	4.83	10.45	17.29	19.22	13.24	17.16	18.15	13.03	9.57	12.12	145.59

5.9 Validation of final model set up

5.9.1 Validation approach

For the validation of the nutrient load prediction of the Hauraki Plains Catchment model the years 2009 and 2012 were used. The loads calculated for these years were not used in the water quality model calibration. The model was calibrated on loads, but in the validation model performance will also be assessed based on concentrations. In addition, the flow results have been translated from a daily time step in WFLOW to a periodic time step in the WFD Explorer. To validate whether these results were correctly translated, the measured flow, WFLOW results and the WFD Explorer flow were compared per period for the modelled years (2008 till 2013).

An overall statistical performance analysis for periodic and mean annual load prediction is presented in Section 5.9. As this analysis considers all years modelled with the WFD Explorer, this analysis has been included in a separate section.

5.9.2 Validation of coupled flow model schematisation

The WFD Explorer model flow simulations were validated against the WFLOW model and measured flow (Appendix E.1,Table 5.18). When comparing the WFD Explorer to WFLOW outflow it is apparent that the Waihou River deviates most (Nash-Sutcliffe = 0.78, RVE = -0.04, COF = 0.09). A comparison between WFD Explorer output to the measured flow the Waihou River is also poor, especially at Site Okauia (NS = -2.21, RVE = 0.11, COF = 0.90). Okauia was not included in the comparison in Section 4.5.1, but the offset is most likely due to similar causes as at Pinedale, with an overestimation of flow by WFLOW due to the inability of the model to capture complex hydrological processes associated with underlying aquafers.

Overall the WFD Explorer model has good predictive capability for flow (NS = 0.86, RVE = 0.04, COF = 0.07) and the partitioning of the WFLOW results to the WFD-Explorer schematisation is done accurately (NS = 0.99, RVE = 0.04, COF = 0.03).

Table 5.18 Validation of the WFD Explorer model flow results against the WFLOW model results and measured flow. The validation is based on the Nash-Sutcliff (NS), Relative Volume Error (RVE) and Coefficient of Fit (COF) statistics. These statistics are described in Section 4.4.1.

		WFD Explorer vs. WFLOW				WFD Explorer vs. Measured flow			
Catchment	**Station**	**NS**	**RVE**	**COF**	**Performance rating**	**NS**	**RVE**	**COF**	**Performance rating**
Waihou	Okauia	0.81	0.04	0.08	Very good	-2.21	0.11	0.90	Unsatisfactory
	Te Aroha	0.89	0.04	0.06	Very good	0.04	0.05	0.28	Good
Ohinemuri	Queens-Head	0.99	0.04	0.03	Very good	0.54	-0.20	0.27	Good
	Karangahake	0.97	0.07	0.06	Very good	0.44	-0.17	0.27	Good
Waitoa	Waharoa Control	0.97	0.04	0.04	Very good	0.51	0.27	0.32	Good
	Mellon Rd Recorder	0.98	0.01	0.01	Very good	0.28	0.19	0.32	Good
Piako	Kiwitahi	0.98	0.08	0.06	Very good	0.85	0.09	0.11	Very good
	Paeroa-Tahuna	0.99	0.02	0.02	Very good	0.82	0.11	0.13	Very good
Outflow	Waitakaruru	0.96	0.07	0.07	Very good	-	-	-	-
	Piako	0.98	0.01	0.01	Very good	-	-	-	-
	Waihou	0.78	-0.04	0.09	Very good	-	-	-	-
Overall	All stations	0.99	0.04	0.03	Very good	0.86	0.04	0.07	Very good

5.9.3 Load validation

The analysis of statistical performance for periodic and annual load prediction for the Hauraki Plains catchment model is presented in Section 5.9. In this section the load prediction for the years 2009 and 2012 is visually assessed.

As a first step the RLoadest results for the validation years 2009 and 2012 were compared with other load calculating techniques (Flow-Weighted and Beale-Ratio calculation). This is the same approach as what was followed in Stephens (2015). This comparison shows a large difference for the year 2012 at measurement station Karangahake (see Appendix E.2).

To further validate the water quality model the periodic attenuated TN and TP load output was compared with the calculated load by RLoadest. As the RLoadest calculations were made with a relatively small sample of water quality measurements (n = 12 per year), the RLoadest model shows that the calculated monthly loads are quite uncertain, especially during high flow periods. This uncertainty has been incorporated in the graphical validation to give a better idea of the data on which the model is calibrated and validated (Figure 5.14 and Figure 5.15).

In this section only the downstream measurement stations are represented and only the validation years 2009 and 2012 are shown. The visual assessments of the other measurement stations and years are shown in Appendix E.2.

TN

Depending on the validation year, TN loads varied by up to 50% compared with the loads calculated with RLoadest. This variation is highest at Karangahake, with a variation of 30% at Te Aroha, 20% at Mellon Rd Rec and >5% at Paeroa-Tahuna Rd Br. Figure 5.14 shows that the measurement stations at Te Aroha and Mellon Rd have a clear over prediction during high flow periods. Karangahake is under predicted by the model during high flow periods.

TP

Simulated TP load varied by up to 80% compared with the loads calculated with RLoadest. As for TN, this variation is highest at Karangahake, with a variation of 50% at Mellon Rd Rec, 30% at Te Aroha, and 5% at Paeroa-Tahuna Rd Br. Figure 5.15 shows that for station Te Aroha the model over predicts TP during high flow periods but station Mellon Rd Rec over predicts during low flow periods. At Karangahake loads are predicted well, with the exception for the load prediction for Period 7 in 2012 (see Figure 5.15).

The difference between the modelled mean annual load and RLoadest calculated annual load at Karangahake for year 2012 is most likely due to errors with the RLoadest calculation, as described before (see Section 3.5).

See Appendix E.2 for the RLoadest model boundaries.

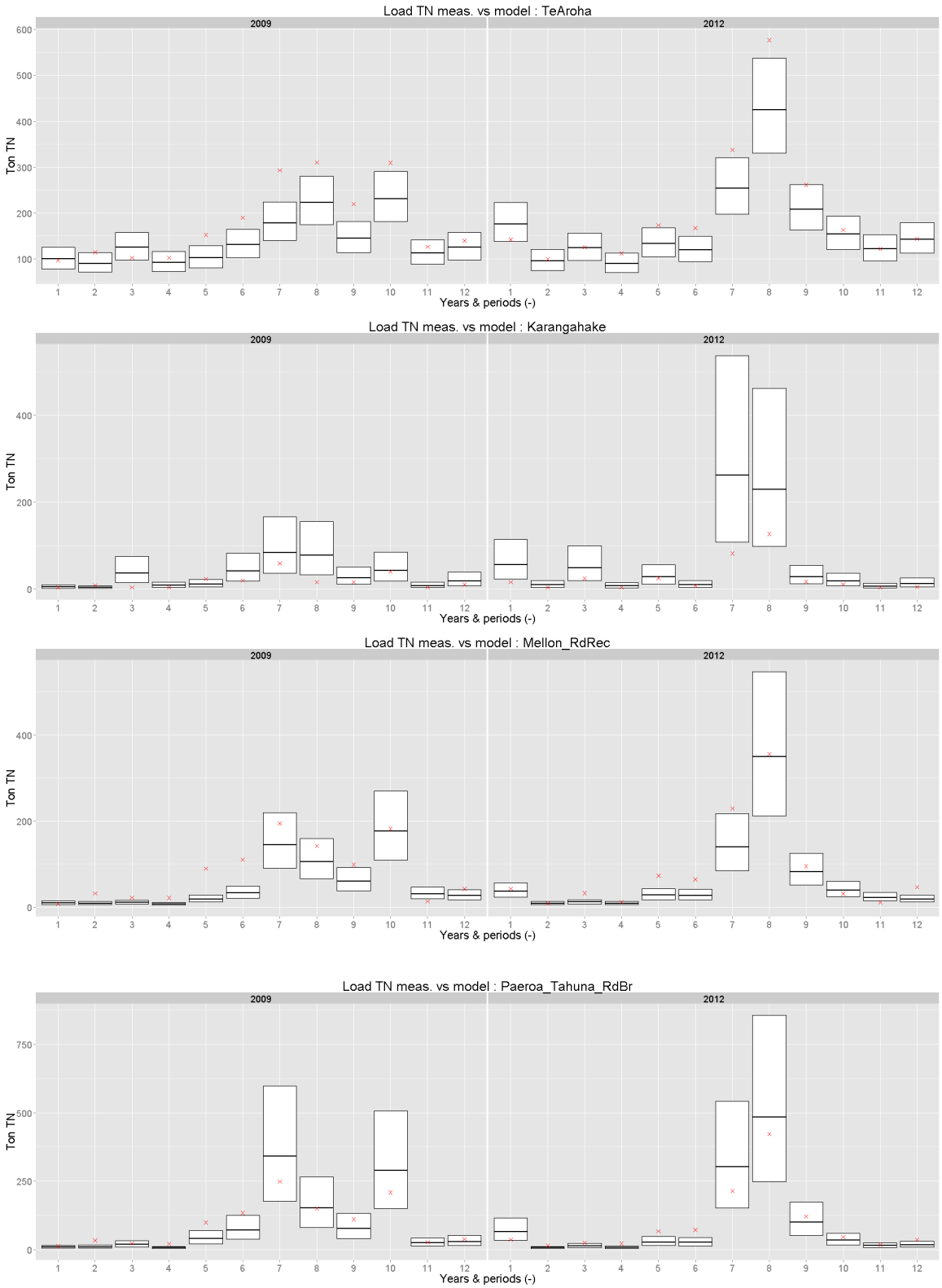

Figure 5.14 Measured (RLoadest) and modelled nitrogen load results for validation years 2009 and 2012 for the stations Te Aroha, Karangahake, Mellon Rd Rec and Paeroa-Tahuna Rd Br (top to bottom). In this graph the Hauraki Plains water quality model (red cross) is compared with the RLoadest load prediction (black line in middle of the bar) and the 95% certainty of the prediction (top bar to bottom bar) for all the years that the model predicts.

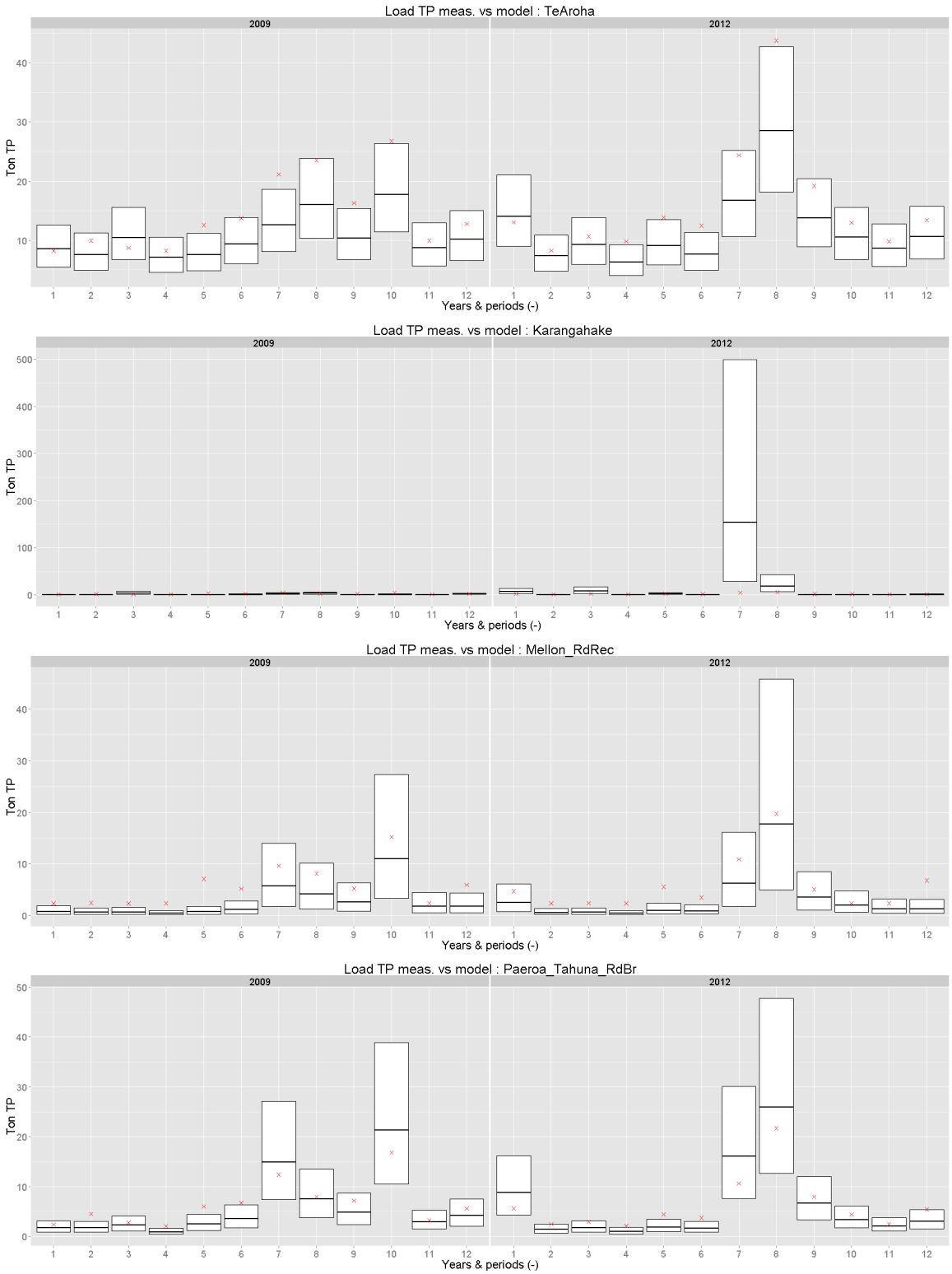

Figure 5.15 Measured (RLoadest) and modelled phosphorus load results for validation years 2009 and 2012 for the stations Te Aroha, Karangahake, Mellon Rd Rec and Paeroa-Tahuna Rd Br (top to bottom). In this graph the Hauraki Plains water quality model (red cross) is compared with the RLoadest load prediction (black line in middle of the bar) and the 95% certainty of the prediction (top bar to bottom bar) for all the years that the model predicts.

Table 5.19 Calibrated mean annual TN and TP loads modelled with the WFD-Explorer for all study years.

Year	Nitrogen Load				Phosphorus Load			
	Modelled by WFD-Explorer per station (ton / yr)				Modelled by WFD-Explorer per station (ton / yr)			
	Te Aroha	Karangahake	Paeroa-Tahuna Rd br	Mellon Rd Rec	Te Aroha	Karangahake	Paeroa-Tahuna Rd Br	Mellon Rd Rec
2008	2313.15	392.52	1551.94	1268.69	181.22	26.42	93.04	84.38
2009	2153.88	211.04	1101.62	949.72	171.61	26.23	77.55	68.07
2010	2207.86	338.04	1237.09	1113.78	169.66	26.28	76.83	70.57
2011	2141.04	245.08	1092.12	982.28	169.87	26.50	78.41	72.55
2012	2423.73	330.05	1092.18	997.15	191.40	26.44	73.68	67.80
2013	2013.54	189.93	829.25	853.36	157.73	26.15	53.61	61.01

Table 5.20 Percentage difference to calculated RLoadest loads. The average, minimum and maximum have been shown per measurement station over the years. The range is the difference between minimum and maximum.

Year	Nitrogen Load				Phosphorus Load			
	Percentage difference WFD-Explorer Load to Rloadest Load per station (%)				Percentage difference WFD-Explorer Load to Rloadest Load per station (%)			
	Te Aroha	Karangahake	Paeroa-Tahuna Rd br	Mellon Rd Rec	Te Aroha	Karangahake	Paeroa-Tahuna Rd Br	Mellon Rd Rec
2008	25.13	-36.94	11.61	54.36	25.73	-75.17	21.54	84.86
2009	30.12	-42.07	3.45	51.40	36.33	93.53	13.71	119.16
2010	28.78	-28.62	1.62	50.29	35.17	10.59	6.72	118.26
2011	7.26	-47.21	-4.41	28.32	17.90	-5.02	6.43	122.33
2012	18.63	-54.03	-0.07	29.57	34.61	-86.09	0.28	80.26
2013	24.63	-43.27	91.64	125.74	46.66	55.05	64.53	244.87
AVERAGE	22.42	-42.02	17.31	56.61	32.73	-1.18	18.87	128.29
MIN	7.26	-54.03	-4.41	28.32	17.90	-86.09	0.28	80.26
MAX	30.12	-28.62	91.64	125.74	46.66	93.53	64.53	244.87
RANGE	22.86	25.41	96.04	97.42	28.77	179.63	64.25	164.60

5.9.4 Validation of in-stream concentrations

In-stream TN and TP concentrations were validated by comparing model concentration output with the RLoadest calculations based on discrete monitoring data as input (see Section 3). The actual water quality measurements were not used as these represent only monthly measurements and are highly dependent on the amount of flow at the time of sampling.

Total nitrogen

As shown in Figure 5.16, TN concentration results show a high comparison to the mean concentration calculated from the load calculations by RLoadest, and seem to be well-correlated with the monthly water quality measurements. The results show a clear seasonal pattern with low concentrations in summer (January-April) and higher concentrations during winter (June-September) at most locations. At Karangahake and in Paeroa-Tahuna Rd Br, the variation between modelled and measured concentration is much greater.

At Paeroa-Tahuna Rd Br the cause of high variability is uncertain. However as only one measurement per month is taken this may be due to a measurement error or sample bias towards low flow conditions.

Total phosphorus

As shown in Figure 5.17, TP concentration results show a high degree of similarity with mean concentration as calculated from the load calculations by RLoadest. This appears to be well-correlated with the monthly water quality measurements for all stations except Karangahake and Mellon Rd Rec. At Te Aroha there seems to be no or very low seasonal variability in TP concentration.

Modelled concentrations at measurement station Karangahake show a poor representation of the RLoadest calculations, as the load distribution was based solely on the flow results of WFLOW as the exponential load prediction formula minus point sources and background load, which delivered negative load values. Therefore, the load remained constant throughout each year even though the total flow quantity varies.

The measurement station Mellon Rd Rec also shows a poor representation. The cause for the negative load is similar to the explanation at Karangahake, however as most periods did not end up to be a negative load value, the anthropogenic loads have been scaled to zero where negative load values applied (instead of replacing the yearly input load by the default load scaled to the flow results).

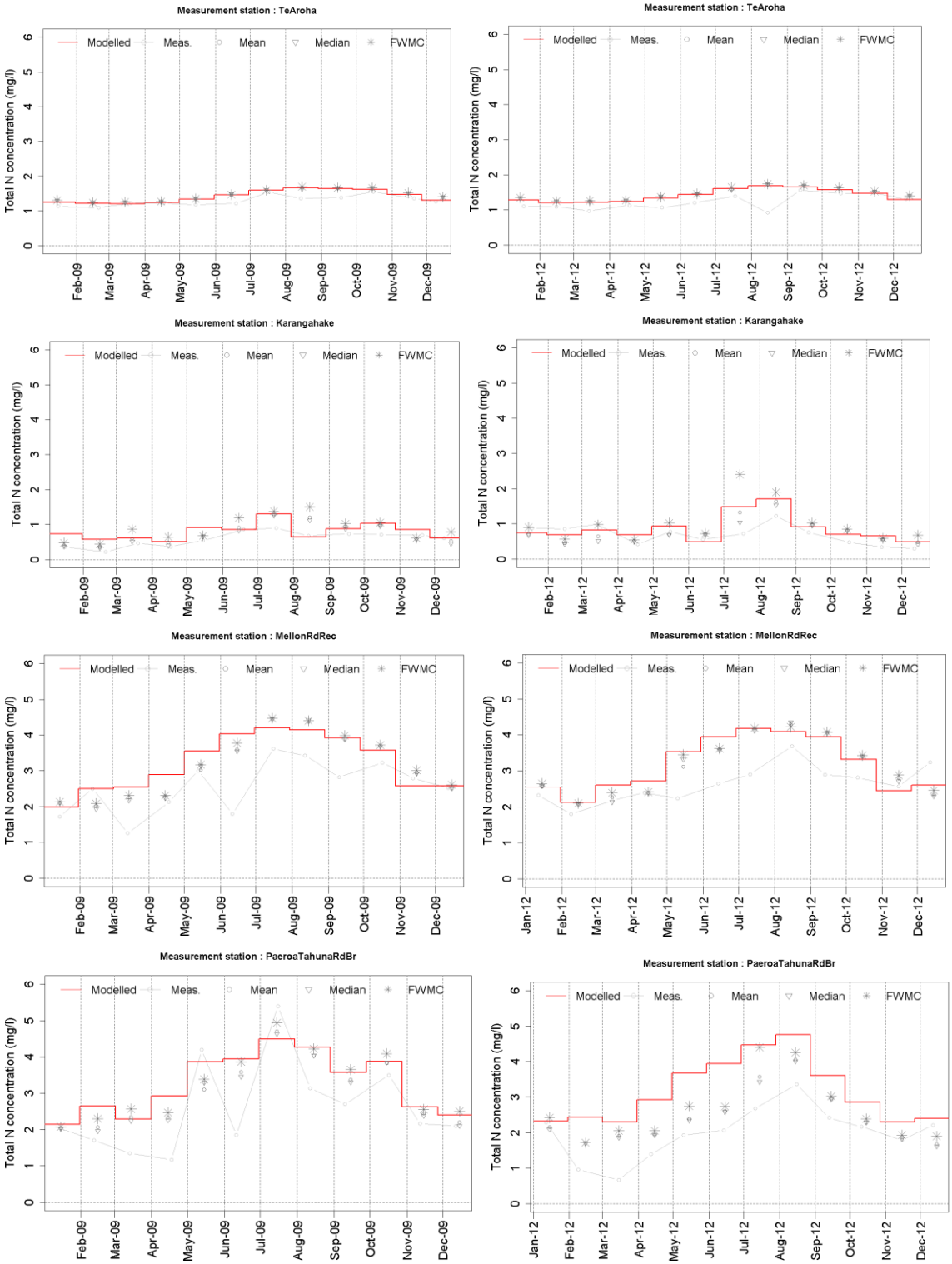

Figure 5.16 Measured (RLoadest daily calculation) and modelled total nitrogen concentration results for validation years 2009 and 2012 at the downstream measurement stations Te Aroha, Karangahake, Mellon Rd Rec and Paeroa-Tahuna Rd Br.

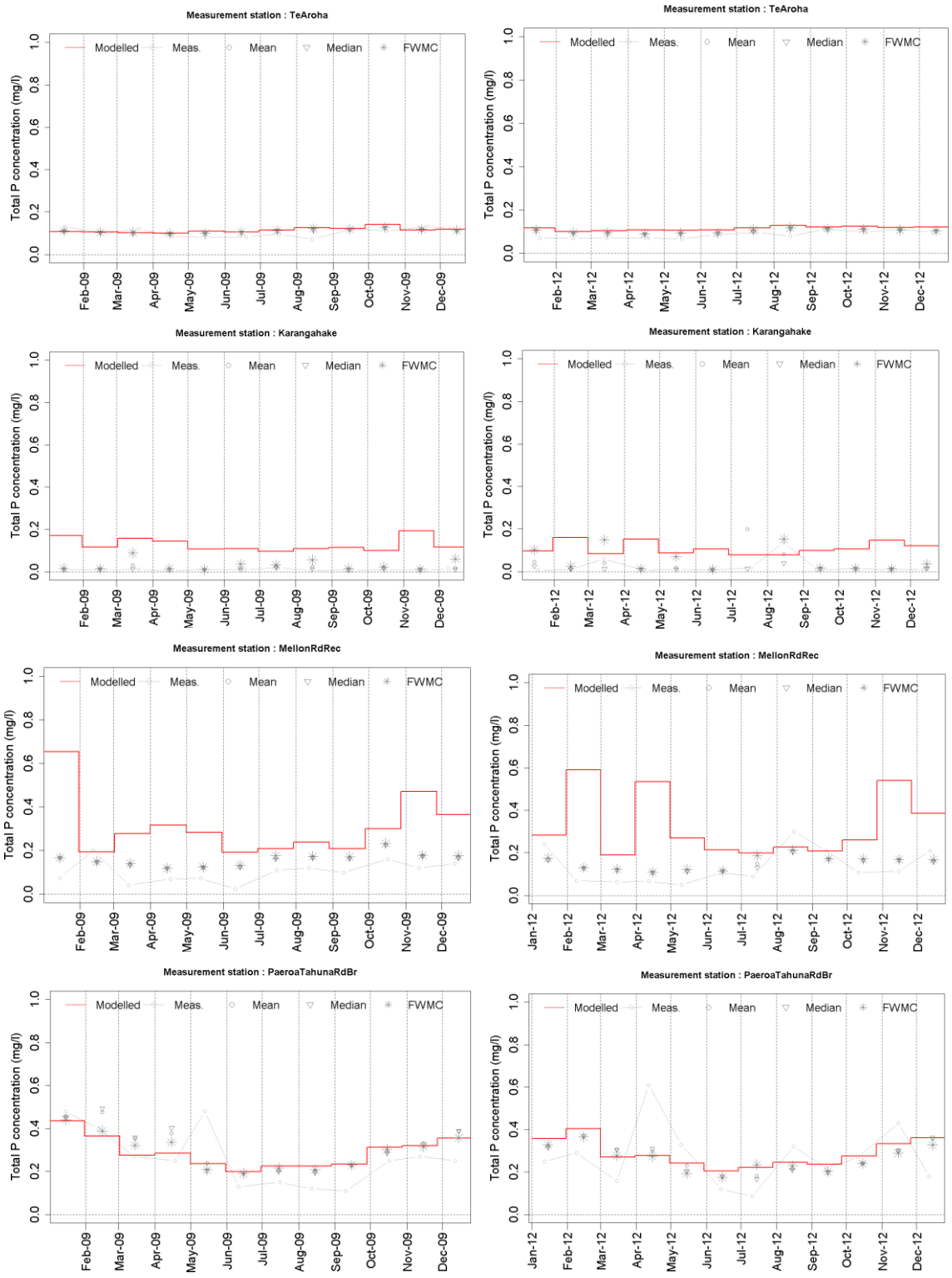

Figure 5.17 Measured (RLoadest daily calculation) and modelled total phosphorus concentration results for validation years 2009 and 2012 at the downstream measurement stations Te Aroha, Karangahake, Mellon Rd Rec and Paeroa-Tahuna Rd Br. In Karangahake July 2012 a Flow Weighted Mean Concentration of 1.4 was calculated, which is not visible in the plot due to the scale of the y-axis.

5.10 Statistical evaluation of model performance

To give a value criterion to how the model performs, a statistical analysis of model performance was undertaken to assess the ability of the model to predict periodic loads and annual loads. For this analysis the r-squared (r^2), Nash-Sutcliff coefficient (NS, described in Section 4.4.1), unbiased root-mean square difference (uRMSD), the normalised model bias (uBias) and the root-mean square error (RMSE) were reported for the 8 water quality measurement stations. The uRMSD and uBias were both used with a conservative approach to give a performance rating to each of these stations in terms of the ability to predict period loads and annual loads.

The RMSE (Equation 5-1) is a common statistic routinely used to compare water quality models. This statistic gives an indication of differences between the modelled and measured values. The closer the RMSE gets to zero for each parameter, the better the model is considered to be for simulating the measurements. However, the range of the RMSE result is dependent on the nature of the data. For example, the same model performance for higher loads would therefore result in a higher RMSE. Hence, this statistic should be used carefully in model comparisons.

Equation 5-1 The root-mean square error (RMSE).

$$RMSE = \sqrt{\frac{1}{N}\sum_{n=1}^{N}[(M_n \cdot D_n)^2]}$$

where:
D = measurements
M = modelled
n = index number
N = number of sample size

The r-squared (Equation 5-2) is only valid if the model is able to replicate the observations exactly, and not whether the model has a consistent bias for over or under prediction due to a constant offset while observed trends are simulated accurately. This statistic only provide an indication whether the simulated result is exactly the same as the observed result ($R^2 = 1.0$).

Equation 5-2 The r-squared (R^2).

$$R^2 = \left(\frac{\frac{1}{N-1}\sum_{n=1}^{N}[(M_n - \bar{M}) - (D_n - \bar{D})]}{\sigma_M \cdot \sigma_D}\right)^2$$

The Nash-Sutcliff statistic is not corrected for sample size. Therefore, a low sample size (n) with the same values as a larger sample size could lead to lower scores. The Nash-Sutcliff coefficient is described in Section 4.4.1.

Los and Blaas (2010) have described a combination of two statistics, uRMSe (Equation 5-3) and nBias (Equation 5-4), that together describe the overall accuracy of water quality model performance. Both statistics are corrected for the number of observations and the range of values. The uRMSE gives insight in how well the model follows the relationship and the nBias gives insight in whether there is a constant over or under prediction of the model. In the same paper a performance rating was proposed.

Equation 5-3 The unbiased root-mean square difference (uRMSD; Los and Blaas(2010)).

$$uRMSD = \frac{sign(\sigma_M - \sigma_D)}{\sigma_D} \sqrt{\frac{\sum_{n=1}^{N}[(M_n - \bar{M}) - (D_n - \bar{D})]^2}{N}}$$

Equation 5-4 The normalised model bias (nBias; Los and Blaas(2010)).

$$nBias = \frac{\bar{M} - \bar{D}}{\sigma_D}$$

Table 5.21 Performance rating derived from the uRSMD and nBias, as described in Los and Blaas (2010).

Performance rating	uRSMD	nBias
Very good	±0.20 > X	±0.20 > X
Good	±0.74 > X	±0.74 > X
Reasonable	±1.00 > X	±1.00 > X
Poor	X > ±1.00	X > ±1.00

5.10.1 Statistical results

Overall the statistics results for periodic model performance are considered good for predicting TN and reasonable for TP load (Tables 5.22 and 5.23). Model performance is also considered reasonable for TN and good for TP annual loads.

When the model performance is assessed per individual station, models prediction overall is mostly good for TN and reasonable or good for TP for periodic loads. Mellon Rd Rec performs poor for the periodic prediction of TP loads. However, when model performance is assessed per station for annual load the model shows a generally poor performance for TN, with the exception of the Piako River, which performs good. The annual prediction of TP is also poor, with the exception of stations in the Ohinemuri River, which are reasonable, and the measurement station Paeroa-Tahuna Rd Br (Piako river) which is good. A more detailed understanding of the reasons for poor model performance is described in Section 5.10.2.

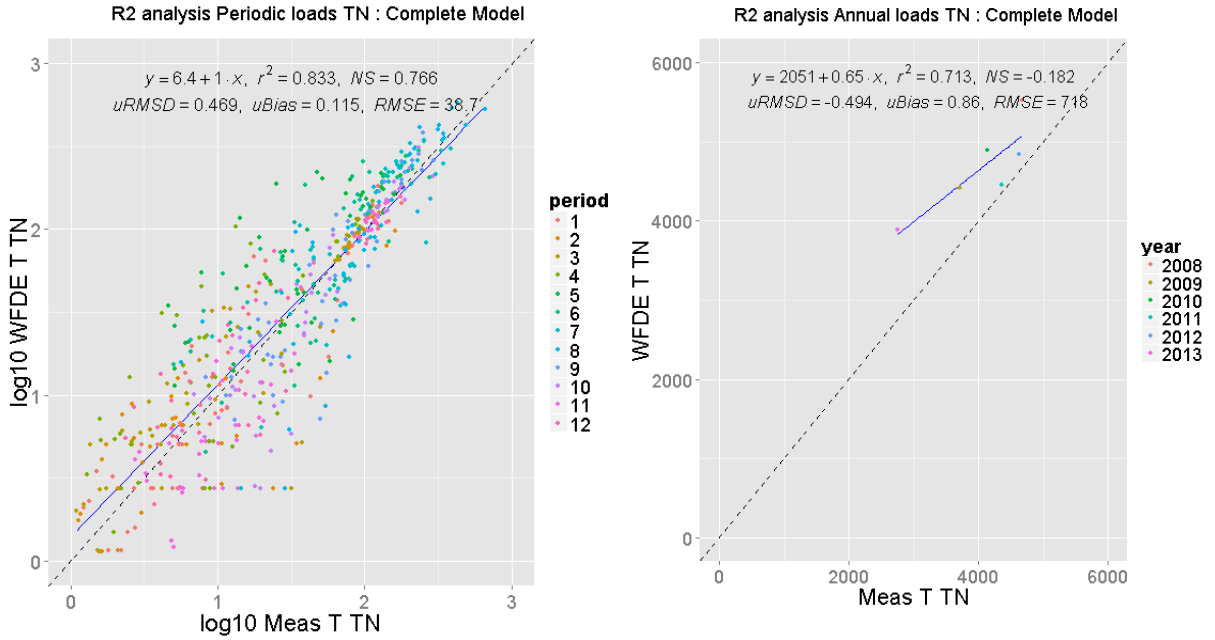

Figure 5.18 Overall Hauraki Plains model performance for predicting nitrogen load compared with the measured load (modelled by RLoadest).

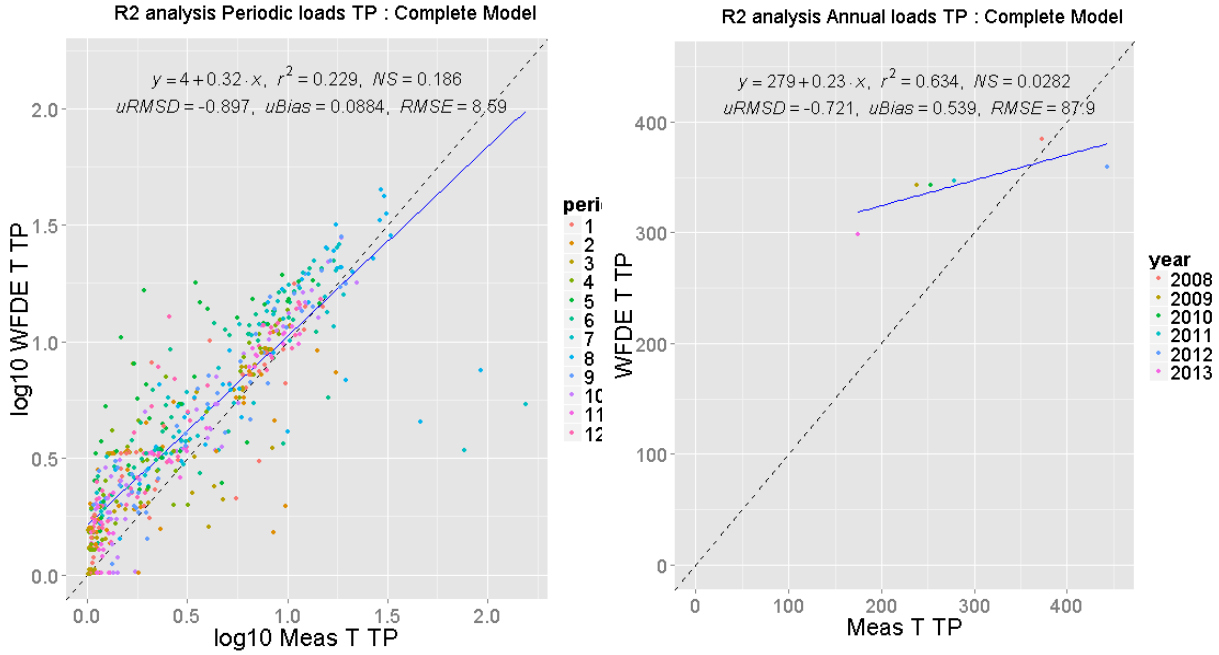

Figure 5.19 Overall Hauraki Plains model performance for predicting phosphorus load compared with the measured load (modelled by RLoadest).

Table 5.22 Overview of the performance of the 8 water quality measurement stations and the overall model periodic and annual prediction of total nitrogen. The performance is expressed in uRSMD and nBias and has been given a published performance rating (Los and Blaas, 2010).

TN		Periodic			Annual		
Catchment	**Station**	**uRSMD**	**nBias**	**Performance rating**	**uRSMD**	**nBias**	**Performance rating**
Waihou	Okauia	0.546	0.365	Good	-0.595	1.600	Poor
	Te Aroha	0.565	0.388	Good	-0.674	2.210	Poor
Ohinemuri	Queens-Head	-0.651	-0.689	Good	-0.641	-2.380	Poor
	Karangahake	-0.539	-0.348	Good	-0.584	-1.430	Poor
Waitoa	Waharoa Control	0.756	0.321	Reasonable	0.701	2.890	Poor
	Mellon Rd Recorder	0.661	0.337	Good	-0.607	2.110	Poor
Piako	Kiwitahi	-0.380	0.290	Good	-0.412	0.233	Good
	Paeroa-Tahuna	-0.383	0.246	Good	-0.458	0.287	Good
Overall	All stations	0.469	0.115	Good	-0.494	0.860	Reasonable

Table 5.23 Overview of the performance of the 8 water quality measurement stations and the overall model periodic and annual prediction of total phosphorus. The performance is expressed in uRSMD and nBias and has been given a published performance rating (Los and Blaas, 2010).

TP		Periodic			Annual		
Catchment	**Station**	**uRSMD**	**nBias**	**Performance rating**	**uRSMD**	**nBias**	**Performance rating**
Waihou	Okauia	0.650	0.699	Good	-0.631	1.840	Poor
	Te Aroha	0.647	0.689	Good	-0.574	2.870	Poor
Ohinemuri	Queens-Head	-0.818	0.150	Reasonable	-0.913	-0.530	Reasonable
	Karangahake	-0.769	0.220	Reasonable	-0.912	-0.516	Reasonable
Waitoa	Waharoa Control	0.997	0.477	Reasonable	0.548	2.640	Poor
	Mellon Rd Recorder	-0.738	1.050	Poor	-0.433	4.140	Poor
Piako	Kiwitahi	0.491	0.600	Good	-0.168	2.080	Poor
	Paeroa-Tahuna	-0.463	0.285	Good	-0.434	0.568	Good
Overall	All stations	-0.897	0.088	Reasonable	-0.721	0.539	Good

5.10.2 Cause of model offset

For both the annual prediction of TN and TP load, the normalised bias (uBias) indicates that the performance is poor. This means that the model significantly over or under predicts the mean annual load. To determine the cause for this systematic offset in the predictions an additional analysis was done, which used a simplistic approach of comparing measured load; the flow-load rating curve results for the measured flow, WFLOW flow and WFD Explorer; and the modelled load (see Appendix E.6).

For Te Aroha the main offset for both TN and TP can be explained by an offset in the flow prediction by WFLOW (TN ≈ 18%; TP ≈ 18%) and an incorrect routing of flow in the WFD Explorer schematisation (TN ≈ 13%; TP ≈ 15%).

For TN predictions at Karangahake the main cause is an offset in the flow prediction by WFLOW (TN ≈ 40%).To a smaller extent the flow-load relationship (TN: 6%, highly variable by year) and incorrect routing of flow in the WFD Explorer schematisation (TN ≈ 7%). TP predictions are mainly offset by the model load input (TP ≈ 60%, highly variable by year). Also for TP, the offset in flow prediction by WFLOW is a cause (TP ≈ 50%, highly variable by year) and to a large extent also the flow-load relation (TP ≈ 30%, highly variable by year).

For TN predictions at Mellon Rd Rec the sole cause is an offset in the flow prediction by WFLOW (TN ≈ 70%, variable by year). For TP the main cause at this station is the offset in the flow prediction by WFLOW (TP ≈ 60%, variable by year), but to a large extend also the flow-load relation (TP ≈ 20%, highly variable by year) and the model load input (20%, variable by year).

Paeroa-Tahuna Rd Br in general has a good prediction for TN and TP. In the years 2008 and 2013 there is a clear offset do to the WFLOW flow prediction and do to the flow-load relations.

5.11 Total loads to the Hauraki Gulf

Total modelled TN and TP load to the Hauraki Gulf is provided in Table 5.26. The Piako and Waihou segments of the model have been calibrated up to the lowest downstream measurement stations (Te Aroha, Karangahake, Paeroa-Tahuna Rd Br and Mellon Rd Rec). Both the Waitakaruru and the downstream catchment of the Piako and Waihou Rivers are calibrated based on an estimated monthly distribution, named as “Other” (Section 5.8). Even though the loads of the Waitakuru are represented, these loads cannot be validated as there is no gauged water quality station present in this catchment. As there are no measurement stations at the outflow of any of these rivers, the resulting outflow, concentration and load cannot be validated.

Table 5.24 Total nitrogen and total phosphorus load to the Firth of Thames per year as calculated by the Hauraki Plains catchment model.

Year	**Total nitrogen** Modelled load contribution to the Firth of Thames (ton / yr)				**Total phosphorus** Modelled load contribution to the Firth of Thames (ton / yr)			
	Waihou	Piako	Waitakaruru	**Total**	Waihou	Piako	Waitakaruru	**Total**
2008	3689.6	3636.8	258.3	7584.8	299.1	255.5	30.0	584.6
2009	3142.0	2671.4	194.2	6007.6	280.3	214.0	26.1	520.4
2010	3419.4	3063.2	224.5	6707.0	277.5	215.2	26.0	518.7
2011	3170.5	2701.4	196.4	6068.3	274.5	215.5	24.6	514.6
2012	3650.7	2822.6	230.8	6704.1	303.9	213.3	27.5	544.6
2013	2905.2	2229.1	170.0	5304.3	256.3	173.4	22.4	452.0

Figure 5.20 Total nitrogen and total phosphorus load contribution (top – bottom) according to the Hauraki Plains Model to the Firth of Thames by the Waihou, Piako and Waitakuru in the validation years 2009 and 2012 (left-right).

6 Application of model framework to evaluate possible management scenarios

6.1 Introduction

The complete modelling framework has been designed as a management tool which can be applied to help evaluate the impact of different management strategies for reducing nutrient inputs to the Firth of Thames with temporal resolution. The method of load implementation used in the model schematisation means that scenarios can be targeted at different soil types, land-use practices or location in the catchment. The model can therefore be used as an integrated catchment management tool to help find a sustainable solution for farming and nutrient contribution to the rivers of the Hauraki Plains catchment and their outflow in the Firth of Thames.

In this Chapter the model is tested to run a number of hypothetical mitigation scenarios to understand and test how the model can be applied as a catchment planning tool. The scenarios applied and their results are intended as a demonstration only and a more detailed evaluation is required in order to test these options and potential alternatives further, including a cost-benefit analysis which takes into consideration farm economic impacts.

6.2 Possibilities for scenario calculations and implementation

Management scenarios can be carried out using any one or a combination of the following approaches:

- Hydrological scenarios (in WFLOW) - adjustment of the meteorological input data to reflect a specific historical year or period, e.g. simulating a dry or wet period.
- Emission scenarios (in WFD Explorer):
  - Adjustment of designed load inputs for land-uses and/or point sources, as prescribed in the WFD Explorer import file.
  - Manipulation of load sources in the WFD Explorer schematisation, including the addition, elimination or modification of specific or collective load types.

The adjustment of farm-specific OVERSEER load information is an approach suited to situations where there have been significant changes to the operation of an individual farm, leading to large changes in farm nitrogen and phosphorus losses. Loads can be adjusted for individual farms or all farms where new or modified OVERSEER output is available.

Modification of loads through the WFD Explorer framework is a suitable approach for testing mitigation scenarios targeted across the entire catchment. This approach can be applied without the need to regenerate individual farm nutrient budgets using OVERSEER. Loads can be altered for a specific source (e.g., an individual farm), enterprise type (e.g. all dairy farms), soil type, geographical location or specific land-use activities (e.g. cropping). Loads can also be partially reduced through adjustment of the removal efficiency (or retention factor) for each specific load source.

6.3 Performed scenarios

In this assessment three scenarios were calculated and compared with the initial model results. As in the limit-setting process the scenarios of a 5%, 10% and 15% reduction of the loads flowing out in the Firth of Thames have been discussed, the choice has been made to model the effect of these three scenarios on dairy nutrient loads to assess the effects on total loading to the Firth. The contribution of the dairy industry to the total load was assessed per sub-catchment. These scenarios focus on nitrogen, as phosphorus is not expected to reach problematic concentrations in the Hauraki Plains catchment.

The nitrogen reduction of dairy farms is implemented by a percentage reduction implemented per period and per dairy nitrogen source. Another way to implement this is by reducing the yearly dairy source load by 5% and distributing this proportionally over the periods. The model is set up in such a way that there will be a linear relation as the load decreases within the years. As the difference in flow between years affects the load released in that year, the value of the decrease in load between years is also likely to differ.

In the model calculation the reduction is implemented on the input loads, which will be attenuated and summed to determine the load at the specific site.

6.4 Testing of scenario framework

To validate the workflow of the model, scenario calculations executed within the model were also compared with a spreadsheet approach. As the attenuation is assumed to be constant, this calculation can be done simply by reducing the previous model results of a tracer study in a spreadsheet calculation. By comparing both the spreadsheet and the modelled simulation results, possible errors in the model can be identified.

The results of the modelling and spreadsheet approach resulted in the same outcomes which validates the model setup for scenario modelling.

6.5 Scenario results

The scenario results have been included in the confidential Appendix F.

7 Delta Data Viewer

7.1 Introduction

Through the current study as well as Netherlands TKI co-funding, a smart geographic data viewer application of the WFD Explorer model application has been developed for both the Waituna and Hauraki catchments. The Delta Data Viewer (DDV) is intended as a simple and graphical model application to support decision makers in defining and simulating mitigation scenarios in an interactive way. The DDV uses disaggregated model output from the WFD water quality framework, providing an application with short calculation times (± 8 seconds, depending the scale of the model). The application is therefore highly suitable for use in stakeholder meetings.

This DDV application (see Figure 7.1) allows the user to view the basic data to make policy decisions (e.g. land-use, soil and farm types), create load reduction scenarios, calculate these scenarios, analyse the results and compare the effect of these scenarios in an interactive way. The DDV can work with multiple geographic file formats (KML/KMZ, WPS/WMS, GeoJSON, SHP, TMS etc.) and provides multiple interactive functions (drawing of polygons, lines and points; server file browser; accessing attribute files of data layers; view capturing etc.). DDV applications can be hosted on a webserver, making them accessible by internet via different browsers (Internet Explorer, Chrome, Firefox etc.) and to different platforms (PC, tablets, smart phones). The applications work through touch screen and with mouse actions.

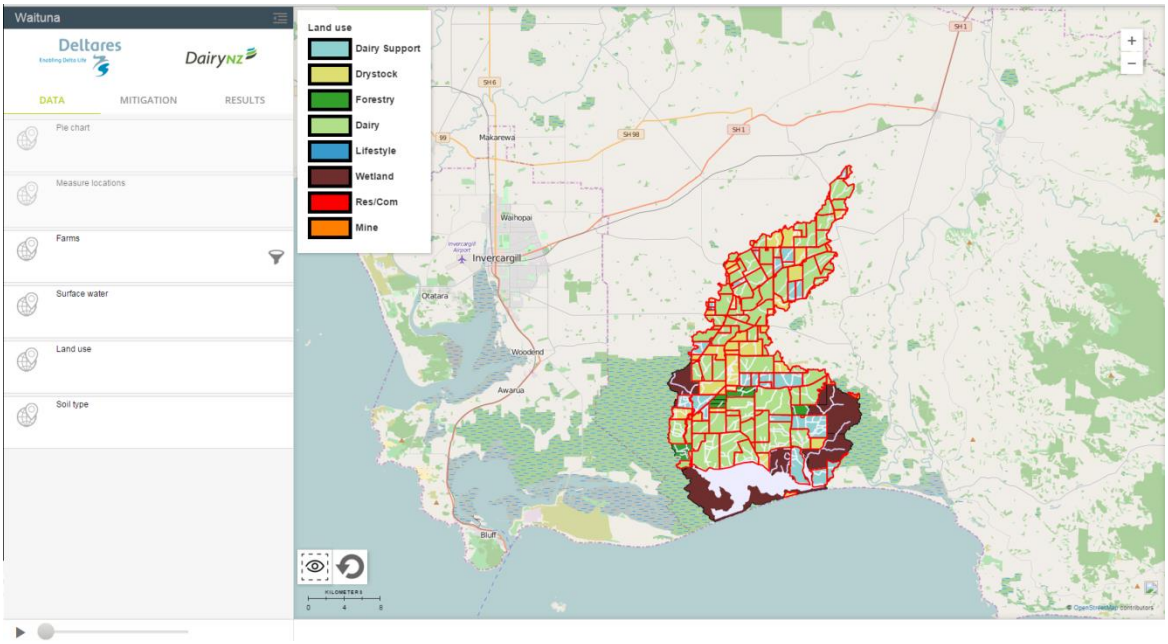

Figure 7.1 The DDV user interface for the Waituna model application. On the left top-side the user can make a selection to view the data (containing basic-data and calculation results) or the measures (measures applied to the individual farms). With the legend, the user can select which parts of the basic-data should be presented (in this case which land-use, property boundaries (red lines) and the rivers are shown).

The Hauraki and Waituna WFD model applications have served as test cases for this DDV development. As the development of the Hauraki model and the DDV application for WFD Explorer models occurred simultaneously, the Waituna model has been used to fully set up and test the DDV application.

7.2 Accessibility and workflow

The Waituna DDV application is secured by a username and password. This ensures that sensitive information, for example individual property nutrient loss information, can only be viewed by authorized persons.

The DDV provides the interface for the specific model application (see Figure 7.1). This interface is hosted on a webserver, which also contains the processing workflows (Figure 7.2). The “calculation workflow” consists of (1) pre-processing of the data provided by the DDV, (2) the actual Waituna model calculation and (3) post-processing the results which are uploaded to the DDV.

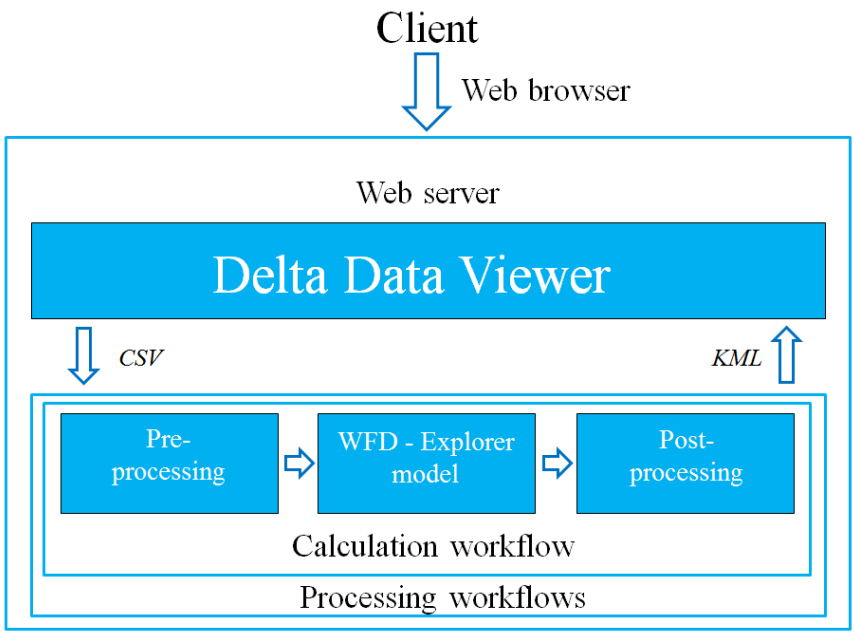

Figure 7.2 Schematic overview of the interaction between the client, the DDV application and the processing workflows. Both the DDV application and the processing workflows are hosted on the same webserver.

7.3 Applying mitigation scenarios

The purpose of the Waituna model application based on the WFD Explorer is to explore possible future limit setting scenarios. To define these scenarios, the DDV contains basic layers, describing the soil type, the land-use type, the surface waters, the farms and the point sources. Currently only the farm property boundaries (diffuse sources) can be used to apply mitigation scenarios. These property boundaries need to be selected in order to apply a scenario. This can be done by individually selection on a map or by using a filter based on the basic layers (for example select all the farms that are involved in dairy production). After selection, the mitigation tab button will show the mitigations that can be applied. Currently, these choices are percent reduction or an annual aerial maximum loading rate for the selected farms. After applying the measures, the calculation can be started.

7.4 Calculation and results

In the Waituna application the calculation of the scenarios takes approximately 5 seconds. When the calculation has finished, the scenario result is shown under the “results” tab.

The scenario results provide an overview of the measures that have been applied for the scenario calculation. For every water quality substance represented in the scenario, the annual average concentration throughout the surface water network as well as a bar-graph showing the origin of the loads in the receiving water body is given. These results give decision makers an overview of where additional measures how the different catchments contribute to the loading of substances in downstream areas or the receiving environment.

8 Summary and conclusions

8.1 Summary

The aim of the current study was to develop a water quality modelling framework for the Hauraki Plains catchment to quantify total catchment nutrient loads discharging to the Firth of Thames. The final framework, which integrates a distributed hydrological model with monthly load model, provides a complete catchment management tool which can now be applied to explore possible management options to reduce nutrient loading at the catchment scale together with land owners and water managers.

The model framework is based on farm-specific estimates of N and P loss which for dairy farms are based on the results of OVERSEER modelling for 12 representative case study farms distributed throughout the Hauraki Plains catchment. Actual farm data can be applied in the model in future should this information become available. The use of individual farms in the model schematisation greatly improves the spatial resolution of the load estimates and provides much greater flexibility to investigate different management options. As monthly land-use leaching data was unavailable, the assumption was made that all anthropogenic land-use loads can be scaled equally based on the hydrological conditions. However, the model has been implemented in such a way that it is suitable for future updates with farm and point source specific load estimates, which would make the need for hydrological load scaling obsolete. Scenarios can be targeted at specific land-use types, soil types, geographical locations or different land-use activities on individual farms, as well as point sources.

The modelling approach taken is based on open-source software and, given the availability of input data, can easily be replicated to other catchments across New Zealand.

8.1.1 Modelling framework

The water quality modelling framework applied to the Hauraki Plains catchment has been set up using an in-project developed Model Tool Setup module in Python. The hydrological component of the framework (WFLOW) is run under the Delft-FEWS user interface and data management platform. This has been coupled to the WFD Explorer user interface and associated framework components. The final framework enables the user to simulate the hydrology for the catchment on a detailed spatial scale and to define the farms and point sources as separate emission sources, to add additional emissions to the system, to estimate water quality concentrations in the river network and to calculate the contributions of the different sub-catchments to the total nutrient load by the Waihou, Piako and Waitakuru river to the Firth of Thames. Scenario calculations can be made using nitrogen and phosphorus leaching values (OVERSEER model output or from literature) or by applying detailed emission reductions on specific farms, emission types and soil types within the WFD Explorer framework.

The project is a larger pilot study after the Waituna Lagoon model study to test a spatially refined modelling approach for wider application to more extensive and hydrologically complex catchments in New Zealand. The specifics that have been tested in the Hauraki pilot study are:

- Working with a larger and more complex catchment
- Applying a higher temporal resolution to the model
- Making use of extrapolated leaching values from literature and OVERSEER

- Getting a better understanding of the contribution of phosphorus by erosion
- Gaining a comprehensive estimate of total N and P loading from the Hauraki Plains catchment to the Hauraki Gulf.

8.1.2 WFLOW hydrological model

The WFLOW model simulates discharge associated with surface runoff and shallow subsurface flows. Compared with the Waituna WFLOW model the Hauraki Plains catchment is highly spring fed. Especially in the Waihou River it makes a significant difference when the inflow from springs is considered. As WFLOW is a model for surface and subsurface flow, the springs are not automatically incorporated into the model framework and instead need to be added manually. This made the calibration of the model a more challenging task than anticipated, especially given a general lack of quantitative information around the spatial and temporal distribution of spring flows.

The WFLOW model performance was assessed based on a coefficient of fit (COF) rated by an arbitrary scale. The results suggest that model performance is very good for the Piako catchment (COF : 0.10-0.17), good for the Ohinemuri catchment (COF : 0.33 – 0.34), satisfactory – unsuitable for the Waihou River (COF: 0.59 – 15,51) and unsatisfactory – satisfactory for the Waitoa River (COF : 1.37 – 0.83).

The cause for poor model performance in the Waihou is attributed to the complexity and uncertainty around the contribution of ground water aquifers to the overall catchment water balance. The spatial extent of these aquifers is unlikely to follow the catchment topographic boundary as derived from the digital elevation model meaning that surface recharge and groundwater discharge is not fully accounted for. At Waitoa the capacity of the river catchment and system to retain peak rainfall under semi-saturated conditions seems much higher than what has been estimated by the model.

The WFLOW model is fit for purpose in terms of providing the required periodic flow input needed to undertake water quality calculations with the WFD Explorer water quality model. However, the uncertainty in flow predictions is likely the predominant cause of the modelled offset in load predictions in the Waihou, Ohinemuri and Waitoa Rivers.

8.1.3 Water Quality Model WFD-Explorer

A detailed model schematisation comprised of basins (farms), river segments and associated linkages was developed to represent the spatial distribution of catchment load sources. By combining the WFLOW hydrology with emissions from different sources, river water quality could be calculated by the WFD Explorer. From this data the contribution of nitrogen and phosphorus loads to the Firth of Thames from the individual sub-catchment flows could be derived.

Nutrient load input to the WFD Explorer reflected sources related to specific agricultural land-uses, background loads and point sources. Different types of land-uses and for farms even block types were defined in the WFD Explorer as separate emission types. Nutrient losses for Dairy farms were based on 12 model farm calculations with other land-use values acquired from the literature whilst point source estimates were derived from empirical data in Vant (2012). Based on a daily load estimation for the downstream water quality measurement stations by the package RLoadest, the anthropogenic land-use loads were distributed monthly.

The daily flow results from WFLOW were aggregated to monthly flow input for the WFD Explorer. The distribution of these flows on the WFD Explorer model schematisation was done automated with the model setup tool. A comparison between the WFLOW and the WFD Explorer results for water flows suggested that both models have highly comparable flow outputs (overall, r^2 = 0.994) with the lowest comparison at the Waitoa river (measurement station Mellon Rd Recorder, r^2 = 0.981). This slight difference in flow is explained by a small inaccuracy of the model setup tool as it does not follow the elevation, but proximity of streams.

By calibration of model output for annual loads against measured water quality a simplified attenuation factor was derived for TN. This factor was estimated to be 4%. As this value is much lower than attenuation factors applied to other modelling studies (range 20-40%, e.g. van den Roovaart et al. 2014), it is likely that the magnitude of input N to the model framework prior to attenuation has been under estimated. However, as the model output is calibrated against monitored in-stream discharges, this does not affect the estimates of total loading to the downstream receiving environment. For TP no attenuation was applied given the model considered stable-state and conservation of TP throughout the hydrological system (e.g., inability to be readily returned to an atmospheric form).

A more detailed assessment of the partitioning between measured TP and DRP at various monitoring locations was undertaken to determine the particulate P (PP) fraction of the total P load. This fraction is associated with phosphorus sources from sediment erosion, runoff and organic matter. This fraction is not measured in nutrient leaching studies or specifically reflected in the OVERSEER results. By analysing the upstream measurement stations in the catchment, where erosion is more likely to occur due to its steeper topography, a linear regression model was applied, the results of which suggest that the main source of PP is derived from the land-uses Exotic forest and Dairy. These results were used in the model to introduce an additional erosional P load source on those land-uses only.

The performance of the calibrated catchment water quality modelling framework was statistically assessed using the unbiased root-mean square difference (uRMSD) and the normalised model bias (nBias) (Los and Blaas, 2010). The results suggest that model performance is good for the simulation of periodic (approximately monthly) TN load (uRMSD = 0.469, nBias = 0.115), and reasonable for annual TN load (uRMSD = -0.494, nBias = 0.860). When TN prediction is compared annually between rivers, model performance for the Piako is good and all other rivers poor. For TP model performance was determined to be reasonable for periodic loads (uRMSD: -0.897, nBias: 0.088) and good for annual loads (uRMSD: -0.721, nBias: 0.539). Between rivers model performance for TP was good downstream and poor upstream for the Piako River, reasonable for the Ohinemuri River, and poor for all other rivers.

The low model rating for individual rivers when assessed for annual load prediction is found in the model bias. The WFD Explorer uses the WFLOW results to determine the annual load. This causes model uncertainties to accumulate. The main cause of this is the over and under prediction of flow by WFLOW (TN & TP, Waihou, Ohinemuri and Waitoa Rivers). A secondary and minor cause was found to be the incorrect translation of the WFLOW schematisation to the WFD Explorer by the model setup tool (TN, Waihou & Karangahake; TP, Waihou), and in some cases, a simplification of using the flow-load rating curves which are not suitable for capturing trends and point source contributions (TP, Ohinemuri and Waitoa Rivers).

As there is no seasonal distribution of point sources and background load available, this conflicts with the chosen approach of scaling the anthropogenic land-use load. This is most apparent in the Ohinemuri and Waitoa Rivers for TP.

Due to the poor flow predictions in some river systems, the model has a poor annual prediction for TN and TP load based on the statistical tests applied. Despite this, the model framework is still considered to be fit for purpose as a management screening tool to test the likely impact of various mitigations in the Hauraki Plains catchment. The model also provides a first overall estimate of TN and TP loading from the entire Hauraki Plains catchment, including the large areas of land situated below the current monitoring locations. However, the values estimated should be treated as a best estimate only, as the model could not be calibrated or validated for the reaches below the last monitoring locations. Predicting the correct flows have proven to be challenging in this catchment. When this is improved and more data is provided on the monthly distribution of point source loads in the Hauraki Plains, the predicted annual load value will improve substantially.

8.1.4 Recommendations WFD- Explorer Hauraki Plains model

The monitoring data on nutrient concentration and flows is limited because there is no monitoring downstream of the terminal stations at Te Aroha, Karangahake, Paeroa-Tahuna and Mellon Road Rec. The Waitakaruru River catchment does not contain any stations where both water quality and flows are measured. This makes it impossible to calibrate and validate the model for these parts of the catchment.

The monthly frequency of measuring water quality has proven to be insufficient to obtain an accurate prediction of the nitrogen and phosphorus load at each monitoring station (as shown at Karangahake in 2012). The yearly load comparison shows a high uncertainty in the predicted loads by RLoadest. This is likely due to frequent high flow periods which are otherwise poorly represented in monitoring data and in the flow-load rating curves. More frequent monitoring during these periods would improve the RLoadest models and thereby the Hauraki Plains catchment model.

The WFLOW model used to predict the flow assumes free flow. In the lower part of the catchment (downstream of the measurement stations Te Aroha, Karangahake, Paeroa-Tahuna and Mellon Road Rec) the land area tends to be extremely flat and dams and culverts exist to protect against flooding. This will impact the flow and thereby the modelled load, however there are no measurement stations below Te Aroha to estimate the impact of this.

The WFLOW model could be improved through the better parameterisation of catchment specific calibration coefficients. These parameters need to be derived from research. Also incorporating a groundwater model (for example MODFLOW) in the flow calculation should substantially improve the model results, especially if the current uncertainties around the temporal and spatial contribution by groundwater systems to base flow can be addressed. This will also have a beneficial impact on the ability of the WFD Explorer model to accurately predict loads. This option has been explored in a case study by Deltares for the Pinedale area in the Hauraki Plains catchment by creating an online coupling between MODFLOW and WFLOW in DeltaShell (see Appendix M).

The OVERSEER modelled farms used to extrapolate the leaching from dairying were limited in number preventing determination of an average loss rate on differing soils from a normal distribution per block type. Here, the full suite of Hauraki Plains catchment soil types has been grouped under three main categories with empirical data collected for 12 real dairy farms, and then extrapolated to the full suite of soil types with dairying land-use. By increasing the amount of modelled dairy farms, the leaching values used can be improved. The optimal situation would be when the model was fed by farm specific OVERSEER results for all pastoral and horticultural property boundaries.

By obtaining OVERSEER model results for individual dairy and dry stock farms as well as refined estimates for nutrient losses for other land-uses under varying rainfall regimes and on varying soil types throughout the Hauraki Plains Catchment, the estimated nutrient leaching can be better validated and improved. The model framework has been set up in such a way that more specific farm data can be incorporated in future.

As land-use specific spatial and periodic information on TN and TP loading is lacking the anthropogenic loads were scaled equally across all time periods. There is a flaw in this approach as management practices (e.g. fertiliser application) and proportional increases of leaching compared with rainfall can differ strongly among land-uses and periods.

The models also likely to improve if the temporal flow and load discharged by the point sources can be incorporated. In absence of this data, the point sources could also be scaled based on their production curves (e.g. Meat works, Dairy processing plants). It is expected that in both cases this will lead to a more realistic temporal distribution of the loads, and thereby a reduction in the number of negative values at the seasonal scaling, which will decrease the offset between the modelled and measured loads.

Due to a limit in water quality measurements of the springs, all spring nutrient concentrations have been extrapolated from one measurement at the Blue Springs. This measurement contained only TN. To improve the nitrogen and phosphorus load estimates contributed from springs, more spatial and temporal measurements are required for both nutrient species.

Even though the land area of Horticulture in the Hauraki Plains model is relatively low, leaching values vary highly between different types of horticultural activities. As it was difficult to estimate concise values for individual activities, a mean value was applied. However, better representation of contaminant leaching from different horticultural land-use types could be considered to improve model outputs from this source.

8.2 Conclusions

The current study provides an integrated catchment water quality tool for the Hauraki Plains catchment which can now be applied to explore possible options for achieving a sustainable solution for managing total loading to the Firth of Thames. The model contains spatially refined source load information and therefore provides great flexibility to investigate different management options. Scenarios can be targeted at specific land-use types, soil types, geographical locations or different land-use activities on individual farms. The model has helped in getting more knowledge on the phosphorus load from erosion and has identified locations that require more frequent monitoring. The model provides a first best estimate of total nitrogen and phosphorus loads from the entire Hauraki Plains catchment, including the large areas of land situated below the current monitoring locations, to the Hauraki Gulf.

The water quality model has a poor annual prediction for TN and TP based on the statistical tests applied and monitoring data available due to the poor representation of water flows in some river reaches. Despite this, the overall framework is still considered to be fit for purpose as a management screening tool to test the likely impact of various mitigations in the Hauraki Plains catchment.

This model setup in combination with the Delta Data Viewer provides a complete catchment management tool to explorer and evaluate the impacts of different management solutions to reach water quality targets together with land owners and water managers. Even though the model input has been scaled to years and temporally disaggregated to months, this data should be treated carefully as there was no annual and monthly specified leaching data available. Therefore, the anthropogenic land-use input data has been annually scaled and periodically distributed based on the modelled flow. The actual anthropogenic land-use specific leaching values could differ substantially due to differences in monthly management practices (e.g., adding fertilizer, wintering of stock) and also leaching rates due to environmental factors (rainfall, temperature).

The model fits the requirement set for this project as a spatially-refined modelling approach which allows individual load sources to be quantified and assessed on relative importance across the catchment based on load inputs acquired from OVERSEER modelling and literature. The model depicts monthly variation correctly; however, the annual loads should be used with caution, although do provide a first best estimate of total loads from the entire catchment to the downstream receiving environment. This offset in model prediction is mainly caused by the complex hydrology and unavailability of temporal variable data of point sources. It is thereby clear how the model could be improved for future use.

The modelling framework applied offers a flexible approach which can easily be applied to other catchments in New Zealand. The framework allows for the simulation of water quality and pollutant loads on finer timescales in future applications through the DELWAQ water quality model included in the WFD Explorer framework. The WFLOW, MODFLOW and WFD Explorer models can potentially be coupled with DeltaShell and fed by OVERSEER results to provide a fully integrated system for environmental modelling of farm nutrient loss data.

This study represents a further step towards developing a robust, nationally applicable and spatially refined (farm-scale) catchment modelling approach for the assessment of wide-scale water quality and water allocation issues within the Dairy industry over the long term.

9 Acknowledgement

We thank the Waikato Regional Council (WRC) for the data provided (e.g., flow and water quality measurements, AGRIBASE shapefile). We thank Dr. Tom Stephens for his guidance in RLoadest, help in determining the source of particulate phosphorus and thorough review of this report.

10 Literature

AgResearch (2014). OVERSEER® Technical manual (ISSN: 2253-461X) - http://www.OVERSEER.org.nz/OVERSEERModel/Information/Technicalmanual.aspx

Bergström, S. (1995). The HBV model. In: Singh, V.P. (Ed.) *Computer Models of Watershed Hydrology*. Water Resources Publications, Highlands Ranch, CO., pp. 443-476.

Burrough, P.A., D. Karssenberg, and van Deursen, W.P.A. (2005). Environmental Modelling with PCRaster. In GIS, Spatial Analysis and Modelling, D.J. Maguire, M.F. Goodchild and M. Batty (Eds.), p. 480 (Redlands, California: ESRI).

Dawson, C.W., R.J. Abrahart, L.M. See (2006) HydroTest : A web-based toolbox of evaluation metrics for the standardised assessment of hydrological forecasts. Environmental Modelling & Software. Vol 22: 1034-1052, doi:10.1016/j.envsoft.2006.06.008

Deltares (2006) Handleiding KRW Verkenner (WFD Explorer). Leven met water.

Gash, J. H. C., I. R. Wright, and C. R. Lloyd (1980) Comparative estimates of interception loss from three coniferous forests in Great Britain. Journal of Hydrology, 48:89–105.

Gash, J. H. C., C. R. Lloyd, and G. Lachaud (1995) Estimating sparse forest rainfall interception with an analytical model. Journal of Hydrology, 170:79–86.

Jenkins, I. and B. Vant, (2011) “Potential for Reducing the Nutrient Loads from the Catchments of Shallow Lakes in the Waikato Region”, Waikato Regional Council, ISSN 1172-4005

Judge, A. and S. Ledgard (2009) Nutrient budgets for Waikato dairy and sheep, beef and deer farms, 1997/98 – 2006/07. Waikato Regional Council, ISSN 1172-4005 (print) ISSN 1177-9284 (Online)

Landcare Research (2007) Digital Elevation Model (DEM) – 25M, Waikato Regional Council, 1015.00@EW.GOVT.NZ, EWDOCS# 881308

Ledgard, S. (2000) Measurement and prediction of nitrate leaching and nitrogen fertilizer requirements of vegetables, AgResearch

Los, F.J., M. Blaas (2010) Complexity, accuracy and practical applicability of different biogeochemical model versions. Journal of Marine Systems Vol 81, 44-74

Longhurst, B., B. De Vantier and S. Ledgard (2016) Hauraki Gulf Catchment Nutrient (N and P) Loss Modelling: Scoping Study (Revised using OVERSEER v 6.2.1), RE500/2014/112, AgResearch

LIC DairyNZ (2015) New Zealand Dairy Statistics 2014/15. Hamilton, New Zealand.

Moriasi, D.N., J.G. Arnold, M.W. Van Liew, R.L. Binger, R.D. Harmel, T.L. Veith (2007) Modelevaluation guidelines for systematic quantification of accuracy in watershed simulations. American Society of Agricultural and Biological Engineers, Vol. 50 (3):885-900, ISSN 0001-2351

Runkel, R.L., Charles, G.C., Timothy, A.C. (2004) Load Estimator (LOADEST): A Fortran Program for Estimating Constituent Loads in Streams and Rivers Techniques and Methods Book 4, (Chapter A5)

Rutherford, Palliser and Wadhwa (2009) Nitrogen exports from the Lake Rotorua catchment - calibration of the ROTAN model.

Stenger, R. and S. Woodward, A. Shorkri and R. Hill (2014) N and P concentration-discharge relationships across a range of Waikato catchments. Fertiliser and Lime Conference

Stephens, T.W. (2015). Trends in water quality of the Hauraki Rivers and nutrient loads into the Firth of Thames: Has land-use driven recent degradation of coastal and freshwater in the Waikato, New Zealand. DairyNZ

Swales, A., M. Gibbs, T. Stephens, G. Olsen, R. Ovenden and K. Costley (2016) Sources of eroded soils and their contribution to long-term sedimentation in the Firth of Thames. NIWA Client Report for DairyNZ and Waikato Regional Council, HAM2016-001

The Agribusiness group (2014A) Nutrient Performance and Financial Analysis of Lower Waikato Horticulture Growers.

The Agribusiness group (2014A) Nutrient Performance and Financial Analysis of Horticultural Systems in the Horizons Region.

Vant, B. (2011) “Water Quality of the Hauraki Rivers and Southern Firth of Thames, 2000-09”, Waikato Regional Council, ISSN 2230-4344 (print), ISSN 2230-4363 (Online)

Vant, B. (2012) “Water Quality of the Hauraki Rivers and Southern Firth of Thames, 2010-12”, Waikato Regional Council, ISSN 2230-4344 (print), ISSN 2230-4363 (Online)

Vertressy, R.A., and H. Elsenbeer (1999). Distributed modelling of storm flow generation in an Amazonian rainforest catchment: effects of model parameterization, Water Resources Research, vol. 35, no. 7, pp. 2173–2187, 1999.

Werner, M., J. Schellekens, P. Gijsbers, M. van Dijk, O. van den Akker, k. Heynert (2012) The Delft-FEWS flow forecasting system. Environmental Modelling & Software, Elsevier, Volume 40, February 2013, pages 65-77

Wilcock, R., K. Muller, G.B. Van Assema, M.A. Bellingham and R. Ovenden (2011). Benefits of wetlands in farming landscapes – The Toenepi Catchment. Fertiliser and Lime Conference

A Description of the WFLOW distributed hydrological model

A.1 Introduction

Conceptually, the WFLOW model is based on the HBV-96 model (Bergström, 1995). WFLOW is a distributed hydrological model. Distributed models remain in contrast to lumped-conceptual models, which merge entire sub-catchment areas into a set of model stores. In WFLOW the landscape is discretized into a model grid, which can have different spatial resolutions. The model grid is obtained by performing a flow drainage analysis on the raw DEM, executing pit-filling and obtaining a consistent drainage map with catchment delineations and a flow direction map, as shown in Figure A.1.

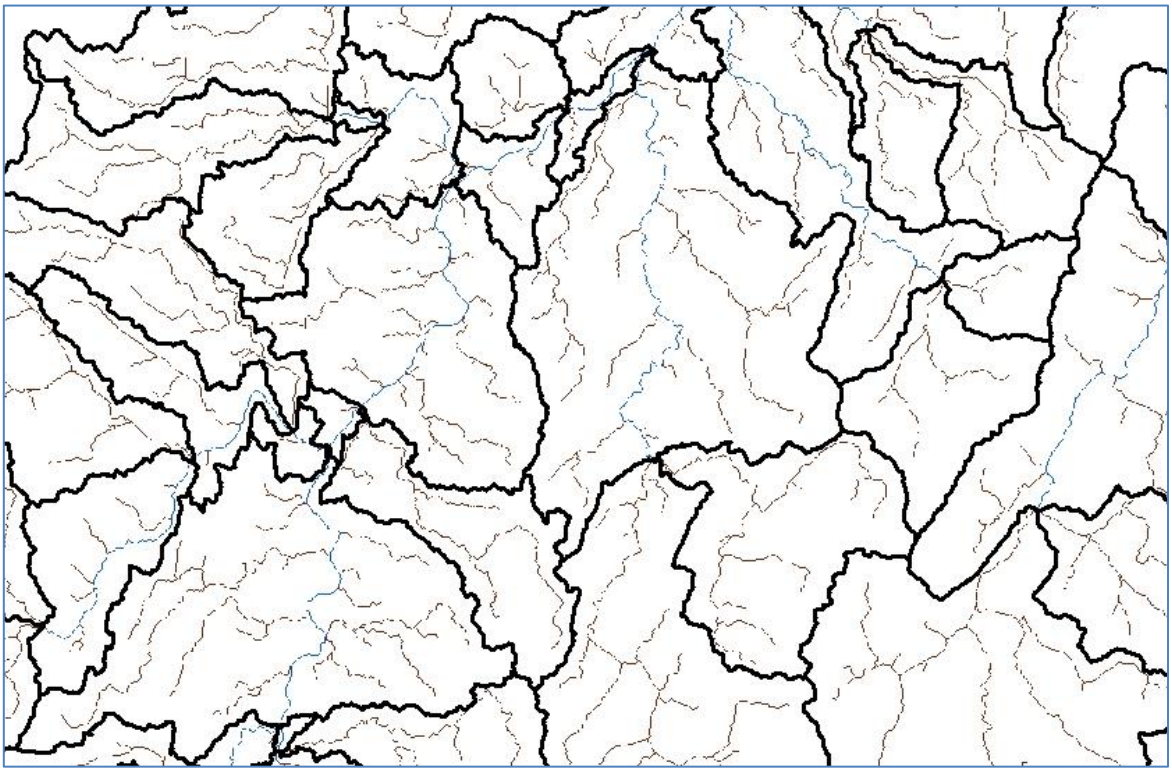

Figure A.1 Example of a drainage map obtained from the elaboration of a raw digital elevation map.

A.2 Model structure

The mode structure is based on the design of the HBV-96 stores, whereby the structure is applied to each grid cell. Some modifications have however been introduced in the distributed HBV structure of the WFLOW model. For example, the hydrological routing represent in HBV by a triangular hydrograph has been removed. Instead, the kinematic wave function is used to route water downstream. All runoff generated in a cell in one of the HBV conceptual reservoirs is added to the kinematic wave reservoir at the end of a time step. There is no lateral connection between the different HBV cells in the model. Wherever possible, all functions that describe the distribution of parameters within a sub-basin have been removed, as this is not needed in the distributed WFLOW application.

A river basin is subsequently divided into a number of grid cells. For each of the cells individually, daily runoff is computed through application of the HBV-96 model. The use of the grid cells offers the possibility to turn the HBV modelling concept, which is originally lumped,

into a distributed model. Figure A.2 shows a schematic view of hydrological response simulation with the HBV-96 modelling concept. The land-phase of the hydrological cycle is represented by three different components: 1) a snow routine, 2) a soil routine and 3) a runoff response routine. Each component is discussed separately below.

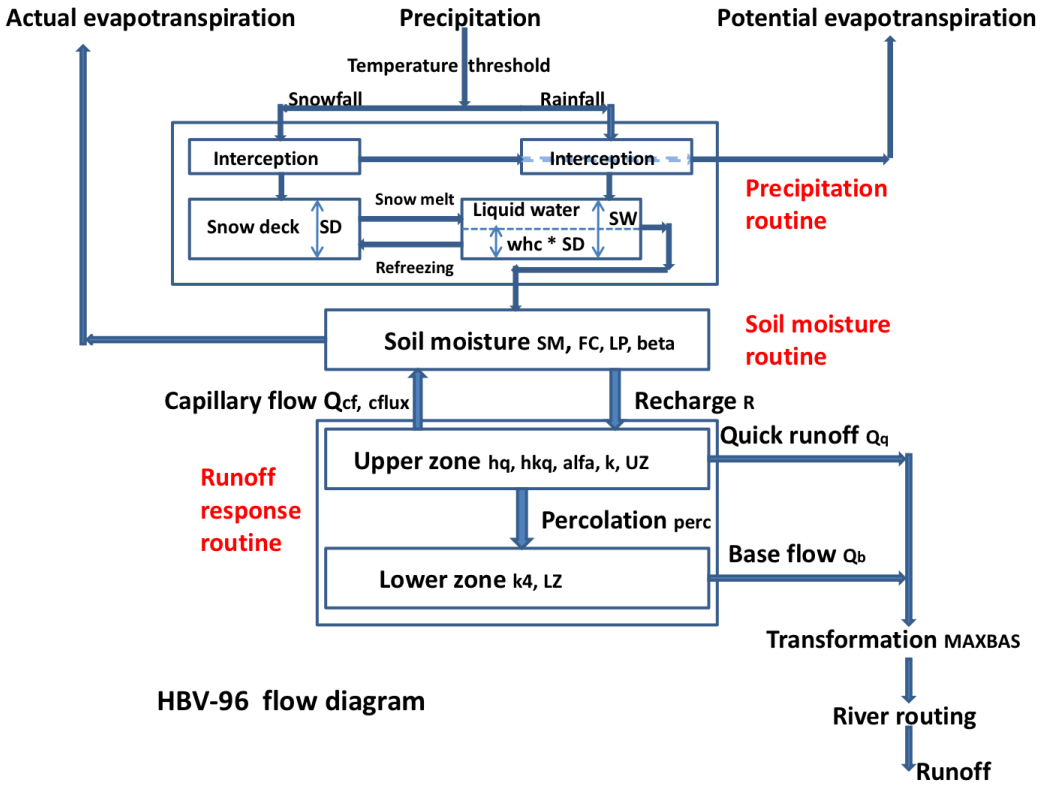

Figure A.2 Schematic view of the relevant components of the HBV model as implemented in WFLOW.

A.3 The snow routine

Precipitation enters the model via the snow routine. If the air temperature (T_a) is below a user-defined threshold ($TT \sim 0$℃) precipitation occurs as snowfall, whereas it occurs as rainfall if $T_a \gg TT$. An additional parameter, *TTI,* defines how precipitation can occur partly as rain of snowfall (see Figure A.3). If precipitation occurs as snowfall it is added to the dry snow component within the snow pack. Otherwise it ends up in the free water reservoir, which represents the liquid water content of the snow pack. Between the two components of the snow pack interactions take place, either through snow melt (if temperatures are above a threshold *TT*) or through snow refreezing (if temperatures are below threshold *TT*). The respective rates of snow melt and refreezing are:

$$Q_m - cfmax * (T_a - TT);\ T_a > TT$$
$$Q_t - cfmax * (TT - T_a);\ T_a \leq TT$$

where Q_m is the rate of snow melt, Q_t is the rate of snow refreezing, and *cfmax* and *cfr* are user defined model parameters (the melting factor [mm/ C°] and the refreezing factor respectively).

The air temperature is related to measured daily average temperatures. In the original HBV-concept, elevation differences within the catchment are represented through a distribution

function (i.e. a hypsographic curve) which makes the snow module semi-distributed. In the modified version that is applied here, the temperature is represented in a fully distributed manner, which means for each grid cell the temperature is related to the grid elevation.

The fraction of liquid water in the snow pack (free water) is at most equal to a user defined fraction, *WHC*, of the water equivalent of the dry snow content. If the liquid water concentration exceeds *WHC*, either through snow melt or incoming rainfall, the surplus water becomes available for infiltration into the soil:

$$Q_{in} = max\ \{(SW - WHC * SD);\ 0.0\}$$

where Q_{in} is the volume of water added to the soil module, *SW* is the free water content of the snow pack and *SD* is the dry snow content of the snow pack.

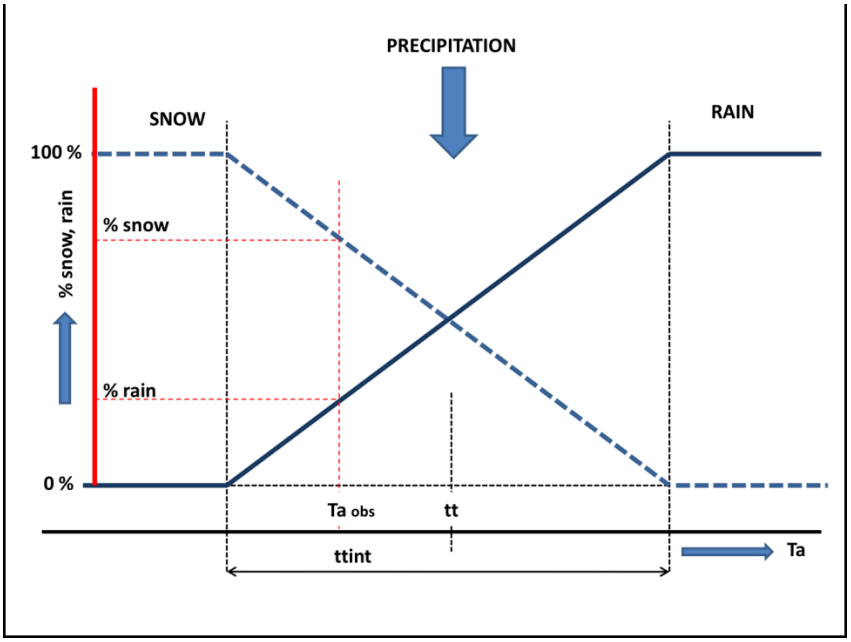

Figure A.3 Schematic view of the snow routine as implemented in WFLOW.

A.4 Potential Evaporation

The original HBV version includes both a multiplication factor for potential evaporation and an exponential reduction factor for potential evapotranspiration during rain events. The *CEVPV* factor is used to connect potential evapotranspiration to specific land-use classes. In the original version the *CEVPFO* is used and it is used for forest land-use only.

A.5 Interception

The parameters *ICF0* and *ICFI* introduce interception storage for forested and non-forested zones respectively in the original model. Within our application this is replaced by a single *ICF* parameter assuming the parameter is set for each grid cell according to the land-use. In the original application it is not clear if interception evaporation is subtracted from the potential evaporation. In this implementation we do subtract the interception evaporation to ensure total evaporation does not exceed potential evaporation. From this storage evaporation equal to the potential rate ET_p will occur as long as water is available, even if it is stored as snow. All water enters this store first, there is no concept of free through fall (e.g. through gaps in the canopy). In the model a running water budget is kept of the interception store:

- The available storage (*ICF*-Actual storage) is filled with the water coming from the snow routine (Q_{in}).
- Any surplus water now becomes the new $Q_{in.}$
- Interception evaporation is determined as the minimum of the current interception storage and the potential evaporation.

A.6 Soil routine

The incoming water from the snow and interception routines (Q_{in}) is available for infiltration in the soil routine. The soil layer has a limited capacity (F_c) to hold soil water, which means if F_c is exceeded, the abundant water cannot infiltrate and, consequently, becomes directly available for runoff (see Figure A.4):

$$Q_{dr} = max\ \{(SM + Q_{in} - F_c);\ 0.0\}$$

where Q_{dr} is the excess soil water (also referred to as direct runoff) and *SM* is the soil moisture content. Consequently, the net amount of water that infiltrates into the soil, I_{net}, equals:

$$I_{net} = Q_{in} - Q_{dr}$$

A part of the infiltrating water (I_{net}) will runoff through the soil layer (seepage). This runoff volume (*SP*) is related to the soil moisture content, *SM*, through the following power relation:

$$SP = (SM / F_c)^{\beta}\ I_{net}$$

where β is an empirically based parameter. Application of this equation implies that the amount of seepage water increases with increasing soil moisture content. The fraction of the infiltrating water which doesn't runoff, I_{net} - *SP*, is added to the available amount of soil moisture (SM). The β parameter affects the amount of supply to the soil moisture reservoir that is transferred to the quick response reservoir. Values of β vary generally between 1 and 3. Larger values of β reduce runoff and indicate a higher absorption capacity of the soil (see Figure A.5).

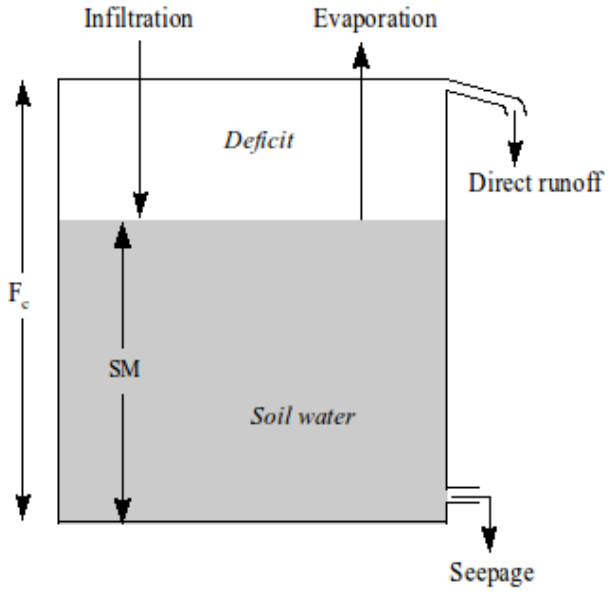

Figure A.4 Schematic view of the soil moisture routine.

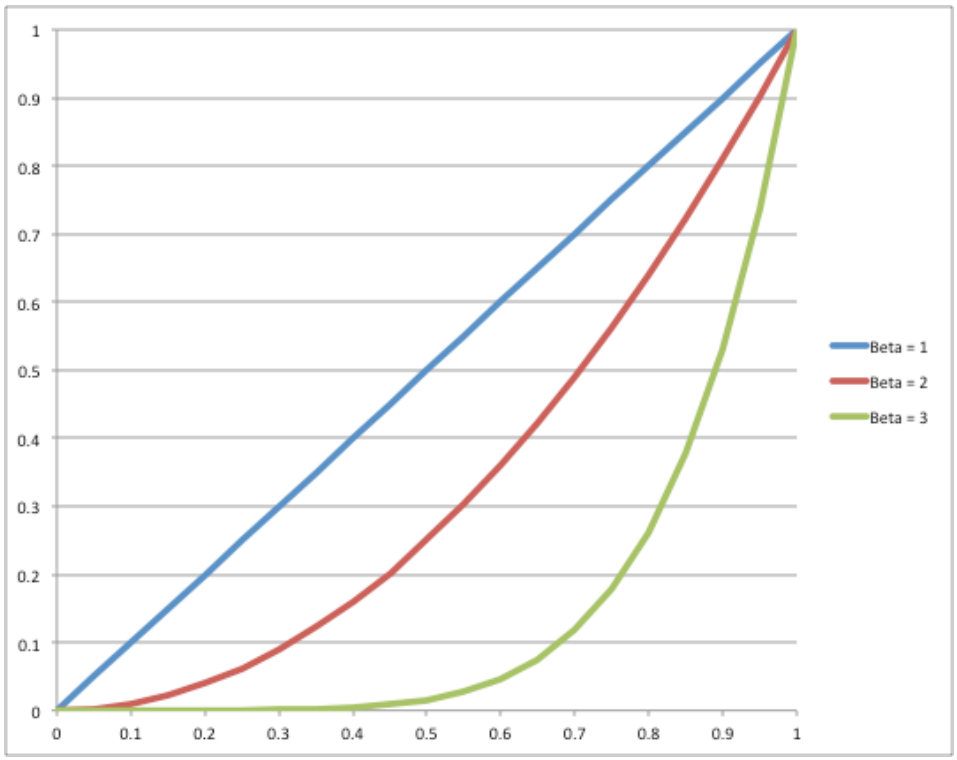

Figure A.5 Relation between SM/Fc (x-axis) and the fraction of water running off (y-axis) for three values of β :1, 2 and 3.

A percentage of the soil moisture will evaporate. This percentage is related to the measured potential evaporation and the available amount of soil moisture:

$$E_a = SM/T_m \, E_p; \; SM \leq T_m$$

$$E_a = E_p; \; SM > T_m$$

where E_a is the actual evaporation, E_p is the potential evaporation and T_m ($\leq F_c$) is a user defined threshold, above which the actual evaporation equals the potential evaporation. T_m is defined as $LP * F_c$ in which LP is a soil dependent evaporation factor ($LP \leq 1$).

In the original model (Berglöv, 2009) a correction to is applied in case of interception. If E_a from the soil moisture storage plus E_i exceeds ET_p-E_i (E_i is equal to the interception evaporation) then the exceeding part is multiplied by a factor (1-*ered*) ≤1, where the parameter *ered* varies between 0 and 1. This correction is presently not included in the WFLOW model.

A.7 The runoff response routine

The volume of water which becomes available for runoff, $S_{dr} + SP$ is transferred to the runoff response routine. In this routine the runoff delay is simulated through the use of a number of linear reservoirs.

Two linear reservoirs are defined to simulate the different runoff processes: the upper zone (generating quick runoff and interflow) and the lower zone (generating slow runoff). The available runoff water from the soil routine (i.e. direct runoff, S_{dr}, and seepage, SP) in principle ends up in the lower zone, unless the percolation threshold, *PERC*, is exceeded, in which case the redundant water ends up in the upper zone:

$$\Delta V_{LZ} = min\{PERC; (S_{dr} + SP)\}$$

$$\Delta V_{UZ} = min\{0.0;(S_{dr} + SP - PERC)\}$$

where V_{UZ} is the content of the upper zone, V_{LZ} is the content of the lower zone and Δ means increase of. Capillary flow from the upper zone to the soil moisture reservoir is modelled according to:

$$Q_{cf} = cflux * (F_c - SM)/F_c$$

where *cflux* is the maximum capillary flux in *mm/day and* F_c is the field capacity. The Upper zone generates quick runoff (C_q) using:

$$Q_q = K * UZ^{(1+\alpha)}$$

here K is the upper zone recession coefficient, and α determines the amount of non-linearity. Within HBV-96, the value of K is determined from three other parameters: α, *KHQ*, and *HQ [mm/day]*. The value of *HQ* represents an outflow rate of the upper zone for which the recession rate is equal to *KHQ*. If we define UZ_{HQ} to be the content of the upper zone at outflow rate *HQ,* the following holds:

$$HQ = K * (UZ_{HQ})^{(1+\alpha)} = KHQ * UZ_{HQ}$$

If we eliminate UZ_{HQ} we obtain:

$$HQ = K * (HQ/KHQ)^{(1+\alpha)}$$

Rewriting for *K* results in:

$$K = KQH^{(1-\alpha)}\, HQ^{-\alpha}$$

The lower zone is a linear reservoir, which means the rate of slow runoff, Q_{LZ}, which leaves this zone during one time step equals:

$$Q_{LZ} = K_{LZ} * V_{LZ}$$

where K_{LZ} is the reservoir constant. The upper zone is also a linear reservoir, but it is slightly more complicated than the lower zone because it is divided into two zones: 1) a lower part in which interflow is generated and 2) an upper part in which quick flow is generated (see Figure A.6).

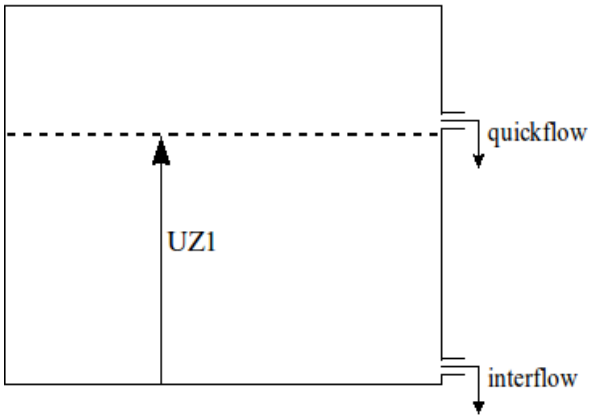

Figure A.6 Schematic view of the upper zone.

If the total water content of the upper zone, V_{UZ}, is lower than a threshold value *UZ1*, the upper zone only generates interflow. On the other hand, if V_{UZ} exceeds *UZ1*, part of the upper zone water will runoff as quick flow:

$$Q_i = Ki * min\ \{UZ1;\ V_{UZ}\}$$

$$Q_q = Kq * max\ \{(V_{UZ};\ UZ1);\ 0.0\}$$

Where Q_i is the amount of generated interflow in one time step, Q_q is the amount of generated quick flow in one time step and K_i and K_q are reservoir constants for interflow and quick flow respectively.

The total runoff rate, *Q*, is equal to the sum of the three different runoff components:

$$Q = Q_{LZ} + Q_i + Q_q$$

The runoff behaviour in the runoff response routine is controlled by two threshold values P_m and *UZ1* in combination with three reservoir parameters, K_{LZ}, K_i and K_q. In order to represent the differences in delay times between the three runoff components, the reservoir constants have to meet the following requirement:

$$K_{LZ} < K_i < K_q$$

B Running WFLOW in Delft-FEWS

The WFLOW model runs in Delft-FEWS by opening the tab: “Tools” and then clicking on the “Manual Forecast”. You have to choose the workflow: “WFLOW historical”. This workflow calls the WFLOW adapter which runs the WFLOW model. The T0 presented in the screen is the end time of the WFLOW simulation. You can edit this yourself. Furthermore, you can choose whether you want to run the model for a cold or warm situation by selecting the tab: ”Select initial state”. By clicking the run button you can start the WFLOW simulation. The result maps and time series are automatically loaded into your Delft-FEWS system. A screenshot of the simulated discharge of WFLOW imported in FEWS at 13-08-2010 is presented in the figure below (Figure B.1).

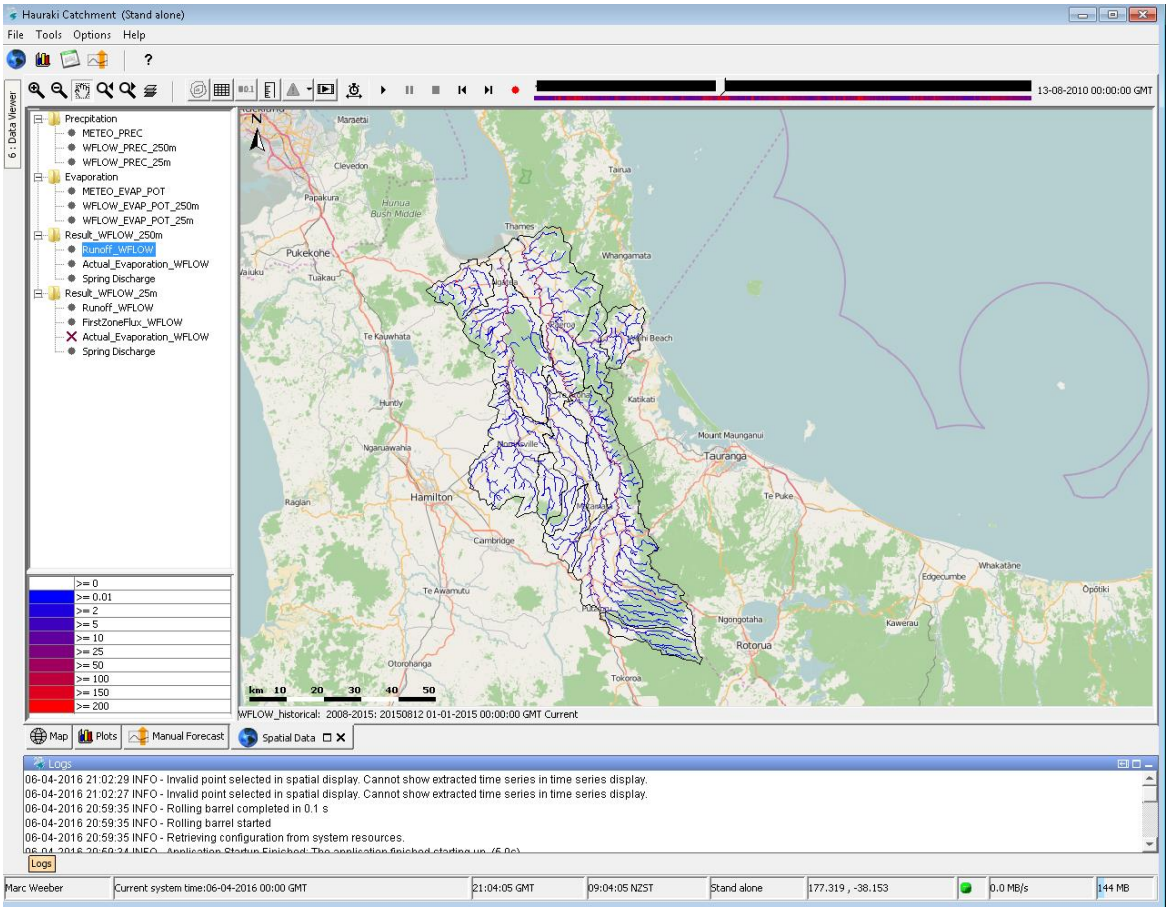

Figure B.1 Example simulated discharge in Delft-FEWS for 13-08-2010.

C Model Setup Tool

C.1 Introduction

The process around setting up the model schematisation has been automated in the WFD-Explorer Python Model Setup Tool. Automating the setup process was required as the Hauraki plains catchment contains too many farms and streams to setup the model manually. The model setup tool requires Python 3.3.5 and consists of the following libraries:

- WFDE_functionalities: contains the functionalities that are required to setup the model within a python class.
- WFDE_formats: contains example formats for the data required to setup the model.
- WFDE_analyses: contains functionalities that can be used to analyses the model results.
- fiona_shapely: a library that contains the geographic alterations and calculations that are required for setting up the model schematisation.
- mpw_csv: a personalized library for operations with CSV files.
- mpw_indexing: a personalized library for indexation.
- mpw_check: a personalized library for frequent used checks on the data provided.

Furthermore, these libraries make use of several published Python libraries, which are either included with the python installation or can most easily be downloaded at:
http://www.lfd.uci.edu/~gohlke/pythonlibs/

Currently the model setup tool requires the following external input to setup the model:

- Rivers (geographic line shapefile with a projected coordinate system)
- All land-use (geographic polygon shapefile with a projected coordinate system)
- Selectable land-use (geographic polygon shapefile with a projected coordinate system)
- Point sources (geographic point shapefile with a projected coordinate system)
- WFLOW results (mm water setup per day per aggregated land-use polygon)

All the geographic files should use the same projected coordinate system. The reason that it has to be a projected coordinate system is that distances are used in the model setup tool. There are several land-use polygon shapefiles that are used in the model setup tool. The largest shapefile with the finest features is the “all land-use shapefile”. This shapefile includes the property boundaries (farmland, but also forest or wetland), but as well additional small land-use elements like rivers, roads and slivers (small discrepancies between polygons). To not overcomplicate the model, these small elements are assigned to the nearest property boundaries. Aggregated this is called the “aggregated land-use shapefile”. The shapefile containing only the property boundaries on which selections will be performed in the model is called the “selectable land-use shapefile”. All these three shapefiles are required to use the model setup tool, but only the “all land-use shapefile” and “selectable land-use shapefile” are loaded in the model setup tool.

The WFLOW results are daily water surplus in mm on the aggregated land-use polygons. Water surplus is the derived runoff from the land after balancing out rainfall, evaporation and shallow groundwater in the WFLOW model. By multiplying the surplus with the area of the polygon the runoff is derived in cubic meters per day, which is used in the model.

C.2 Model setup tool results

The model setup tool will generate the files required for the WFD Explorer to function. The layout of these files are described in Table C.10.1, Table C.10.2, Table C.10.4 and Table C.10.5 and further descriptions can be found in Section 5.6.

Table C.10.1 Attributes for the WFD-Explorer Basins file.

Attribute	Type	Remark
ID	text	Node ID for WFD-Explorer. In this case the source type + "TargetID" field from the land-use GIS file is used. The source type is indicated by the first character (either D or P for diffuse or point source)
Name	text	Specification whether the source is a diffuse or point source
WATERHSURF	float	Horizontal Water surface, set to a default value of 100 m^2. Not yet taken into account by the WFD-Explorer.
WATERVOL	float	Volume of the basin/surface water node, set to a default value of 100 m^3. In this case we do not use the water volume to compute the hydraulic residence time for the removal of nutrients.

Table C.10.2 Attributes for the WFD-Explorer SWU file.

Attribute	Type	Remark
NODEID	text	Node ID for WFD-Explorer. In this case the letter "N" with the number in which order the node was created.
TAG	text	Specification whether the node was created for the river network ("Junction node") or created from the intersect by land-uses ("Load node").
WATERVOL	float	Volume of the basin/surface water node, set to a default value of 100 m^3. In this case we do not use the water volume to compute the hydraulic residence time for the removal of nutrients.
WATERHSURF	float	Horizontal Water surface, set to a default value of 100 m^2. Not yet taken into account by the WFD-Explorer.

Table C.10.3 Attributes for the WFD-Explorer Links file.

Attribute	Type	Remark
LinkID	text	Link ID for WFD-Explorer. This is a combination of the diffuse source, point source or SWU from which the links flows with the SWU the link connects to separated by "_" (for example "DOT6441_N2220").
Tag	text	Specification whether the link was created to join SWUs, a diffuse source or a point source.
NodeFrom	text	The origin node name
NodeTo	text	The destination node name

Table C.10.4 Attributes for the WFD-Explorer Flow file

Attribute	Type	Remark
LinkID	text	The LinkID as defined in the Link file.
FlowType	text	Specification of the FlowType, relative (“R”) or absolute (“A”).
Value	float	The flow value, depending on the FlowType in percentage or m^3/s.
Year	integer	The year for which the flow values are valid.
Period	integer	The period for which the flow values are valid.

Table C.10.5 Attributes for the WFD-Explorer EmDifSources file.

Attribute	Type	Remark
NodeID	text	The NodeID as defined in the Basins file
EmissionTypeId	text	In this model the EmissionTypeIds specified are the block types and runoff from the WFLOW model.
VariableId	text	In this model the VariableIds specified are Q (discharge), totN (total nitrogen) and totP (total phosphorus)
Value	float	This is the quantity of the VariableId that is presented to the model from this specific Basin node. For discharge the unit is m^3/s and for substances g/s.
Percentage	float	This percentage is an attenuation factor that is subtracted from the load before it enters the model.
Year	integer	The year for which the flow values are valid.
Period	integer	The period for which the flow values are valid.

C.3 Tutorial

The following tutorial will guide the user through setting up a WFD-Explorer model with the Model Setup Tool. The requirement for the model setup tool to work is that python 3.3.5 has been installed including the required packages.

First import the functionalities part of the Model Setup Tool:
import WFDE_functionalities

Setting up a new model case

1. Make a Case

A new model case is created with the following function. When setting up the class the user needs to provide a suitable path to create the case folder, the periods in which a model year is divided and the years that are being modelled.

```
Hauraki = WFDE_functionalities.WFDExplorerModelSetup("d:/Hauraki_case1",\
          calc_periods = [1,2,3,4,5,6,7,8,9,10,11,12], \
          calc_years = [2008,2009,2010,2011,2012,2013])
```

When a case has already been created the case can be reopened using:
Hauraki = WFDE_functionalities.WFDExplorerModelSetup("d:/Hauraki_case1")

2. Import the required data

When the class has been set up the user should import the data which is required for generating the schematisation. Make sure that all geographic data (shape file, coordinates etc.) are in the same projection coordinate system. A projection coordinate system is required as some operations make use of distance calculations. This is not checked in the library. This data consists of:

- a “river network shapefile” containing the WFLOW schematisation of the surface water stretches,
Hauraki.import_surfacewater_line_shape(path_rivershapefile)

- an “aggregated land-use shapefile” covering the catchment with the complete load and flow tiles (roads, surface water and slivers are added to the defined tiles).
Hauraki.import_land_unit_shape(path_landunitsshapefile)

- a “selectable land-use shapefile” covering the catchment with the defined land-use tiles (actual land-use tiles like farming, natural area etc. excluding roads, surface water and slivers).
Hauraki.import_diffuse_sources_shape(path_diffusesources_shapefile)

- a “point sources shapefile” containing the outflow location of the point sources
Hauraki.import_point_sources_shape(path_pointsources_shapefile)

As the inflows of land-uses and point sources are distributed over the nearest river stretches an intersection of the WFLOW schematisation with the aggregated land-use shapefile is made.
Hauraki.intersect_surfacewater_landunit()

Create the WFD-Explorer schematisation

1. Create junction nodes

The first step in transferring the WFLOW-schematisation into a WFD-Explorer schematisation is defining the junctions where several river reaches merge into one or the opposite. On these junctions, junction nodes are placed. These junction nodes make sure that the WFD-Explorer schematisation follows the pattern of the WFLOW-schematisation.
Hauraki.get_junctionnodes()

2. Create load nodes

Using the junction nodes, the load nodes are added to the river stretches. The stretches have been divided by the covering tiles in the previous intersection. They have been further separated by the junction nodes. For each river stretch a load node is added. Between the load nodes and the junction nodes a link network is created. Now the WFD-Explorer schematisation depicts the WFLOW schematisation.

As in the intersection between the aggregated land-use shapefile and the river network shapefile some gaps can occur, the uncertainty of linking coordinates for the start and the end of the stretches can be set. The uncertainty will be in the unit of the coordinate

system provided with the shapefile. If the correct links find no or several connections within the set uncertainty, an error will occur.
Hauraki.add_loadnodes(uncertainty = 0.0000005)

3. Set link direction

Even though the WFD-Explorer schematisation depicts the WFLOW schematisation, the links have not been set in the flow direction. Based on the outflow locations (in this case in the Firth of Thames the junction nodes N46, N14 and N4) the links are set into the correct direction. The information provided to make the link and flow files is updated.
Hauraki.Links.set_link_directions(outflow_nodes = ["N46","N14","N4"])

4. Add diffuse sources

Here the diffuse sources originating from the land-uses are added to the model schematisation. The location of the diffuse sources is determined by calculating the centroid of the selectable land-use polygons. From these centroids the nearest load node is calculated. All load nodes located within 125% of this distance will be connected through a link with the land-use centroid. On these locations flow and substances coming from this land-use polygon will enter the river network.
The function requires that the uniquely identifying column for the polygons in the ”selectable land-use shapefile” is indicated.
Hauraki.add_diffuse_sources("TargetID")

5. Add point sources

The same exercise as done for the diffuse sources is also performed for the point sources. However, in this case there is no need to determine a centroid and there will only be a link by the nearest load node, as point sources like waste water treatment plants and meat works will enter the river in one location.
Hauraki.add_point_sources("map letter")

Create the flows and emissions

1. Import the required data

Several input files need to be loaded to create the distribution of the substances. These input files are automatically loaded when available and will also be automatically generated when the case is created.

The input files can be filled or edited under the folder:
“[CASE_PATH]/input/diffuse_sources”
And:
“[CASE_PATH]/input/point_sources”

When the files are located in another folder and need to be imported from there, these files can manually be referenced with the following functions. These functions require a path to the CSV file and the delimiter used to store the file:
Hauraki.import_substances_considered(path_substances, sep = ";")

Hauraki.import_land_use_categories_considered(path_landuse_categories, sep = ";")

Hauraki.import_soiltype_per_tile("TargetID",path_soiltype_tiles,";")

Hauraki.import_other_areas_per_tile("TargetID",path_other_tiles,";")

Hauraki.import_catchment_per_tile("TargetID",path_catchment,";")

Hauraki.import_specification_per_tile("TargetID",path_specified,";")

2. Distribute the flows

This function calculates the mm WFLOW results per aggregated polygon towards a cubic meter per day runoff value. These values are then further aggregated based on the periods and years. The data supplied in the WFLOW results should be indicated in the function.

Input in the function is:

- the corresponding number between the WFLOW polygon results and the polygons in the “aggregated land-use shapefile”;
- the property name in the “aggregated land-use shapefile”;
- the column in the shapefile that contains the area of the shapefile in m^2;
- the years present in the WFLOW results;
- the days that each year contains;
- the output years that need to be generated and
- in how many periods the day results of those years should be aggregated.

```
Hauraki.derive_flows_from_WFLOW(WFLOW_nr_feature = 'IDENT',\
    naming_feature = 'TargetID', area_feature = 'AREA', \
    data_years = [2008,2009,2010,2011,2012,2013],\
    data_timesteps_per_year = [366,365,365,365,366,365],\
     output_years = [2008,2009,2010,2011,2012,2013], output_periods = 12)
```

3. Distribute the diffuse source substances

This function distributes the provided substance values for the diffuse sources (land-uses) over these sources based on land-use categories, catchment, specifics and soil type. These substances can be further divided based on block type and a specific type of land-use a proportion of the block type can be determined. Per land-use polygon a distribution of soil types can be created.

The files that are used as input for creating the substances from diffuse sources can be found at the following location:
“[CASE_PATH]/input/diffuse_sources”

Input in the function is:

- the property name in the “selectable land-use shapefile”;
- the property land-use assigned in the “selectable land-use shapefile”;
- the path where the diffuse source substance data is stored (will automatically look for the standard location if not filled);
- the path to a CSV with the land-use, soil type, block type area distribution.
- the output years that need to be generated;
- the days that each year contains;

- in how many periods the day results of those years should be aggregated and
- the distribution that should be followed per period if only the total year contribution is specified.

```
Hauraki.create_diffuse_loads_from_landuse(naming_feature = "TargetID",\
    landuse_feature = "DAIRYNZ_CO",\
    path_folder_substance_data = path_diffuse_substance_data, \
    path_area_landuse = path_area_landuse,\
    output_years = [2008,2009,2010,2011,2012,2013],\
    year_days = [366,365,365,365,366,365], periods = 12,\
    distribution = [0.0833, 0.0833, 0.0833, 0.0833, 0.0833, 0.0833, 0.0833,
    0.0833, 0.0833, 0.0833, 0.0833, 0.0833] )
```

4. Distribute the point source substances

This function distributes the provided substance values for the point sources over these sources based on the actual value provided per point source.

The files that are used as input for creating the substances from point sources can be found at the following location:
"[CASE_PATH]/input/point_sources"

Input in the function is:

- the point source identifier in the "point sources shapefile";
- the point source type that has been assigned in the "point sources shapefile";
- the path where the point source substance data is stored (will automatically look for the standard location if not filled);
- the output years that need to be generated;
- the days that each year contains;
- in how many periods the day results of those years should be aggregated and
- the distribution that should be followed per period if only the total year contribution is specified.

```
Hauraki.create_point_loads_from_file(naming_feature = "map letter", \
    descriptive_feature = "type", path_folder_substance_data =
    path_point_substance_data,\
    output_years = [2008,2009,2010,2011,2012,2013],
    year_days = [366,365,365,365,366,365], periods = 12,\
    distribution = [0.0833, 0.0833, 0.0833, 0.0833, 0.0833, 0.0833, 0.0833,
    0.0833, 0.0833, 0.0833, 0.0833, 0.0833])
```

5. Write to file

At last the results generated with the Model Setup Tool are exported to a format that is suitable to be loaded in the WFD-Explorer. These functionalities are separated in two parts, where the first functionality will create the file and the second will export it from the Model Setup Tool.

Only for the creation of the flow file, the years to export and periods need to be specified.

```
Hauraki.Swu.create_file()
Hauraki.Swu.export_csv()
```

```
Hauraki.Links.create_file()
Hauraki.Links.export_csv()

Hauraki.Flows.create_file(year = [2008,2009,2010,2011,2012,2013],\
    period = [1,2,3,4,5,6,7,8,9,10,11,12])
Hauraki.Flows.export_csv()

Hauraki.Basins.create_file()
Hauraki.Basins.export_csv()

Hauraki.EmDifSources.create_file()
Hauraki.EmDifSources.export_csv()
```

C.4 Further documentation

For further documentation and feasibilities of the Model Setup Tool the description can be found in the python scripts.

D Analysis of flows and load

D.1 Difference between years for flow

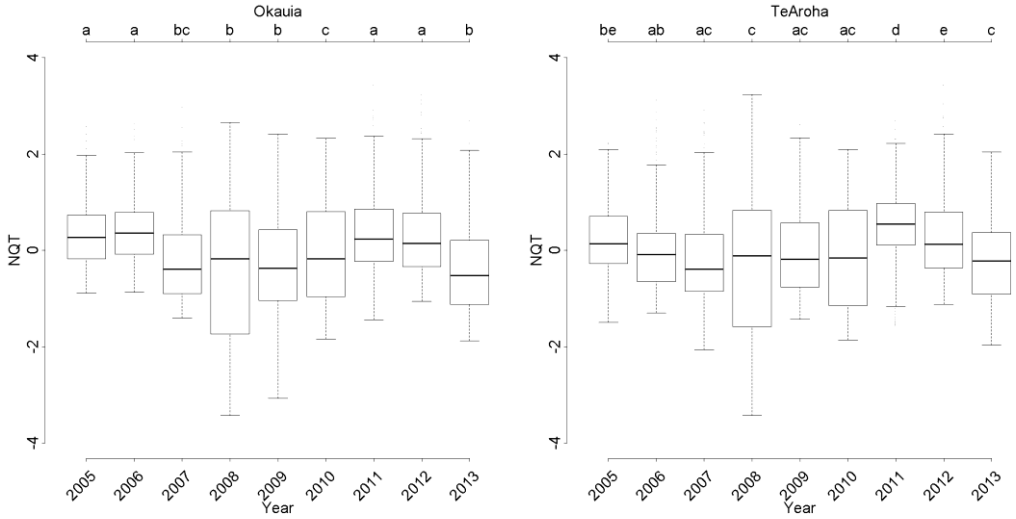

Figure D.1 Mean annual flow at Waihou measurement stations Okauia and Te Aroha, 2005-2013. The left figure represents the upstream measurement station. Note that the flows have been normalised using the Normal Quantile Transformation and the significant difference between the means of the flows have been tested using the "Posthoc Tukey test". Similar years for flow are indicated by a shared letter, where the entire code is shared meaning a similarity to any other year with that exact code and otherwise a similarity with any other year observing one or more shared letters.

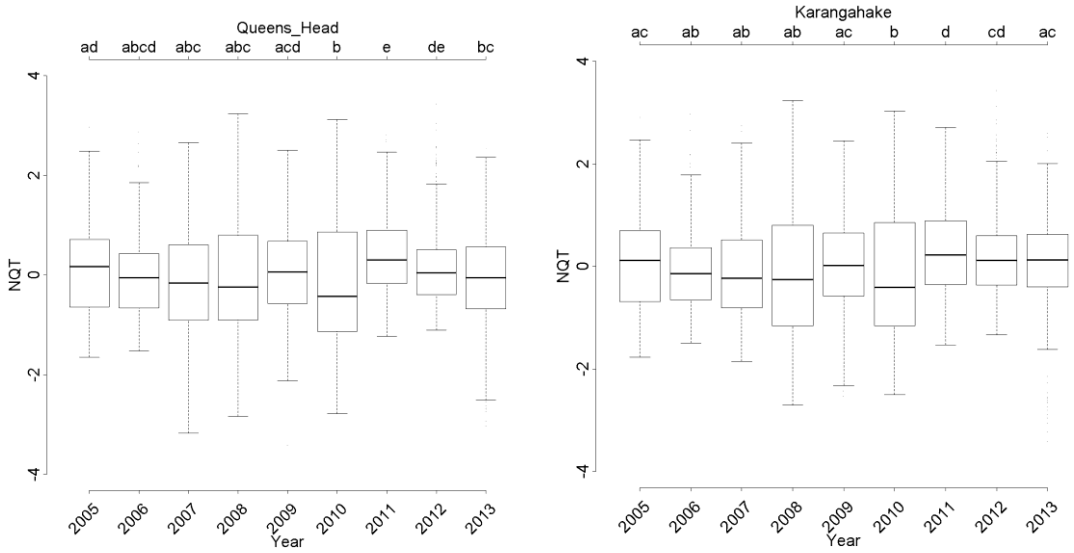

Figure D.2 Mean annual flow at Ohinemuri measurement stations Queens Head and Karangahake, 2005-2013. The left figure represents the upstream measurement station. Note that the flows have been normalised using the Normal Quantile Transformation and the significant difference between the means of the flows have been tested using the "Posthoc Tukey test". Similar years for flow are indicated by a shared letter, where the entire code is shared meaning a similarity to any other year with that exact code and otherwise a similarity with any other year observing one or more shared letters.

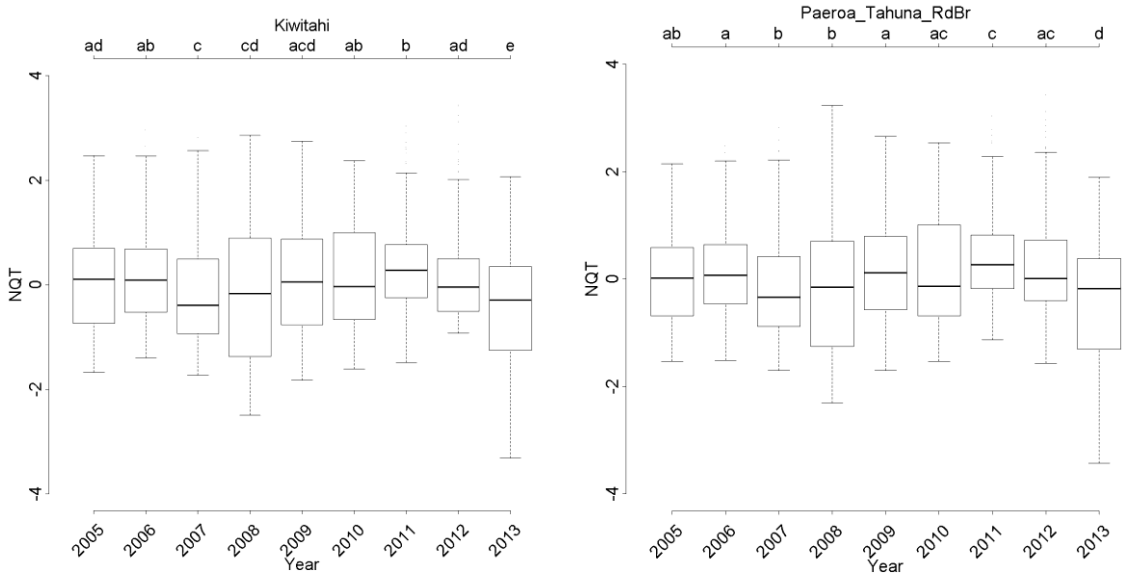

Figure D10.3 Mean annual flow at Piako measurement stations Kiwitahi and Paeroa-Tahuna Rd Br., 2005-2013. The left figure represents the upstream measurement station. Note that the flows have been normalised using the Normal Quantile Transformation and the significant difference between the means of the flows have been tested using the "Posthoc Tukey test". Similar years for flow are indicated by a shared letter, where the entire code is shared meaning a similarity to any other year with that exact code and otherwise a similarity with any other year observing one or more shared letters.

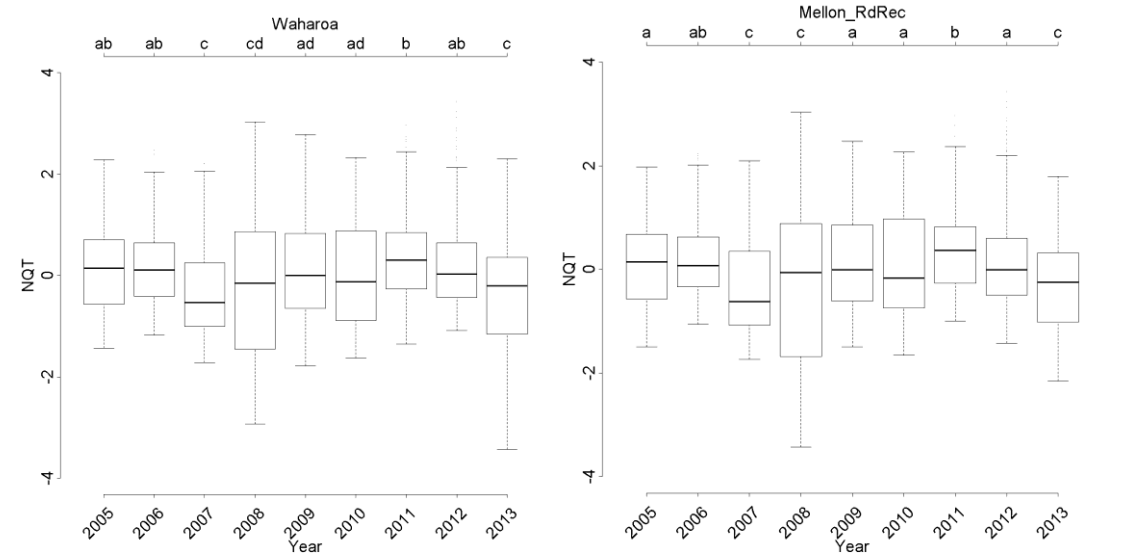

Figure D.4 Mean annual flow at Waitoa measurement stations Landsdowne Rd (Waharoa Control) and Mellon Rd Rec, 2005-2013. The left figure represents the upstream measurement station. Note that the flows have been normalised using the Normal Quantile Transformation and the significant difference between the means of the flows have been tested using the "Posthoc Tukey test". Similar years for flow are indicated by a shared letter, where the entire code is shared meaning a similarity to any other year with that exact code and otherwise a similarity with any other year observing one or more shared letters.

D.2 Difference between years for concentration

One – way ANOVA

Okauia

data: NQT_TN and Year
F = 1.0665,
num df = 8, denom df = 99,
p-value = 0.3928

One – way ANOVA

Te Aroha

data: NQT_TN and Year
F = 1.492,
num df = 8, denom df = 72,
p-value = 0.1753

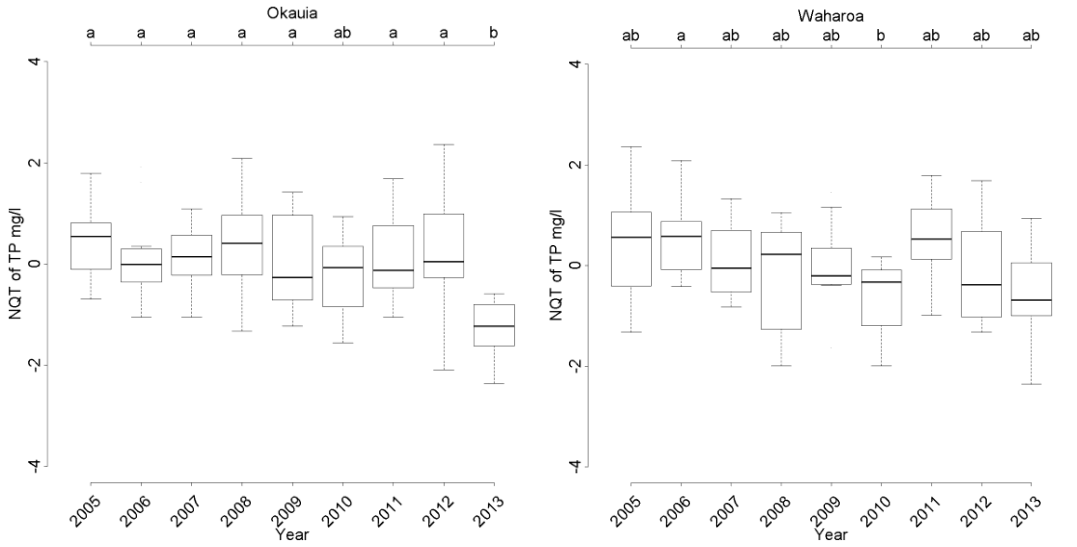

Figure D10.5 TN and TP concentration at Waihou measurement stations Okauia and Te Aroha 2005-2013. The left figure represents the upstream measurement station. Note that the concentrations have been normalised using the Normal Quantile Transformation and the significant difference between the means of the flows have been tested using the "Posthoc Tukey test". Similar years for flow are indicated by a shared letter, where the entire code is shared meaning a similarity to any other year with that exact code and otherwise a similarity with any other year observing one or more shared letters.

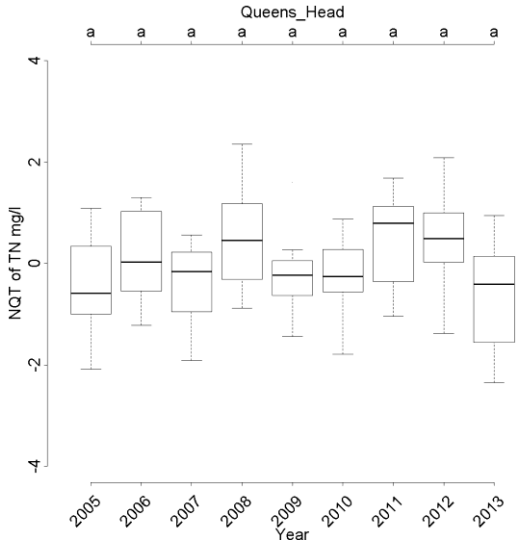

One – way ANOVA

Karangahake

data: NQT_TN and Year
F = 1.3248,
num df = 8, denom df = 72,
p-value = 0.2453

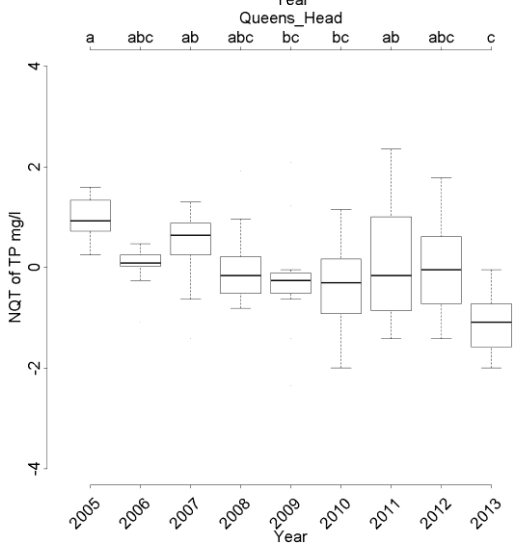

One – way ANOVA

Karangahake

data: NQT_TP and Year
F = 1.0172,
num df = 8, denom df = 72,
p-value = 0.431

Figure D.6 TN and TP concentration at Ohinemuri measurement stations Okauia and Te Aroha 2005-2013. The left figure represents the upstream measurement station. Note that the concentrations have been normalised using the Normal Quantile Transformation and the significant difference between the means of the flows have been tested using the "Posthoc Tukey test". Similar years for flow are indicated by a shared letter, where the entire code is shared meaning a similarity to any other year with that exact code and otherwise a similarity with any other year observing one or more shared letters.

One – way ANOVA

Kiwitahi

data: NQT_TN and Year
F = 0.7557, num df = 8, denom df = 99, p-value = 0.6423

One – way ANOVA

Paeroa-Tahuna Rd Br

data: NQT_TN and Year
F = 1.0922,
num df = 8, denom df = 27,
p-value = 0.3984

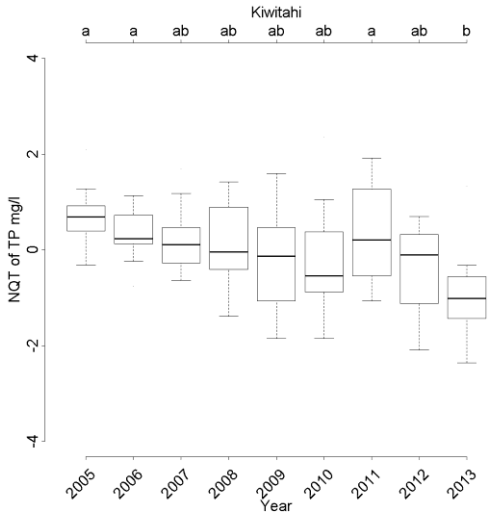

One – way ANOVA

Paeroa-Tahuna Rd Br

data: NQT_TP and Year
F = 1.2208,
num df = 8, denom df = 27,
p-value = 0.3247

Figure D.7 TN and TP concentration at Piako measurement stations Kiwitahi and Paeroa-Tahuna Rd Br 2005-2013.. The left figure represents the upstream measurement station. Note that the concentrations have been normalised using the Normal Quantile Transformation and the significant difference between the means of the flows have been tested using the "Posthoc Tukey test". Similar years for flow are indicated by a shared letter, where the entire code is shared meaning a similarity to any other year with that exact code and otherwise a similarity with any other year observing one or more shared letters.

One – way ANOVA

Waharoa

data: NQT_TN and Year
F = 1.019,
num df = 8, denom df = 99,
p-value = 0.4269

One – way ANOVA

Mellon_RdRec

data: NQT_TN and Year
F = 0.47437,
num df = 8, denom df = 99,
p-value = 0.8716

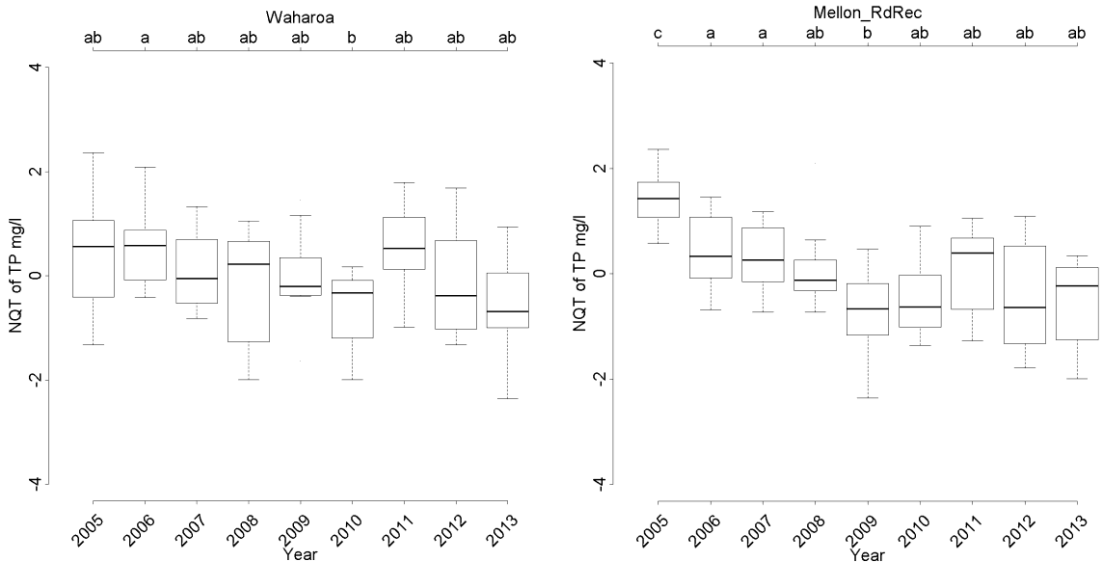

Figure D.8 TN and TP concentration at Waitoa measurement stations Landsdowne Rd Br (Waharoa Control) and Mellon Rd 2005-2013. The left figure represents the upstream measurement station. Note that the concentrations have been normalised using the Normal Quantile Transformation and the significant difference between the means of the flows have been tested using the "Posthoc Tukey test". Similar years for flow are indicated by a shared letter, where the entire code is shared meaning a similarity to any other year with that exact code and otherwise a similarity with any other year observing one or more shared letters.

D.3 Concentration and flow relation

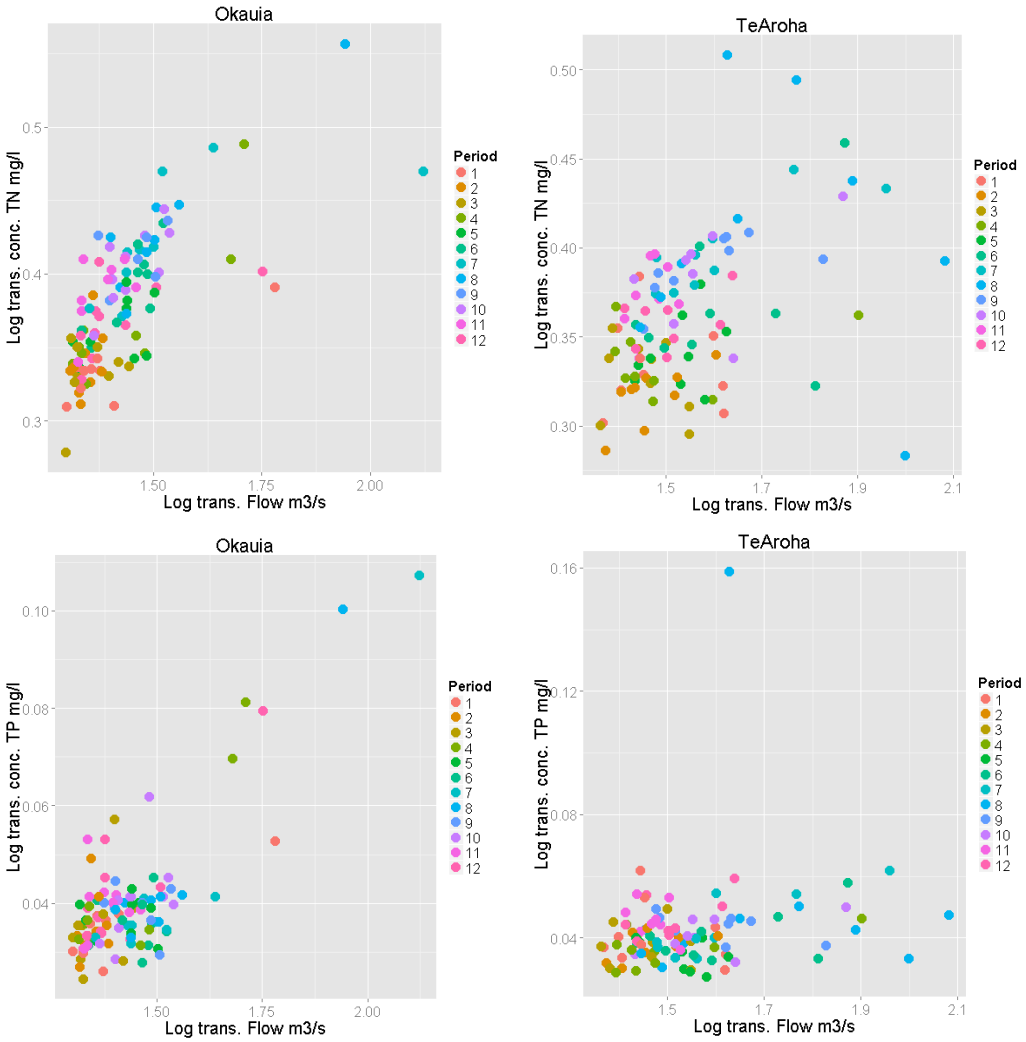

Figure D.1 Waihou measurement stations Okauia and Te Aroha. The left figure represents the upstream measurement station. The period numbering corresponds to month (e.g., 1 = January, 2 = February)

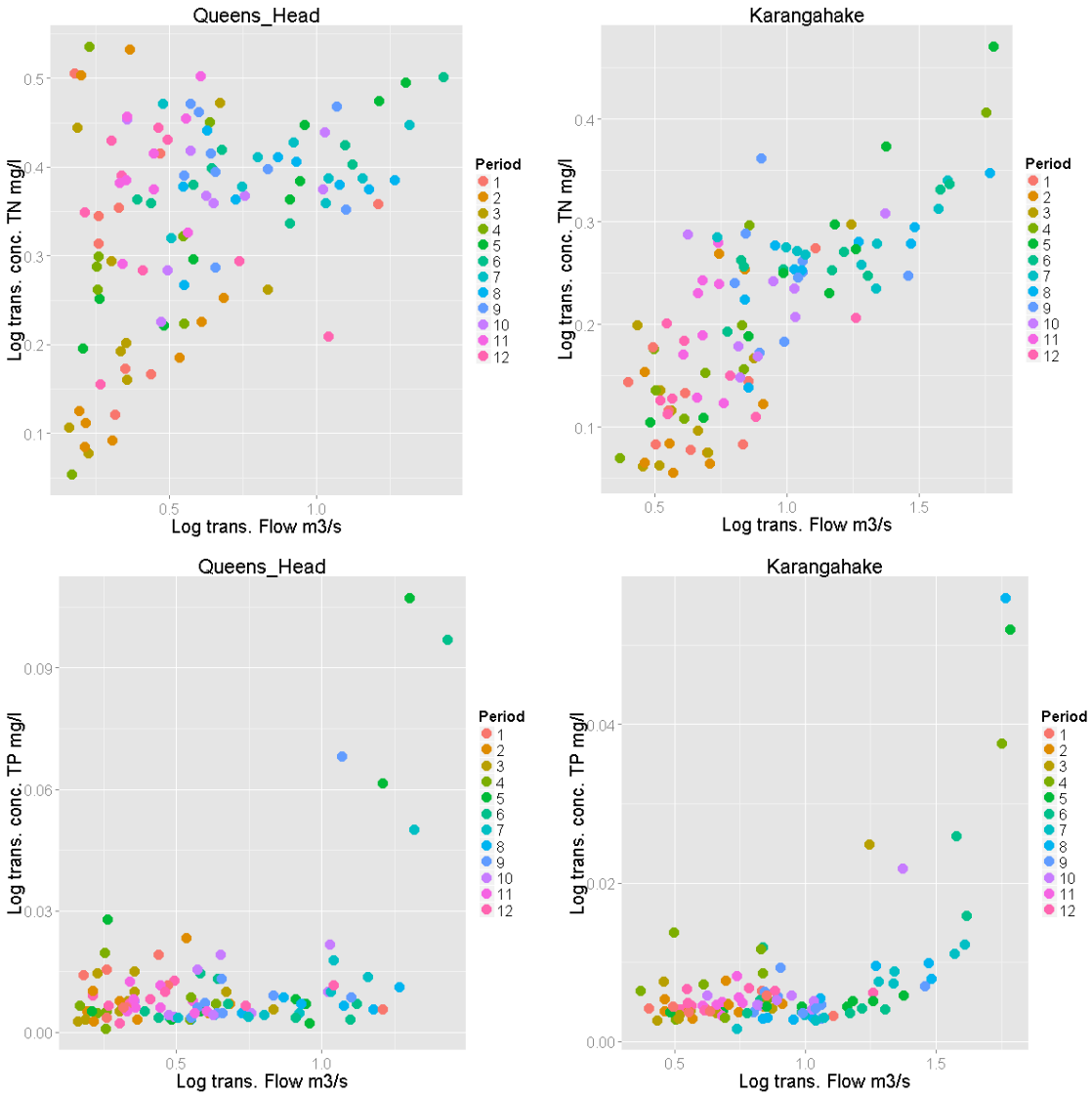

Figure D.2 Ohinemuri measurement stations Queens Head and Karangahake. The left figure represents the upstream measurement station. The period numbering corresponds to month (e.g., 1 = January, 2 = February)

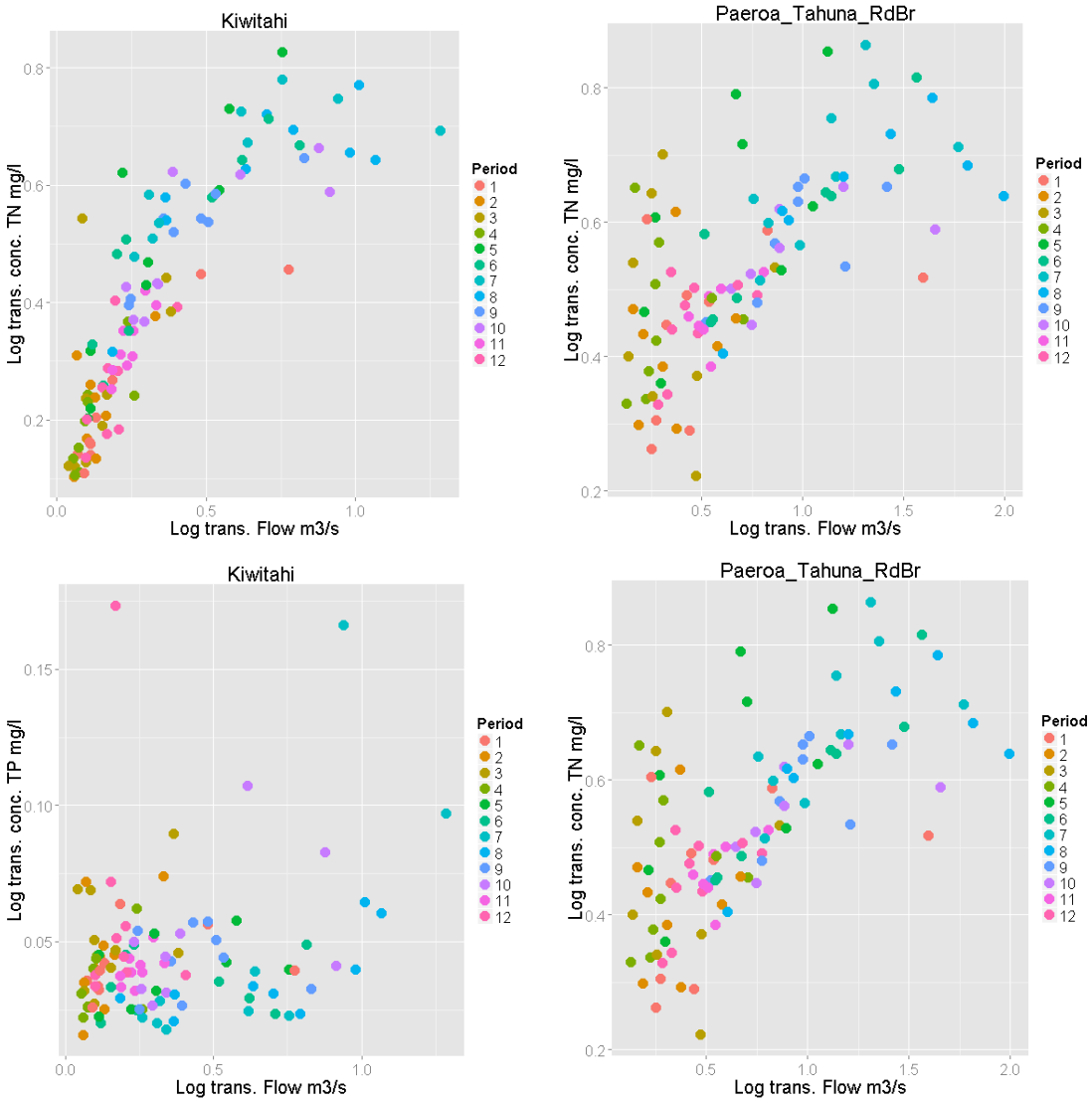

Figure D.3 Piako measurement stations Kiwitahi and Paeroa-Tahuna Rd Br. The left figure represents the upstream measurement station. The period numbering corresponds to month (e.g., 1 = January, 2 = February)

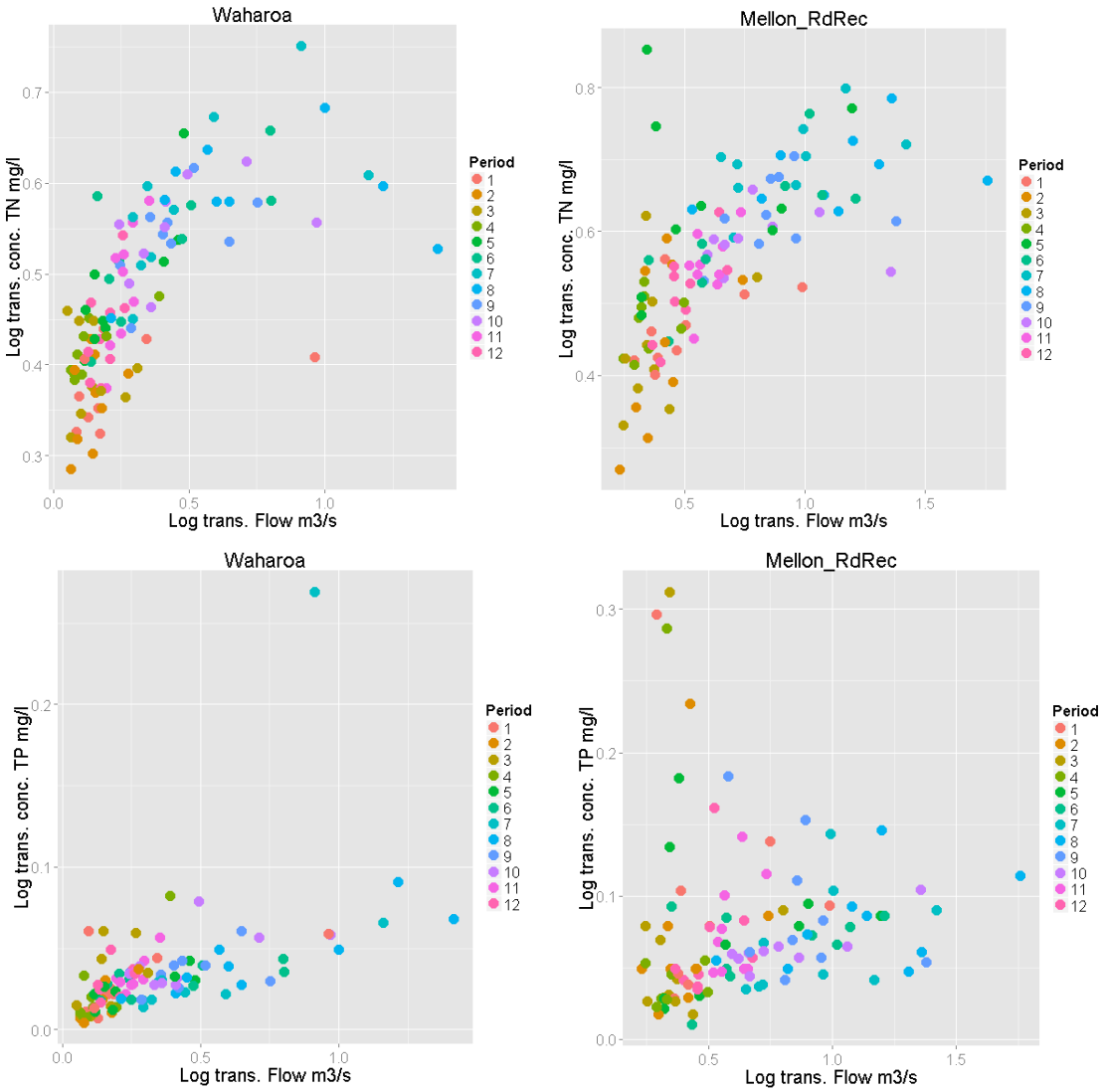

Figure D.4 Waitoa measurement stations Landsdowne Rd (Waharoa Control) and Mellon Rd Rec. The left figure represents the upstream measurement station. The period numbering corresponds to month (e.g., 1 = January, 2 = February)

D.4 Load analysis

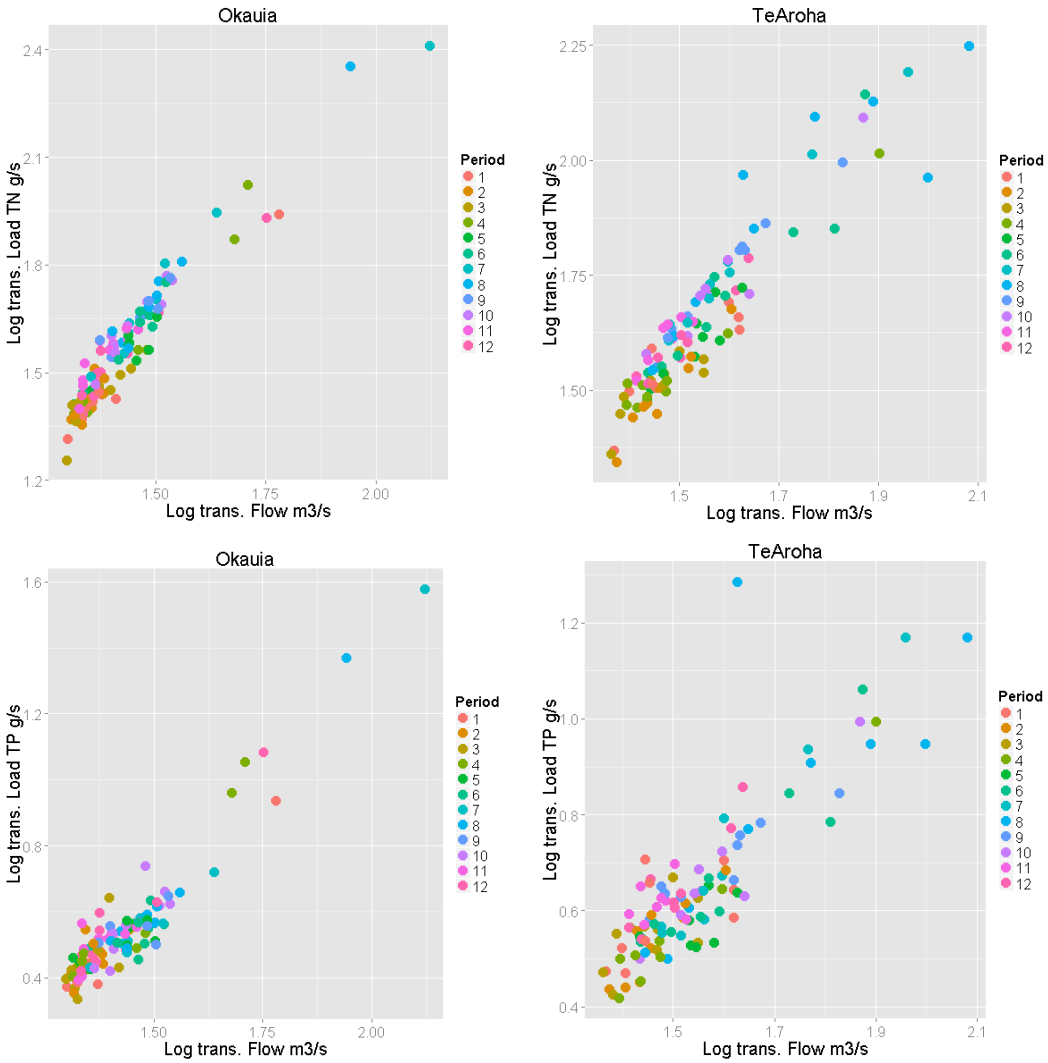

Figure D.5 Waihou measurement stations Okauia and Te Aroha. The left figure represents the upstream measurement station. The period numbering corresponds to month (e.g., 1 = January, 2 = February)

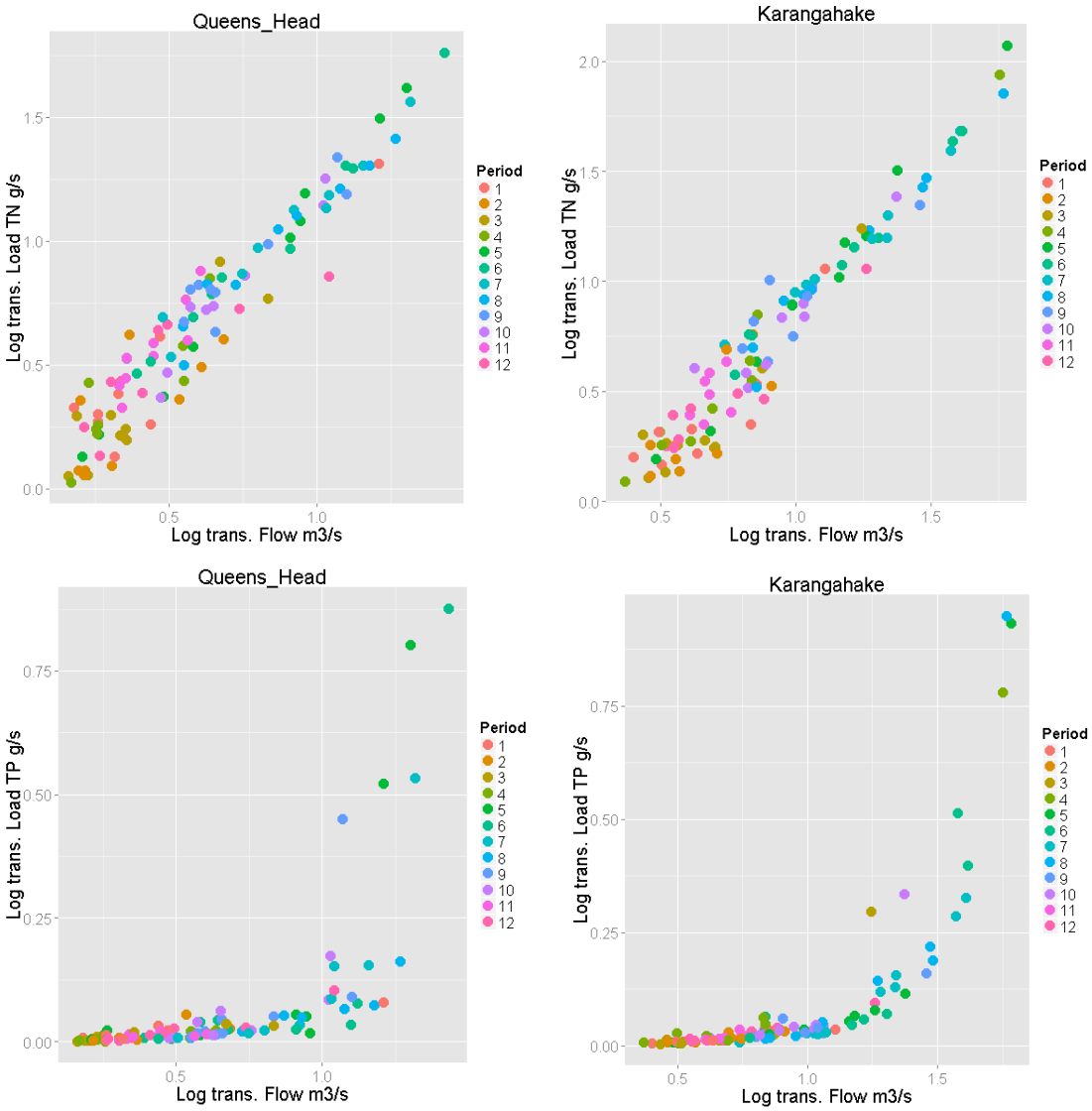

Figure D.6 Ohinemuri measurement stations Queens Head and Karangahake. The left figure represents the upstream measurement station. The period numbering corresponds to month (e.g., 1 = January, 2 = February)

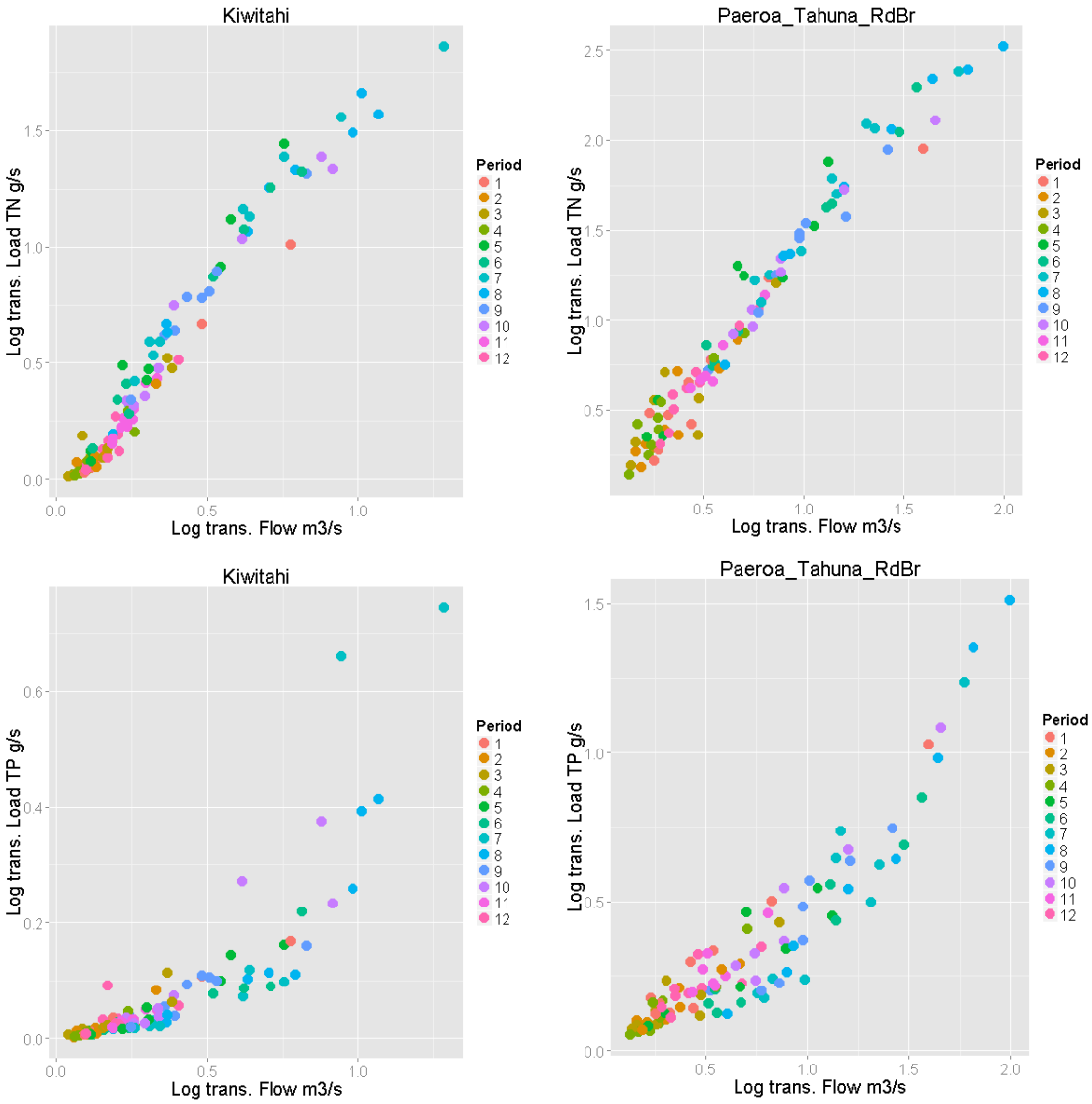

Figure D.7 Piako measurement stations Kiwitahi and Paeroa-Tahuna Rd Br. The left figure represents the upstream measurement station. The period numbering corresponds to month (e.g., 1 = January, 2 = February)

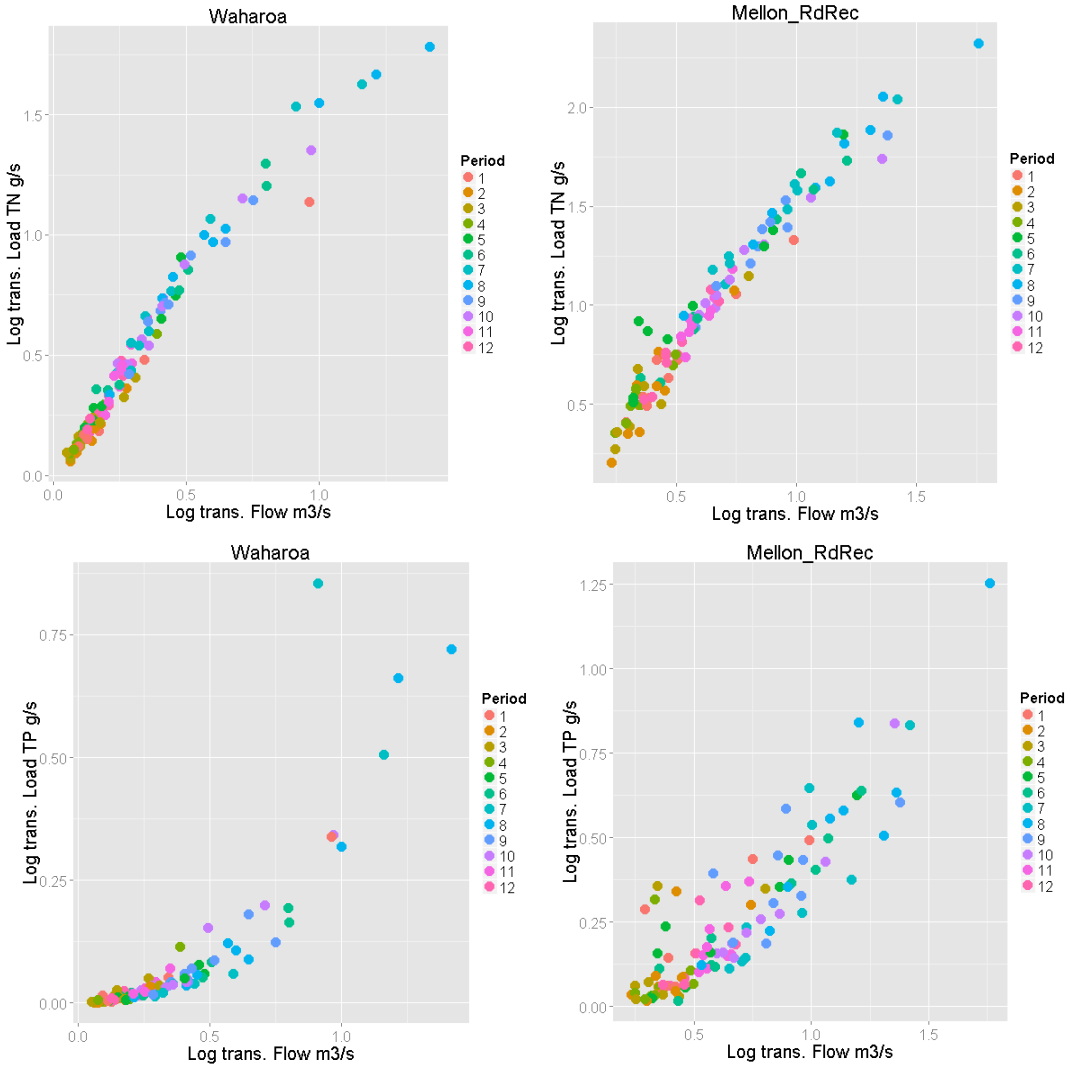

Figure D.8 Waitoa measurement stations Landsdowne Rd (Waharoa Control) and Mellon Rd Rec. The left figure represents the upstream measurement station. The period numbering corresponds to month (e.g., 1 = January, 2 = February)

D.5 Modelled loads (RLoadest)

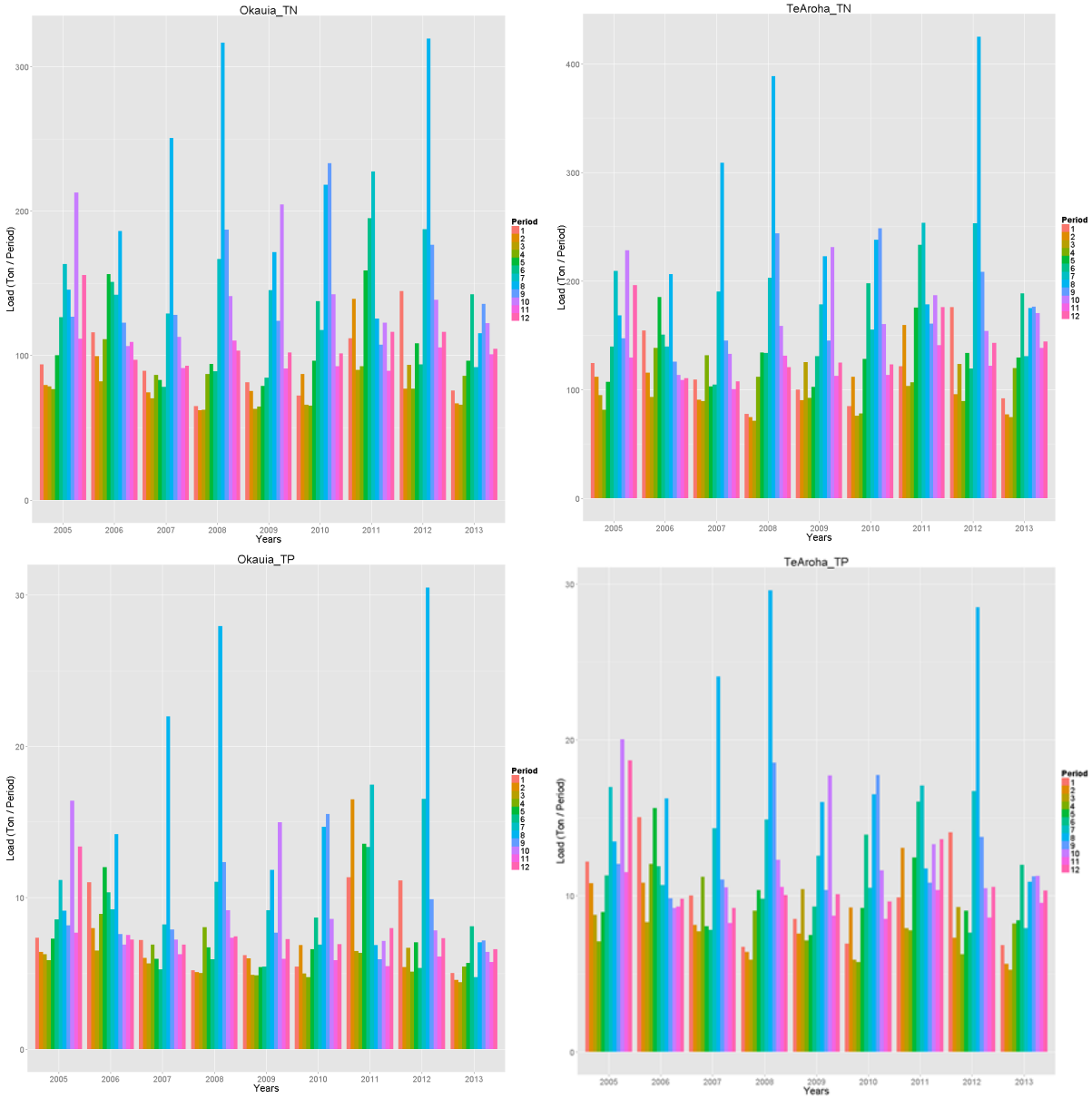

Figure D.9 RLoadest results presented over the periods and years for the Waihou measurement stations Okauia and Te Aroha. The first measurement station is upstream. The period numbering corresponds to month (e.g., 1 = January, 2 = February)

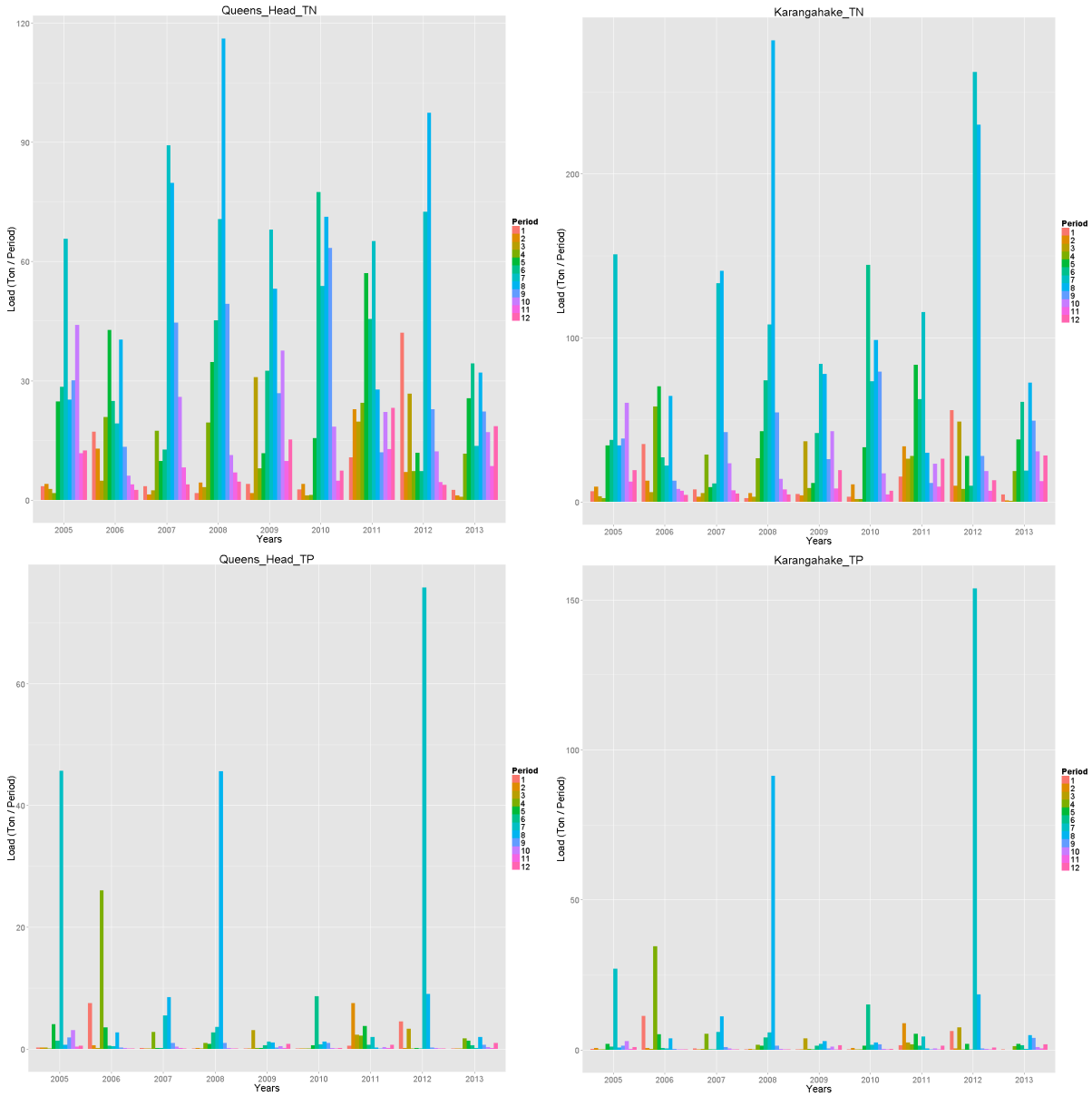

Figure D.10 RLoadest results presented over the periods and years for the Ohinemuri measurement stations Queens Head and Karangahake. The first measurement station is upstream. The period numbering corresponds to month (e.g., 1 = January, 2 = February)

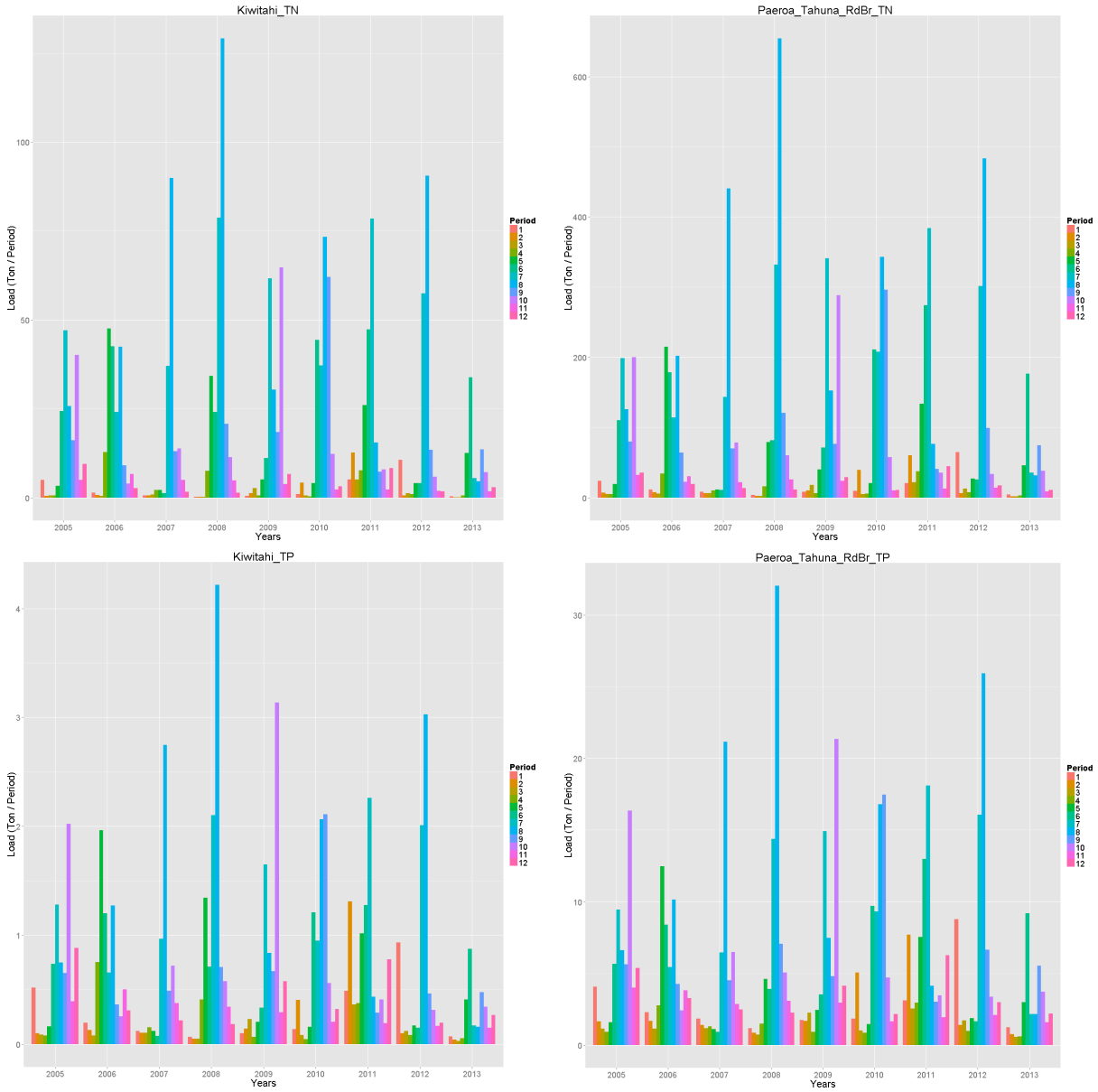

Figure D.11 RLoadest results presented over the periods and years for the Piako measurement stations Kiwitahi and Paeroa-Tahuna Rd Br. The first measurement station is upstream. The period numbering corresponds to month (e.g., 1 = January, 2 = February)

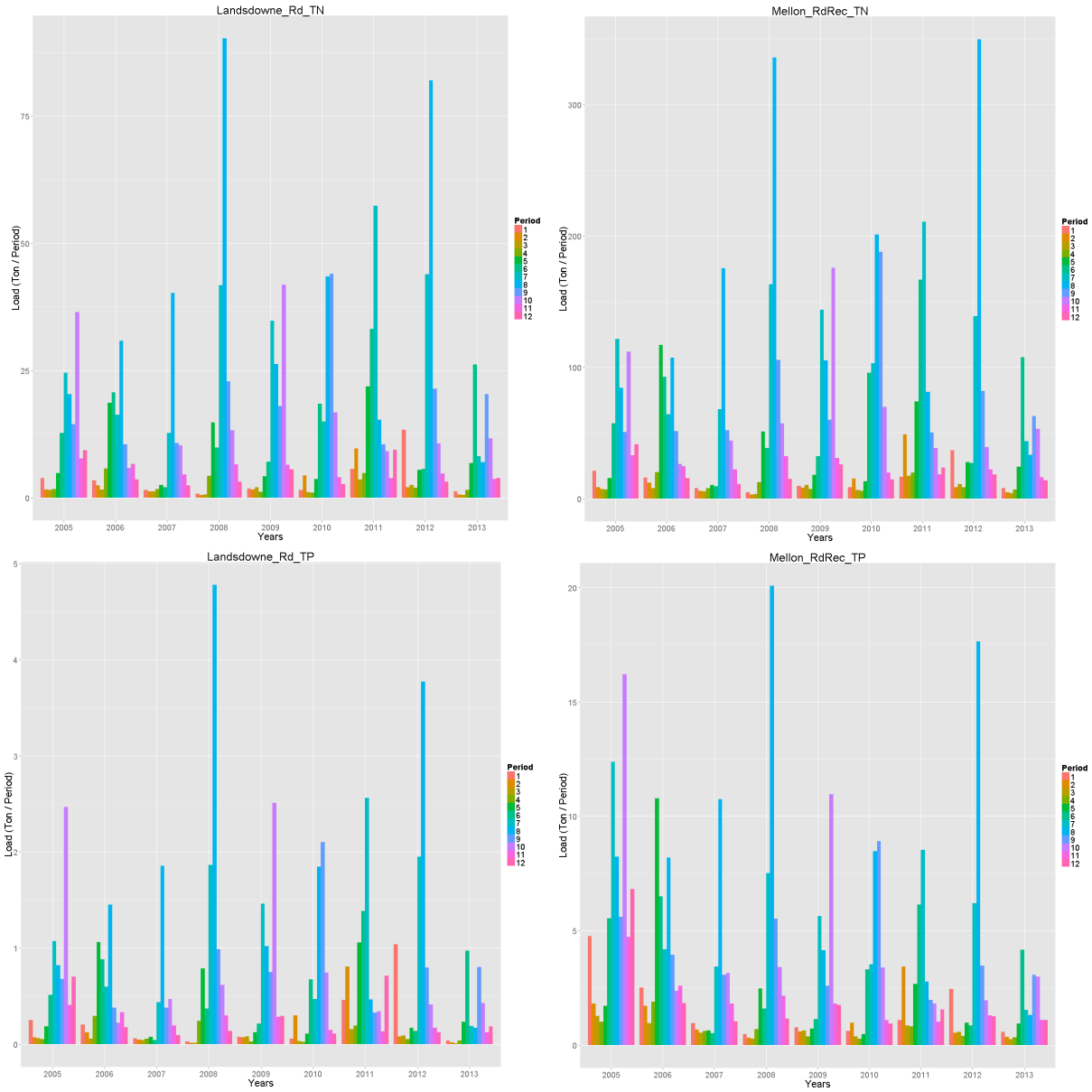

Figure D.12 RLoadest results presented over the periods and years for the Waitoa measurement stations Landsdowne Rd and Mellon Rd Rec. The first measurement station is upstream. The period numbering corresponds to month (e.g., 1 = January, 2 = February)

D.6 Modelled loads relation to flow (RLoadest)

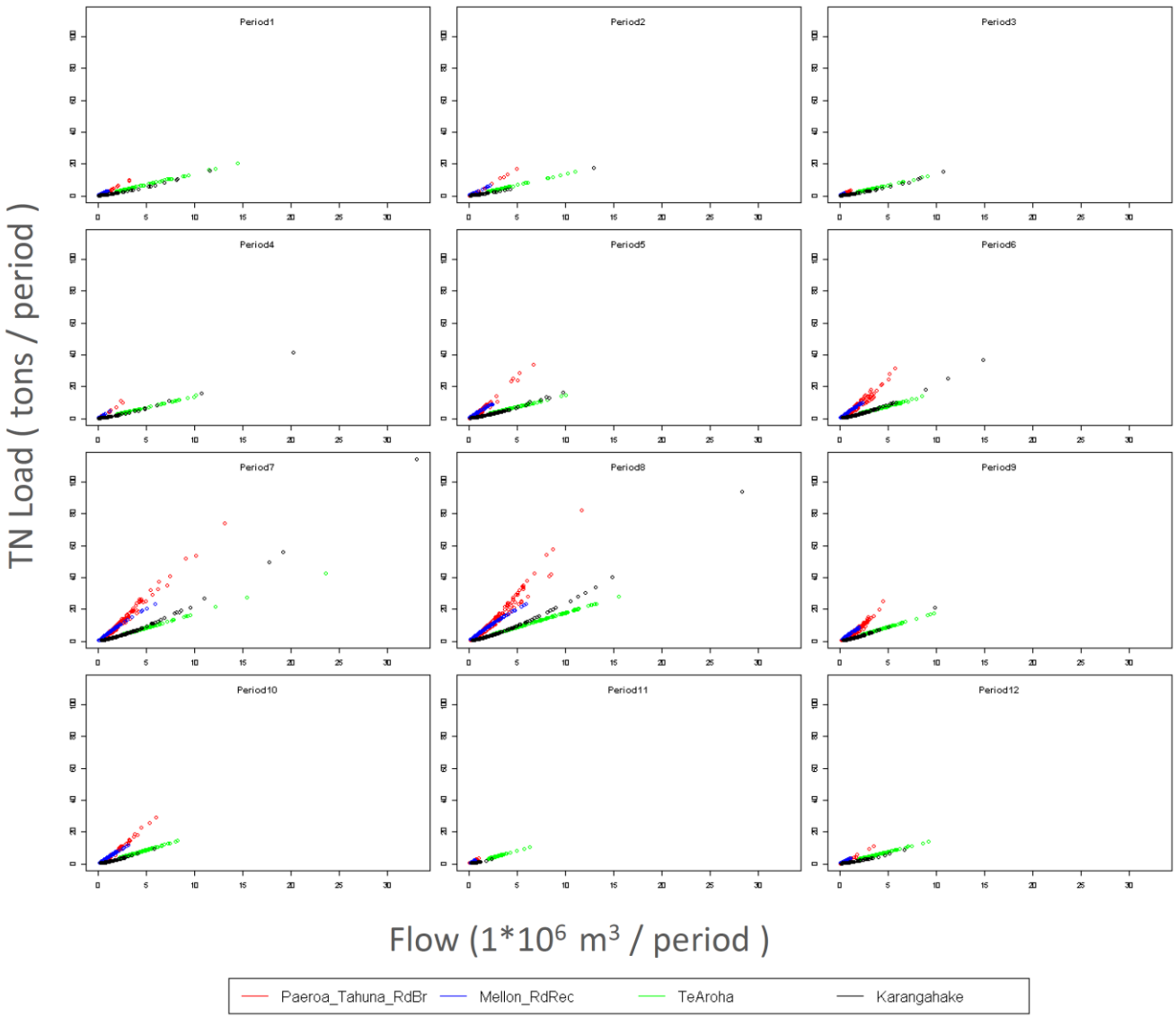

Figure D.13 Linear nitrogen load (calculated with RLoadest) to flow relation for the measurement stations Paeroa-Tahuna Rd Br, Mellon Rd Rec, Te Aroha and Karangahake for the years 2005-2013. These linear relations have been idealised by the RLoadest load calculations. However, the relation between period flow and load are still useful for the calibration. The period numbering corresponds to month (e.g., 1 = January, 2 = February)

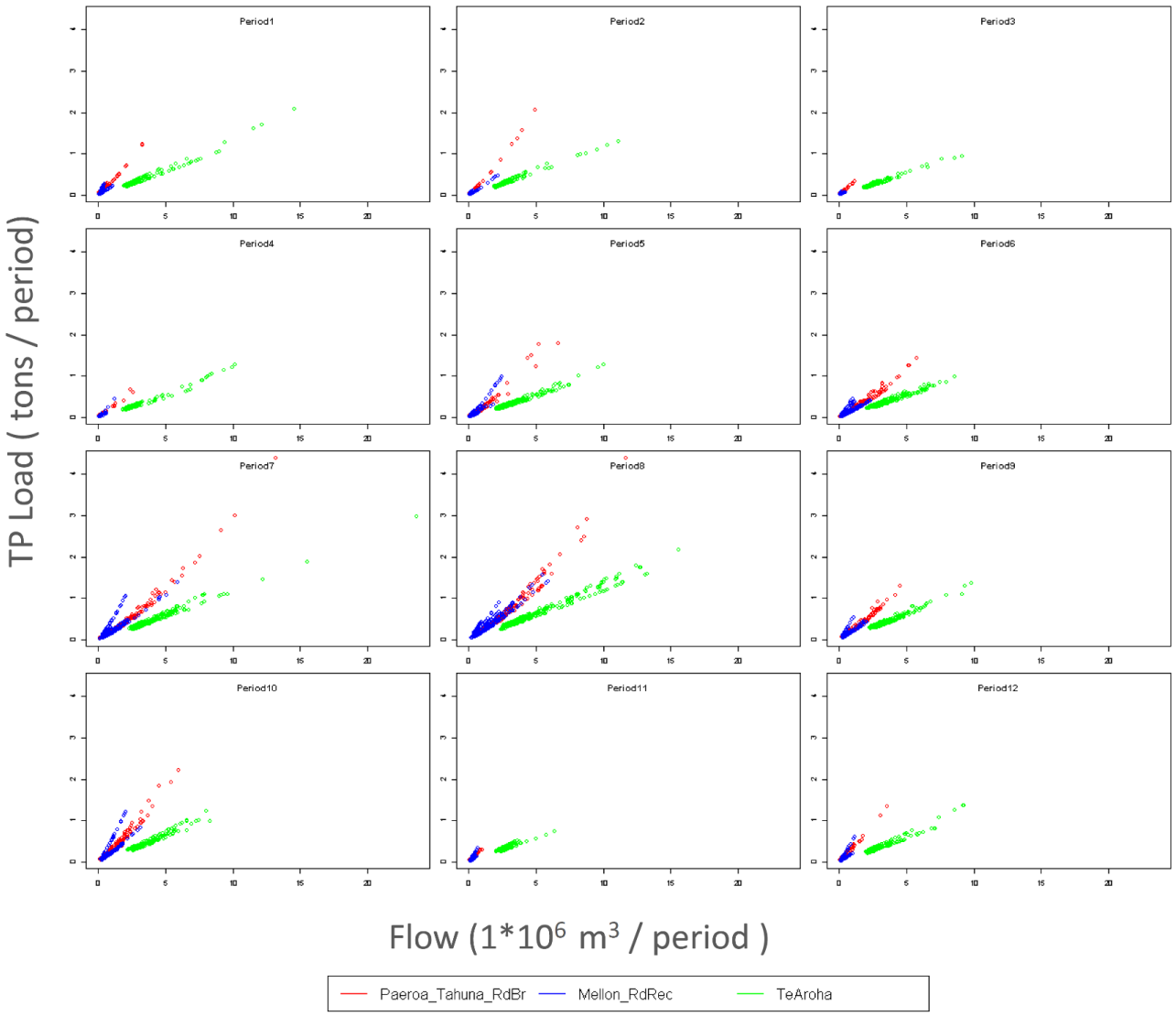

Figure D.14 Linear phosphorus load (calculated with RLoadest) to flow relation for the measurement stations Paeroa-Tahuna Rd Br, Mellon Rd Rec and Te Aroha for the years 2005-2013. These linear relations have been idealised by the RLoadest load calculations. However, the relation between period flow and load are still useful for the calibration. The period numbering corresponds to month (e.g., 1 = January, 2 = February)

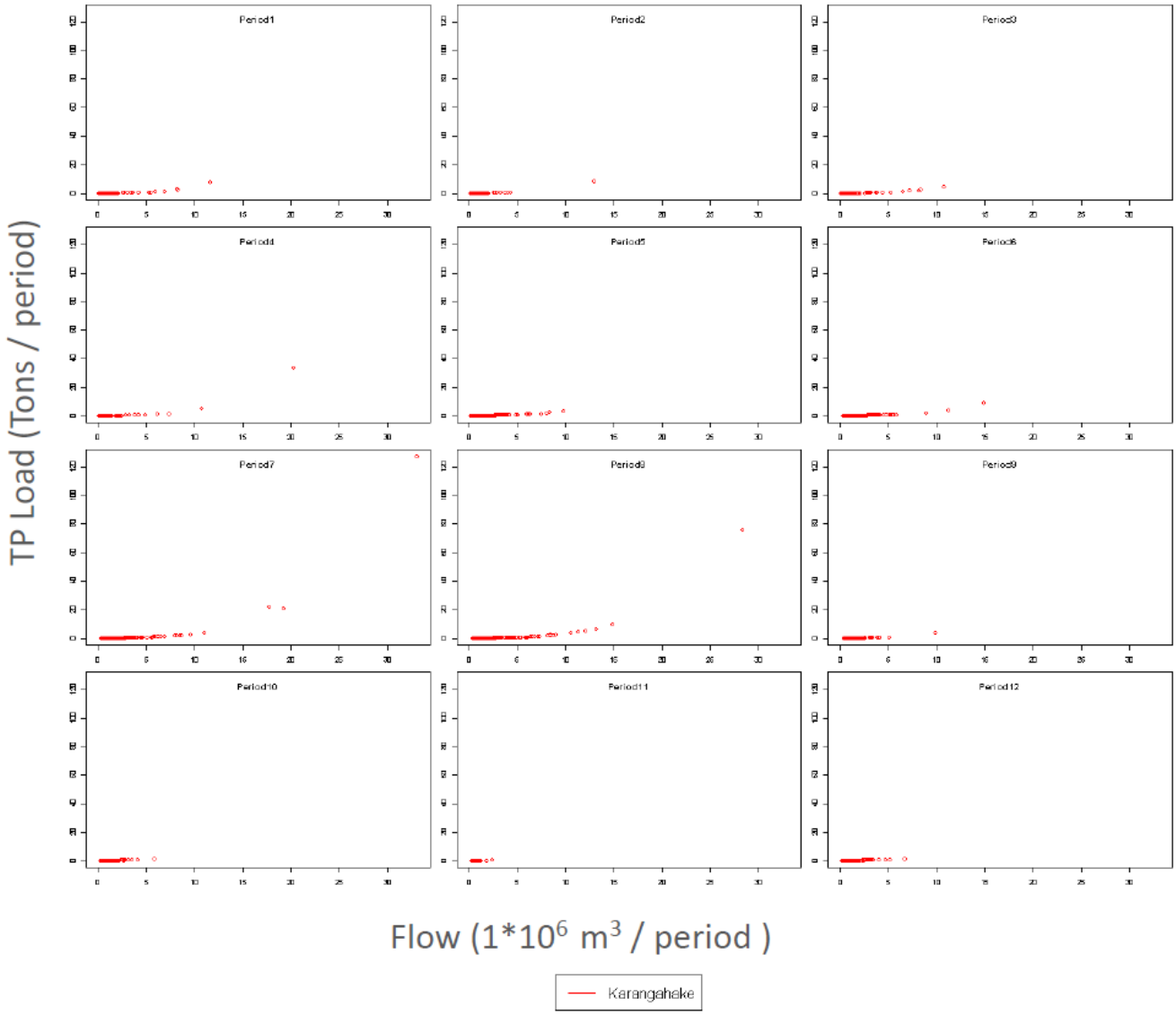

Figure D.15 Linear phosphorus load (calculated with RLoadest) to flow relation for the measurement station Karangahake for the years 2005-2013. These linear relations have been idealised by the RLoadest load calculations. However, the relation between period flow and load are still useful for the calibration. The period numbering corresponds to month (e.g., 1 = January, 2 = February)

E Validation

E.1 Flow validation

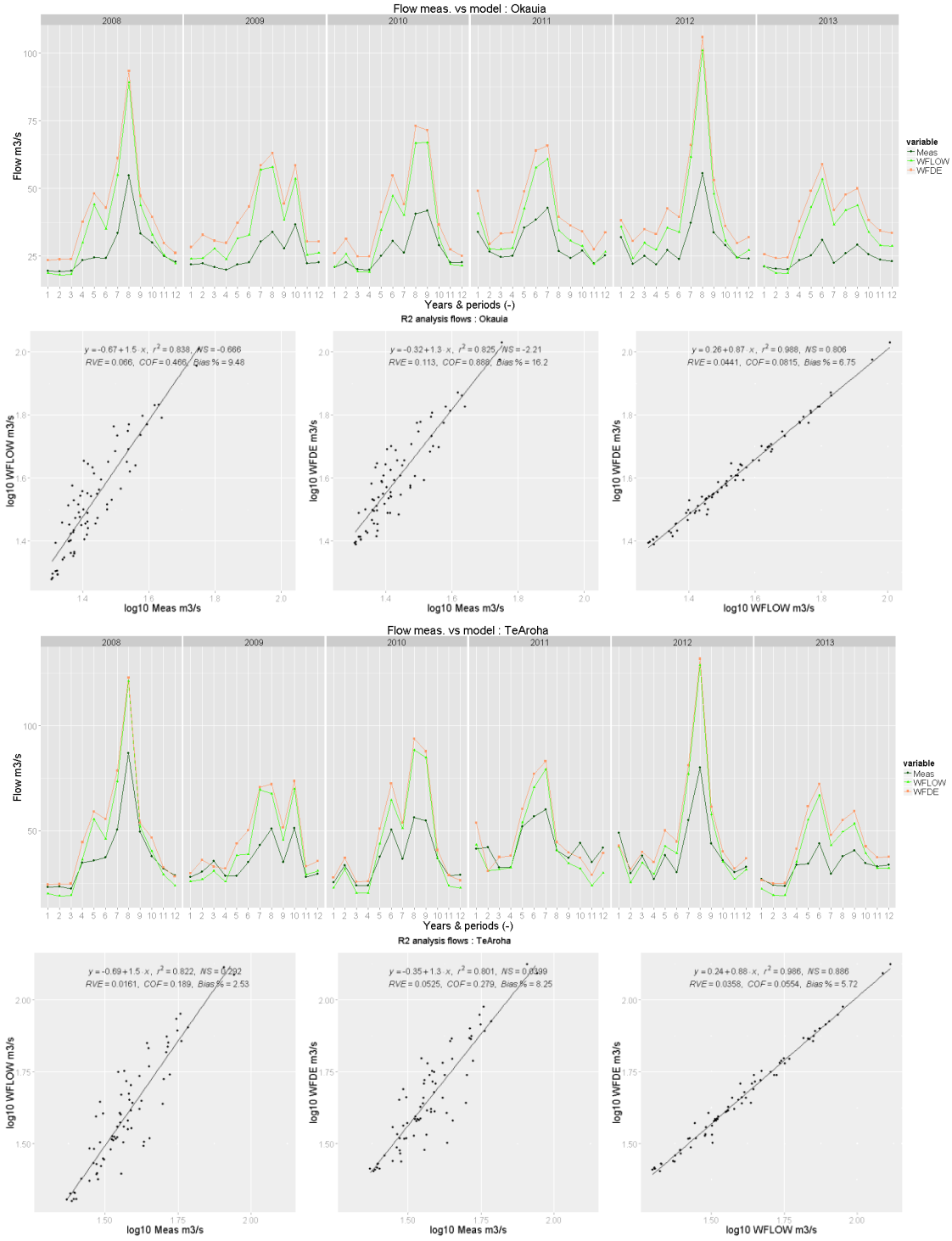

Figure E.1 Flow validation for the Waihou measurement stations Okauia and Te Aroha. The flow has been projected and analysed per period for measured flow, WFLOW model result and WFD-Explorer model result.

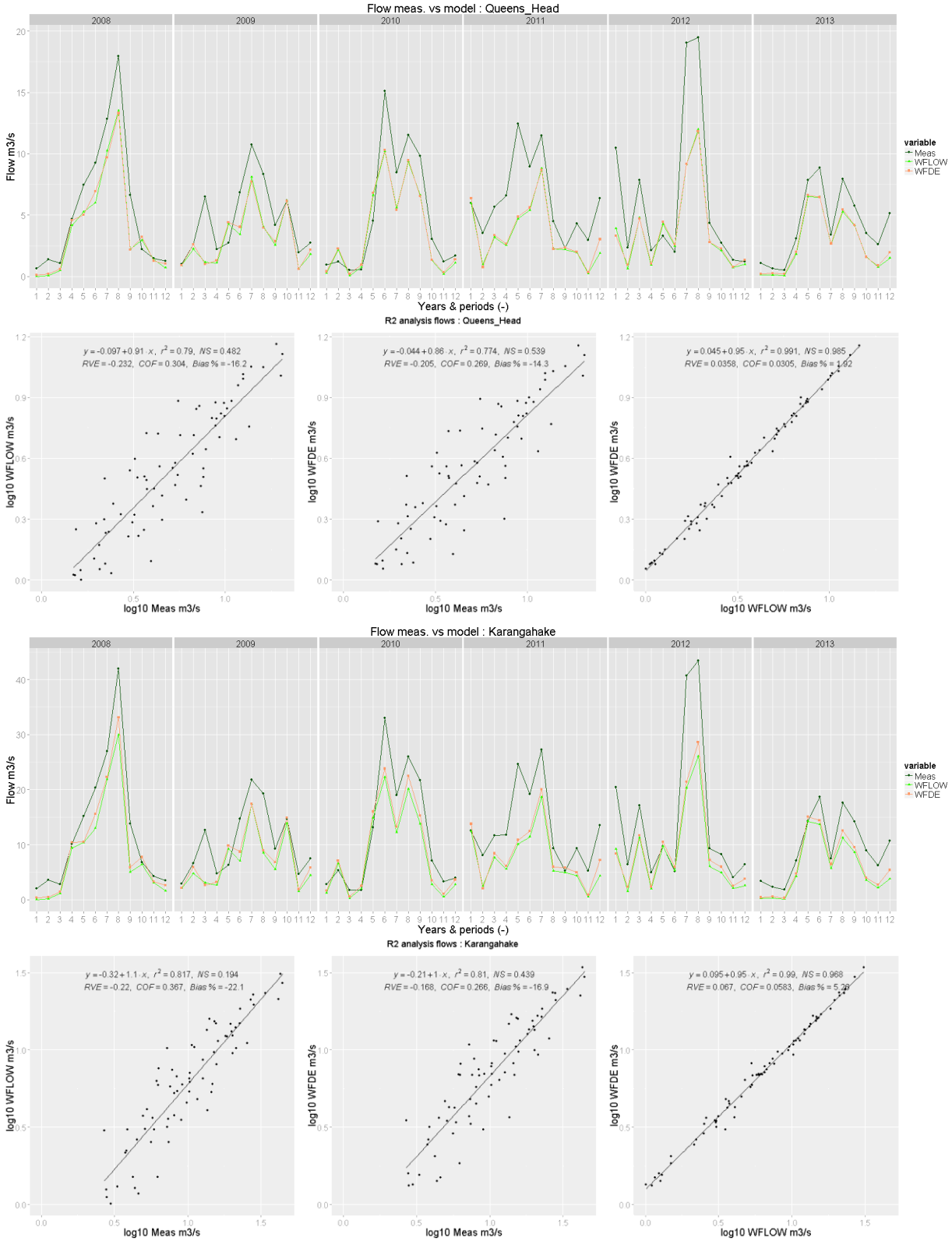

Figure E.2 Flow validation for the Ohinemuri measurement stations Queens Head and Karangahake. The flow has been projected and analysed per period for measured flow, WFLOW model result and WFD-Explorer model result.

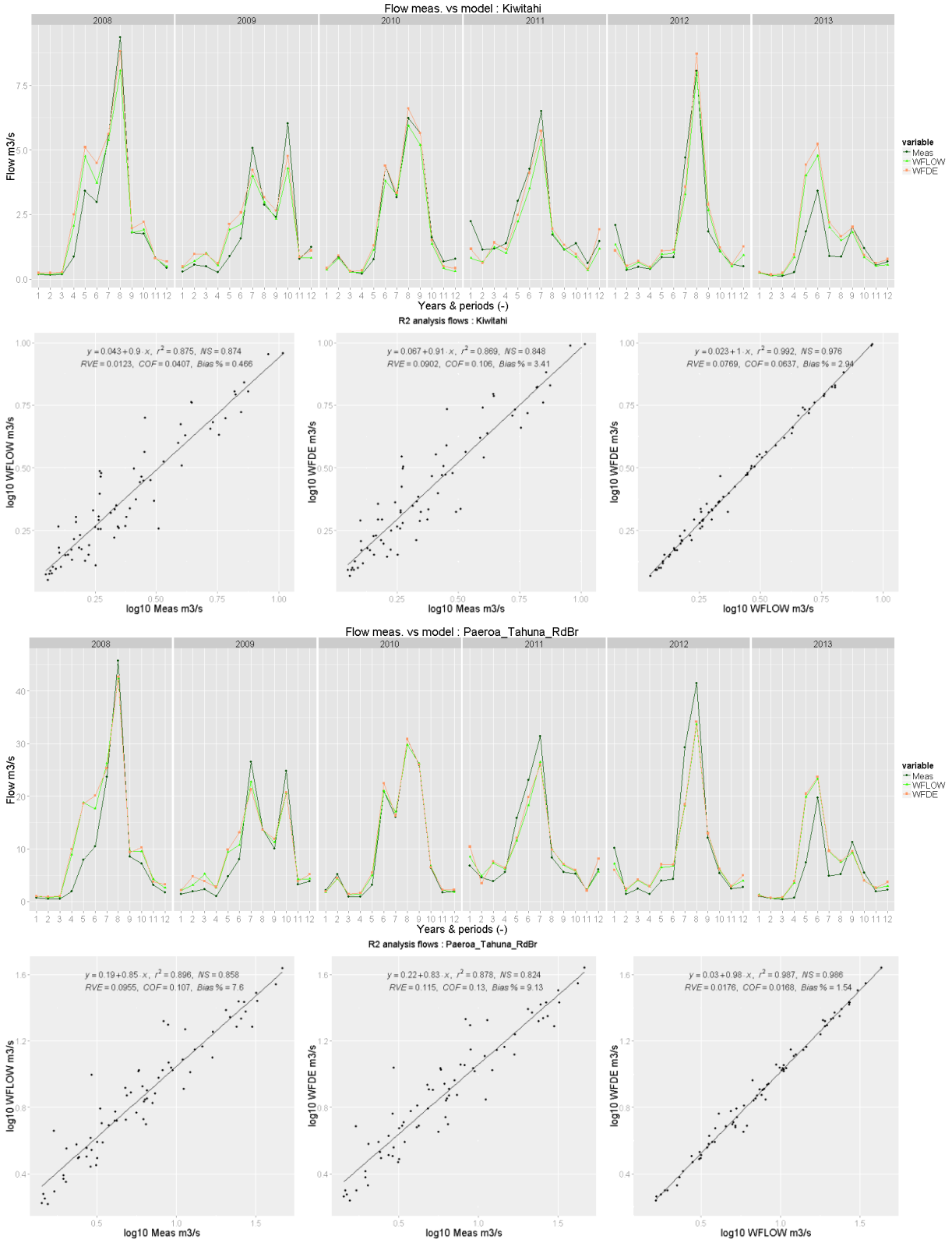

Figure E.3 Flow validation for the Piako measurement stations Kiwitahi and Paeroa-Tahuna Rd Br. The flow has been projected and analysed per period for measured flow, WFLOW model result and WFD-Explorer model result.

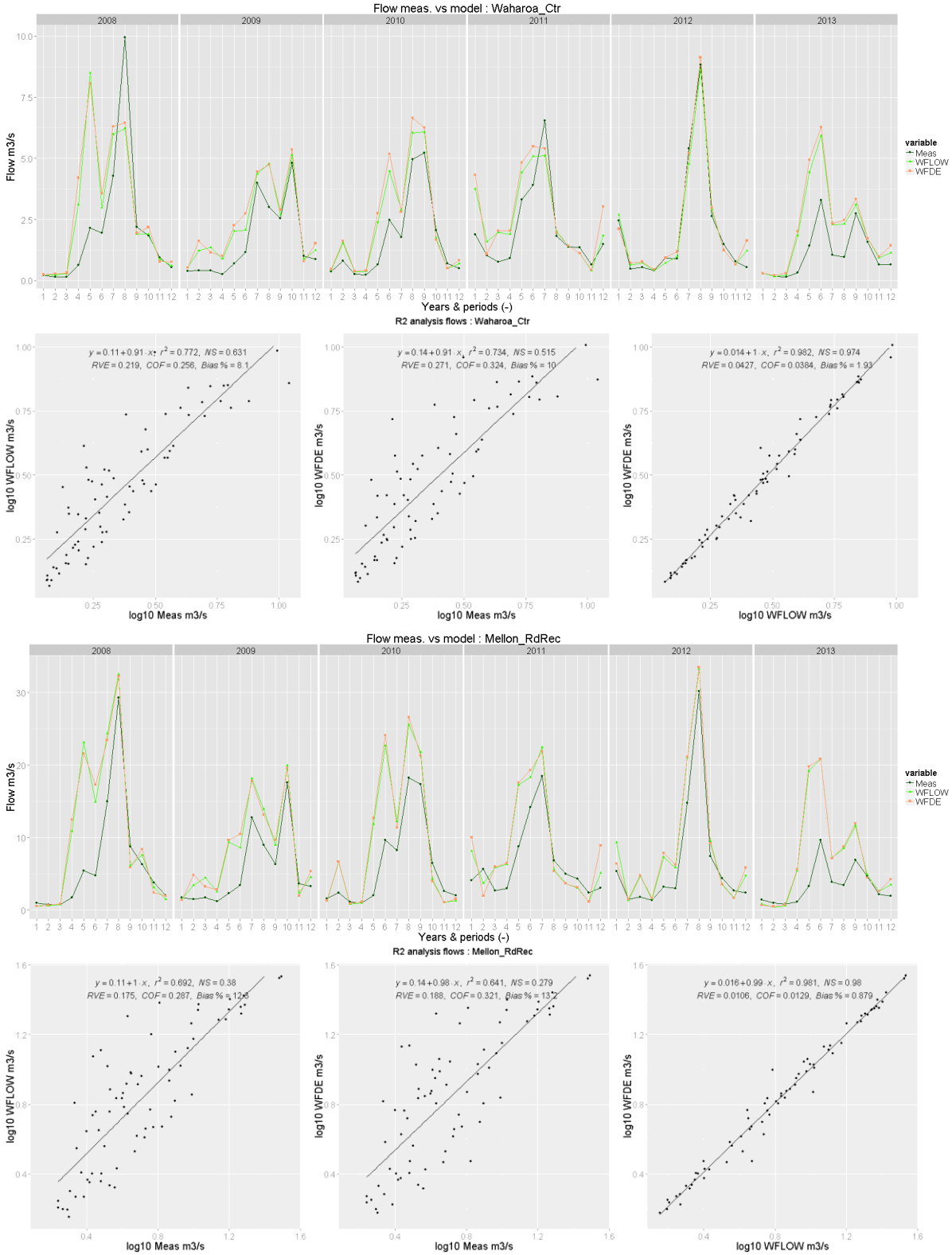

Figure E.4 Flow validation for the Waitoa measurement stations Landsdowne Rd (Waharoa Control) and Mellon Rd Rec. The flow has been projected and analysed per period for measured flow, WFLOW model result and WFD-Explorer model result.

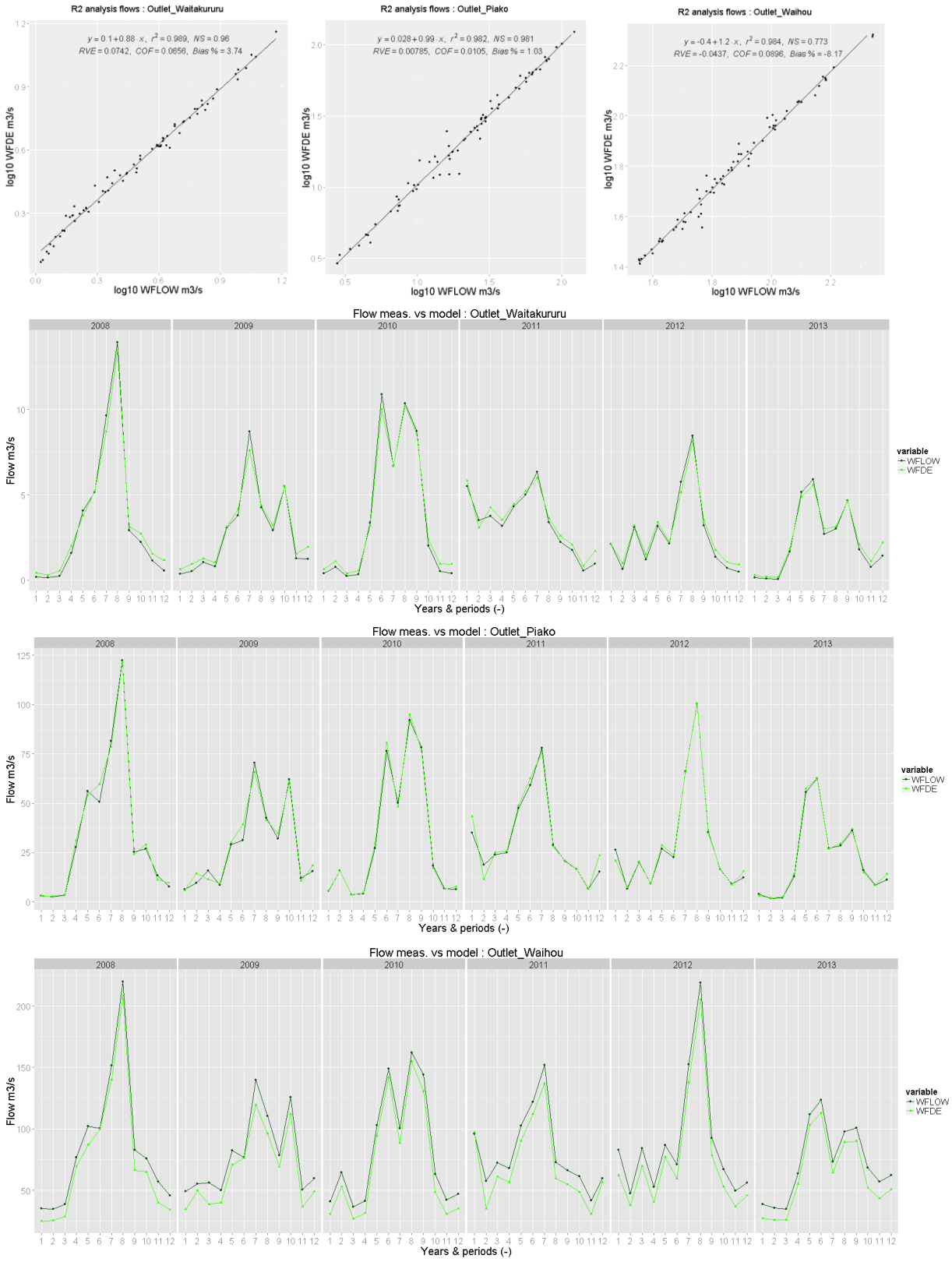

Figure E.5 Flow validation for the outflows of the Waitakaruru, Piako and Waihou River. The flow has been projected and analysed per period for WFLOW model result and WFD-Explorer model result. There is no measured flow available for the outflow locations.

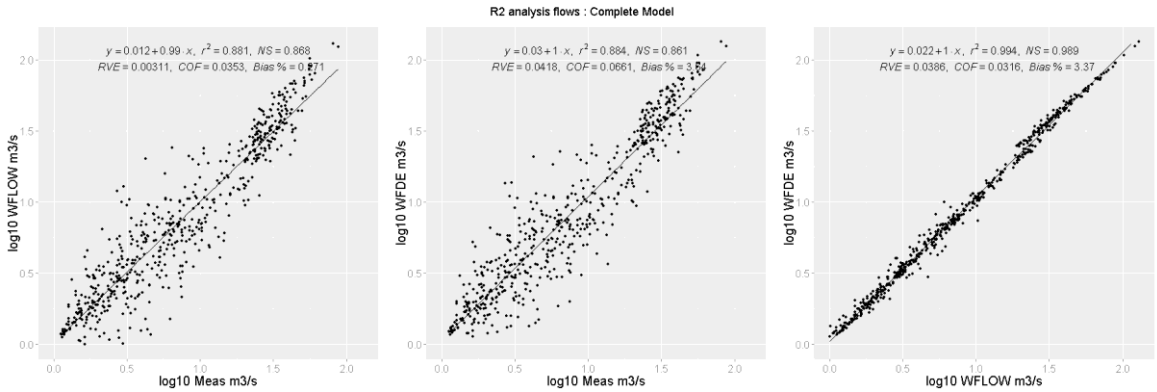

Figure E.6 Flow validation for the concatenated downstream stations of the Hauraki Plains catchment. The flow has been projected and analysed for measured flow, WFLOW model result and WFD-Explorer model result.

Table E.1 Flow per year to the Firth of Thames, from the river mouths and along the different measurement stations as calculated by the WFD-Explorer.

	WFD-Explorer flow per year (1*10^6 m3 per year)											
	Firth of Thames	*Waihou*					*Piako*					*Waitakaruru*
Year	*Inflow*	*Outflow*	Waihou		Ohinemuri		*Outflow*	Piako		Waitoa		*Outflow*
			Te Aroha	Okauia	Karangahake	Queens head		Paeroa-Tahuna Rd Br	Kiwitahi	Mellon Rd Rec	Landsdowne Rd	
2008	1358.59	888.20	595.19	496.32	113.62	48.18	427.46	146.17	32.90	127.90	35.08	42.93
2009	1169.43	792.59	561.10	486.63	88.25	37.73	341.55	113.01	24.44	99.92	29.08	35.29
2010	1302.31	865.89	571.11	480.33	110.76	45.46	390.80	121.52	25.63	112.78	29.56	45.62
2011	1270.17	839.17	569.81	494.81	98.40	42.25	387.91	119.01	23.19	105.68	33.20	43.09
2012	1288.89	903.10	627.06	540.81	110.54	45.24	351.95	109.12	23.22	103.44	27.02	33.84
2013	1040.91	740.11	531.28	465.59	76.12	32.49	271.73	87.82	19.42	87.50	26.36	29.06

E.2 RLoadest load calculation technique comparison

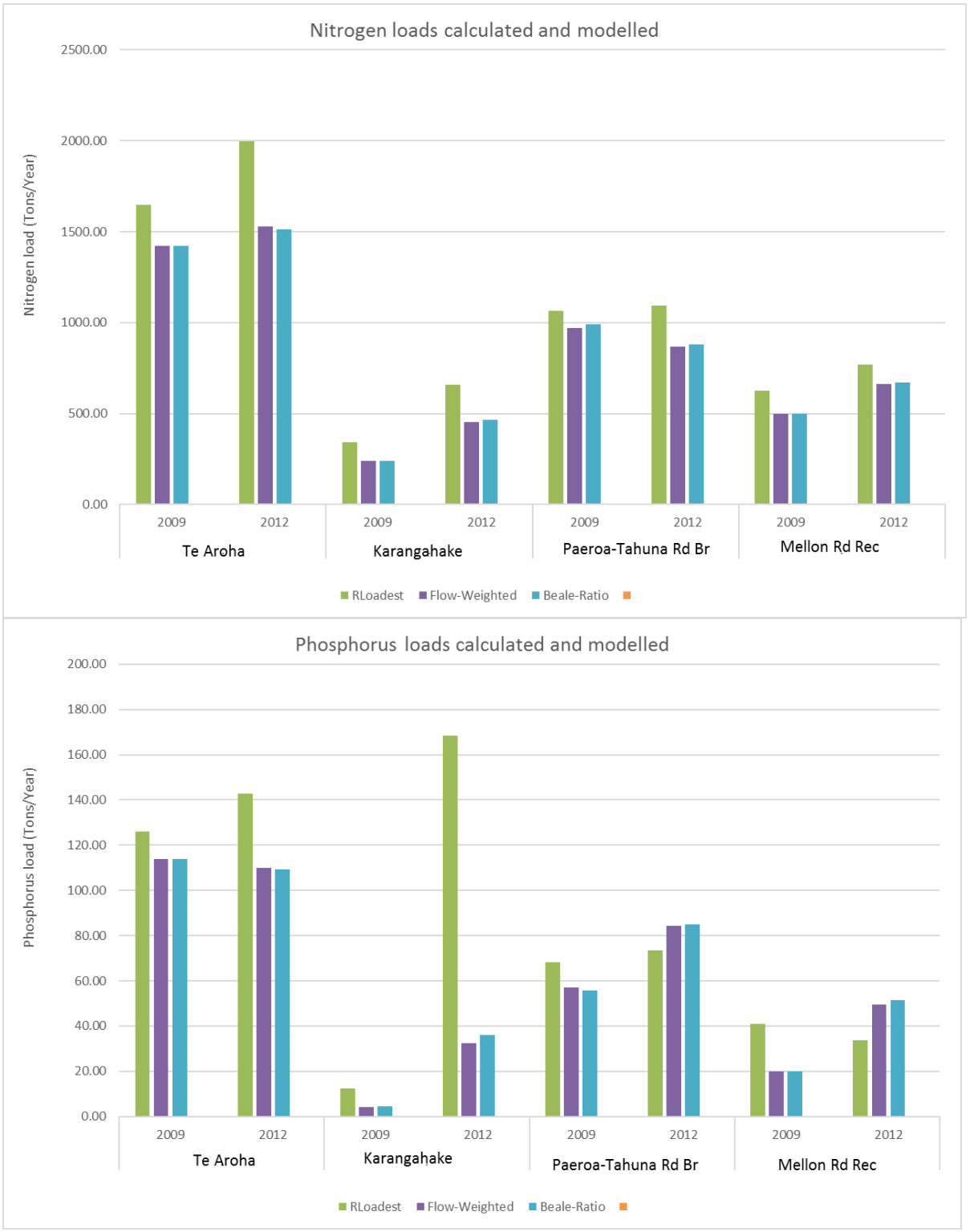

Figure E.7 Variation in load calculation techniques to calculate the total nitrogen and total phosphorus load of the summed stations Te Aroha, Karangahake, Mellon Rd Rec and Paeroa-Tahuna Rd Br. Here the techniques RLoadest, Flow-Weighted and Beale-Ratio calculation. The full comparison has been described in Stephens (2015).

E.3 Load validation

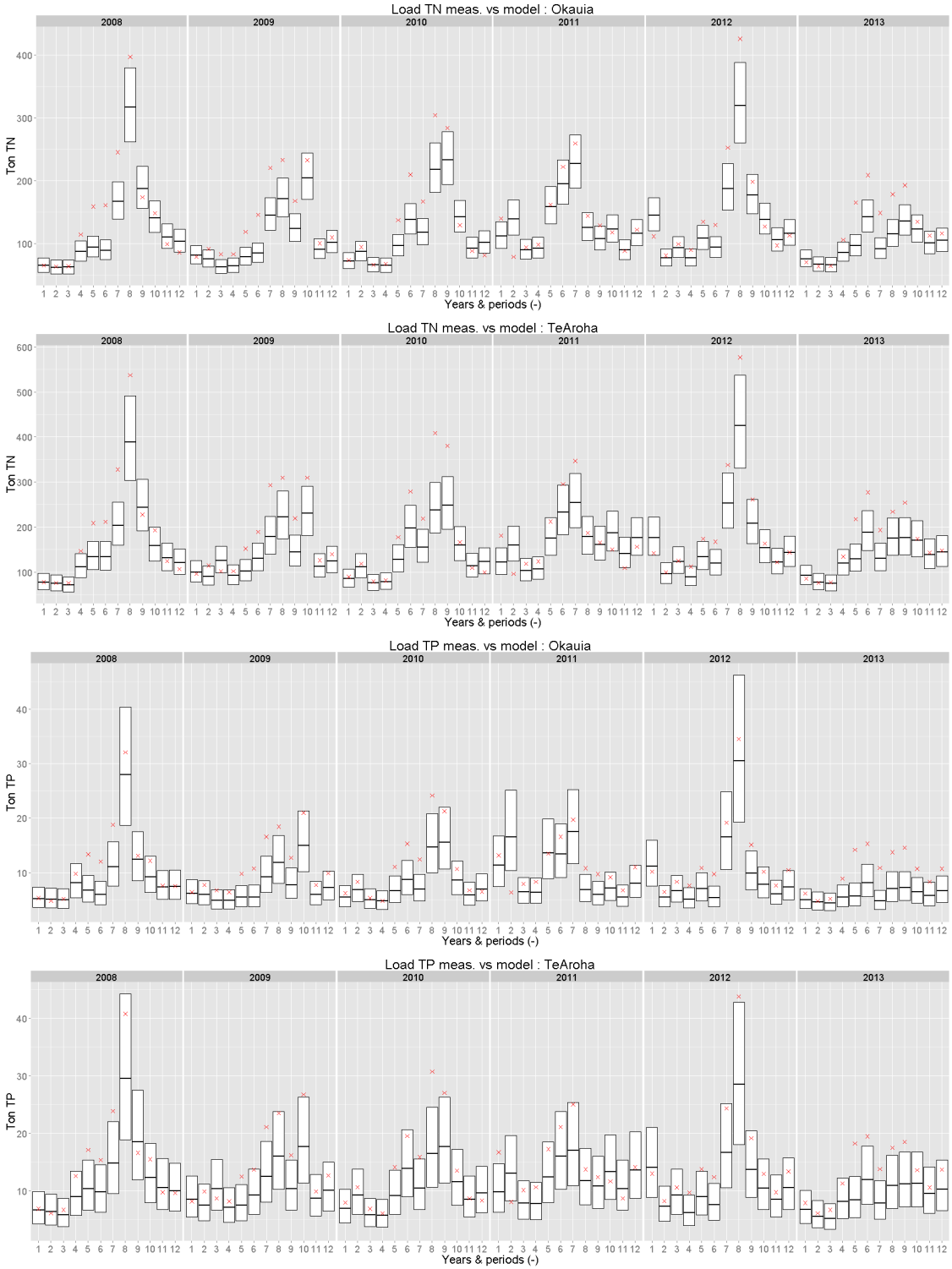

Figure E.8 Modelled nitrogen (top plots) and phosphorus (bottom plots) loads for the Waihou measurement stations Okauia and Te Aroha. In this graph the Hauraki Plains water quality model (red cross) is compared with the RLoadest load prediction (black line in middle of the bar) and the 95% certainty of the prediction (top bar to bottom bar) for all the years that the model predicts.

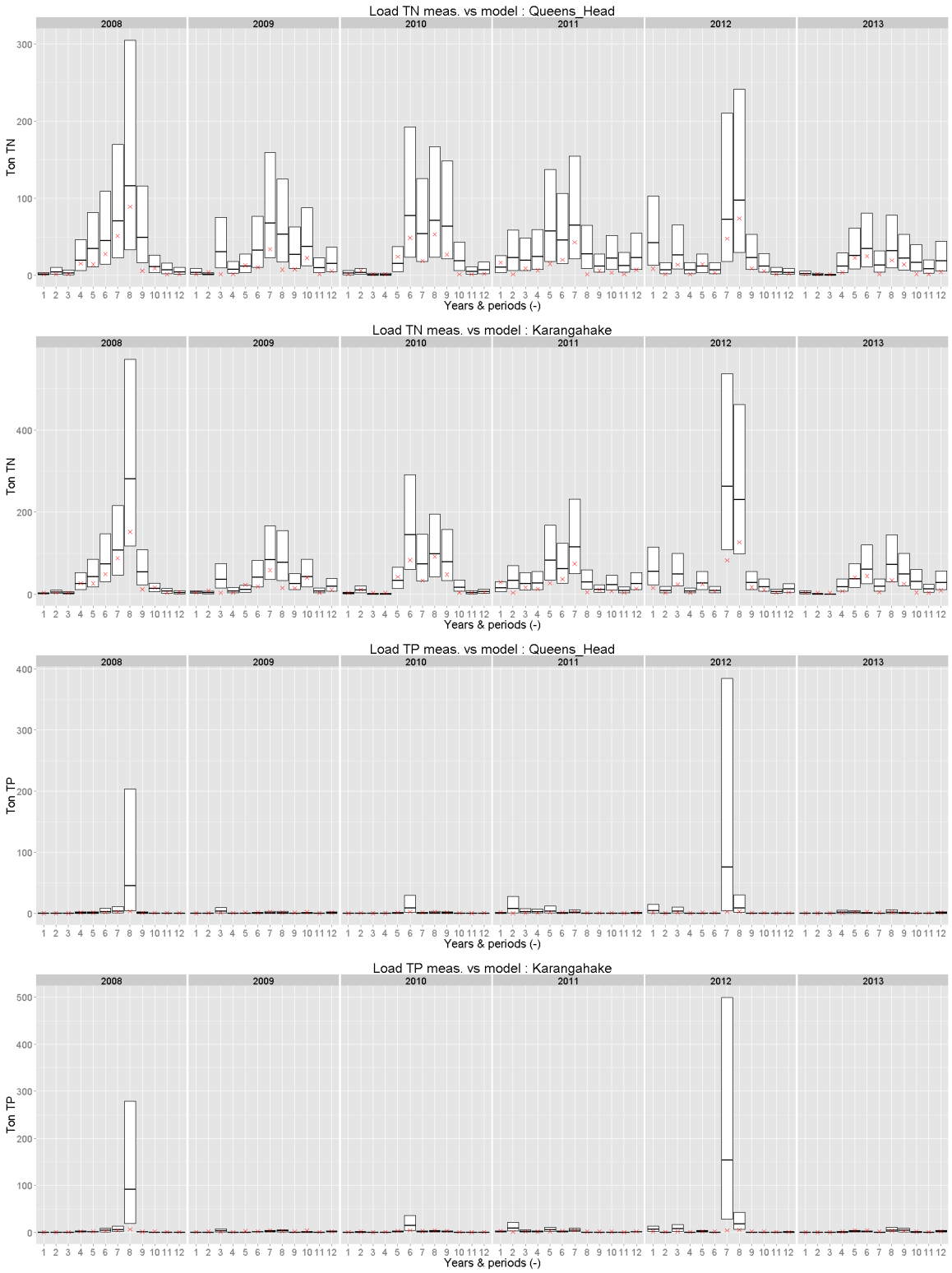

Figure E.9 Modelled nitrogen (top plots) and phosphorus (bottom plots) loads for the Ohinemuri measurement stations Queens Head and Karangahake. In this graph the Hauraki Plains water quality model (red cross) is compared with the RLoadest load prediction (black line in middle of the bar) and the 95% certainty of the prediction (top bar to bottom bar) for all the years that the model predicts.

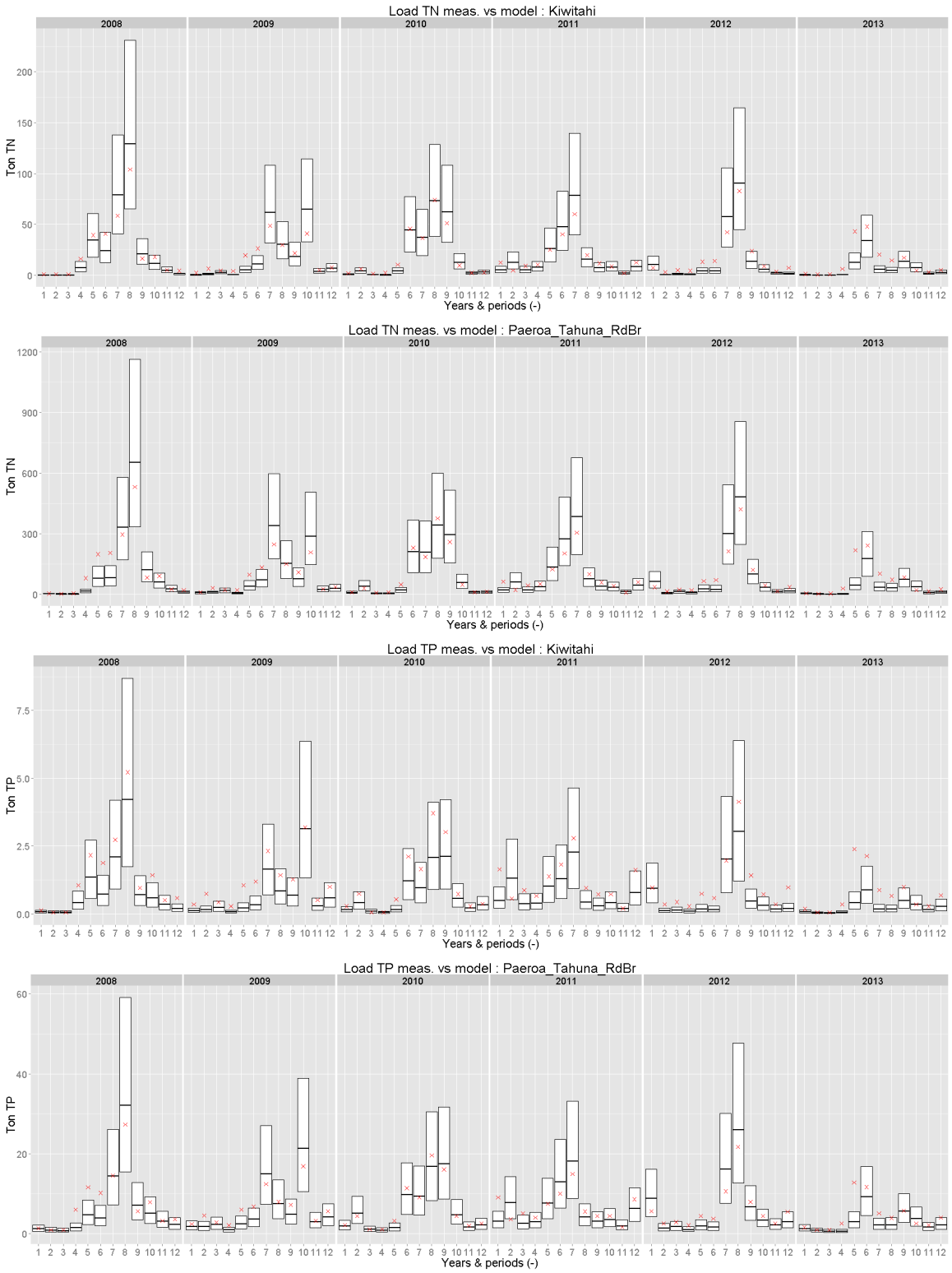

Figure E.10 Modelled nitrogen (top plots) and phosphorus (bottom plots) loads for the Piako measurement stations Kiwitahi and Paeroa-Tahuna Rd Br. In this graph the Hauraki Plains water quality model (red cross) is compared with the RLoadest load prediction (black line in middle of the bar) and the 95% certainty of the prediction (top bar to bottom bar) for all the years that the model predicts.

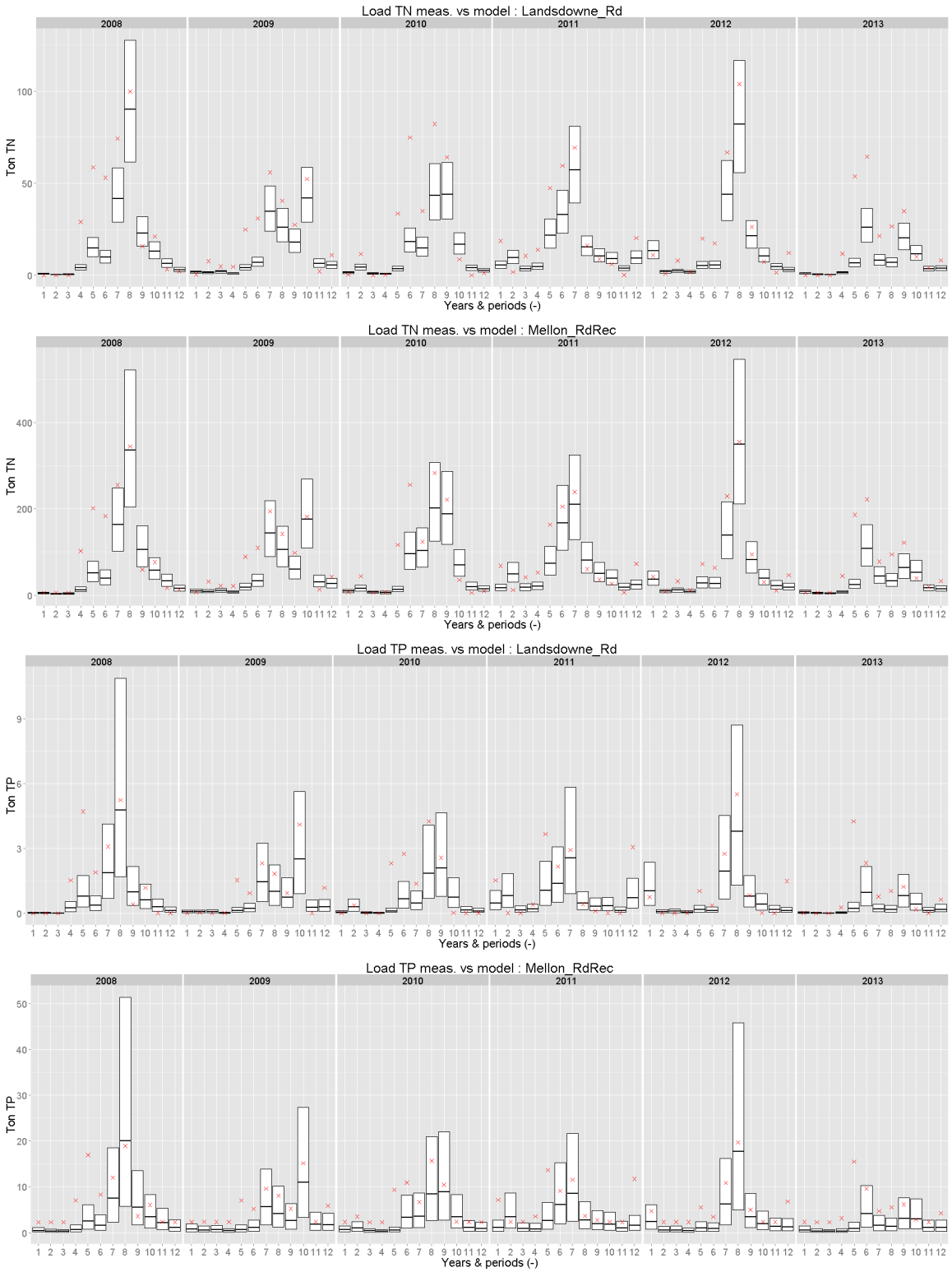

Figure E.11 Modelled nitrogen (top plots) and phosphorus (bottom plots) loads for the Waitoa measurement stations Landsdowne Rd (Waharoa Control) and Mellon Rd Rec. In this graph the Hauraki Plains water quality model (red cross) is compared with the RLoadest load prediction (black line in middle of the bar) and the 95% certainty of the prediction (top bar to bottom bar) for all the years that the model predicts.

Table E.2 RLoadest model uncertainty for the nitrogen load at the downstream measurement stations. The upper boundary (UB) and lower boundary (LB) of the 95% certainty interval for the load calculation is presented. The difference (DIF) is calculated by subtracting the lower boundary from the upper boundary. The RLoadest predictions are relatively uncertain due to the infrequent water quality measurements (12 periods per year).

		Nitrogen Load											
		Predicted by Rloadest per station (ton / yr)											
		Te Aroha			Karangahake			Paeroa-Tahuna Rd br			Mellon Rd Rec		
	Uncertainty	LB	UB	DIF	LB	UB	DIF	LB	UB	DIF	LB	UB	DIF
Year	2008	1449.47	2324.44	874.97	265.33	1252.98	987.66	717.44	2449.15	1731.71	508.50	1260.83	752.33
	2009	1299.14	2079.63	780.49	157.01	727.71	570.70	554.33	1863.22	1308.89	391.64	955.18	563.53
	2010	1345.87	2153.59	807.72	204.00	946.42	742.43	634.73	2127.51	1492.78	462.68	1128.48	665.80
	2011	1564.96	2510.22	945.26	198.77	931.58	732.81	590.61	2009.38	1418.77	475.40	1170.69	695.29
	2012	1599.36	2572.66	973.29	302.67	1456.00	1153.33	559.62	1936.06	1376.45	471.73	1189.55	717.82
	2013	1268.08	2029.69	761.61	144.04	669.67	525.64	223.60	761.24	537.64	236.65	574.36	337.71

Table E.3 RLoadest model uncertainty for the nitrogen load at the downstream measurement stations. The upper boundary (UB) and lower boundary (LB) of the 95% certainty interval for the load calculation is given. The difference (DIF) is calculated by subtracting the lower boundary from the upper boundary. The RLoadest predictions are relatively uncertain due to the infrequent water quality measurements (12 periods per year).

		Phosphorus Load											
		Predicted by Rloadest per station (ton / yr)											
		Te Aroha			Karangahake			Paeroa-Tahuna Rd Br			Mellon Rd Rec		
	Uncertainty	LB	UB	DIF	LB	UB	DIF	LB	UB	DIF	LB	UB	DIF
Year	2008	92.83112	214.0597	121.23	25.19791	311.6324	286.43	37.6451	139.5982	101.95	13.71368	114.2216	100.5079
	2009	81.20312	186.7113	105.51	5.402654	28.54229	23.14	33.81728	123.6108	89.79	9.539147	76.69905	67.15991
	2010	80.95404	186.1849	105.23	8.538835	53.85838	45.32	35.70323	130.477	94.77	9.961322	79.67768	69.71636
	2011	92.60502	214.3586	121.75	10.30569	61.94788	51.64	36.12561	134.6279	98.50	9.88059	81.28045	71.39986
	2012	91.03616	212.2087	121.17	41.79821	580.7307	538.93	35.77768	134.9382	99.16	10.97508	95.79859	84.8235
	2013	69.04964	160.1327	91.08	6.295743	37.12965	30.83	16.11286	59.16527	43.05	5.380314	43.92399	38.54368

E.4 Concentration validation

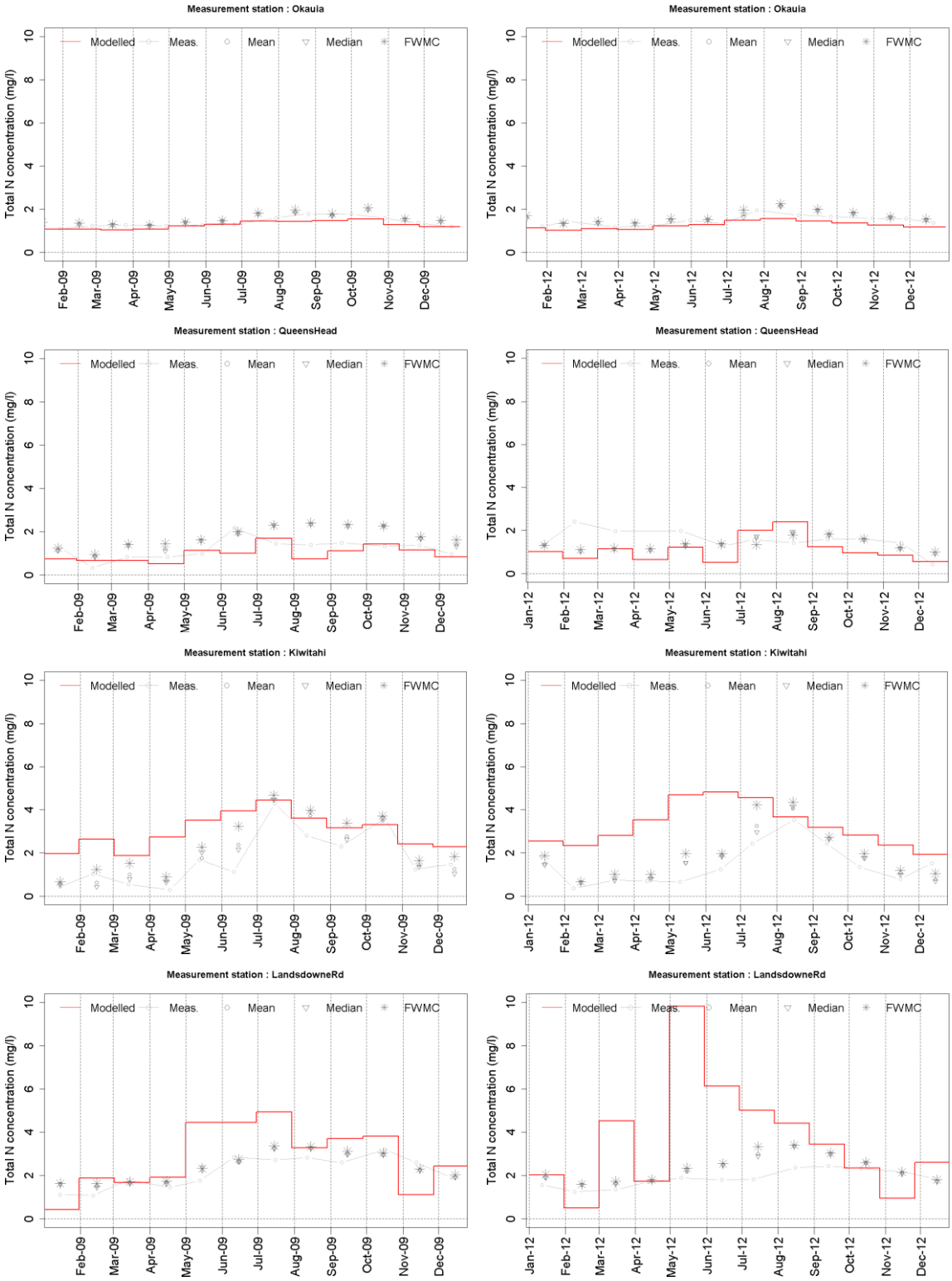

Figure E.12 Measured (RLoadest daily calculation) and modelled total nitrogen concentration results for validation years 2009 and 2012 at the upstream measurement stations Okauia, Queens Head, Kiwitahi and Landsdowne

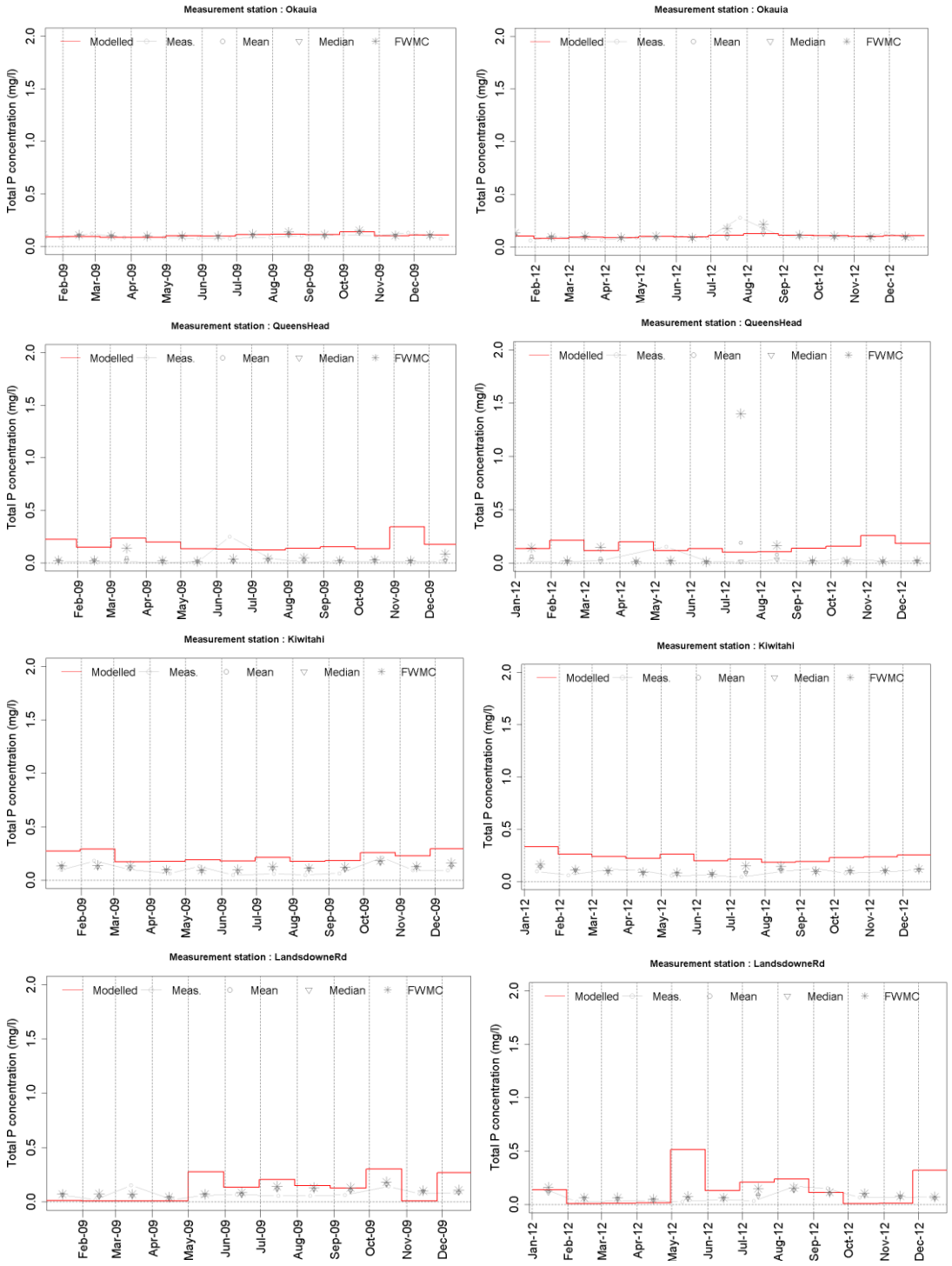

Figure E.13 Measured (RLoadest daily calculation) and modelled total phosphorus concentration results for validation years 2009 and 2012 at the upstream measurement stations Okauia, Queens Head, Kiwitahi and Landsdowne Rd.

E.5 Model performance

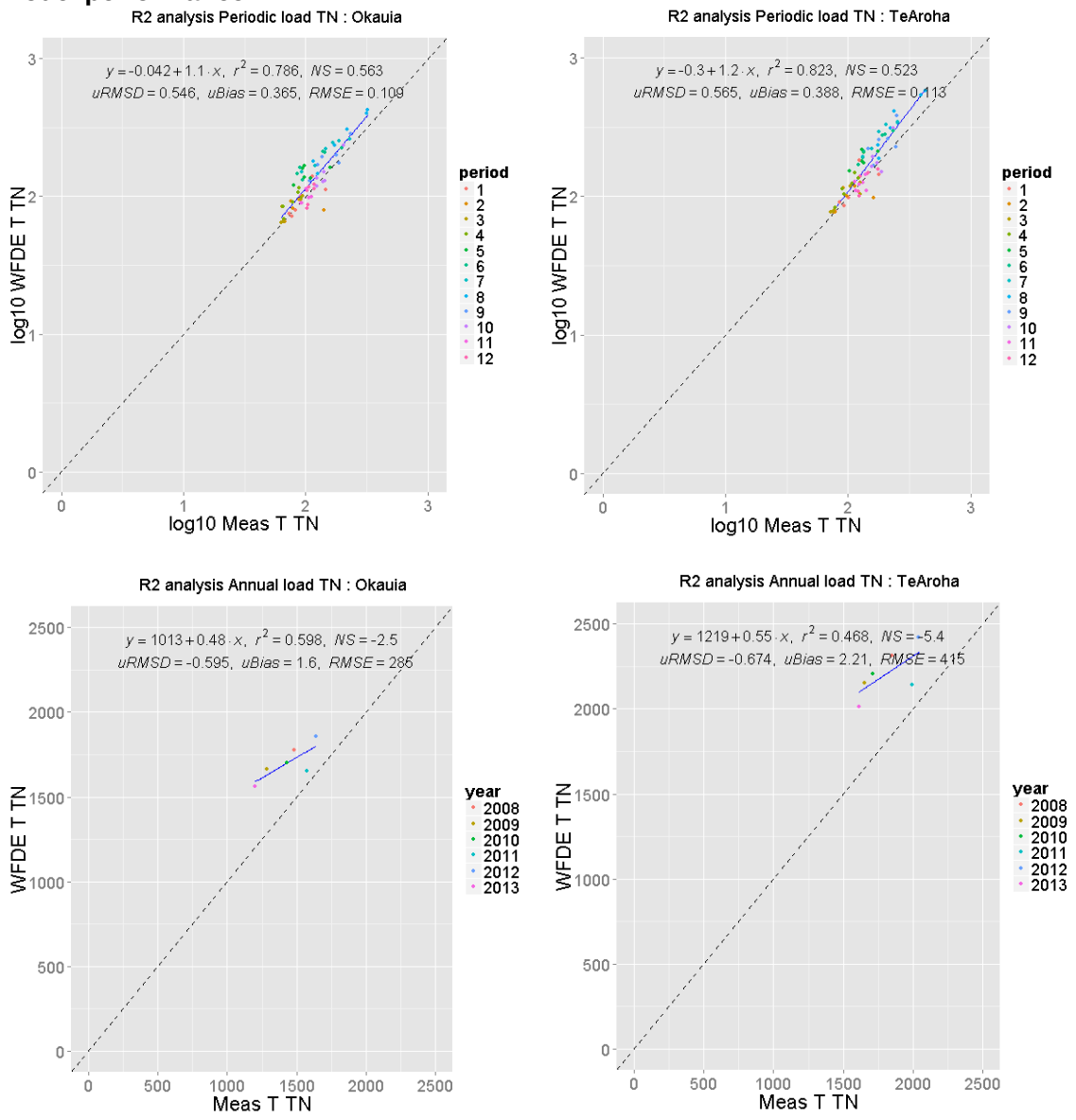

Figure E.14 Modelled total nitrogen loads per period and annual for the Waihou measurement stations Okauia and Te Aroha statistically compared by using the r-squared (r^2), Nash-Sutcliffe coefficient (NS), unbiased root-mean square difference (uRSMD), normalised Bias (uBias) and root-mean square error (RMSE). In this graph the Hauraki Plains water quality model is compared with the RLoadest load prediction.

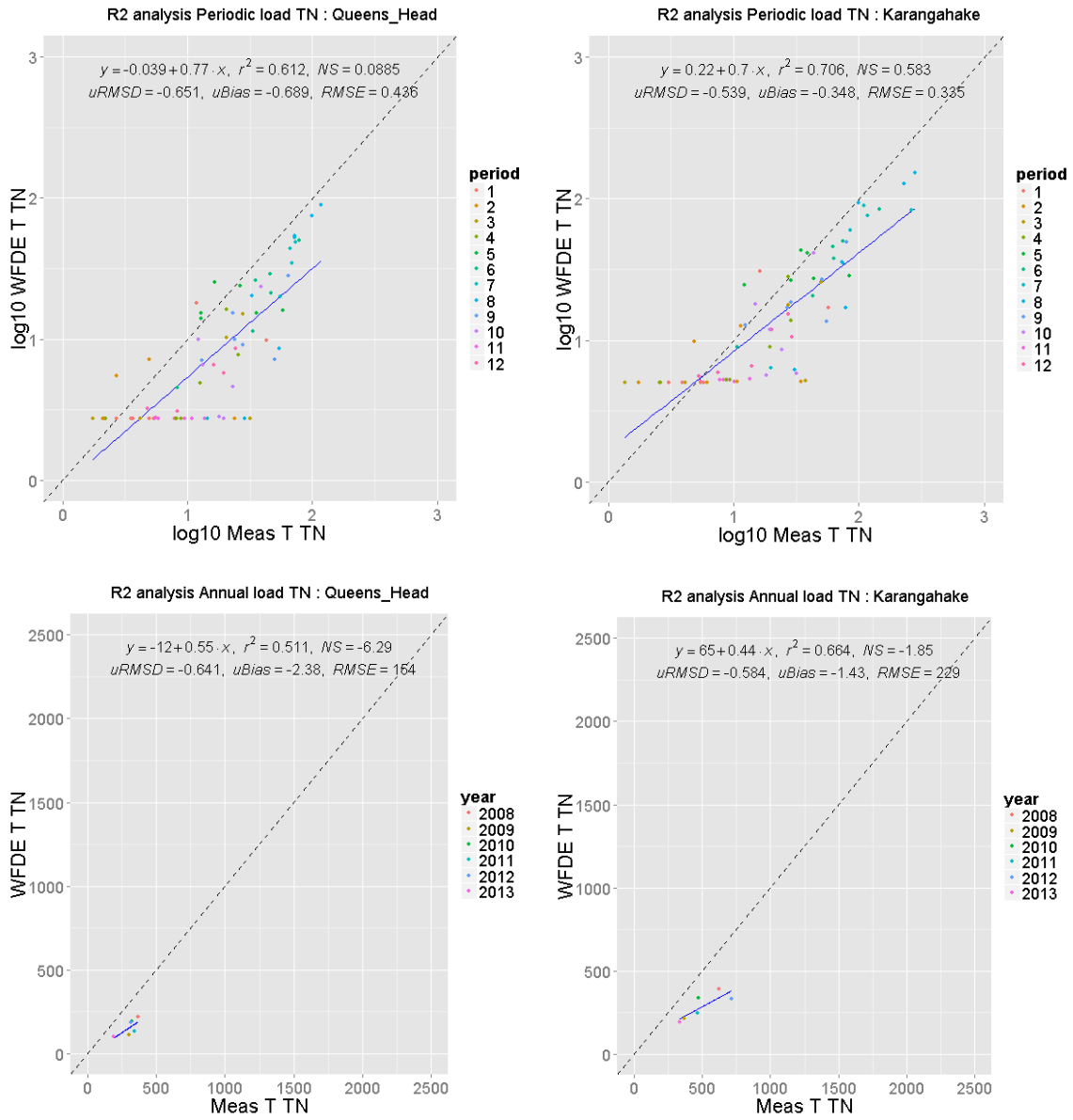

Figure E.15 Modelled total nitrogen loads per period and annual for loads for the Ohinemuri measurement stations Queens Head and Karangahake statistically compared by using the r-squared (r^2), Nash-Sutcliffe coefficient (NS), unbiased root-mean square difference (uRSMD), normalised Bias (uBias) and root-mean square error (RMSE). In this graph the Hauraki Plains water quality model is compared with the RLoadest load prediction.

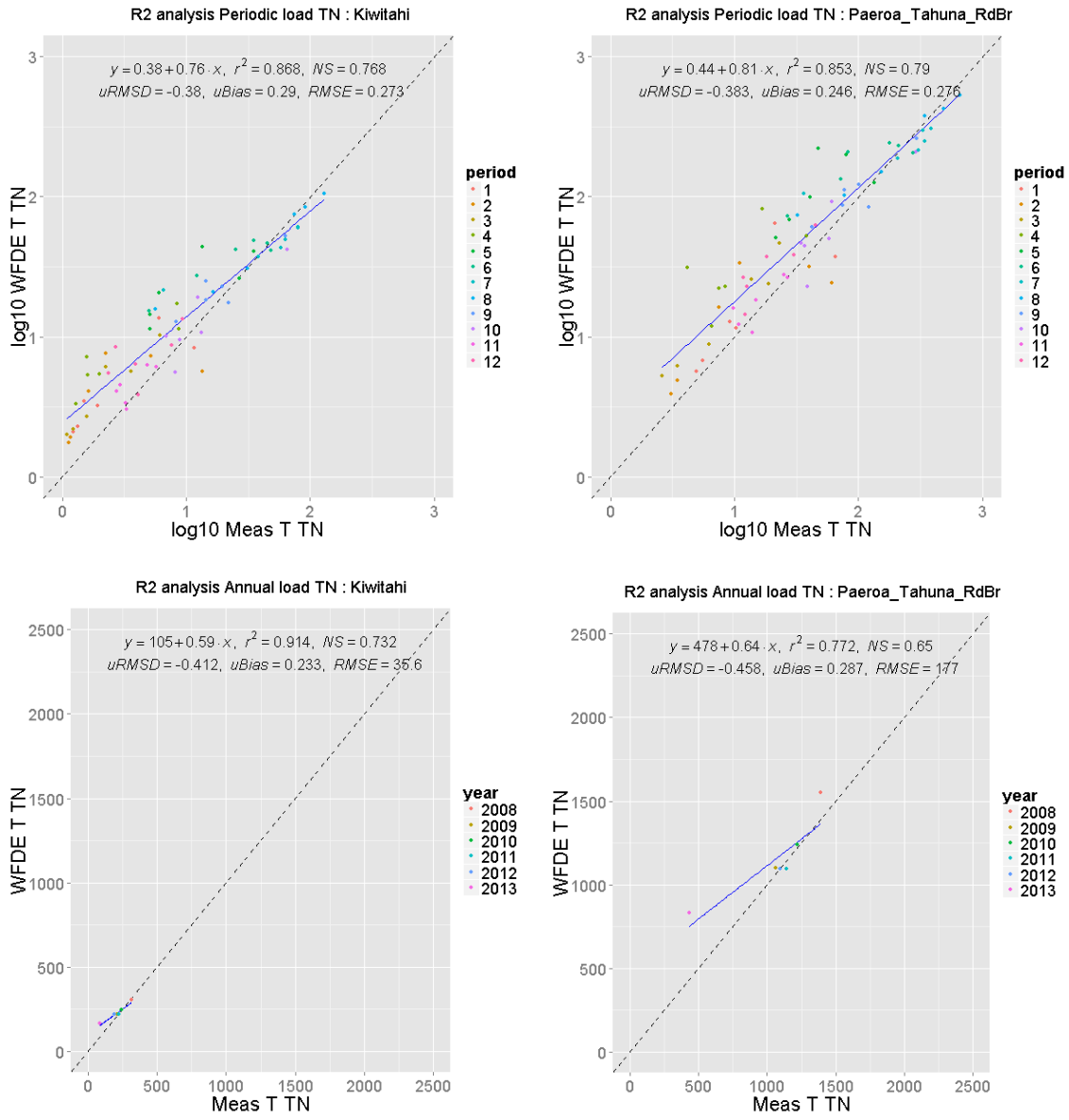

Figure E.16 Modelled total nitrogen loads per period and annual for loads for the Piako measurement stations Kiwitahi and Paeroa-Tahuna Rd Br statistically compared by using the r-squared (r^2), Nash-Sutcliffe coefficient (NS), unbiased root-mean square difference (uRSMD), normalised Bias (uBias) and root-mean square error (RMSE). In this graph the Hauraki Plains water quality model is compared with the RLoadest load prediction.

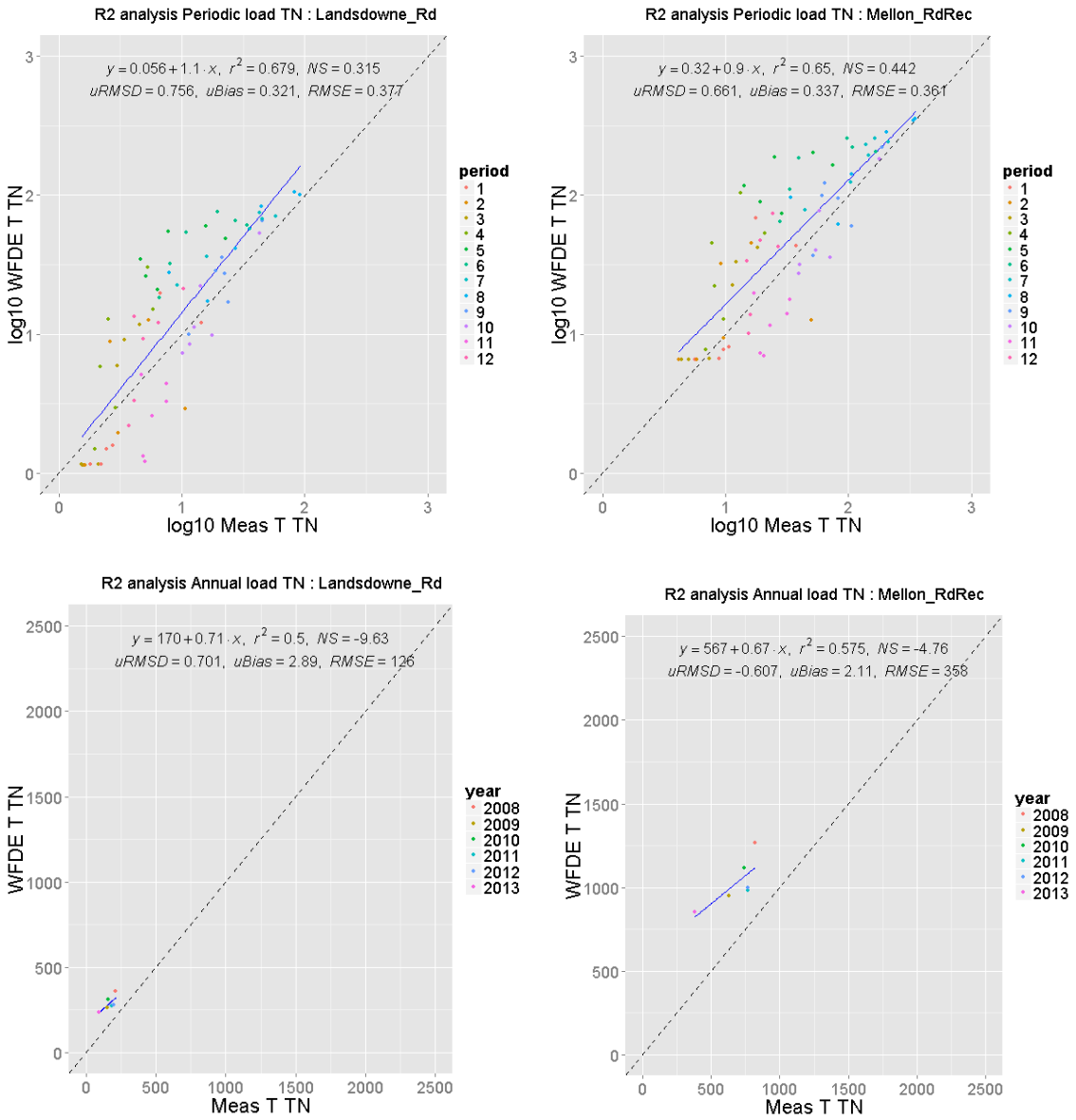

Figure E.17 Modelled total nitrogen loads per period and annual for loads for the Waitoa measurement stations Landsdowne Rd Br and Mellon Rd Rec *statistically compared by using the r-squared (r^2), Nash-Sutcliffe coefficient (NS), unbiased root-mean square difference (uRSMD), normalised Bias (uBias) and root-mean square error (RMSE). In this graph the Hauraki Plains water quality model is compared with the RLoadest load prediction.*

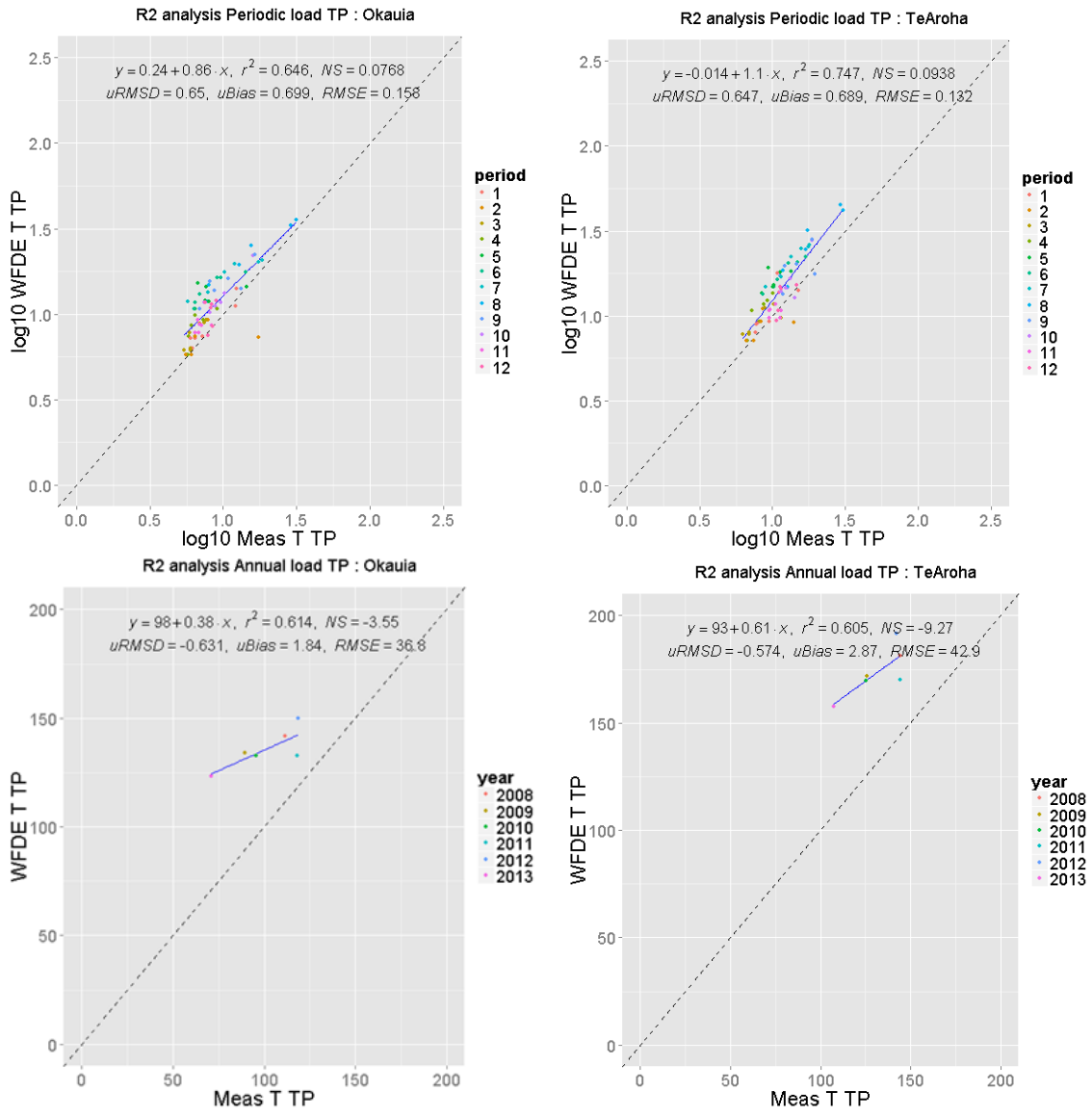

Figure E.18 Modelled total phosphorus loads per period and annual for loads for the Waihou measurement stations Okauia and Te Aroha statistically compared by using the r-squared (r^2), Nash-Sutcliffe coefficient (NS), unbiased root-mean square difference (uRSMD), normalised Bias (uBias) and root-mean square error (RMSE). In this graph the Hauraki Plains water quality model is compared with the RLoadest load prediction.

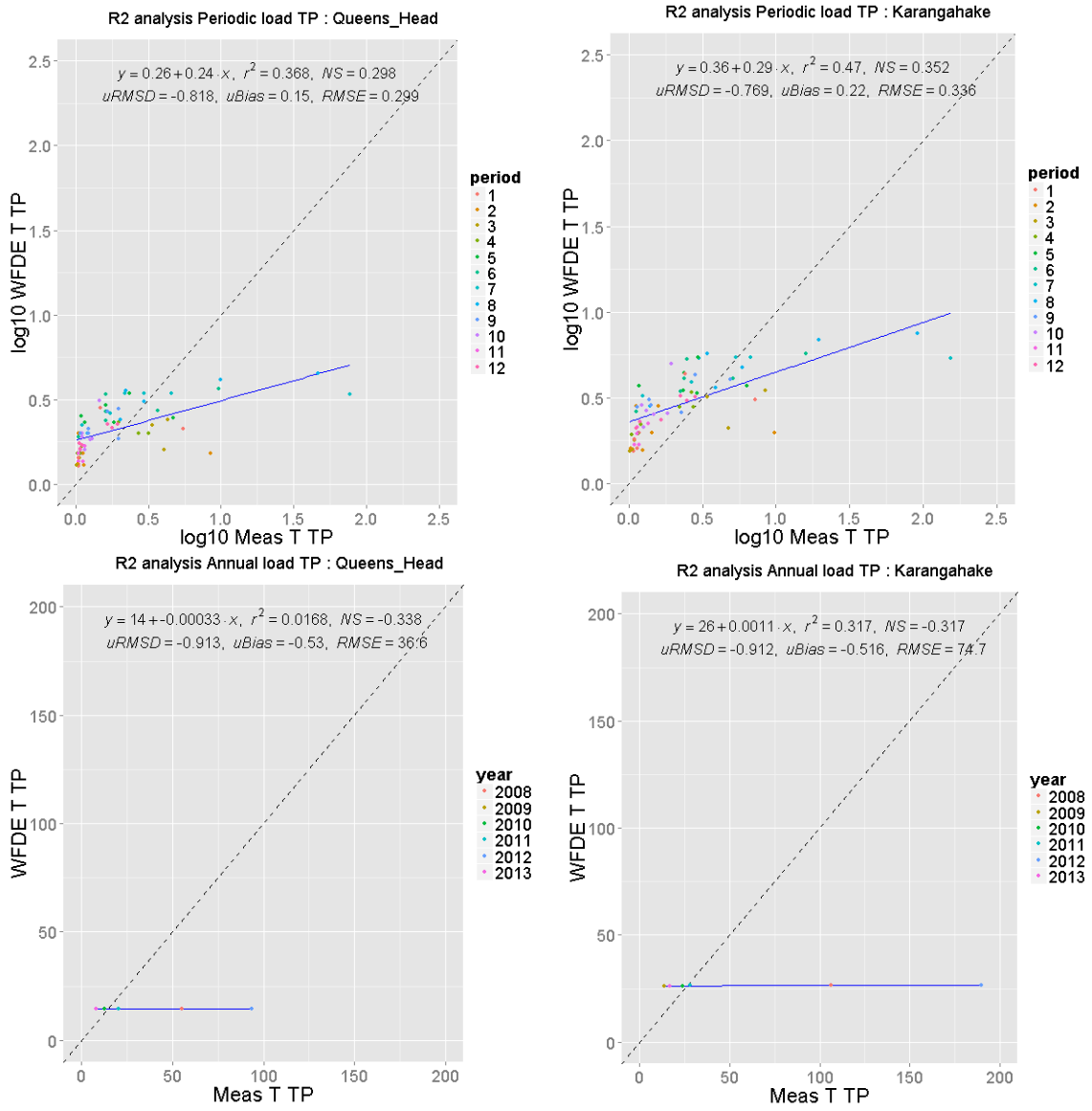

Figure E.19 Modelled total phosphorus loads per period and annual for loads for the Ohinemuri measurement stations Queens Head and Karangahake statistically compared by using the r-squared (r^2), Nash-Sutcliffe coefficient (NS), unbiased root-mean square difference (uRSMD), normalised Bias (uBias) and root-mean square error (RMSE). In this graph the Hauraki Plains water quality model is compared with the RLoadest load prediction.

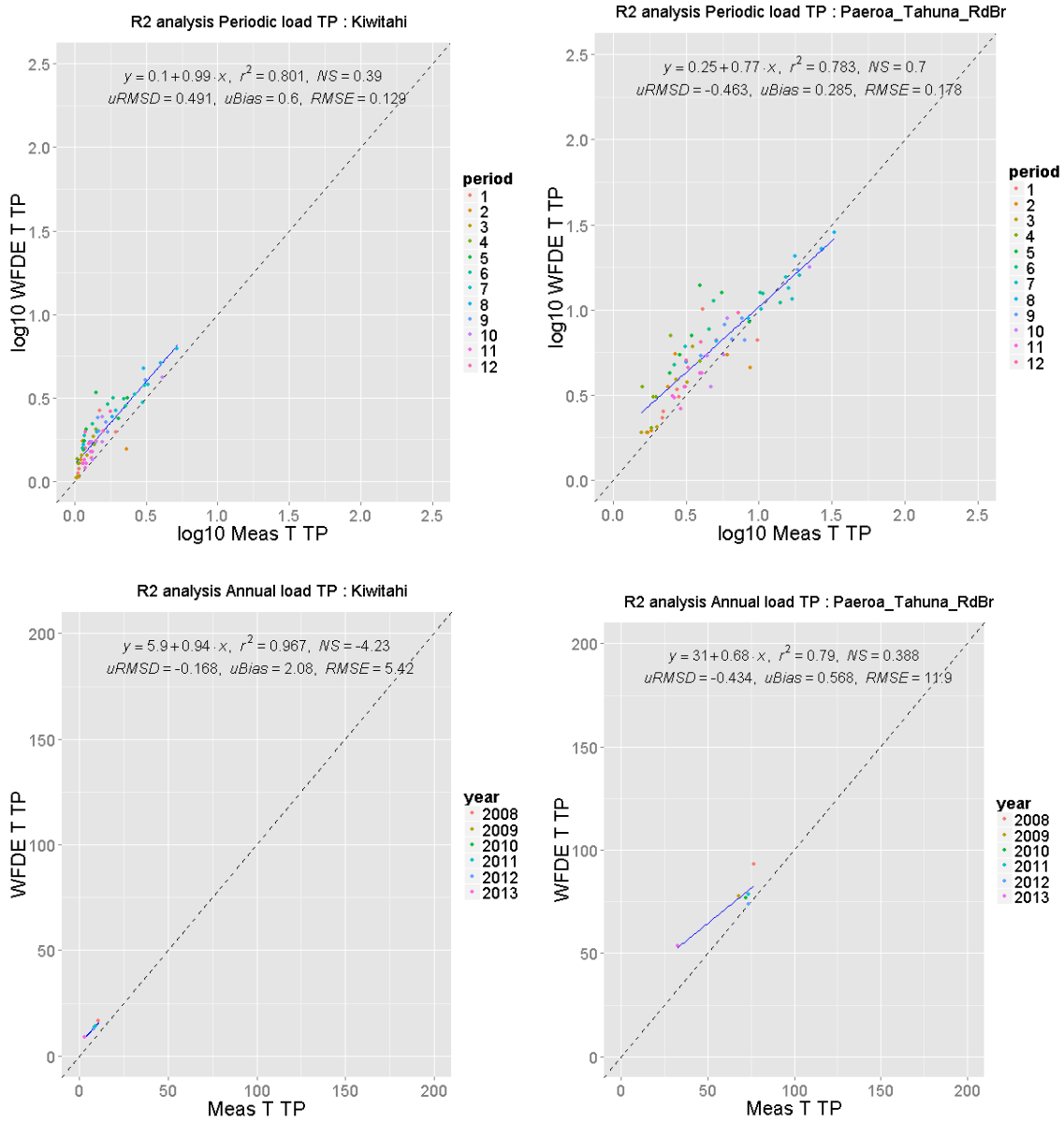

Figure E.20 Modelled total phosphorus loads per period and annual for loads for the Piako measurement stations Kiwitahi and Paeroa-Tahuna Rd Br statistically compared by using the r-squared (r^2), Nash-Sutcliffe coefficient (NS), unbiased root-mean square difference (uRSMD), normalised Bias (uBias) and root-mean square error (RMSE). In this graph the Hauraki Plains water quality model is compared with the RLoadest load prediction.

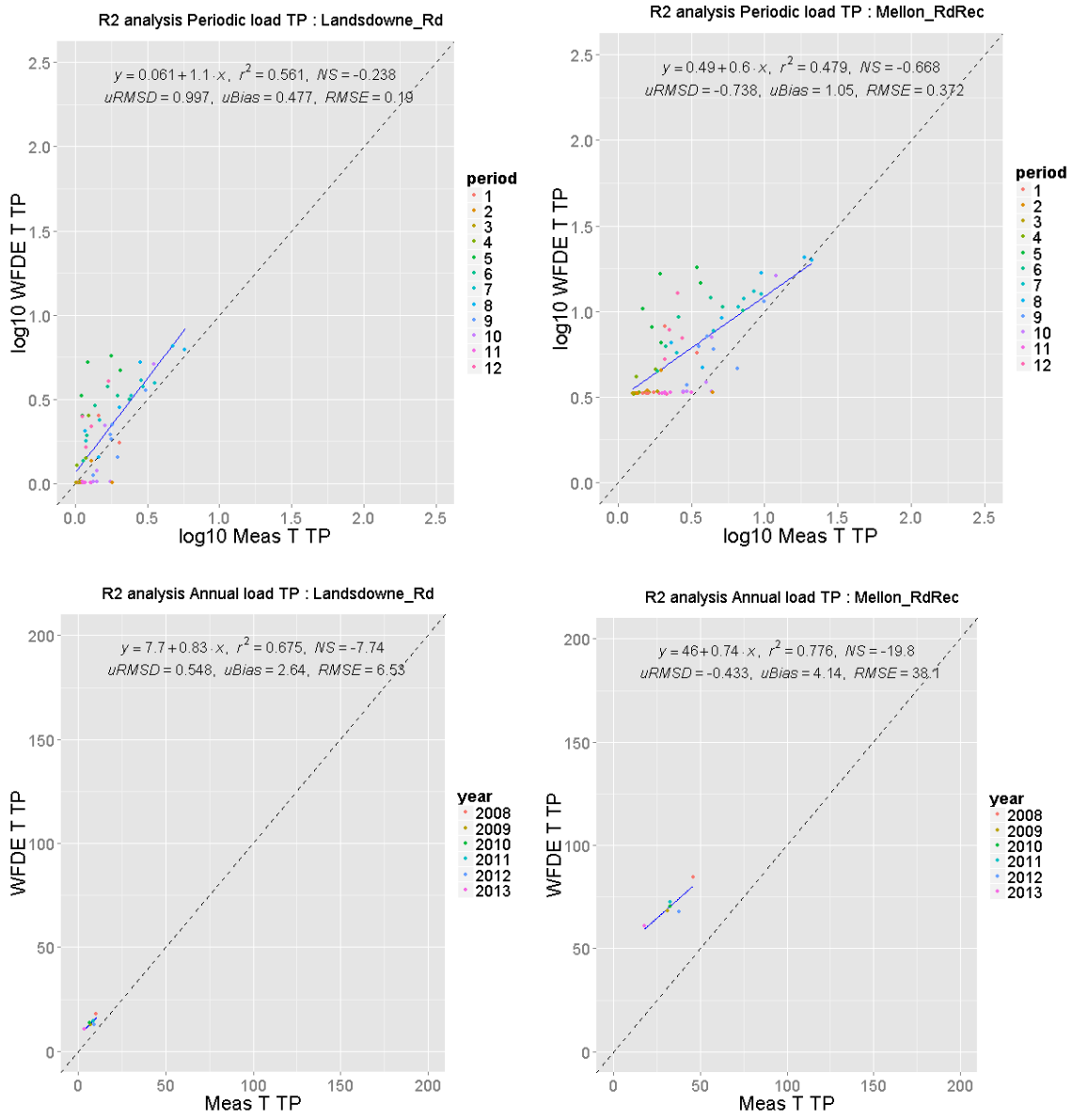

Figure E.21 Modelled total phosphorus loads per period and annual for loads for the Waitoa measurement stations Landsdowne Rd Br and Mellon Rd Rec *statistically compared by using the r-squared (r^2), Nash-Sutcliffe coefficient (NS), unbiased root-mean square difference (uRSMD), normalised Bias (uBias) and root-mean square error (RMSE). In this graph the Hauraki Plains water quality model is compared with the RLoadest load prediction.*

E.6 Cause of annual model bias

Introduction

As the annual results are nearly all classified poor (TN: Waihou, Ohinemuri, Waitoa; TP: Waihou, Waitoa, Piako – Kiwitahi) a further investigation of this cause of error was undertaken.

For this investigation a simplified approach was used. In this approach the assumption is made that the periodic loads calculated by RLoadest are accurate and can be summed to derive the actual annual load. This load forms the foundation for the comparison. Flows were measured, modelled by WFLOW and redistributed for the WFD Explorer model setup. Using the flow-load rating curves as derived in Section 5.7.3, the periodic loads as calculated from these flows were generated. These were summed to derive an annual load. For the final comparison the load modelled by the WFD Explorer was included.

Having these actual, derived and modelled annual loads lined up per downstream station makes is feasible to understand where in the modelling process the bias occurs. Knowing the approximate reason for the model prediction bias will help future improvement of the model.

Interpretation

Relation measured flow
When “Relation measured flow” has a large percentage of deviation compared to the RLoadest load the cause should be searched in the flow-load rating curves.

Possible explanations:

- the flow-load rating curves are poor, most likely due to insufficient measurements. This should lead to a large percentage of deviation in each year.
- The flow-load rating curves perform poorly in years of extreme flow. This should lead to a large percentage of deviation in high load or low load years.
- There is no trend component included in the flow-load rating curves.

Relation WFLOW flow
When “Relations WFLOW flow” has a large deviation compared to the load derived at “Relation measured flow” the cause should be searched in the WFLOW model performance.

Possible explanations:

- Continuous under or over prediction of the flow
- Incorrect predictions of extreme flow events (e.g., low flow, peak flow).

Section 4.5 gives an indication of which stations might be affected by an insufficient flow prediction by WFLOW.

Relation WFDE flow
When “Relations WFDE flow” has a large deviation compared to the load derived at “Relation WFLOW flow” the cause should be searched in the incorrect allocation of flows to the river catchments in the WFD Explorer model setup. This is caused by the automated approach of setting up the WFD Explorer model.

Possible explanations:

- The flow is incorrectly allocated in the WFD Explorer to a different river catchment.
- The flow is incorrectly allocated in the WFD Explorer upstream or downstream of the stations location.

The annual outflow of the WFLOW model and WFD Explorer model were compared and no flow was lost due to incorrect model setup.

WFDE model result
When “WFDE model result” has a large percentage of deviation when compared to the load derived at “Relation WFDE flow” the cause should be searched in incorrect load input.

Possible explanations:

- incorrect allocation or magnitude of source loads
- incorrect annual load scaling
- the lack of annual variability in background and point sources
- spatial variation in land-use leaching rates which is not captured in the model
- the incorrect attribution of total phosphorus load from erosion

Results

Table E.10.6 The attributed model bias per model year for the downstream stations. This model bias was derived by comparing the RLoadest load; flow-load rating curve prediction for measured, WFLOW modelled and WFD Explorer modelled flow and the WFD Explorer load (in that order). Green indicates an model bias of -5% <X<5%, yellow -10%<X<10%, orange -25%<X<25%, red -50%<X<50% and dark red X<-50% OR X>50%. A greater the percentage (negative or positive) means that this factor has a worse influence on the model performance.

Downstream station	Years	TN						TP					
		Rloadest load	Relation Measured flow	Relation WFLOW flow	Relation WFDE flow	WFDE model result	Modelled Load	Rloadest load	Relation Measured flow	Relation WFLOW flow	Relation WFDE flow	WFDE model result	Modelled Load
		T	%	%	%	%	T	T	%	%	%	%	T
Te Aroha	2008	1848.62	-1.39%	17.84%	12.57%	-3.90%	2313.15	144.13	-3.98%	15.98%	13.26%	0.48%	181.22
	2009	1655.32	-1.51%	20.76%	14.87%	-4.00%	2153.88	125.88	0.04%	20.02%	15.77%	0.49%	171.61
	2010	1714.51	-1.21%	20.40%	13.75%	-4.17%	2207.86	125.51	2.20%	17.98%	15.37%	-0.38%	169.66
	2011	1996.15	-0.78%	-2.16%	13.29%	-3.09%	2141.04	144.09	7.05%	-4.87%	15.31%	0.40%	169.87
	2012	2043.07	-6.73%	18.48%	10.92%	-4.04%	2423.73	142.19	3.42%	17.95%	12.92%	0.32%	191.40
	2013	1615.65	-6.70%	19.38%	15.63%	-3.69%	2013.54	107.55	8.14%	20.13%	19.13%	-0.73%	157.73
Karangahake	2008	622.49	-11.86%	-32.63%	7.53%	0.02%	392.52	106.40	-77.23%	-15.86%	1.63%	16.29%	26.42
	2009	364.29	-0.47%	-51.70%	7.90%	2.20%	211.04	13.55	-26.16%	-31.47%	4.14%	147.03%	26.23
	2010	473.59	-2.50%	-36.45%	9.15%	1.17%	338.04	23.77	-13.20%	-48.97%	5.86%	66.90%	26.28
	2011	464.22	-2.91%	-53.59%	7.46%	1.83%	245.08	27.90	-15.39%	-56.93%	3.83%	63.47%	26.50
	2012	717.98	-12.86%	-46.29%	5.30%	-0.19%	330.05	190.14	-20.09%	-75.78%	0.36%	9.41%	26.44
	2013	334.81	-13.92%	-41.87%	7.63%	4.89%	189.93	16.87	-50.43%	-15.66%	2.59%	118.55%	26.15
Mellon Rd Rec	2008	821.92	-1.95%	59.39%	2.04%	-5.13%	1268.69	45.64	0.66%	64.12%	0.36%	19.73%	84.38
	2009	627.30	-1.68%	54.52%	3.36%	-4.80%	949.72	31.06	31.15%	61.59%	4.77%	21.66%	68.07
	2010	741.11	-1.74%	55.09%	2.91%	-5.98%	1113.78	32.33	20.94%	62.94%	3.66%	30.73%	70.57
	2011	765.51	-0.96%	27.70%	5.42%	-3.85%	982.28	32.63	34.29%	46.61%	19.70%	21.73%	72.55
	2012	769.59	0.49%	32.80%	0.31%	-4.04%	997.15	37.61	17.37%	40.09%	1.24%	21.57%	67.80
	2013	378.03	-0.48%	126.85%	4.52%	-5.15%	853.36	17.69	25.13%	167.32%	9.29%	43.12%	61.01
Paeroa-Tahuna Rd Br	2008	1390.44	-8.80%	22.72%	2.34%	-4.64%	1551.94	76.55	-5.70%	24.89%	2.73%	-0.39%	93.04
	2009	1064.85	-0.73%	5.31%	2.78%	-3.91%	1101.62	68.20	1.80%	7.03%	3.46%	1.42%	77.55
	2010	1217.35	1.07%	2.13%	2.64%	-4.21%	1237.09	71.99	2.43%	1.63%	2.72%	-0.07%	76.83
	2011	1142.45	2.56%	-7.39%	3.67%	-3.24%	1092.12	73.68	1.82%	-2.80%	5.07%	2.34%	78.41
	2012	1092.90	15.36%	-13.95%	2.19%	-3.67%	1092.18	73.47	4.98%	-8.67%	1.98%	2.00%	73.68
	2013	432.72	27.37%	64.84%	6.28%	-6.85%	829.25	32.58	12.92%	46.09%	5.92%	-0.40%	53.61

Conclusion

For TN the largest deviation can be found in the “Relation WFLOW flow”, meaning most of the deviation can be attributed to the performance of WFLOW. Only for Paeroa-Tahuna Rd Br the result is good as has been described in Section 4.5 (with year 2013 as exception, but this might be an added effect of the poor flow-load relation for that year).

At Te Aroha the result show that there is an approximate 13% additional flow at this station in the WFD Explorer due to incorrect allocation in the WFDE schematisation (see “Relation WFDE flow”). In Karangahake this effect is also visible but to a smaller extent (approximately 7%).

In Karangahake the flow-load rating curve substantially under predicts the TN load for the years 2008, 2012, and 2013. A possible explanation could be that the TN load is regulated by other factors in addition to flow, for example point sources, which do not discharge continuously throughout the year. The opposite is apparent at Paeroa-Tahuna Rd Br, where

the flow-load relation tends to under predict the first year and over predict in the last year. This could be due to the occurrence of a trend in the TN load, these trends are neglected in the load-flow relations approach.

For TP most deviation can be found in the “Relation WFLOW flow” and in the “WFDE model result”. The cause for deviation in the “Relation WLOW flow” is most likely to be the same as for TN, an offset in the flow prediction by WFLOW to the actual flow. The deviation in the “WFDE model result” is severe and occurs in both Karangahake and Mellon Rd Rec. Both are caused by the even distribution of point sources and background loads throughout the year. In both catchments the point sources are a serious contribution in comparison to the total load coming from the catchment. Distributing the point sources evenly throughout the year makes the anthropogenic periodic load partition calculated from the total period load negative. This is then scaled back to zero. At Mellon Rd Rec this occurs during several periods, and in this case the option has been chosen to set the anthropogenic load for these periods to zero. In Karangahake this occurs nearly all periods and here the option was chosen to keep using the default load input for all years.

In addition, a large part of the deviation for stations Karangahake and Mellon Rd Rec can be found in the “Relation Measured flow”. This is most likely caused by the fact that the flow-load rating curves can’t accurately predict periodic load from flow for these stations. This may be because a large part of the load at both stations is contributed by point sources. Another likely reason that Karangahake is difficult to predict by the flow-load rating curves is the exponential increase of TP with flow. This might be due to increases in erosion, which does not occur under average flow conditions (e.g., a large part of the Ohinemuri catchment is used for exotic forest, the Ohinemuri flows through a relatively narrow canyon and higher flow levels might therefore cause more erosion).

Discussion

This analysis of the probable cause of model bias contains a high level of assumptions. Future research should answer whether the made assumptions are correct. The used technique to pinpoint model bias to model setup steps is very coarse (e.g., it is likely that when WFLOW calculates flows higher then measured the use of flow-load rating curves increases the related load even further do to that the flow is out of the scope of the relation). Overall this assessment of the model bias has shown to be useful and provides an overview of future steps to improve the models annual prediction capacity.

F Scenario results

Appendix included in confidential Appendixes

G Land-use categorisation

For setting up the model the diffuse sources need to be categorised and spatially located. These diffuse sources consist of land-uses (anthropogenic and natural). To create this spatial layer, the information provided by the LCDB4 layer, AGRIBASE and CLUES have been combined to a new spatial layer. These layers differ in spatial resolution and the information that they contain. AGRIBASE contains the most detail spatially and in classes for farming. For the natural land-uses the LCDB4 layer is needed as these are not described in AGRIBASE. Also the LCDB4 is in high detail. The CLUES layer is low in spatial resolution and strongly rasterized and thereby only used for validation and where AGRIBASE and LCDB4 don't suffice.

The categories that have been used in this new spatial layer can be classified as the following:

Table G.1 Land-use classes used in the Hauraki Plains Catchment model

Category	Land-use
Farming	Dairy
	Dairy support
	Drystock
	Horticulture
	Lifestyle
	Other farming
Forestry	Exotic forest
Residential	Res/Com
Natural	Wetland
	Shrubland
	Indigenouis forest
	Other landscape

To come to these categories, the first classification was based on AGRIBASE by categorising these classes as shown in Table G.2. However, AGRIBASE doesn't provide a full coverage of the Hauraki Plains Catchment. Also AGRIBASE cannot be used to classify the categories forestry, natural and residential. As not all farm boundaries were present in the AGRIBASE layer, there was still a fair amount of farm boundaries that needed to be defined by hand.

The remaining non-farming area was intersected with the land-uses of the LCDB4 layer. Areas still remaining after the intersection with LCDB4 were separated in Res/com, roads, rivers and slivers (partial manually). Slivers are mostly the remaining area between property boundaries. For Res/com only areas that intersected with a grouped CLUES Urban class raster covering an area larger than 17 acres (70.000 m^2) were taken into account.

All natural, forestry and farming land-uses were further classified using the categories in the AGRIBASE, LCDB4 and CLUES layers.

Table G.2 Categorising of AGRIBASE classes towards the Hauraki Plains Catchment model classes.

FARM_TYPE	Description	CAT
ALA	Alpaca and/or Llama Breeding	Other farming
ARA	Arable cropping or seed production	Horticulture
BEF	Beef cattle farming	Drystock
DAI	Dairy cattle farming	Dairy
DEE	Deer farming	Other farming
DOG	Dogs	Lifestyle
DRY	Dairy dry stock	Dairy support
EMU	Emu bird farming	Other farming
FIS	Fish, Marine fish farming, hatcheries	Lifestyle
FLO	Flowers	Horticulture
FOR	Forestry	-
FRU	Fruit growing	Horticulture
GOA	Goat farming	Other farming
GRA	Grazing stock	Dairy support
HOR	Horse farming and breeding	Other farming
LIF	Lifestyle block	Lifestyle
MTW	Meatworks	Res/Com
NAT	Native Bush	-
NEW	New Record - Unconfirmed Farm Type	-
NOF	Not farmed (i.e. idle land or non-farm use)	-
NUR	Plant Nurseries	Horticulture
OPL	Other planted types (not covered by other types)	-
OST	Ostrich bird farming	Other farming
OTH	Enterprises not covered by other classifications	-
PIG	Pig farming	Other farming
POU	Poultry farming	Other farming
SHP	Sheep farming	Drystock
SNB	Mixed Sheep and Beef farming	Drystock
TOU	Tourism (i.e. camping ground, motel)	Res/Com
UNS	Unspecified (i.e. farmer did not give indication)	-
VEG	Vegetable growing	Horticulture

A second classification of the remaining area was made using the LCDB4 layer.
The LCDB4 land-uses were transformed to the Hauraki Plains Catchment model land-uses as shown in Table G.3.

Table G.3 Categorising of LCDB4 classes towards the Hauraki Plains Catchment model classes.

LCDB4 Class	**LCDB3 NAME**	**CAT**
1	Built-up Area (Settlement)	
2	Urban Parkland/Open Space	Res/Com
6	Surface Mines and Dumps	Other landscape
5	Transport Infrastructure	Res/Com
10	Sand and Gravel	-
16	Gravel and Rock	-
12	Landslide	-
14	Permanent Snow and Ice	-
15	Alpine Grass/Herbfield	-
20	Lake or Pond	-
21	River	-
22	Estuarine Open Water	-
30	Short-rotation Cropland	-
33	Orchard Vineyard & Other Perennial Crops	-
40	High Producing Exotic Grassland	-
41	Low Producing Grassland	-
43	Tall Tussock Grassland	-
44	Depleted Grassland	-
45	Herbaceous Freshwater Vegetation	Wetland
46	Herbaceous Saline Vegetation	Other landscape
47	Flax	Other landscape
50	Fernland	Shrubland
51	Gorse and Broom	Shrubland
52	Manuka and/or Kanuka	Indigenous forest
58	Matagouri or Grey Sub	Shrubland
54	Broadleaved Indigenous Hardwoods	Exotic forest
55	Sub Alpine Shrubland	Shrubland
56	Mixed Exotic Shrubland	Shrubland
71	Exotic Forest	Exotic forest
64	Forest - Harvested	Exotic forest
68	Deciduous Hardwoods	Exotic forest
69	Indigenous Forest	Indigenous forest
70	Mangrove	-

The remaining uncertain classes where classified using CLUES (see Table G.4).

Table G.4 Categorising of CLUES classes towards the Hauraki Plains Catchment model classes.

CLUES class	**CAT**
DAIRY	Dairy
SBHILL	Drystock
SBINTEN	Drystock
APPLES	-
DEER	-
KIWIFRUIT	-
MAIZE	-
NAT_FOR	-
ONIONS	-
OTHER	-
OTHER_ANIM	-
PLANT_FOR	-
POTATOES	-
SBHIGH	Drystock
SCRUB	-
UNGR_PAST	-
URBAN	-

Where both AGRIBASE and LCDB4 didn't suffice to classify the land-use, the classification in Table G.5 was used.

Table G.5 Remaining land-use classification based on AGRIBASE and LCDB4.

FARM TYPE CODE	**FARM TYPE Description**	**LCDB4 CODE**	**LCDB4 TYPE Description**	**CAT**
UNS	Unspecified (i.e. farmer did not give indication)	40	High Producing Exotic Grassland	Lifestyle
OPL	Other planted types (not covered by other types)	40	High Producing Exotic Grassland	Horticulture
NEW	New Record - Unconfirmed Farm Type	40	High Producing Exotic Grassland	Lifestyle
OTH	Enterprises not covered by other classifications	40	High Producing Exotic Grassland	Lifestyle
OTH	Enterprises not covered by other classifications	1	Built-up Area (Settlement)	Res/Com
NEW	New Record - Unconfirmed Farm Type	30	Short-rotation Cropland	Horticulture
OPL	Other planted types (not covered by other types)	30	Short-rotation Cropland	Horticulture
FOR	Forestry	40	High Producing Exotic Grassland	Exotic forest
NAT	Native Bush	40	High Producing Exotic Grassland	Indigenous forest
NOF	Not farmed (i.e. idle land or non-farm use)	40	High Producing Exotic Grassland	Lifestyle

H WFD-Explorer loads

This appendix supplies more detailed information on the variance of leaching values applied for different land-uses. Based on discussions with the DairyNZ water quality team and external experts, values for total nitrogen and total phosphorus leaching were selected for each dominant land-use in the model.

Table H.1 Land-use loads as derived from literature and unpublished data applicable to the Hauraki Plains catchment.

Land-use	Source	Kg TN/ Ha/Yr	Kg TP/ Ha/Yr	Comments
Dairy	Rutherford et al. (2009)	35.0 – 55.0	-	Lake Rotorua catchment
	DairyNZ (unpublished data)	7.1 – 103.9 (mean = 40.1; median = 42.1)	0.19 – 1.14 (mean = 0.71; median = 0.61)	Waituna catchment (van den Roovaart et al. 2014)
	Judge and Ledgard (2009)	32 – 45	0.80 – 0.90	Waikato catchment, OVERSEER 1997 – 2008
Dairy support	DairyNZ (unpublished data)	3.1 – 54.8 (mean = 21.3; median = 21.0)	<0.01 – 2.66 (mean = 0.69; median = 0.44)	Waituna catchment (van den Roovaart et al. 2014)
Drystock	Olubode-Awosola et al., unpublished/confidential	13.1	0.95	Waikato-Waipa catchment
	Rutherford, Palliser and Wadhwa (2009)	20.0, 30.0, 35.0		Rotorua catchment
	DairyNZ (unpublished data)	5 - 40 (mean = 17.5 ,median = 14.9)	0.14 – 1.13 (mean = 0.52 ,median = 0.41)	Waituna catchment (van den Roovaart et al. 2014)
	Judge and Ledgard (2009)	9.0 – 10.0 (Sheep), 13.0 – 14.0 (Beef)	2.00	Waikato catchment, OVERSEER 1997 – 2008
Lifestyle	DairyNZ (unpublished data)	7.0	0.10	Waituna catchment (van den Roovaart et al. 2014)
Other farming	Judge and Ledgard (2009)	15.0 - 17.0	1.00 – 2.00	Deer farming,, Waikato catchment, OVERSEER 1997 – 2008

Land-use	Source	Kg TN/ Ha/Yr	Kg TP/ Ha/Yr	Comments
Horticulture	Rutherford, Palliser and Wadhwa (2009)	25.0	-	Rotorua catchment
	Ledgard (2000)	219.0 (onions), 321.0 (potatoes)	-	Franklin district, yearly rainfall was 30% above average
	Plant & Food (unpublished)	110.0 – 250.0 (winter spinach), 180.0 (winter cabbage)	-	Pukekohe district
	Haynes and Francis (1996)	276.0 (potatoes)	-	Pukekohe district, value redundant due to improved practise of N fertiliser and cover crop
	Martin et al. (2001)	167.0 – 219.0 (potatoes)	-	Pukekohe district, value redundant due to improved practise of N fertiliser and cover crop
	The Agribusiness group (2014A)	58.0 (extensive), 65.0 (intensive), 73.0 (traditional)	1.10 (extensive), 1.30 (intensive), 1.90 (traditional)	Lower Waikato catchment
Horticulture	The AgriBusiness Group (2014B)	8.0 (pastoral), 56.0 (potato), 117.0 (barley)	-	Horizons region
	Stuart Ford (The AgriBusiness Group, pers. comm.)	55.0 (potatoes), 75.0 (onions)	-	Puke district
Res/com	Rutherford, Palliser and Wadhwa (2009)	10.0 (urban), 50.0 (rural septic tank)	-	Rotorua catchment
	DairyNZ (unpublished data)	3.0	0.10	Waituna catchment (van den Roovaart et al. 2014)
Wetland	DairyNZ (unpublished data)	3.0	0.30	Waituna catchment (van den Roovaart et al. 2014)

Land-use	Source	Kg TN/ Ha/Yr	Kg TP/ Ha/Yr	Comments
Shrubland, Indigenous forest, Exotic forest and Other Landscape	Rutherford, Palliser and Wadhwa, (2009)	4.0 (forest), 5.0 (bare ground)	-	Rotorua catchment
	DairyNZ (unpublished data)	2.5	0.25	Waituna catchment (van den Roovaart et al. 2014)
	Jenkins & Vant (2007)	3.0 (indigenous forest)	0.30 (indigenous forest)	Waikato district
Roads, slivers and rivers	DairyNZ (unpublished data)	2.5 (road)	0.10 (road)	Waituna catchment (van den Roovaart et al. 2014)

I Phosphorus load from erosion

I.1 Introduction

In the first calibration of the Hauraki Plains Catchment water quality model mainly the loads for phosphorus differed significantly from the observed loadings and those reported in Vant (2011). In the model an over prediction of roughly 20% was expected in comparison to the observed and reported loadings as attenuation had not yet been accounted for.

As shown in Figure I.1 the phosphorus load is severe under predicted at the measurement station Okauia (- 464 – -235% in difference) and less severe at Te Aroha (- 44 – -8% in difference), which are both located in the upstream Waihou River. Also there is an unusually high measured phosphorus load in the year 2008 for the stations Queenshead and Karangahake, which we not further take into account for the calibration of the model.

During the setup of the Waituna Catchment water quality model a similar under prediction of the phosphorus load was found. This was attributed to an additional load coming from erosion. This erosion can be caused by river bank collapse, naturally or do to treading of life stock. Another large potential cause of erosion is forest harvesting. As in New Zealand forestry is mainly practiced on sloped land harvesting would barren a large area which is prone to erosion.
In this model study the aim is to get a better understanding of whether the phosphorus load from erosion plays a role in the Hauraki Plains catchment and if so to which types of land-use this load should be assigned.

To explore the under predictions in P load in the Hauraki catchment a further analysis was undertaken.

I.2 Method

Particular phosphorus
We assume that particulate phosphorus (PP) is a good indicator of the phosphorus load component associated mostly with erosion processes in upstream locations. At the upstream stations water flows relatively rapid due to the slope of the landscape. As the water has a smaller residence time the effect of instream processes, for example uptake by plants, is limited. To exclude the effect that processes might have and to focus on the effect of erosion, this analysis will focus on the upstream stations. At these upstream stations it can be assumed that the fraction of PP, which is calculated from subtracting DRP from TP, mostly represents particular material that has entered the stream due to land-use.

In this study there is insufficient information to separate PP by organic or inorganic (sedimentary) components. However, both are currently not accounted for in the model as only nutrient loads from the root zone are used as input. Therefore, we can add the found effect of phosphorus load from PP as an additional load source per land-use in our model.

Calculation of phosphorus load
In this study the contribution per land-use is derived by calculating the load of phosphorus per station. For this calculation the yearly flow at each water quality station is required. As the flow is not measured at all stations, a flow gauge in a comparable catchment was applied, based on the selection criteria by Jenkins & Vant (2011). To use this flow gauge additional

flows from anthropogenic point sources (sewage water treatment plants, factories etc.) and springs need to be corrected and the overall flow needs to be corrected for catchment size. For the load calculation a simplified approach was used with small alterations from the formula described in Walling and Webb (1981 and 1988) the calculate an average year loading of phosphorus over the years 2004-2013. Base of these alterations is that the load calculation is made with an average yearly flow as flow stations need to be imposed on other catchments and corrections need to be made on a yearly basis.

$$Flow = \bar{Q} \cdot n$$
$$Ls = \bar{C} \cdot Flow$$

where $\bar{Q}$ represents the average flow during the years (m^3/s), *n* the number of seconds in one year (365 days) and *Flow* stands for yearly flow. In the second equation $\bar{C}$ represents the average of the concentration over the years (mg/l) and Ls the average load year load. The load per station is than corrected for the yearly phosphorus load contributed by anthropogenic point sources and springs. The remaining load is assumed to be directly affected by the land-use and the flow velocity.

Variance inflation factor
The variance inflation factor (VIF) is a method to exclude predicting variables that show a large correlation with the rest of the predicting variables. This method has been described in Kutner, et. al. (2004). If used these predicting variables would not represent their own effect in such but also the correlating predictors.

Correlation
As a first indicatory analyses a correlation between the land-uses per catchment and the load of PP at that specific catchment is performed. As a multi parameter effect by different land-uses is expected the correlation will not present a clear model of how the load of PP is influenced by land-use.

Linear Model
Secondary a Linear model (LM) is setup based on hectares of land-use to predict the yearly load of PP at the measurement station. Using land-use in hectares will result in the Kg/Ha/Yr as estimated factor in the model.

Recalculation of the load
Based on the acquired load of PP per land-use Kg/ha/Yr the model is re-run and the phosphorus load on the stations is re-compared with the measurements and described loads in Vant (2011).

I.3 Results

Load calculation

Table I.1 Summary of the different measurement stations in the Hauraki Plains

River	Contributary	Confluence	Measurement station	Station Type	Catchment size (Ha)
Kauaeranga	-	-	Smiths Cableway	FLOW	11961
Hikutaia	-	-	OldMaratotoRd	WQ	6186
Piako river	Mangawara (1)	-	Jefferis	FLOW	
Piako river	Waitoa river (2)	-	Waharoa Control	FLOW	10747
Piako river	Waitoa river (2)	-	LandsdowneRdBr	WQ	10705
Piako river	Waitoa river (2)	-	MellonRdRec	FLOW & WQ	40482
Piako river	-	-	PiakonuiRd	WQ	588
Piako river	-	-	Kiwitahi	FLOW & WQ	10539
Piako river	-	-	Paeroa-TahunaRdBr	FLOW & WQ	53208
Waihou	Waiohutu stream (1)	-	Waiohutu	WQ	613
Waihou	Waiohutu stream (1)	-	Matamata-TaurangaRd	WQ	19868
Waihou	Oraka stream (2)	-	Pinedale	FLOW	12963
Waihou	Oraka stream (2)	-	LakeRd	WQ	26323
Waihou	-	-	WhitesRd	WQ	4450
Waihou	-	1 & 2	Okauia	FLOW & WQ	82350
Waihou	-	-	TeAroha	FLOW & WQ	111651
Ohinemuri	Waitekauri river (1)	-	USOhinemuriConfl	WQ	4236
Ohinemuri	-	-	SH25Br	WQ	2584
Ohinemuri	-	-	QueensHead	FLOW & WQ	13614
Ohinemuri	-	1	Karangahake	FLOW & WQ	28652
Waitakaruru	-	-	CoxheadRd	WQ	5987

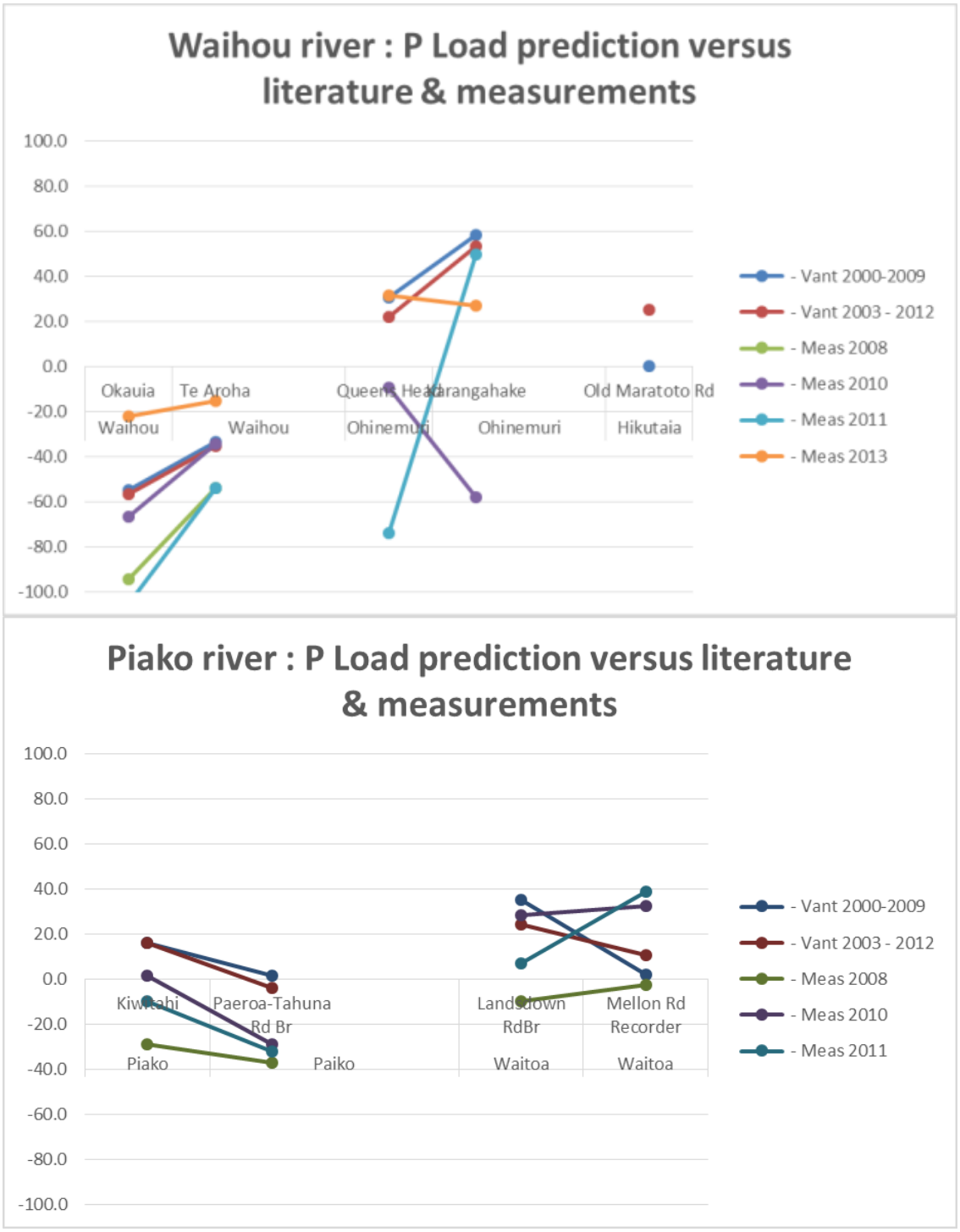

Figure I.1 Difference between the measured loads and the load calculated with the Hauraki Plains Water quality model. Figures A and B represent the performance of the model on the phosphorus load. In each plot the contributory river and the measurement stations are indicated. Connected dots are measurement stations that are located within the same contributory river where the measurement station on the left is located upstream. Note that the scale of the Y axes varies between the plots. For the measurement station Old Maratoto Rd in the to the Waihou River Hikutaia only load calculations by Vant (2011) are available.

Table I.2 Summary of the point sources and springs contributing to the upstream catchment of the measurement stations

River	Measurement station	Point sources	Springs
Kauaeranga	Smiths Cableway	-	(uncertain)
Hikutaia	OldMaratotoRd	-	-
Piako river (1)	Jefferis	-	-
Piako river (2)	Waharoa Control	-	24
Piako river (2)	LandsdowneRdBr	-	24
Piako river (2)	MellonRdRec	L, P, S & U	24
Piako river	PiakonuiRd	-	-
Piako river	Kiwitahi	-	-
Piako river	Paeroa-TahunaRdBr	A & T	-
Waihou (1)	Waiohutu	-	(uncertain)
Waihou (1)	Matamata-TaurangaR	-	1, 5, 11, 12, 13, 19, 20, 21 & 22
Waihou (2)	Pinedale	-	8 & 9
Waihou (2)	LakeRd	G, H & Q	6, 7, 8,9 & 10
Waihou	WhitesRd	-	17
Waihou	Okauia	F, G, H & Q	1,2, 3, 4, 5, 6 , 7, 8, 9, 10, 11, 12, 13, 14, 15, 19, 20, 21, 22 & 23
Waihou	TeAroha	F, G, H, Q & R	1,2, 3, 4, 5, 6 , 7, 8, 9, 10, 11, 12, 13, 14, 15, 19, 20, 21, 22 & 23
Ohinemuri (1)	USOhinemuriConfl	-	-
Ohinemuri	SH25Br	-	-
Ohinemuri	QueensHead	D & O	-
Ohinemuri	Karangahake	D & O	-
Waitakaruru	CoxheadRd	-	-

Table I.3 Calculation of the load of total phosphorus (TP), dissolved reactive phosphorus (DRP) and particulate phosphorus (PP) per water quality measurement station by using their related flow station in Vant (2012)

River	Measurement station	Flow station	Concentration (10 year average mg/l)			Original Load (T / yr)		
			TP	DRP	PP	TP	DRP	PP
Hikutaia	OldMaratotoRd	Kauaeranga @ Smiths	0.01	0.00	0.01	0.83	0.26	0.56
Piako (2)	LandsdowneRdBr	Waitoa @ Waharoa Control	0.08	0.03	0.05	4.73	1.72	3.01
Piako (2)	MellonRdRec	Waitoa @ Mellon Rd	0.23	0.14	0.09	39.90	25.01	14.89
Piako	PiakonuiRd	Piako @ Kiwitahi	0.03	0.01	0.02	0.08	0.03	0.05
Piako	Kiwitahi	Piako @ Kiwitahi	0.11	0.06	0.05	6.16	3.14	3.02
Piako	Paeroa-TahunaRdBr	Piako @ Paeroa-Tahuna Rd	0.30	0.20	0.10	81.72	54.23	27.50
Waihou (1)	Waiohutu	Oraka @ Pinedale	0.03	0.01	0.02	0.09	0.04	0.05
Waihou (1)	Matamata-TaurangaRd	Waihou @ Okauia	0.05	0.02	0.03	6.86	3.24	3.62
Waihou (2)	LakeRd	Oraka @ Pinedale	0.16	0.10	0.05	36.06	23.59	12.47
Waihou	WhitesRd	Oraka @ Pinedale	0.08	0.08	0.01	5.60	5.16	0.44
Waihou	Okauia	Waihou @ Okauia	0.10	0.07	0.03	80.46	55.27	25.18
Waihou	TeAroha	Waihou @ Te Aroha	0.10	0.05	0.05	115.17	58.99	56.18
Ohinemuri (1)	USOhinemuriConfl	Ohinemuri @ Queens Head	0.01	0.00	0.01	0.66	0.14	0.52
Ohinemuri	SH25Br	Ohinemuri @ Queens Head	0.02	0.01	0.02	0.59	0.17	0.42
Ohinemuri	QueensHead	Ohinemuri @ Queens Head	0.03	0.01	0.02	4.28	1.20	3.08
Ohinemuri	Karangahake	Ohinemuri @ Karangahake	0.02	0.00	0.01	4.96	1.11	3.85
Waitakaruru	CoxheadRd	Mangawara @ Jefferis	0.07	0.03	0.04	4.28	1.95	2.32

Table I.4 Load attributed by the land-uses in the upstream catchment of each water quality measurement station. This is calculated by subtracting the loads contributed by point sources and springs from total phosphorus and Dissolved reactive phosphorus (DRP). The remainder after dissolved reactive phosphorus is brought to 0 is subtracted from particulate phosphorus (PP).

River	Measurement station	Corrected	Land-use Load (T / yr)		
			TP	DRP	PP
Hikutaia	OldMaratotoRd	FALSE	0.83	0.26	0.56
Piako (2)	LandsdowneRdBr	FALSE	4.73	1.72	3.01
Piako (2)	MellonRdRec	TRUE	12.98	0.00	12.98
Piako	PiakonuiRd	FALSE	0.08	0.03	0.05
Piako	Kiwitahi	FALSE	6.16	3.14	3.02
Piako	Paeroa-TahunaRdBr	FALSE	71.70	44.20	27.50
Waihou (1)	Waiohutu	FALSE	0.09	0.04	0.05
Waihou (1)	Matamata-TaurangaR	FALSE	6.86	3.24	3.62
Waihou (2)	LakeRd	FALSE	23.72	11.25	12.47
Waihou	WhitesRd	FALSE	5.60	5.16	0.44
Waihou	Okauia	FALSE	62.85	37.67	25.18
Waihou	TeAroha	FALSE	91.51	35.33	56.18
Ohinemuri (1)	USOhinemuriConfl	FALSE	0.66	0.14	0.52
Ohinemuri	SH25Br	FALSE	0.59	0.17	0.42
Ohinemuri	QueensHead	TRUE	1.41	0.00	1.41
Ohinemuri	Karangahake	TRUE	2.09	0.00	2.09
Waitakaruru	CoxheadRd	FALSE	4.28	1.95	2.32

Table I.5 Summary of the spring data.

Spring code	WRC Spring code	Flow (1*10^6 * m3/yr)
1	221_2	5.07
2	279_1	1.84
3	279_6	11.32
4	490_9	7.16
5	636_1	2.24
6	669_6	27.48
7	669_7	27.46
8	669_11	6.19
9	669_13	18.94
10	669_18	21.47
11	824_6	7.86
12	872_5	2.78
13	872_6	2.78
14	1122_14	142.11
15	1122_27	140.42
16	1122_29	55.11
17	1122_41	46.80
18	1158_1	42.06
19	1174_4	29.74
20	1174_6	25.30
21	1174_9	11.73
22	1174_10	17.98
23	1204_5	18.87
24	1249_38	1.45

Table I.6 Summary of the anthropogenic point source data.

Point source code	Flow (1*10^6 * m3/yr)	Load DRP (T/yr)
A	1.51	10.00
B	1.42	4.96
C	0.76	1.60
D	0.68	2.87
E	0.65	2.09
F	0.60	5.27
G	0.44	3.20
H	0.11	0.59
I	0.11	0.41
J	0.06	0.21
K	0.03	0.25
L	0.01	0.13
M	0.01	0.08
N	0.01	0.05
O	3.26	0.00
P	1.99	21.28
Q	0.87	8.55
R	0.23	6.05
S	0.16	5.27
T	0.16	0.03
U	0.09	0.23
V	0.04	0.31

Correlation

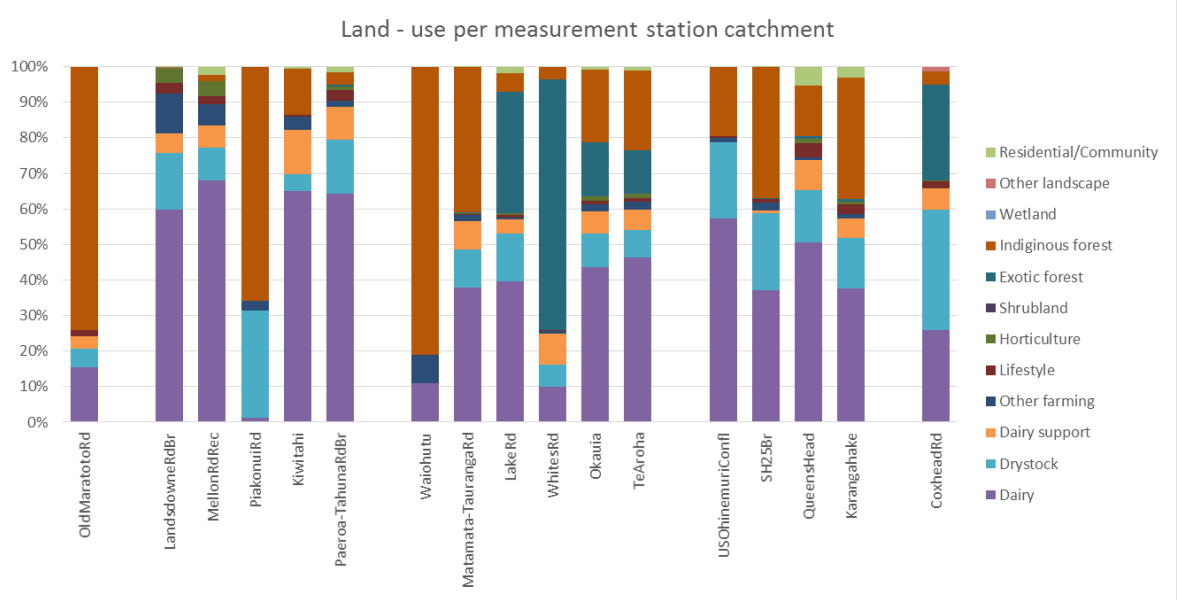

Figure I.1 Land-use coverage in the catchment upstream of each measurement station.

Table I.7 land-use coverage in km² in the catchment upstream of each measurement station.

River	Measurement station	Landuse (Km2)											
		Dairy	Drystock	Dairy support	Other farming	Lifestyle	Horticulture	Shrubland	Exotic forest	Indiginous forest	Wetland	Other landscape	Residential/Community
Hikutaia	OldMaratotoRd	9.37	3.04	2.14	0.00	0.99	0.06	0.00	0.00	44.63	0.00	0.00	0.00
Piako (2)	LandsdowneRdBr	61.60	16.54	5.79	11.37	3.31	4.16	0.00	0.00	0.00	0.00	0.37	0.10
Piako (2)	MellonRdRec	266.82	36.43	24.72	23.02	8.67	16.84	0.00	0.00	6.61	0.00	0.45	8.85
Piako	PiakonuiRd	0.06	1.67	0.00	0.16	0.00	0.00	0.00	0.00	3.67	0.00	0.00	0.00
Piako	Kiwitahi	65.62	4.95	12.50	3.75	0.60	0.00	0.00	0.00	13.13	0.00	0.00	0.51
Piako	Paeroa-TahunaRdBr	327.14	77.90	46.66	9.29	14.49	5.36	0.00	2.11	18.13	0.64	0.00	7.61
Waihou (1)	Waiohutu	0.64	0.00	0.00	0.47	0.00	0.00	0.00	0.00	4.76	0.00	0.00	0.00
Waihou (1)	Matamata-TaurangaRd	71.78	20.12	14.99	3.27	0.74	0.52	0.00	0.29	77.57	0.00	0.00	0.02
Waihou (2)	LakeRd	95.80	32.31	9.56	1.37	1.72	1.02	0.00	82.42	12.88	0.00	0.00	4.29
Waihou	WhitesRd	4.40	2.66	3.89	0.23	0.20	0.00	0.00	30.81	1.59	0.00	0.00	0.00
Waihou	Okauia	334.53	74.03	46.83	15.94	6.71	9.30	0.13	117.36	156.75	0.00	0.00	6.91
Waihou	TeAroha	484.96	79.81	59.56	22.52	10.19	13.44	0.13	127.63	235.03	0.00	0.00	11.23
Ohinemuri (1)	USOhinemuriConfl	23.23	8.72	0.00	0.47	0.25	0.00	0.00	0.00	7.87	0.00	0.00	0.00
Ohinemuri	SH25Br	9.06	5.24	0.19	0.55	0.25	0.02	0.00	0.06	8.98	0.00	0.00	0.02
Ohinemuri	QueensHead	64.26	18.44	10.63	1.20	4.95	1.69	0.00	0.88	17.92	0.00	0.00	6.80
Ohinemuri	Karangahake	101.68	38.92	14.76	3.66	7.07	1.97	0.00	2.26	92.42	0.00	0.00	8.39
Waitakaruru	CoxheadRd	14.92	19.44	3.31	0.01	1.16	0.19	0.00	15.45	2.12	0.00	0.74	0.00

The VIF shows high collinearity at the predictor variables Indigenous forest and Lifestyle (in that order). The remaining predictor variables give a VIF score lower than 6 (thresholds between 5 up to 10 are commonly used).

These are excluded from the analysis. Also Shrubland (2 occurrences) and Wetland (1 occurrence) are excluded due their direct association with measurement stations.

The land-uses Dairy, Drystock, Dairy support, Other farming, Horticulture, Exotic forest, Other landscape and Residential / Community are used in the correlation and linear model.

Linear model

For the linear model the same predictor variables were used as for the correlation. The intent of this model is to predict the Load of PP per catchment, and thereby work out the Kg/Ha/yr PP that needs to be assigned to the different land-uses.

The forward-stepwise linear regression results in the lowest AIC value (AIC = 191.69) and is therefore selected as the best model to predict the phosphorus load coming from PP per land-use. This results in an additional phosphorus load of ~0.46 Kg/Ha/Yr for Dairy and ~0.86 Kg/Ha/Yr for Exotic forest. Both are only applicable for land-use that is on a sloped area.

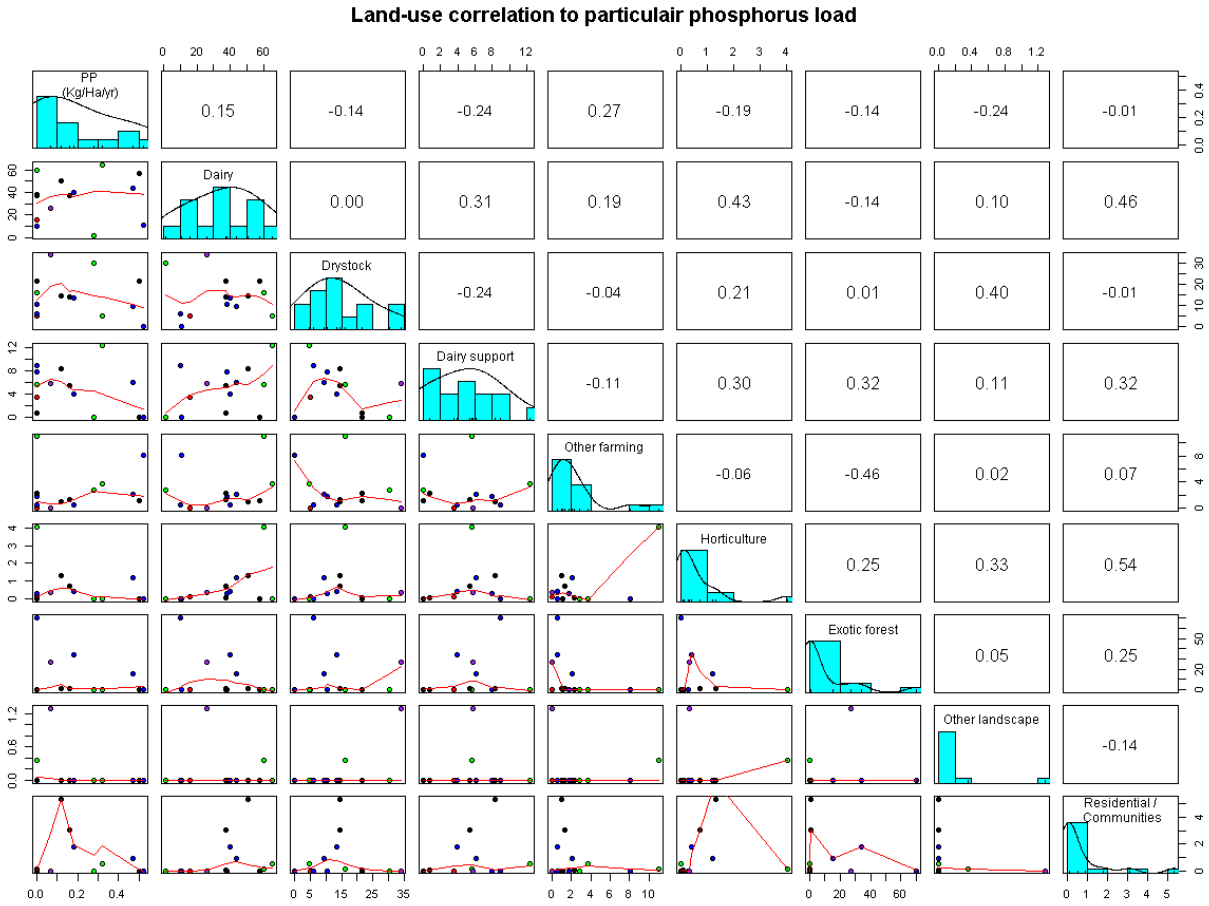

Figure I.2 Correlation between particulate phosphorus load per hectare per year and different land-uses. Note that if the number on the right side is larger the correlation is stronger.

Water quality model

When these newly acquired additional phosphorus loads are applied to the water quality model, this results in the following:

These graphs show that adding particular phosphorus to the water quality model results in a model improvement for the measurement locations Okauia, Te Aroha and Paeroa-Tahuna Rd Br. However, for the measurement location Kiwitahi it increases the over prediction for the phosphorus load.

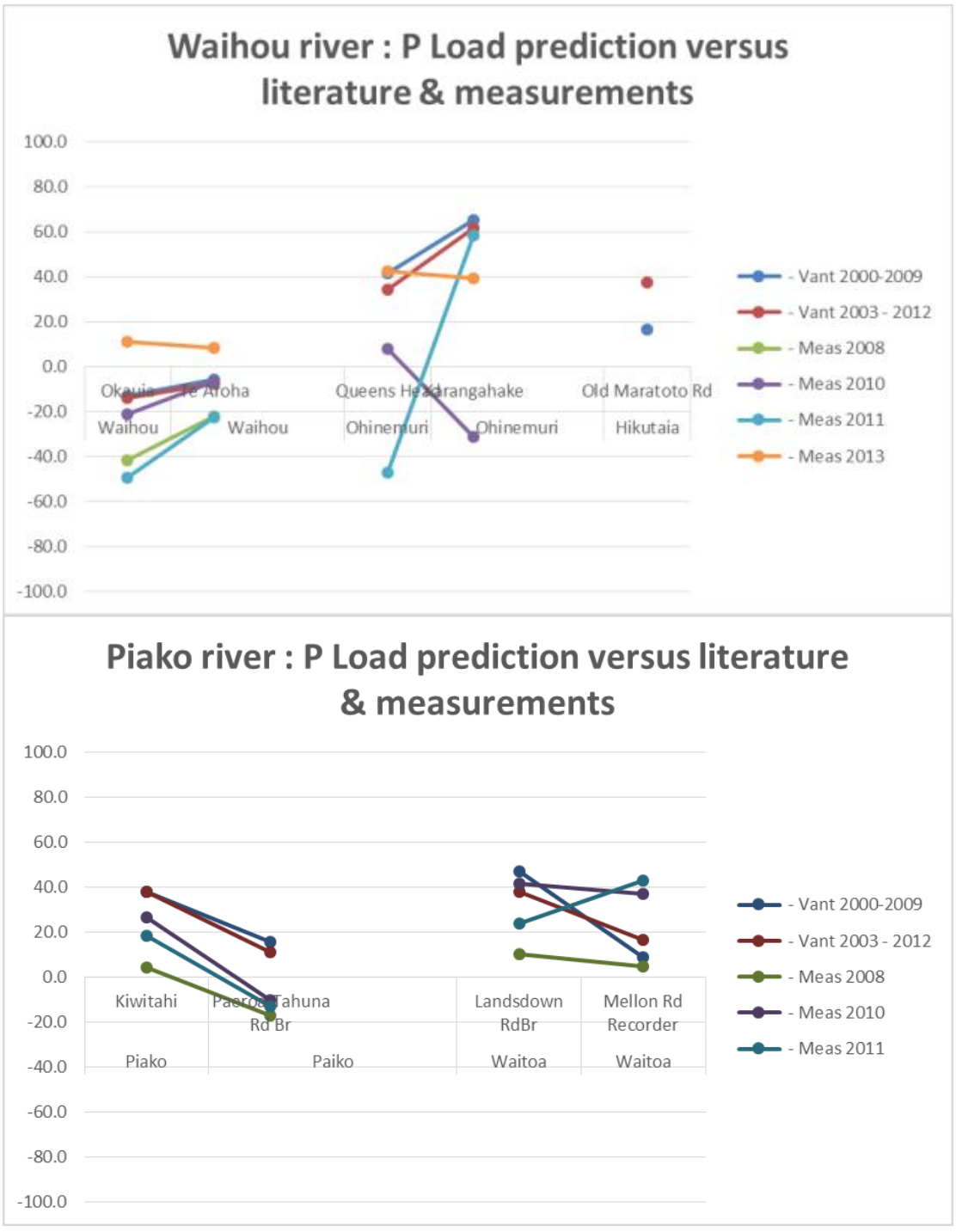

Figure I.3 Differentiation of the measured and reported phosphorus load compared with the load modelled by the Hauraki Plains water quality model for the different measurement stations. In each occasion the upstream and downstream stations within the same river have been linked with a line.

```
Step:  AIC=193.07
LoadPartP ~ Dairy + DairySupp + Horticulture + ExotForest + OthLandscape

               Df Sum of Sq      RSS    AIC
<none>                       5795000 193.07
- OthLandscape  1    913247  6708247 193.12
- Horticulture  1   1055295  6850295 193.41
- DairySupp     1   1524655  7319655 194.34
- Dairy         1  10124985 15919985 205.22
- ExotForest    1  31448296 37243296 217.12

Residuals:
     Min       1Q   Median       3Q      Max
-1298.54   -98.22   172.82   450.06   717.84

Coefficients:
              Estimate Std. Error t value Pr(>|t|)
(Intercept)  -396.3747   334.6240  -1.185 0.270196
Dairy           0.8061     0.2156   3.739 0.005716 **
DairySupp      -1.5594     1.0749  -1.451 0.184891
Horticulture   -3.3528     2.7778  -1.207 0.261909
ExotForest      0.7741     0.1175   6.589 0.000171 ***
OthLandscape   13.7210    12.2201   1.123 0.294076
---
Signif. codes:  0 ‘***’ 0.001 ‘**’ 0.01 ‘*’ 0.05 ‘.’ 0.1 ‘ ’ 1

Residual standard error: 851.1 on 8 degrees of freedom
  (5 observations deleted due to missingness)
Multiple R-squared:  0.9904,    Adjusted R-squared:  0.9845
F-statistic: 165.9 on 5 and 8 DF,  p-value: 7.436e-08
```

Figure 1 Result backward stepwise linear regression

```
Step:  AIC=191.69
LoadPartP ~ Dairy + ExotForest

               Df Sum of Sq     RSS    AIC
<none>                      8059837 191.69
+ DairySupp     1    868141 7191695 192.09
+ OthLandscape  1    417719 7642118 192.94
+ ResCom        1    118273 7941564 193.48
+ Horticulture  1     67011 7992826 193.57
+ Drystock      1     35418 8024419 193.62
+ OthFarming    1       600 8059237 193.69

Residuals:
    Min      1Q  Median      3Q     Max
-2215.8  -159.7   211.0   334.0  1133.8

Coefficients:
              Estimate Std. Error t value Pr(>|t|)
(Intercept) -193.73586  285.22858  -0.679    0.511
Dairy          0.46565    0.04506  10.334 5.32e-07 ***
ExotForest     0.85778    0.10683   8.029 6.31e-06 ***
---
Signif. codes:  0 ‘***’ 0.001 ‘**’ 0.01 ‘*’ 0.05 ‘.’ 0.1 ‘ ’ 1

Residual standard error: 856 on 11 degrees of freedom
  (5 observations deleted due to missingness)
Multiple R-squared:  0.9867,    Adjusted R-squared:  0.9843
F-statistic: 408.4 on 2 and 11 DF,  p-value: 4.778e-11
```

Figure I.4 Result forward stepwise linear regression

J Division of P and N load over periods

This appendix provides the percentages used for the distribution of the land-use loads. Bear in mind however that for phosphorus at Karangahake the relation was exponential and predicted a too low load to correct for background and point sources. Therefore the total load has been kept equal to the reported loads and the distribution of load over the year has been based on the proportional amount of flow in that period.

J.1 Nitrogen

Table J.1 Percentage scaling of land-use loads over periods per year for Te Aroha

Nitrogen scaling (%)	Period1	Period2	Period3	Period4	Period5	Period6	Period7	Period8	Period9	Period10	Period11	Period12	Total
2008	2.36	2.19	2.23	7.19	11.53	11.80	20.16	35.27	13.21	10.61	5.74	4.61	126.87
2009	3.70	4.98	4.14	4.12	7.62	10.30	17.70	19.03	12.51	18.95	5.86	6.72	115.64
2010	3.21	5.23	2.46	2.64	9.44	16.58	12.44	25.98	24.07	8.77	4.64	3.89	119.34
2011	9.74	3.68	5.21	5.63	11.86	17.85	21.53	10.21	8.72	7.59	4.68	7.91	114.61
2012	6.98	3.92	5.78	4.86	9.23	8.80	20.90	38.15	15.62	8.56	5.55	7.34	135.70
2013	2.89	2.25	2.29	6.43	12.17	16.52	10.65	13.57	15.02	9.31	7.12	7.36	105.58

Table J.2 Percentage scaling of land-use loads over periods per year for Karangahake

Nitrogen scaling (%)	Period1	Period2	Period3	Period4	Period5	Period6	Period7	Period8	Period9	Period10	Period11	Period12	Total
2008	0.00	0.00	0.00	6.94	6.45	13.51	25.41	44.91	2.27	3.71	0.00	0.00	103.22
2009	0.00	1.42	0.00	0.00	5.81	4.48	16.48	2.96	3.32	10.76	0.00	1.91	47.15
2010	0.00	2.31	0.00	0.00	11.72	24.24	8.84	26.46	13.01	0.00	0.00	0.12	86.71
2011	7.82	0.00	3.90	2.57	6.82	9.46	21.19	0.00	2.22	0.96	0.00	2.92	57.87
2012	3.60	0.00	6.38	0.00	6.44	0.91	23.74	37.02	3.72	1.96	0.00	0.25	84.02
2013	0.00	0.00	0.00	1.12	10.84	11.97	0.00	9.07	6.45	0.05	0.00	1.50	41.00

Table J.3 Percentage scaling of land-use loads over periods per year for Paeroa-Tahuna Rd Br

Nitrogen scaling (%)	Period1	Period2	Period3	Period4	Period5	Period6	Period7	Period8	Period9	Period10	Period11	Period12	Total
2008	0.31	0.21	0.36	8.33	20.81	21.61	31.27	56.30	8.65	9.52	2.51	2.17	162.05
2009	1.04	3.27	2.22	2.01	10.22	13.93	26.05	15.69	11.42	21.88	2.63	3.76	114.12
2010	0.93	3.04	0.62	0.96	4.96	24.13	19.56	39.80	27.29	5.00	1.00	1.20	128.49
2011	6.47	2.25	4.64	5.23	12.91	21.25	32.20	10.50	6.11	4.37	0.81	6.28	113.03
2012	3.61	1.39	2.39	2.11	6.86	7.37	22.33	44.46	12.65	4.60	1.64	3.69	113.09
2013	0.40	0.09	0.26	2.96	23.02	25.45	10.78	7.46	8.81	2.04	1.34	2.48	85.07

Table J.4 Percentage scaling of land-use loads over periods per year for Mellon Rd Rec

Nitrogen scaling (%)	Period1	Period2	Period3	Period4	Period5	Period6	Period7	Period8	Period9	Period10	Period11	Period12	Total
2008	0.00	0.00	0.00	12.75	25.78	23.23	32.50	43.66	6.83	9.15	1.41	0.96	156.29
2009	0.19	3.35	2.05	2.03	10.89	13.54	24.44	17.64	12.02	22.88	0.90	4.76	114.68
2010	0.14	5.06	0.00	0.16	14.68	32.86	15.27	35.97	28.03	3.73	0.00	0.44	136.33
2011	8.16	0.76	4.61	6.11	20.81	26.07	30.33	7.00	3.81	2.64	0.05	8.82	119.19
2012	4.82	0.36	3.48	0.76	8.69	7.56	29.19	45.35	11.43	3.17	0.60	5.48	120.88
2013	0.00	0.00	0.00	5.08	23.58	28.27	9.30	11.60	15.19	4.33	1.70	3.50	102.56

Table J.5 Percentage scaling of land-use loads over periods per year for Other

Nitrogen scaling (%)	Period1	Period2	Period3	Period4	Period5	Period6	Period7	Period8	Period9	Period10	Period11	Period12	Total
2008	0.00	0.00	0.00	6.03	12.67	13.60	22.43	37.54	7.96	6.84	1.55	0.52	109.14
2009	0.14	1.93	1.03	1.16	6.70	9.28	18.36	14.82	8.79	15.89	1.41	2.46	81.97
2010	0.00	2.36	0.00	0.00	8.63	19.27	12.45	26.99	20.48	3.85	0.60	0.19	94.82
2011	5.82	0.41	2.76	3.35	11.22	16.94	22.68	7.02	4.88	3.24	0.58	3.92	82.83
2012	3.18	0.38	2.86	1.32	7.09	6.24	21.04	37.04	10.57	4.01	1.22	2.49	97.45
2013	0.00	0.00	0.00	3.13	13.83	17.37	8.22	10.39	10.54	3.90	1.90	2.33	71.60

J.2 Phosphorus

Table J.6 Percentage scaling of land-use loads over periods per year for Te Aroha

Phosphorus scaling (%)	Period1	Period2	Period3	Period4	Period5	Period6	Period7	Period8	Period9	Period10	Period11	Period12	Total
2008	5.03	4.59	4.75	11.64	16.42	14.32	24.00	42.86	16.16	14.86	8.32	7.94	170.89
2009	7.06	8.64	7.35	6.89	11.11	12.77	21.21	23.63	15.39	26.66	8.44	11.12	160.27
2010	6.32	9.00	5.06	4.59	13.58	19.29	15.26	31.86	28.10	12.26	7.33	6.76	159.41
2011	16.21	6.75	8.80	9.22	16.87	20.61	25.55	13.18	11.22	10.60	7.36	12.97	159.34
2012	12.04	7.11	9.57	8.03	13.29	11.21	24.83	46.28	18.80	11.97	8.15	12.16	183.45
2013	5.84	4.68	4.83	10.45	17.29	19.22	13.24	17.16	18.15	13.03	9.57	12.12	145.59

Table J.7 Percentage scaling of land-use loads over periods per year for Karangahake. This distribution has been based on the years flow distribution at Karangahake.

Phosphorus scaling (%)	Period1	Period2	Period3	Period4	Period5	Period6	Period7	Period8	Period9	Period10	Period11	Period12	Total
2008	0.30	0.43	1.25	9.11	9.19	13.63	19.52	29.01	5.17	6.78	2.86	2.76	100
2009	2.41	6.61	2.97	3.57	10.99	9.71	19.45	10.09	7.64	16.74	2.12	7.68	100
2010	1.49	6.40	0.54	2.22	14.37	21.32	11.81	20.22	13.77	3.13	0.93	3.82	100
2011	13.89	2.05	8.43	6.15	10.91	12.51	20.02	5.98	5.88	4.95	0.86	8.36	100
2012	7.48	2.07	10.47	2.13	9.44	5.35	19.23	25.73	6.46	5.36	2.24	4.04	100
2013	0.54	0.71	0.42	6.13	19.59	18.69	8.34	16.27	12.44	5.20	3.53	8.13	100

Table J.8 Percentage scaling of land-use loads over periods per year for Paeroa-Tahuna Rd Br

Phosphorus scaling (%)	Period1	Period2	Period3	Period4	Period5	Period6	Period7	Period8	Period9	Period10	Period11	Period12	Total
2008	0.88	0.42	0.32	9.27	19.61	16.98	24.64	48.12	8.67	12.69	4.36	4.90	150.86
2009	2.51	6.85	3.44	1.87	9.24	10.65	20.32	12.55	11.47	28.90	4.58	8.42	120.79
2010	2.28	6.36	0.76	0.63	4.10	19.06	14.95	33.66	27.49	6.76	1.65	2.82	120.53
2011	14.61	4.71	7.51	5.63	11.88	16.69	25.41	8.00	6.10	5.94	1.33	13.93	121.73
2012	8.23	2.91	3.72	1.98	5.96	5.23	17.24	37.74	12.70	6.23	2.80	8.24	112.99
2013	1.09	0.17	0.15	2.97	21.77	20.15	7.68	5.34	8.82	2.88	2.27	5.61	78.90

Table J.9 Percentage scaling of land-use loads over periods per year for Mellon Rd Rec

Phosphorus scaling (%)	Period1	Period2	Period3	Period4	Period5	Period6	Period7	Period8	Period9	Period10	Period11	Period12	Total
2008	0.00	0.00	0.00	12.24	39.22	15.36	25.79	43.57	3.34	9.82	0.00	0.00	149.34
2009	0.00	0.45	0.00	0.00	12.57	7.50	18.91	15.22	7.67	34.02	0.00	9.87	106.20
2010	0.00	2.73	0.00	0.00	19.35	23.17	11.08	35.19	21.06	0.26	0.00	0.00	112.83
2011	12.39	0.00	0.00	3.36	30.33	17.67	23.94	3.63	0.81	0.00	0.00	25.14	117.25
2012	5.76	0.00	0.00	0.00	8.64	2.65	22.96	45.42	7.18	0.00	0.00	12.45	105.05
2013	0.00	0.00	0.00	1.98	35.29	19.45	5.99	8.64	10.32	1.32	0.00	5.11	88.09

Table J.10 Percentage scaling of land-use loads over periods per year for Other

Phosphorus scaling (%)	Period1	Period2	Period3	Period4	Period5	Period6	Period7	Period8	Period9	Period10	Period11	Period12	Total
2008	6.09	6.31	5.82	13.44	21.01	14.90	24.16	46.50	12.54	15.39	7.94	0.46	174.56
2009	8.03	10.60	6.96	6.30	11.39	11.62	20.52	21.23	13.33	33.13	7.98	0.80	151.90
2010	7.45	11.17	5.94	4.13	12.93	19.36	14.65	34.62	25.43	10.21	5.52	0.35	151.76
2011	19.02	8.51	7.90	9.58	18.54	18.86	24.91	11.24	8.92	8.31	5.54	1.09	142.43
2012	13.94	8.39	7.70	6.78	11.85	8.96	22.76	46.95	15.35	9.69	7.12	0.87	160.37
2013	6.72	6.28	5.82	9.52	21.70	18.98	11.20	14.23	14.86	10.13	9.35	0.78	129.57

K User manual WFD Explorer Hauraki Plains Model

K.1 Introduction

Contact DairyNZ for further information on this section.

L User manual Delta Data Viewer

L.1 Introduction

Contact DairyNZ for further information on this section.

M WFLOW-MODFLOW model Pinedale/Oraka

M.1 Introduction

This memo describes the current status of the coupled WFLOW-MODFLOW model for Pinedale/Oraka.

M.1.1 Background

In the WFLOW model for Hauraki a significant discrepancy between observed and modelled discharge at station Pinedale emerged. This is shown in Figure M.1, taken from the Delft-FEWS system for Hauraki. Calibration could not bridge this gap.

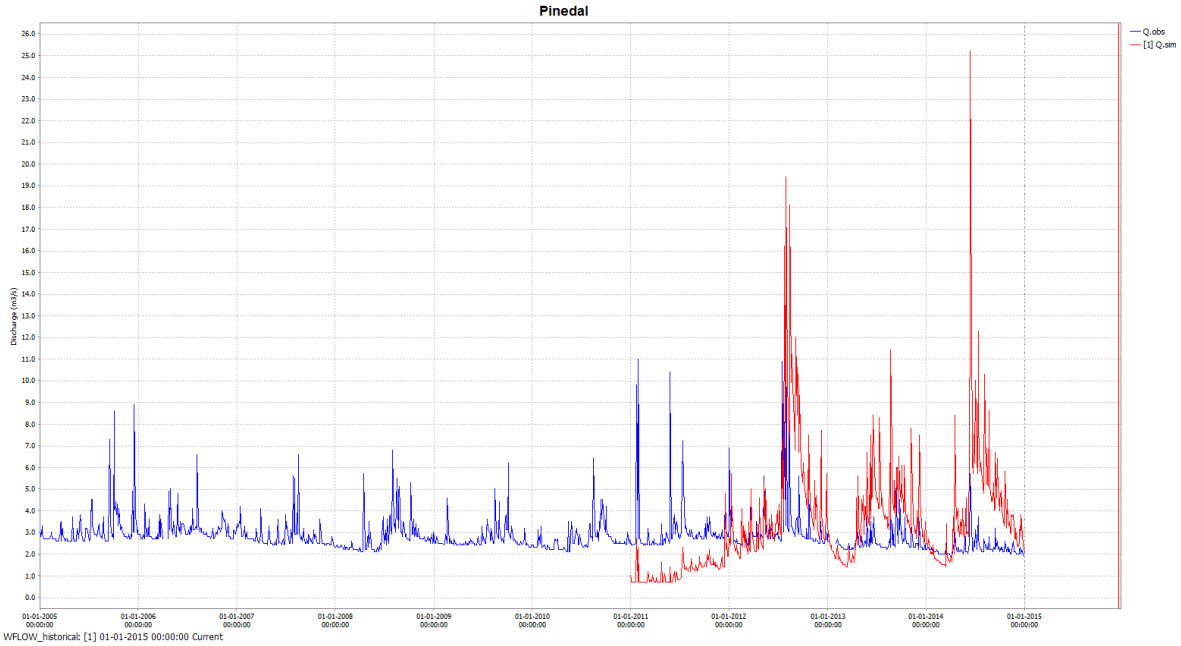

Figure M.1 Discharge at station Pinedale. Results from the Delft-FEWS system.

- blue line = Observations
- red line = WFlow model

It was discussed – by DairyNZ, GNS and others – that groundwater flow in deeper aquifers could play an important role. It was even suggested that the groundwater “catchment” may have a significantly different form than the surface water catchment. In other words, the groundwater head divides may be at different locations than the watershed divides, leading to water flow to other catchments via groundwater.

In WFLOW groundwater flow crossing the model boundaries is not possible. Further, the groundwater flow process is relatively simple, using a 1-layer approach. In order to include flow to/from deeper groundwater layers and flow across the model boundaries, a more sophisticated groundwater schematisation is needed. Coupling to a groundwater flow model is a possible solution.

MODFLOW is perfect candidate for such a coupling. Like WFLOW it is a raster based model. Besides it is widely used in the world and accepted as a standard for groundwater modelling.

M.1.2 Objectives

The objectives of the Pinedale/Oraka pilot case are:

1 Demonstrate the coupling: is it working, are both models sensitive to each other?
2 Evaluate the coupled model in terms of discharge at the Pinedale station: could the discharge be improved compared to the observations?

Because the available geological and geo-hydrological data is very limited, the Pinedale/Oraka case is not meant to develop a detailed, calibrated model. The goal is to demonstrate the potential added value of the coupling.

M.2 WFLOW – MODFLOW coupling

M.2.1 BMI approach

WFLOW[1] and MODFLOW[2] are coupled using the concepts of 'BMI', implemented by Deltares in both modelling codes. BMI is the abbreviation of 'Basic Model Interface', which is a globally used standard to convert existing models into reusable, plug-and-play components.

In the present coupling the two models remain independent, but interact with each other through a wrapper program written in Python[3]. The wrapper takes care of running each model and exchanging relevant information/data between the models.

The advantage of this approach is that the models can be developed independent of each other and linked in an easy and flexible way. However, the modeler is responsible for consistency between the model and the model concepts.

M.2.2 Pinedale/Oraka

In the Pinedale/Oraka model (Section M.3) the saturated groundwater flow in WFLOW is replaced by MODFLOW. This means that the saturated groundwater flow process should be disabled in WFLOW, since it is handled by MODFLOW and duplication in concepts should be avoided. On the contrary, surface runoff and surface water flow should not be parameterized in MODFLOW, because these processes are part of WFLOW. Other consistency issues – which should be considered and solved by the modeler – comprise the overlapping area of the models, cell sizes, time discretisation (time steps), simulation period etc. These issues are further described in Section M.3.

M.3 Pinedale/Oraka model

M.3.1 WFLOW

The Hauraki WFLOW model was used for the coupled model. This WFLOW model has already been delivered to DairyNZ and has been made operational in a Delft-FEWS system. The model has not been modified for this case study.

In Figure M.2 the model area of the WFLOW model is shown. The red lines show the subcatchments. The Pinedale subcatchment is the southern-most subcatchment. The 250 m variant of the model has been used.
The model has a simulation period from 01-Jan-2011 up to 31-Dec-2014 (a 4-year period). The time step size is 1 day, constant over the simulation period.

[1] *The WFLOW-SBM variant.*

[2] *The "component version" of MODFLOW built by Deltares.*

[3] *In future this might be replaced by an interface in DeltaShell.*

Figure M.2 Hauraki subcatchments in WFLOW.

M.3.2 MODFLOW

The MODFLOW model was developed with geo-hydrological data from GNS[4]. The available geo-hydrological data comprises:

- K value (hydraulic conductivity) for the near-surface soil layer, available on point locations in a regular grid (see Figure M.3). The data points cover an area called Oraka by GNS.
- 'Decay' function to calculate K value at a depth below surface:

$$K_z = K_0 * e^{-(z-10)/f}$$
$$where: f = 75/(1 + 150 * s)$$

with: z = depth
K_0 = K value for near-surface soil layer (see bullet above)
K_z = K value at depth z
s = slope

[4] *Delivered to Deltares by GNS*

- The above mentioned parameters K_0 (see also upper bullet) and f were provided by GNS.

No specific geological or hydrogeological information about the subsurface layering was available, so with the above mentioned data a simple model schematisation was built:

- Quasi 3-D model with 3 layers to represent both the top layer and deeper layers and to account for the decrease in K value with depth.
- The K value calculated with the GNS data was applied as horizontal K value. The vertical K value was assumed to be 5 times lower.
- In each layer a “general head boundary”[5] (ghb) was applied at the lateral boundaries of the model. This makes it possible for groundwater to flow over the boundary of the model – both in and out flow is possible.
- The MODFLOW model area is shown in Figure M.4 .
  - It coincides with the area where the GNS data is present.
- The cell size is set to 250 m, conformal to the WFLOW model.

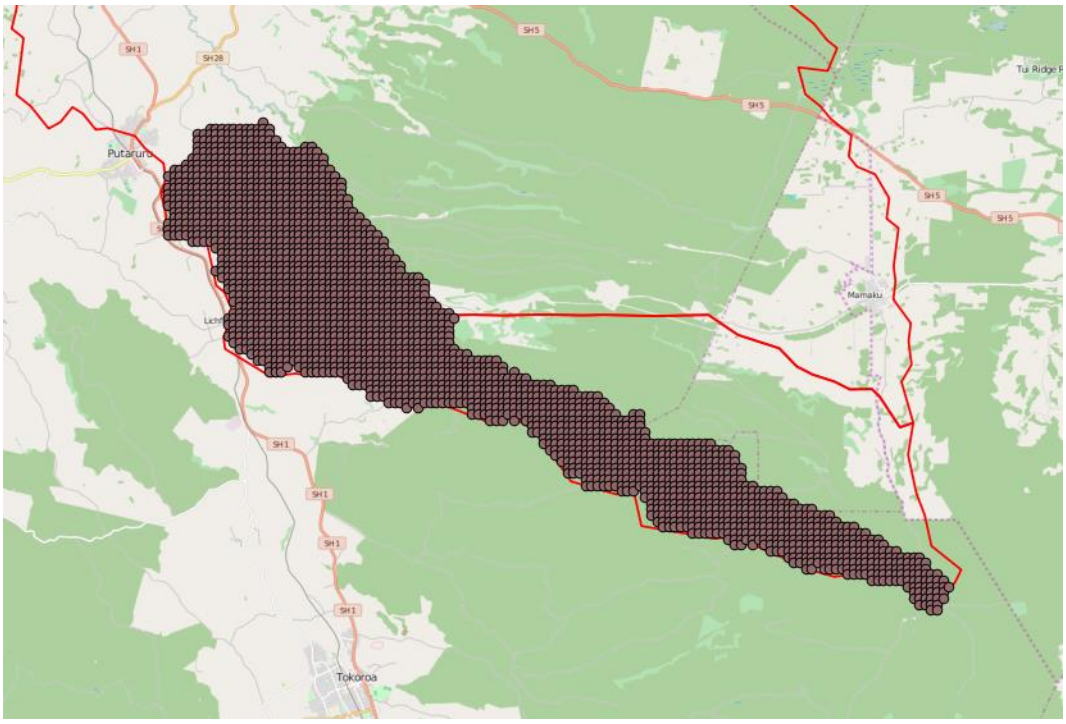

Figure M.3 Oraka data points received from GNS.

[5] *A general head boundary is parameterized by a level (head) and a conductance (the reverse of a resistance). The higher the conductance (lower resistance) the larger the influence of the level and the closer the modelled head will be “pulled” to that level.*

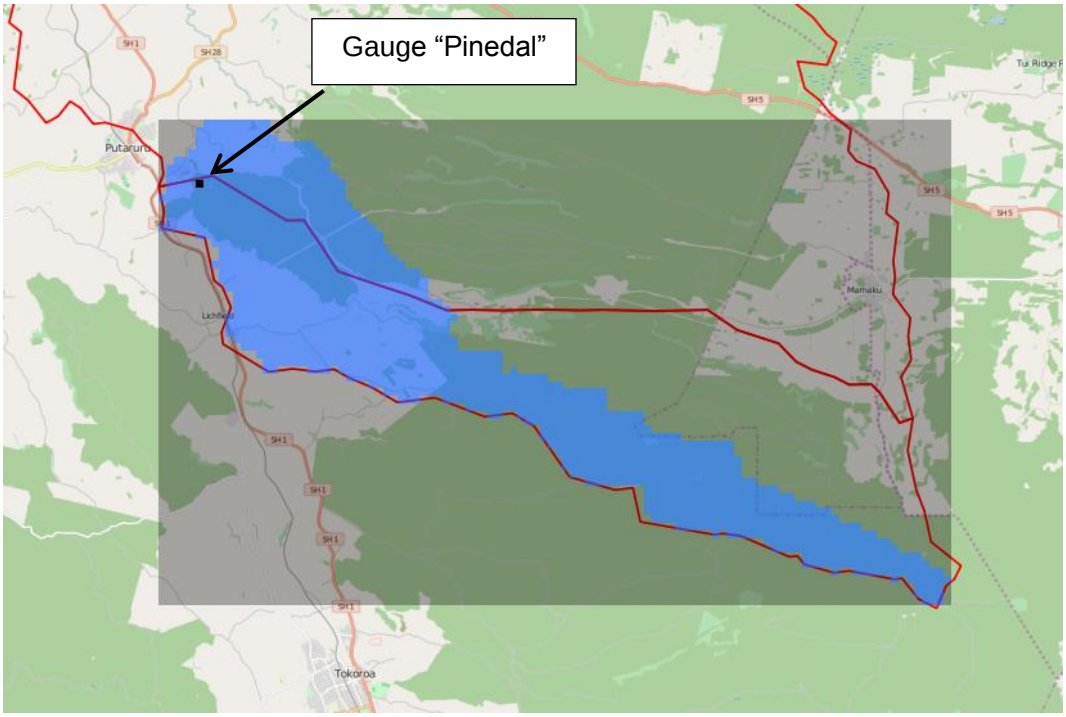

Figure M.4 MODFLOW model rectangle. Blue = active model area, Gray = inactive model area, Black dot = gauge (discharge station) Pinedale.

M.3.3 WFLOW-MODFLOW coupling

During the simulation – run by the Python wrapper – the following parameters are exchanged:

- The groundwater recharge flux is taken from WFLOW[6] and given to MODFLOW at the start of a MODFLOW time step. The recharge is averaged over the time elapsed since the previous MODFLOW time step.
- The groundwater head of the upper layer is taken from MODFLOW[7] and given to WFLOW at the start of a WFLOW time step. The head is averaged over the time elapsed since the previous WFLOW time step.

Because the time steps of the WFLOW and MODFLOW models are the same, the above mentioned averaging is not relevant. However, in future applications it is possible to have different time steps, e.g. to apply longer time steps for the groundwater model – and thus reduce computation time – if the groundwater flow process is much slower than the surface processes.

WFLOW and MODFLOW are run in sequence. Iteration within a time step – which is potentially needed since recharge and head are correlated – is not yet supported in the coupling. We think that the uncertainty introduced by this is relatively small given the daily time steps and the ‘slowness’ of the groundwater flow process.

The parameters are exchanged only in the overlapping area of the two models:

- Because the MODFLOW area is fully covered by the WFLOW area the recharge of MODFLOW is entirely replaced by the WFLOW recharge.

[6] *Averaged over the time elapsed since the previous MODFLOW time step.*

[7] *Averaged over the time elapsed since the previous WFLOW time step.*

- Because the WFLOW area is larger than the MODFLOW area the head of MODFLOW is burned-in into the head of WFLOW. That means that outside the MODFLOW area WFLOW keeps its own head.

M.4 Results

At station Pinedale the discharge of the coupled model differs from the discharge of the WFLOW model (see Figure M.5). That means that WFLOW is sensitive to MODFLOW: the exchanged head has influence on the discharge. In other words, the groundwater head from MODFLOW is not overruled or damped by WFLOW.

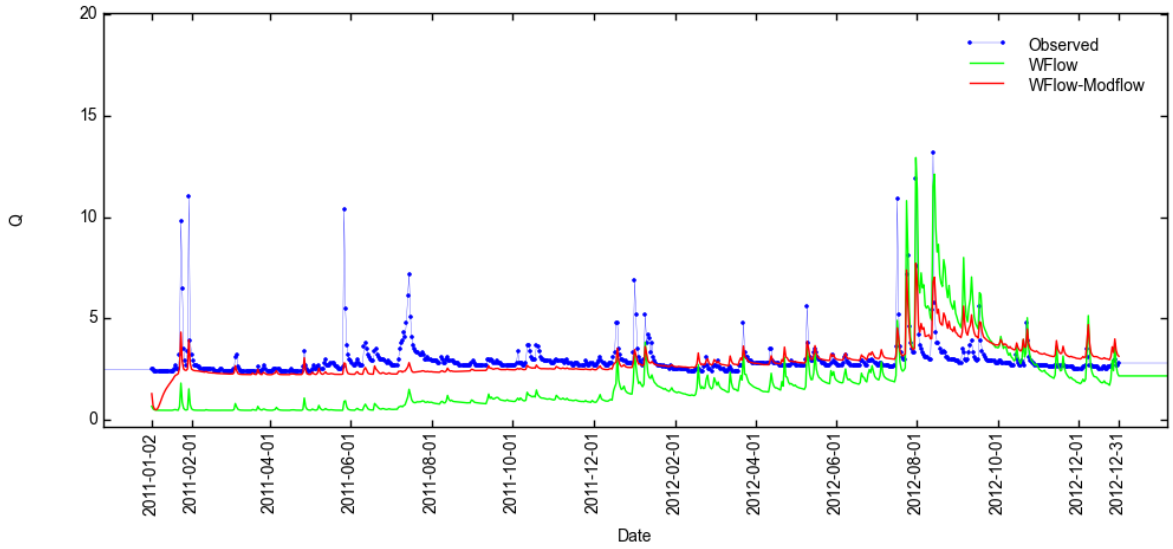

Figure M.5 Observed and modelled discharge at station Pinedale.

• • blue dots = Observations
▬ green line = WFLOW model (without MODFLOW)
▬ red line = WFLOW model with MODFLOW coupling

The combination with MODFLOW results in an increase of the base flow and in lower peaks. The base flow now comes much closer to the observations. With a quick manual modification of some basic parameters, it was possible to tune the base flow. The manual tuning was done by changing:

- The level of the general head boundaries. This level controls the heads near the catchment boundary and have thus an influence on the runoff. The model is highly sensitive for this parameter. Due to the lack of real data/information the parameterization has been kept very simple without any spatial variation (i.e. the same values were applied at all boundary cells). In future this parameter could be tuned if a better understanding of the flow.
- The horizontal and vertical K values. These parameters are estimated with the general approach provided by GNS. The model is sensitive to these parameters, because they control the lateral and vertical groundwater flow and the extent to which deeper aquifers are connected to shallower aquifers.

M.5 Conclusions

The two main conclusions are:

1 The coupling was tested and it was shown that it works as expected. The two models are sensitive to each other.

2 Further with the tested model the base flow at the Pinedale station comes much closer to the observations, although the peaks are too low. The result is promising: potentially there is a big added value. It was possible to influence the discharge with a quite simple MODFLOW model. With a quick manual modification of some basic parameters, it was possible to tune the base flow.